A modelling approach to diagnose the impacts of global changes on hydrology suspended sediment and organic carbon in an Asian tropical basin : the case of the Red River (China and Vietnam)

Xi Wei

Université Fédérale
Toulouse Midi-Pyrénées

THÈSE

En vue de l'obtention du

DOCTORAT DE L'UNIVERSITÉ DE TOULOUSE

Délivré par l'Institut National Polytechnique de Toulouse

Présentée et soutenue par

Xi WEI

Le 2 décembre 2019

Une approche de modélisation pour diagnostiquer les impacts des changements globaux sur l'hydrologie, les sédiments en suspension et le carbone organique dans un bassin tropical asiatique: cas du fleuve Rouge (Chine et Vietnam)

Ecole doctorale : **SDU2E - Sciences de l'Univers, de l'Environnement et de l'Espace**

Spécialité : **Surfaces et interfaces continentales, Hydrologie**

Unité de recherche :
ECOLAB - Laboratoire d'Ecologie Fonctionnelle et Environnement

Thèse dirigée par
Sabine SAUVAGE

Jury

M. Aldo SOTTOLICHIO, Rapporteur
M. Xixi LU, Rapporteur
M. José-Miguel SáNCHEZ-PéREZ, Examinateur
M. Sylvain OUILLON, Examinateur
M. Henrique Llacer ROIG, Examinateur
M. Orange DIDIER, Examinateur
Mme Sabine SAUVAGE, Directrice de thèse

Mme Marine HERMANN, invitée

Acknowledgement

If you are going to ask me which part of the thesis is the most difficult part to write. My answer will be the acknowledgment part, as difficult as the discussion! The discussion, conclusion and perspective are to justify and to summary my scientific work, but the acknowledgment is to review and to put a full stop for my three-year both life and work.

"*Life is like a box of chocolate, you never know what you are gonna get.*" I clearly knew that I would like to do a PhD abroad, but honestly, I did not expect that it was in France. The attractive and interesting part of life is its unpredictability: a person you met, an idea came out, a choice you made…Like a complex permutation and combination. Life provided me with a French "chocolates" in 2015, and then I made a choice to come to France, a country with history and culture, a country famous for liberty, equality and fraternity. Now when I look back, I am grateful for the "chocolate" I got and the choice I made. I really appreciate **the China Scholarship Council (CSC)** for founding and providing me with a chance for studying abroad. Surely, this opportunity is a significant treasure for both my life and scientific work. I also appreciate my supervisors **Sabine Sauvage** and **José-Miguel Sánchez-Pérez** for providing me with a PhD subject and accepting me as a member of the EcoLab. I appreciate the understanding and support of my **family**. I know they worry a lot for my health condition after my surgery and I know they prefer me staying close to them in order for me to better recover and to be taken care of. Since I was a kid, they always respect my choice and let me decide the way I want to take. Their selfless love and support are always with me wherever I go. In this context, in January 2017, I took pieces of luggage and flew 12 hours to France without any fear and with full of expectations for my new adventure, though I barely knew French and this country, beginning my life in Toulouse and my study in the EcoLab, and now I still remember the first breath I took when landed in France.

During these three years, what I have learned is more than my PhD subject. The way and method of self-learning and doing research will absolutely benefit my future research works. In the beginning, works here were really tough for me. Reading one scientific article would cause me several weeks and after reading I forgot what I had read about, and I did not understand what the authors talked about. **Sabine** always encouraged and comforted me during the beginning, and she makes me realize that patience and enthusiasm are important for research works. For getting through the difficult beginning, my teammates: **Roxelane Cakir**, **Clement Fabre** and **Jeremy Guilhen**, helped me dealing many problems with the modelling. They are representatives of the good education system of engineering schools. Appreciation is also due to **Juan Luis Lechuga Crespo**, who is always willing to help me to figure out the problems, and to **Chuxian Li**, who is teaching me many learning methods. After one year and a half, I gradually got to know my research and work, and more and more professional questions came to me. Luckily, **Sabine**, **José**, **Sylvain Ouillon**, **Thi Phuong Quynh Le**, **Didier Orange**, **Marine Herrmann**, these researchers are there

to guide me to go forward. They contributed to the conceptualization and methodology for my PhD work, helped me to improve my scientific articles, taught me to be rigorous in research. With their expertise, I am able to keep going and finish my thesis. And I am so glad to be supervised by them, especially my director **Sabine** who not only taught me something related to my scientific work but also life philosophy. Thanks for her toleration and understanding during these three years. Thanks **José** for proposing the directions and ideas for my study and the time he spending in guiding me. Thanks **Sylvain** for being there for my problems and questions. He was so friendly showing us around when we were in Hanoi. He proposed many nice ideas for my study and worked together with me to figure the questions out. Thanks **Quynh** for providing the organic carbon sampling data which allowed me to test the equations for calculating the organic carbon. Modelling work cannot be isolated from in-situ observations. The combining of in-situ and modelling methods help researchers better and easier carry out studies an solve problems. Great respects should give to the filed-work researchers with their continuous efforts on sampling work. **Quynh** is also a hard-working researcher who inspires and encourages me a lot. Thanks **Didier** and **Marine** for introducing us the LOTUS project and taking us as a member in this project. It is a nice project and I personally think this kind of cooperations can be also greatly applied to other developing countries. Thanks **Didier** for providing mang expertise ideas and suggestions of Vietnam which really helped me better understand my study area. The time in Hanoi with Didier was also cheerful. He is such a friendly and kind person whom you will always be happy around. Thanks Marine for helping me improving my scientific writing a lot. She taught me how to be more rigorous and convictive in scientific paper. She works efficiently, and carefully and always on schedule which I really admire.

I would like to express my gratitude to **Franck Gilbert**, director of the EcoLab, **Genevieve Soucail**, director of the SDU2E doctoral school, **Stephane Bonnet**, associate director of the doctoral school. They are great group leaders. They are contributed to improve PhD study life and support PhD students when we come across problems. They organize activities and classes for PhD students, and they try their best to make international PhD students feel welcome and comforting. I really appreciate these efforts they made. Merci à **Annick Correge**, **Marie-Jose Tavella**, **Yannick Combarieu**, **Paule Tabarelli** et **Caroline Duthier**, qui se soucient de moi, qui ont un cœur en or et qui me font toujours sourire. Chaque fois que je leur demande de l'aide, ils font de leur mieux pour m'aider et sont patients avec mon mauvais français. Ce sont des personnes avec qui je souhaite rester en contact et continuer de partager des mots affectueux dans l'école.

In my daily life, there are also many lovely people around. I am extremely grateful to my good friends here in Toulouse: **Chuxian** and **Roxelane**, inviting me out and introducing me new people. I am so grateful that **Roxelane** introduced me the Madagascar groups (**Christopher Marifeno Honoré**, **Arivony Rakotonirina**, **Anaïs Estrade Totobesola** and **Ali Andria**). They are so kind and easygoing, making my life

here cheerful. Friends here in France like **Abby Wanyu Liu**, **Vanessa Cristina Dos Santos**, **Manon Dalibard, Juan Luis Lechuga Crespo** and **Pankeyes Datok**, also outside France: **Huier Liu**, **Xue Mi**, **Bo**, **Victor Postel** and **Ramón Fuentes**, they are so lovely. These people support me a lot during my stay in France. They listen to me, help me dealing with my troubles, comfort me, encourage me to be strong and to continue my study. They with my family are like a pillar of my life and spirit. The time with them was relaxing and cheerful. Accompanies from **Marilen Haver**, **Lulu He**, **Yuewei Wang**, **Mei Zhang**, **Ya Huang**, **Margaux Jacober**, **Melody Darsou**, **Columba Martínez-Espinosa**, **Amina Mami**, **Juan Durango-Cordero**, **Amine Benabdelkader**, **Clement**, **Jeremy**, **Mélanie Raimonet**, **Thomas Rosset**, **Vivien Ponnou-Delaffon**, **Amine Zettam**, **Francesco Angelo Salvatore Ulloa Cedamanos**, **Xinda Wu**, **Liliana Dorticos**, **Minerva Llull**, **Rebeca Martinez** and **Roberta Bruschi** will build my good memories in France too. Among these people, we have witnessed each other's glory and important moments: some became doctors and outstanding researchers, some became great mothers, etc. I feel so lucky to live and grow with these people.

Thanks again for those people who have helped and cared about me during these three years. Their help and love are such a preciousness. I will always carry these beautiful memories with me wherever I will be. May we meet again, in France or in China, or somewhere around the world.

My journey of PhD in Toulouse is over, but my next journey just begins…I will take what I have learned here, both in science and life, to continue improving myself, to continue studying, to continue devoting to research and science.

Contents

Preface

In densely populated Asia, the river systems are under strong influences of anthropogenic interferences, such as intensive agricultural activities, urban expansion and rapid industrial growth. In addition, influences from the natural environment, such as climate variability and climate changes (El Nino, La Nina, typhoon and extreme weather), also affect the river basins. The tropical region in Asian (South Asia) has been identified as hot spots of many biogeochemical processes, such as riverine export of sediment, carbon and nitrogen. Basic and in-depth studies of these biogeochemical processes in the regions are necessary and important. However, there are many limitations on data access, such as restriction by governments, difficulty in monitoring and sampling due to remote places and funding issue, and the accuracy and authenticity of the data. The Red River is a river basin integrating above problems and issues.

This research was developed in the framework of the Land-Ocean-aTmosphere regional coUpled System study center (LOTUS), an international joint Vietnamese/French laboratory funded by the Institut de Recherche pour le Développement (IRD). The scientific objective of the LOTUS is to understand and monitor the functioning and variability of the transport and fate of water and associated matter in the atmosphere-continent-ocean coupled system in coastal regions of Vietnam and South East Asia (SEA). Based on that main objective, our specific objective is to provide validated high frequency (daily) time series on annual to multi-annual time scales of the fluxes of water and matter across and at the outlet of the Red River basin, in order to study the functioning and variability of those fluxes and to provide upper boundary conditions for estuarine and ocean models.

The Red River is an international river crossing three developing countries (China, Vietnam and Laos). Lack of data sharing between countries and difficulty of in-situ observations and samplings, make the study through the whole basin difficult. Therefore, for studying a large basin with limited data access, modelling would be a good tool, but even so, some base dataset for setting up and calibrating the model is indispensable (such as meteorology, topography, soil, land cover and in-situ observations and sampling). During the first half period of the study, we spent plenty of time searching and collecting data. No free access to climate data (temperature and rainfall), therefore, satellite data became the priority. Nowadays, satellite data become popular and is a practical tool to study geoscience, and more and more precise results are produced by satellite data. After investigating and comparing some satellite productions, we finally chose CFSR (for temperature) and TRMM (for rainfall) as the meteorology inputs for the model. Topography, soil and land cover data were also downloaded from satellite data. The first hydrology dataset we could obtain was provided by IRD (contacts: Didier Orange). Then, under the cooperation with the LOTUS laboratory, we got the dataset from the Vietnam Ministry of Natural Resources and Environment (MONRE), which we used for calibrating the model. Dissolved and

particulate organic carbon sampling data was provided by the Institute of Natural Product Chemistry (INPC, contacts: Thi Phuong Quynh Le), a lab under Vietnam Academy of Science and Technology (VAST); also some sampling values could be found in the thesis annexes of Thi Ha Dang, 2006.

In order to better understand the Red River basin, a trip to Hanoi was funded by the LOTUS. A meeting was hosted by the LOTUS there, aiming to introduce the project and build connections with all the participate researchers. We presented the initial results in this meeting. Researchers who had been working there for years took us to have a look at the Red River basin around Lao Cai, Hoa Binh and Son Tay and shared their knowledge about this basin. These field trips are helpful for me to have an insight of the actual characteristics of the Red River basin and in the process of modelling steps.

With these above contexts, this work was able to carry on.

List of Figures

List of Tables

List of Abbreviations

Q: Discharge

SS: Suspended Sediment

SSC: Suspended Sediment Concentration

CSS: Concentration de Sédiments en Suspension (in French)

SF: Sediment Flux

FS: Flux de Sédiment (in French)

SE: Soil Erosion

SSY: Specific Sediment Yield

SOC: Soil Organic Content

OC: Organic Carbon

DOC: Dissolved Organic Carbon

DOC: Carbone Organique Dissous (in French)

POC: Particulate Organic Carbon

COP: Carbone Organique Particulaire (in French)

TOC: Total Organic Carbon

COT: Carbone Organique Total (in French)

SWAT: Soil and Water Assessment Tool

HRU: Hydrologic Response Unit

DEM: Digital Elevation Model

TRMM: Tropical Rainfall Measuring Mission

CFSR: Climate Forecast System Reanalysis

LOADEST: LOAD ESTimator

NSE: Nash- Sutcliffe Efficiency

FAO: Food and Agriculture Organization of the United Nations

MONRE: Vietnam Ministry of Natural Resources and Environment

LOTUS: Land-Ocean-aTmosphere regional coUpled System study center

IRD: L'Institut de Recherche pour le Développement (in French)

VAST: Vietnam Academy of Science and Technology

INPC: Vietnam Institute of Natural Product Chemistry

Résumé Etendu

La ressource en eau et sa disponibilité attirent l'attention mondiale. La quantité des ressources en eau par habitant est insuffisante en Asie (en particulier dans le sud et le sud-est de l'Asie). L'urbanisation rapide et les activités agricoles intensives se produisent dans les pays en voie de développement d'Asie du Sud-Est, ce qui accroît par conséquent l'utilisation et les prélèvements d'eau. Cependant, les prélèvements d'eau abondants pour l'irrigation et l'utilisation urbaine peuvent avoir des impacts sur les écosystèmes liés à l'eau. Pour faire face à la demande croissante en eau face à des variations climatiques incertaines, des barrages ont été construits dans le monde entier pour le stockage de l'eau. Le développement futur de l'hydroélectricité est principalement concentré dans les pays en voie de développement et les économies émergentes de l'Asie du Sud-Est.

Le réseau fluvial joue un rôle essentiel dans le cycle hydrologique mondial. C'est un lien entre les écosystèmes terrestres et marins, la transformation et le transport des sédiments et des nutriments vers les océans. Le débit des rivières est le résultat d'une série de processus contribuant au cycle hydrologique. Par conséquent, il est de la plus haute importance de comprendre les changements dans le débit des fleuves sous ses facteurs d'influence. En Asie, il existe de nombreuses grandes rivières et fleuves parmi les plus grands au monde en termes de longueur, de superficie de bassin drainé et de volume annuel. Ces grands bassins fluviaux asiatiques présentent certaines caractéristiques importantes, telles que l'influence de la mousson, la diminution des glaciers dans les têtes de bassin, des barrages intensifs, des méga-deltas densément peuplés. Les variations climatiques, notamment les températures et les précipitations, ont des effets sur les systèmes fluviaux à court et à long terme, tels que les inondations et les sécheresses causées par les typhons et El Nino et La Nina, en particulier sous les tropiques. Dans la majeure partie de la zone Asiatique, les précipitations sont importantes lors de la mousson. La quantité de précipitation varie considérablement d'une année sur l'autre en fonction de la force des moussons et de la quantité de vapeur d'eau transportée, ce qui entraîne de grandes fluctuations de débits au cours de l'année. Les précipitations ont diminué dans certaines parties de l'Asie méridionale, en particulier depuis les années 1970.

En conséquence, l'effet des barrages couplé à la variabilité climatique ont un impact sur le régime hydrologique et sur les flux de matières, principalement de matières en suspension. Il a été estimé que plus de 40% du débit mondial des rivières est intercepté par les retenues et plus de 50% du piégeage des sédiments. Le transport des matières en suspension par les rivières et fleuves est une conséquence des processus d'érosion. Le processus de transport des matières en suspension par les rivières et fleuves amène également des éléments nutritifs vers les mers et les océans, processus essentiel du cycle biogéochimique et de la diversité du milieu marin. Le transport associé aux matières en suspension représente plus de 90% du flux total d'éléments tels que les nutriments et les métaux transmis par les cours d'eau, et

environ 43% du transport total de carbone organique des terres vers les océans par les fleuves est sous forme particulaire. Les flux de sédiments fluviaux sont sensibles à de nombreuses influences, allant des activités humaines aux facteurs naturels. Les perturbations humaines peuvent provenir de l'occupation du sol tels que l'érosion des sols suite à la déforestation ou la période d'inter-cultures et pour la partie du chenal de la construction de réservoirs, le captage d'eau et l'extraction de sable. Les facteurs naturels peuvent provenir du climat tels que la mousson, les typhons et l'intensité des précipitations, ainsi que les activités géologiques telles que les tremblements de terre et les glissements de terrain. Comprendre comment les facteurs d'influence agissent sur différentes sources constitue une base, et un travail important pour l'étude du transport de la charge sédimentaire.

Le carbone organique est important pour les organismes hétérotrophes riverains et côtiers. Le carbone organique fluvial provient principalement de trois sources: (1) la source allochtone, d'origines terrestres, telles que l'altération des roches, la lixiviation du sol et les produits décomposés tels que les tissus des plantes terrestres; (2) la source autochtone, provenant de la production primaire au sein même du fleuve, telle que les algues et le phytoplancton; (3) les influences anthropiques des activités agricoles, domestiques et industrielles peuvent également être considérées comme une source allochtone. La teneur en carbone organique du sol est un facteur clé dans le contrôle de l'exportation de carbone organique fluvial (Ludwig et Probst, 1996b; Zhang et al., 2019). L'érosion et la lixiviation des sols sont d'importantes voies de transfert du carbone organique dans le réseau hydrographique. En outre, leurs flux sont également affectés par les caractéristiques du cours d'eau (débit et concentration des sédiments en suspension) et par la présence des barrages. Le climat tropical humide est associé au plus haut flux en carbone et les rivières tropicales sont essentielles pour les flux globaux de carbone organique fluvial vers les océans. Il a été constaté que les fleuves d'Asie continentale affichent les taux d'exportation spécifiques les plus élevés en terme de carbone organique dissous et particulaire (COD et COP). Cependant, les constructions du barrage ont modifié leurs exportations. La plupart des études sur l'estimation des flux de carbone organique sont basées sur des travaux à une échelle mensuelle ou annuelle. Cependant, la plupart des exportations de carbone organique ont lieu lors de périodes de crues liées à des variations journalières. Pratiquement aucune étude n'a estimé les flux de carbone organique sur un pas de temps quotidien. Les COD et les COP exportés par les fleuves tropicaux asiatiques correspondent à une grande partie de toutes les exportations de carbone organique des fleuves asiatiques. Il serait donc nécessaire d'étudier à l'échelle journalière les flux de carbone organique dans cette région afin de mieux comprendre les processus dynamiques de transport de ces éléments sous l'impact des barrages et des variations climatiques.

L'objectif principal de cette étude est de caractériser, comprendre et quantifier les flux d'eau, des matières en suspension et le carbone organique dans le bassin du Fleuve Rouge au pas de temps journalier, en tenant compte des impacts de la variabilité

climatique et des barrages. Les objectifs spécifiques sont: (1) de caractériser l'hydrologie et de quantifier la concentration en matières en suspension (CSS) et les flux (FS) du bassin du Fleuve Rouge à un pas de temps journalier; (2) évaluer les effets de la variabilité climatique et de la construction de barrages sur les débits (Q) et les sédiments de manière séparée; (3) quantifier à l'échelle journalière le carbone organique (OC) particulaire et dissous et évaluer les effets de la variabilité climatique et des barrages sur leur transfert et leur exportation vers le delta du fleuve.

Un modèle hydro-agro-environnemental à base physique, semi-distribué, SWAT, combinant des données climatiques satellitaires (température et précipitations), un modèle numérique d'élévation de terrain (DEM), une carte des sols, l'utilisation des sols et la construction de barrages, a été implémenté. Les données mesurées quotidiennement in situ de débit Q et de CSS de 2000 à 2013 ont été utilisées pour calibrer le modèle en différents points du bassin versant. Une fois le modèle calibré, il a été appliqué pour simuler deux scénarios: les conditions réelles et les conditions naturelles sans les barrages dans ce bassin. Les nouveaux barrages étant opérationnels depuis 2008, la période a été divisée en deux sous-périodes: 2000-2007 et 2008-2013, afin de quantifier séparément les impacts de la variabilité climatique et des barrages. Ensuite, les sources principales, les processus dynamiques de transfert et les flux de Q, FS et OC ont été analysés, ainsi que les impacts de la variabilité climatique et des barrages ont été identifiés et quantifiés.

Les résultats ont montré que dans le bassin du Fleuve Rouge, environ la moitié (47%) des précipitations se sont transformées en flux (697 mm). Les eaux souterraines constituent la principale composante du débit du fleuve dans le bassin du fleuve Rouge, représentant 58% du débit total. Le débit est constitué à 39% de l'écoulement de surface et à 3% de l'écoulement latéral, le reste provenant de l'écoulement des nappes. L'apport en eau des trois principaux affluents du Fleuve Rouge est de 24 km^3 an^{-1} à la station Yen Bai sur le fleuve Thao, 23 km^3 an^{-1} à la station Vu Quang sur la rivière Lo et 43 km^3 an^{-1} à la station Hoa Binh sur la rivière Da, à la sortie du bassin, la station de Son Tay possède un débit de 95 km^3 an^{-1}. 76% de la quantité totale d'eau est produite pendant la saison de la mousson du sud-ouest (de mai à octobre). La rivière Da est le principal contributeur au volume d'eau en aval du bassin, représentant 45% du volume total à Son Tay; les rivières Lo et Thao apportent à peu près le même volume d'eau en aval. Le débit moyen annuel (Q) pour la période 2000-2013 est de 3003 m^3 s^{-1} à Son Tay. Le Q moyen annuel a montré des tendances à la baisse, principalement en raison de la variabilité climatique. Les variations de précipitations et de températures ont entraîné une diminution de 13% de la quantité d'eau disponible, ainsi qu'une diminution de 4% de la teneur en eau du sol dans l'ensemble du bassin, ce qui a entraîné une diminution de 9% du Q du bassin (à la station de Son Tay) sur la période d'étude. La mise en place des barrages a également entraîné des variations sur Q: une réduction de 4% de Q à la station de Son Tay a été montrée. Les différents sous-bassins possèdent des réactions différentes à la variabilité climatique et aux barrages. En ce qui concerne la variabilité climatique pour la période de 2008-2013 à

2000-2007, celle-ci a provoqué la plus forte baisse sur le bassin de la rivière Thao (-21% à Yen Bai), suivi d'une baisse de 10% sur le bassin du Da (à la station de Hoa Binh), tandis qu'elle a entraîné une légère augmentation sur le bassin du Lo (+2% à Vu Quang). Cela est lié à la distribution des précipitations dans ce bassin: l'impact est plus important dans le sous-bassin qui possède le moins de précipitations. Concernant l'impact des barrages, l'impact le plus important a été observé sur la rivière Da (-8%), puis sur la rivière Lo (-2%), puis sur le Thao (-0.4% à Lao Cai et -0.3% à Yen Bai). Une plus grande capacité de stockage dans le barrage entraîne une diminution plus importante de Q.

La CSS dans les trois tributaires diffère énormément. La CSS annuelle moyenne de Lao Cai, de Yen Bai, de Vu Quang, de Hoa Binh et de Son Tay pour la période 2000-2013 est respectivement de 1057, 1003, 172, 57 et 228 mg L^{-1}. Le fleuve Thao a la CSS la plus élevée, suivie par la rivière Lo ; et la rivière Da possède la CSS la plus basse à son exutoire. La CSS moyenne annuelle de 2008-2013 est bien inférieure à celle de 2000-2007. La construction des barrages en 2008 a retenu les particules les plus grossières dans les réservoirs et a modifié la distribution granulométrique en aval; les barrages ont également réduit la dynamique du transport des sédiments en suspension vers l'aval, entraînant une modification de l'érodibilité du canal. En raison des impacts de la variabilité climatique sur le Q et le SSC, les flux de sédiments (SF) ont par conséquent présenté des variations. La SF moyenne annuelle pour 2000-2013 à Lao Cai, à Yen Bai, à Vu Quang, à Hoa Binh et à Son Tay est respectivement de 30,7, 39,8, 6,6, 3,6, et 33,0 Mt^{-1} an^{-1} .90% des exportations annuelles de matières en suspension ont eu lieu pendant la période de mousson du sud-ouest (mai-oct). Le Thao est le plus gros exportateur de FS vers l'aval, tandis que la rivière Da en fournit le moins. Bien que la rivière Da ait un Q supérieur à Hoa Binh par rapport au fleuveThao à Yen Bai, la SSC de la rivière Da est beaucoup plus faible que le fleuve Thao en raison de la rétention des sédiments par les énormes barrages, ce qui a entraîné une exportation moindre de FS sur le Da. Comparativement aux FS de 2000-20007 par rapport à 2008-2013, les flux sont passés de 49,1 à 11,6 Mt an^{-1} à Son Tay. Les baisses de FS ont significativement été impactées par les barrages (-80%). Une plus grande capacité de barrage a entraîné une diminution plus importante des FS. L'impact de la variabilité climatique durant la période de 2008-2013 comparée à 2000-2007 a entraîné une diminution de 10% des FS à Son Tay. Au cours de la période 2000-2013, sans impact des barrages, le bassin du Fleuve Rouge aurait dû fournir un flux spécifique de sédiments de 779 t km^{-2} an^{-1}, ce qui est supérieur à celui d'autres bassins asiatiques avant la construction de barrages (tels que le Yangtze, le Pearl et le Mékong). Cependant, avec la mise en place de nouveaux barrages, le flux spécifique de matière en suspension de 2008-2013 a diminué jusqu'à 85 t km^{-2} an^{-1}. L'érosion annuelle moyenne des sols dans ce bassin est de 5,5 t ha^{-1} an^{-1}. Cependant, les zones critiques (situées au milieu du bassin du Thao et de la partie inférieure du bassin du Da) peuvent provoquer des érosions de sol supérieures à 20 t ha^{-1} an^{-1}. Les précipitations, les pentes et les pratiques agricoles sont les facteurs clés de l'érosion

des sols dans le bassin du Fleuve Rouge. Une relation entre Q mensuel et FS a été établie à chaque station afin de fournir aux gestionnaires et/ou scientifiques une méthode simple pour estimer le SF mensuel sans utiliser le modèle SWAT.

Les résultats de ces deux scénarios ont ensuite été traités pour calculer à l'échelle journalière les concentrations et les flux de COD et de COP. Premièrement, les équations mathématiques pour le calcul des concentrations de COD et de COP ont été calibrées sur la base des données journalières de Q, CSS et des données discrètes de COD et de COP observées de 2003 à 2013. Des simulations de Q et CSS ont ensuite été utilisées pour quantifier les flux de COD et de COP dans les conditions réelles et naturelles afin d'évaluer les impacts potentiels de la variabilité climatique et des barrages sur les exportations de carbone organique.

Nous avons utilisé des équations simples reliant COD à Q et COP à CSS. Les paramètres de ces équations sont liés à la teneur moyenne en carbone organique du sol de la zone de drainage (pour COD et COP), au débit Q (pour COD) et à la concentration en Chlorophylle-a (pour COP). Les relations entre les paramètres et ces variables (la teneur en carbone organique du sol, la concentration en Q et la concentration en Chl-a) permettent d'évaluer les paramètres, puis de calculer les concentrations de COD et de COP à n'importe quel point de ce bassin. Les exportations annuelles moyennes de COD en 2003-2013 sont de 222 kt an^{-1} à Son Tay, ce qui représente 0,26% du transport total de COD des fleuves asiatiques; et l'exportation annuelle moyenne de COP entre 2003 et 2013 est de 406 kt an^{-1} à Son Tay, ce qui représente 0,37% des exportations totales de COP par les fleuves asiatiques. A Son Tay, 85% des exportations totales de COD et 88% des exportations totales de COP ont lieu pendant la saison de la mousson du sud-ouest (de mai à octobre). Comparés à d'autres fleuves asiatiques et tropicaux, les flux de COD et de COP exportés par le Fleuve Rouge ne sont pas très importants, en particulier pour le COP. Cependant, en comparant les flux spécifiques de carbone organique, le bassin du Fleuve Rouge possède des valeurs élevées de COD et de COP. Le flux élevé en COD provient de la forte lixiviation du sol et des roches, tandis que le flux spécifique élevé en COP provient de la forte érosion du sol et de la concentration élevée de matières en suspension.

Dans des conditions naturelles (sans barrages), à la sortie (Son Tay), en raison de la variation de Q induite par la variabilité climatique, le flux de COD a augmenté de 1% entre 2008 et 2007 par rapport à 2003-2007, et la principale inondation de 2008 est un des facteurs importants. Une réduction de 13% des flux de COD est liée aux activités des barrages qui régulent les débits pendant les saisons des pluies. Les flux de DOC sous les conditions naturelles entre 2003-2007 et 2008-2013 ont peu varié (-2%), ce qui indique que la variabilité climatique a peu d'impact sur les flux de COD, tandis que la construction de barrages a entraîné une diminution de 85% du flux de COP. À la sortie (Son Tay), le flux de COP en 2008 n'est que de 45% comparé à 2007 bien que 2008 soit une année d'inondation. Une diminution drastique des flux de SSC et de

sédiments s’est produite la même année. Le transfert de COP a été affecté en conséquence après la construction du barrage. Avec la construction et l'exploitation de nouveaux barrages, le rapport de composition du COT a changé, passant de dominante COP à dominante COD. En outre, les variations dynamiques du COP/COT ont également été modifiées par l’effet des barrages. Avant la construction de nouveaux barrages, le rapport COP/COT était bas autour de mars et était élevé en saison des pluies. Cependant, après la mise en eau de nouveaux barrages, en juin et juillet, ils remplissent des fonctions de contrôle des inondations, de rétention d'eau et de SS, de sorte que le rapport COP/COT est devenu faible pendant la saison des crues. Vers le mois de mars, les barrages rejettent de l'eau pour l'irrigation, tandis que le SS est également libéré, ce qui induit une teneur élevée en COP/COT.

En résumé, les proportions de débit exporté, des flux de SS et de COP provenant du Fleuve Rouge sont faibles par rapport aux autres grands fleuves asiatiques. Cependant, ses flux spécifiques sont élevés en comparaison. Le CSS élevé dans le fleuve Thao et la forte érosion dans la partie centrale du bassin sont les principaux contributeurs au flux spécifique élevé en SS et en COP. La variabilité climatique et la construction de barrages ont montré des impacts sur ce bassin, bien que la réponse de chaque sous-bassin diffère. Le climat a principalement affecté les débits: la diminution des précipitations a eu des impacts plus importants sur les débits du bassin supérieur. Les constructions de barrages ont eu des impacts importants principalement sur les SS et les COP. Les exportations de SS et de COP dans le delta ont donc fortement diminué en raison de la mise en place des nouveaux barrages sur le Fleuve Rouge. La diminution des COP a modifié le rapport COP/COT. Ces changements de SS et d'OC pourraient avoir un effet sur la fonction biogéochimique du delta et des zones côtières en aval.

Les futures études sur l'azote, le phosphore et les pesticides peuvent être poursuivies sur la base de ce modèle. Ce modèle permet également de réaliser des scénarios de changements globaux, tels que les changements climatiques, l'utilisation de la terre, la mise en place de nouveaux barrages. En outre, ce modèle peut être associé à un modèle delta, puis à un modèle marin pour étudier les impacts des changements globaux sur la fonction biochimique de la côte.

Extended Abstract

Water resource and its availability attract global attention. The amount of water resources per inhabitant is deficient in Asia (especially the South and Southeast Asia), and it is the least among the continents. Rapid urbanisation and intensive agricultural actives are happing in developing countries in Southeast Asia which consequently will increase the water use and withdrawals. However, abundant water withdrawals for irrigation and urban use can cause impacts on water-related ecosystems. To face the challenge of increasing water demand under uncertain variations of climate, dams have been built globally for water storage. Future hydropower development is primarily concentrated in developing countries and emerging economies of Southeast Asia.

River network plays a critical role in the global hydrological cycle. It is a link between terrestrial and marine ecosystems, processing and transporting sediments and nutrients to oceans. River flow is a result of a suite of processes contributing to the hydrological cycle. Therefore, understanding changes in river flow under its influence factors is of utmost importance. In Asia, there are many large rivers which are among the largest in the world in terms of length, basin area and annual volume. These large Asian river basins have some special and important features such as monsoon impacts, glacier shrinkage in the headwaters, intensive damming, densely populated mega deltas. Climate variations, particularly temperature and precipitation, have effects on river systems both at short and long time scales, such as floods and droughts caused by typhoons and El Nino and La Nina, especially in the tropics. In much of Asia area, the main influence factors affecting river flow is the monsoon precipitation. The amount of rainfall varies greatly from year to year depending on the strength of the monsoonal flows and the amount of water vapour transported, which leads to large interannual river flow fluctuations. Precipitation has decreased in parts of southern Asia, especially since the 1970s.

As a consequence, dams coupled to climate variability have an impact on water regime and fluxes of matters, mainly suspended sediment (SS). It was estimated that more than 40% of global river discharge is intercepted by the large impoundments, and greater than 50% of potential sediment trapping by dams in regulated basins. The SS transportation by rivers is a key component of the global denudation system. It can measure the rate of denudation of the continents and the erosion processes. The transportation process of suspended sediment by rivers also drives nutrients to the seas which is an essential process for marine biogeochemical cycle and diversity. Sediment-associated transport accounted for more than 90% of the total river-borne flux of elements such as nutrients and metals, and around 43% of the total transport of organic carbon from the land to the oceans by rivers is in particulate form. River sediment fluxes are sensitive to many influences, from human activities to natural effects. Human disturbances can come from landscape such as soil erosion, and from the channel part such as reservoir construction, water abstraction and sand excavation. Natural factors can come from climates such as monsoon, typhoon and rainfall

intensity, geological activity such as earthquake and landslide. Understanding how the influencing factors effecting on different sources would be a base but important work for studying sediment load transportation.

The organic carbon is important to riverine and coastal heterotrophic organisms. Riverine organic carbon mainly comes from three sources: (1) the allochthonous source, which is based on terrestrial origins, such as weathering from rocks, leaching from soil and the decomposed products like the tissue of plants on land; (2) the autochthonous source, which derives from primary production within the river itself, such as from algae and phytoplankton; (3) anthropogenic influences from agricultural, domestic and industrial activities can also be regarded as an allochthonous source. Soil organic carbon content is a key factor controlling the export of riverine organic carbon (Ludwig and Probst, 1996b; Zhang *et al.*, 2019), and soil erosion and leaching are important pathways for organic carbon entering into the river system. Besides, their fluxes are also affected by river conditions (flow and suspended sediment concentration) and dams. The humid tropical climate is associated with the highest carbon yield and tropical rivers are critical to total global fluvial organic carbon fluxes. It was found that rivers in mainland Asia have the highest specific export rates in terms of dissolved and particulate organic carbon (DOC and POC). However, the dam constructions have altered their exports. Most studies on organic carbon fluxes estimation were based on a monthly or an annual scale. However, most organic carbon export happens during flood events linked to daily discharge variations. Hardly any study estimated organic carbon fluxes on a daily time step. The DOC and POC exported by Asian tropical rivers take a large portion of the whole Asian rivers organic carbon exports, and it would be necessary to study the organic carbon fluxes in this region at a daily time step in order to better understand the transport dynamic processes under impacts of dams and water regime variations.

The main goal of this study was to assess the water regime, suspended sediment and organic carbon through the Red River basin based on daily time step, considering the impacts of climate variability and dams. Specific objectives are: (1) to characterize the hydrology and to quantify the suspended sediment concentration (SSC) and fluxes (SF) of the Red River basin at a daily time step; (2) to assess the impacts of climate variability and dam constructions on discharge (Q) and sediment in a separate way; (3) to quantify DOC and POC fluxes at a daily time step and to assesses the impacts of climate variability and dams on their transfer and export to the delta.

A physical-based hydro-ago-environmental model, the Soil and Water Assessment Tool (SWAT), combining with satellite climate data (temperature and rainfall), digital elevation model (DEM), soil map, land use and dam implementations, was used to set up the model, and in-situ daily measured data of discharge Q and SSC from 2000 to 2013 were used to calibrate the model. Once the model was calibrated, it was applied to simulate two scenarios: actual conditions which presented the real scene that happened in the Red River basin; natural conditions which removed the dams within

this basin. The new dams were operation since 2008, therefore, the period was divided into two sub-periods: 2000-2007 and 2008-2013, in order to disentangle and quantify the impacts of climate variability and dams. Then the main sources, the transfer dynamic processes and fluxes of Q, SF and OC were analysed, and the impacts of climate variability and dams were disentangled and quantified.

The results showed that for the Red River basin, around half (47%) of the rainfall turned into the streamflow (697 mm yr^{-1}). The groundwater is the main component for the river flow in the Red River basin, accounting for 58% of the total streamflow. 39% of the streamflow formed the surface runoff and 3% was the lateral flow. The water yield of the three main tributaries of the Red River was 24 km^3 yr^{-1} at Yen Bai station on the Thao River, 23 km^3 yr^{-1} at Vu Quang station on the Lo River and 43 km^3 yr^{-1} at Hoa Binh station on the Da River, respectively; while the water yield at the outlet of the continent basin, Son Tay station, was 95 km^3 yr^{-1}. 76% of the total water yielded during the southwest monsoon seasons (May to October). The Da tributary was the main contributor to the downstream water volume, accounting for 45% of the total volume at Son Tay; the Lo and Thao rivers contributed nearly the same water volume to the downstream. The annual mean discharge (Q) during 2000-2013 was 3003 m^3 s^{-1} at Son Tay. The annual mean Q showed decreasing tendencies mainly due to climate variability. The variations of rainfall and temperature resulted in a 13% decrease of available water with a 4% decrease of soil water content through the whole basin which consequently caused a 9% decrease of the Q for the basin (at Son Tay station). Dams regulations also caused variations on Q: a 4% decrease of Q at Son Tay station was founded. The different sub-basin had different responses to climate variability and dams. For climate variability, compared 2008-2013 to 2000-2007, it caused the largest decrease of Q on Thao river basin (-21% at Yen Bai) following by a 10% decrease on Da basin (at Hoa Binh station) while it induced a slight increase at Lo basin (+2% at Vu Quang). This can relate to the rainfall distribution within this basin: the impact is greater in the sub-basin with less rainfall. For the impact of the dams, the largest impact was on the Da river (-8%), then the Lo river (-2%), and then the Thao river (-0.4% at Lao Cai and -0.3% at Yen Bai). Larger dam capacity caused a larger decrease on Q.

SSC in the three tributaries differs a lot. The mean annual SSC during 2000-2013 at Lao Cai, Yen Bai, Vu Quang, Hoa Binh and Son Tay was 1057, 1003, 172, 57 and 228 mg L^{-1} respectively. The Thao River has the highest SSC, following by the Lo River, and the Da River has the lowest SSC at its outlet. The annual mean SSC of 2008-2013 was much lower compared to 2000-2007. Dam construction retained the coarser particles in the reservoir and altered the downstream particle size distribution; the damming also decreased the dynamics of downstream suspended sediment transport, leading to a change in the channel erodibility. Due to the impacts of climate variability on Q and SSC, sediment fluxes (SF) consequently showed variations. Mean annual SF during 2000-2013 at Lao Cai, Yen Bai, Vu Quang, Hoa Binh and Son Tay was 30.7, 39.8, 6.6, 3.6, 33.0 Mt yr^{-1}, respectively. 90% of the annual sediment export happened during the southwest monsoon period (May-Oct). The Thao River exported the most

SF to downstream while the Da River delivered the least SF. Though the Da River has a higher Q at Hoa Binh than the Thao River at Yen Bai, the SSC of the Da River was much smaller than the Thao River due to the sediment retention by huge dams, resulting in a lower SF export on the Da River. Compared SF during 2000-20007 to 2008-2013, it decreased from 49.1 to 11.6 Mt yr^{-1} at Son Tay. The decreases in SF was significantly contributed by dams (-80%). Larger dam capacity caused a larger decrease in SF. A great quantity of sediment retention in the reservoir should be paid attention by management. The impact of climate variability caused a 10% decrease at Son Tay compared 2008-2013 to 2000-2007. During 2000-2013, without impacts of dams, the Red River basin should have yielded 779 t km^{-2} yr^{-1} specific sediment yield (SSY), which is higher compared to other Asian basins during pre-damming periods (such as the Yangtze, Pearl and Mekong). However, with new dams implementations, the SSY of 2008-2013 decreased to 85 t km^{-2} yr^{-1}. The mean annual soil erosion in this basin was 5.5 t ha^{-1} yr^{-1}. However, hot spots (located in the middle of the Thao basin and the down part of the Da basin) soil erosion could reach above 20 t ha^{-1} yr^{-1}. Precipitation, slope and agriculture practice are the key factors for soil erosion in the Red River basin. A relation between monthly Q and SF was established at each station in order to provide the stakeholders with an easy method to estimate the monthly SF without using the SWAT model.

The outputs from these two scenarios were then used to calculate the DOC and POC concentration and fluxes on a daily step. First, the equations for calculating the DOC and POC concentrations were calibrated based on observed daily Q, SSC and discrete DOC and POC data from 2003-2013. Then, simulated Q and SSC were used to quantify the DOC and POC fluxes under actual and natural conditions for evaluating the potential impacts of climate variability and dams on organic carbon exports.

We used simple equations that related DOC with Q and POC with SSC. The parameters of these equations are linked to the average soil organic carbon content of the drainage area (for both DOC and POC), the mean annual Q (for DOC) and the Chl-a concentration (for POC). The relations between the parameters and those variables (the soil organic carbon content, the Q and the Chl-a concentration) allow people to evaluate the parameters and then to calculate the DOC and POC concentrations at any point within this basin. The mean annual export of DOC during 2003-2013 was 222 kt yr^{-1} at Son Tay, which represented 0.26% of the total Asian rivers DOC transport; and the mean annual export of POC during 2003-2013 was 406 kt yr^{-1} at Son Tay which accounted for 0.37% of the total POC export by the Asian rivers. At Son Tay outlet, 85% of the total export of DOC and 88% of the total export of POC happened during the southwest monsoon seasons (from May to October). Compared to some other Asian and tropical rivers, the export of DOC and POC fluxes through the Red River was not high, especially for POC. However, when comparing the specific organic carbon yields, the Red River basin yielded high DOC and POC values. High DOC yield of the Red River basin comes from the high leaching from soil and rocks while the high POC yield is contributed from high soil erosion and high suspended sediment

concentration.

Under natural conditions (without dams), at the outlet (Son Tay), due to the Q variation induced by climate variability, the DOC flux during 2008-2013 increased 1% compared to 2003-2007, and the flood year 2008 was the main contributor. A 13% reduction of DOC flux was related to dam operations which regulated the discharge during flood seasons. POC fluxes under natural conditions between 2003-2007 and 2008-2013 varied little (-2%) which indicated that climate variability had little impacts on POC fluxes, while the dam constructions caused an 85% decrease in POC flux. At the outlet (Son Tay), the POC flux in 2008 was only 45% of that in 2007 even though 2008 is a flood year. A drastic decrease in SSC and sediment fluxes occurred in the same year. The POC transfer was affected consequently after dam constructions. With the construction and operation of new dams, the composition ratio of TOC changed, from POC-dominating to DOC-dominating. Besides, the dynamic variations of POC/TOC were also changed by dam regulation. Before new dam constructions, the POC/TOC ratio was low around March and high in flood season. However, after new dams impounded, during June and July, the dams fulfil flood-control functions, retaining water and SS, therefore the POC/TOC ratio became low during the flood season. And around March, dams discharge water for irrigation, SS is released too, which induces high POC/TOC.

The proportions of the export of water volume, SS and POC fluxes from the Red River were low compared to other large Asian rivers. However, its specific yields were high. High SSC in the Thao river and high erosion in the middle part of the basin are the main contributors for the high specific yield of SS and POC. The climate variability and dam constructions had shown impacts on this basin, though the response of each sub-basin differed. Climate mainly affected discharge: precipitation decrease had larger impacts on discharge for the upper basin. Dam constructions showed large impacts mainly on SS and POC. SS and POC exported to the delta decreased sharply due to the impoundments of the new dams on the Red River. The decreasing of POC altered the POC/TOC ratio. These changes of SS and OC might have an effect on the biogeochemical function for the downstream delta and coastal areas.

Future studies of nitrogen, phosphorus and pesticide can be carried on based on this model. Also, scenarios of global changes, such as climate changes, land use changes, new dam implementations, can be done by this model. Furthermore, this model can be coupled with a delta model, and then with sea model to investigate the impacts of global changes on the biochemical function in the coast.

Chapter 1

Scientific Context and Objectives

1. CHAPTER Ⅰ: Scientific Context and Objectives

1.1. Water Regime

1.1.1. Water resources worldwide

Water resource and its availability attract global attention. Through the report from the Food and Agriculture Organization of the United Nations (FAO, 2003a), it estimated that the total water resources in the world were about 43,750 km^3 yr^{-1}; at the continental level, America has the largest share of the world's total freshwater resources, account for 45%, followed by Asia (28%), Europe (15.5%) and Africa (9%). In terms of resources per inhabitant in each continent, America has 24,000 m^3 yr^{-1}, Europe 9,300 m^3 yr^{-1}, Africa 5,000 m^3 yr^{-1}, and Asia 3,400 m^3 yr^{-1}. Figure 1-1 demonstrated internal renewable water resources per inhabitant worldwide in 2014.

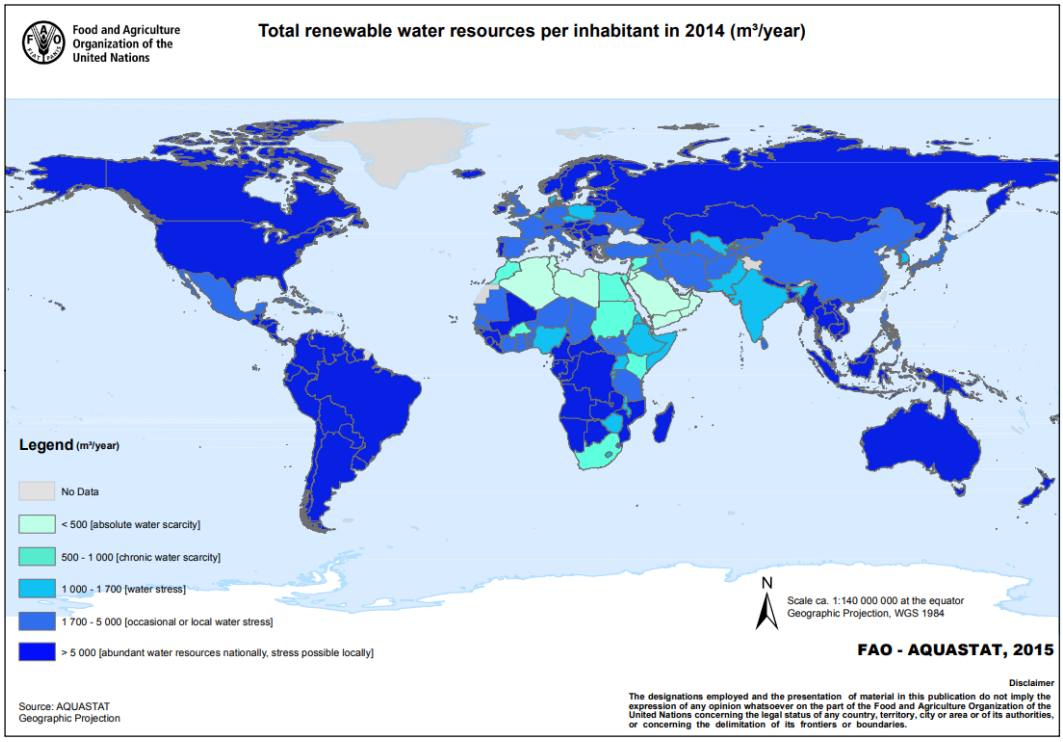

Figure 1-1 World map of total renewable water resources per inhabitant in 2014 (http://www.fao.org/nr/water/aquastat/maps/TRWR.Cap_eng.pdf).

Freshwater scarcity has become a global and local dramatic threat to the sustainable development of human society due to the steadily increasing demand (Mekonnen and Hoekstra, 2016). The main driving forces for the rising global water demand are growing world population, improving living standards, a shift of consumption patterns and expansion of irrigated agriculture (Ercin and Hoekstra, 2014). The continuous increasing water demand is growing faster than the demographic increase, bringing the water crises as the largest global risk in terms of potential impact (World Economic Forum, 2015). Water demand and availability spatially and temporally vary greatly, leading to water scarcity in several parts of the world during specific times of the year (Mekonnen and Hoekstra, 2016). About 66% of the global population, about 4 billion

people, lives under severe water scarcity at least 1 month of the year (Mekonnen and Hoekstra, 2016).

Large water consumption relative to water availability results in decreased river flows, mostly during the dry period, and declining lake water and groundwater levels, which can threaten biodiversity, salinization of soil and groundwater resources (FAO, 2011a).

1.1.2. Water resources and consumptions in Asia

From the report of FAO (2003a, 2011b), we can see that the water resources in Asia are relatively abundant while Asia represents 16% of the world's land surface, receives 22% of its precipitation and produces 27% of its water resources. However, 55% of the world's population is also living in Asia, and population densities in South and Southeast Asia are among the highest in the world. The amount of water resources per inhabitant is deficient, about half the world average, and it is the least among the continents.

Figure 1-2 showed the total renewable water resources per inhabitant for each Asian country in 2011. Though countries like Thailand, Laos, Cambodia and Vietnam have the water resource per inhabitant above the average value of the whole Asian, over 40% of their renewable water resource depends on other countries (FAO, 2003a, 2011b). The withdrawals in the upstream country can affect significantly the volumes of water available to the downstream country. Southeast region is characterized by a zone in which shared river basins play a critical role and make the computation of water resources relatively complex. Large inconsistencies were noted when comparing the flow at borders as recorded by neighbouring countries, e.g. the runoff of the main rivers flowing from China to downstream countries (India, Cambodia and Laos).

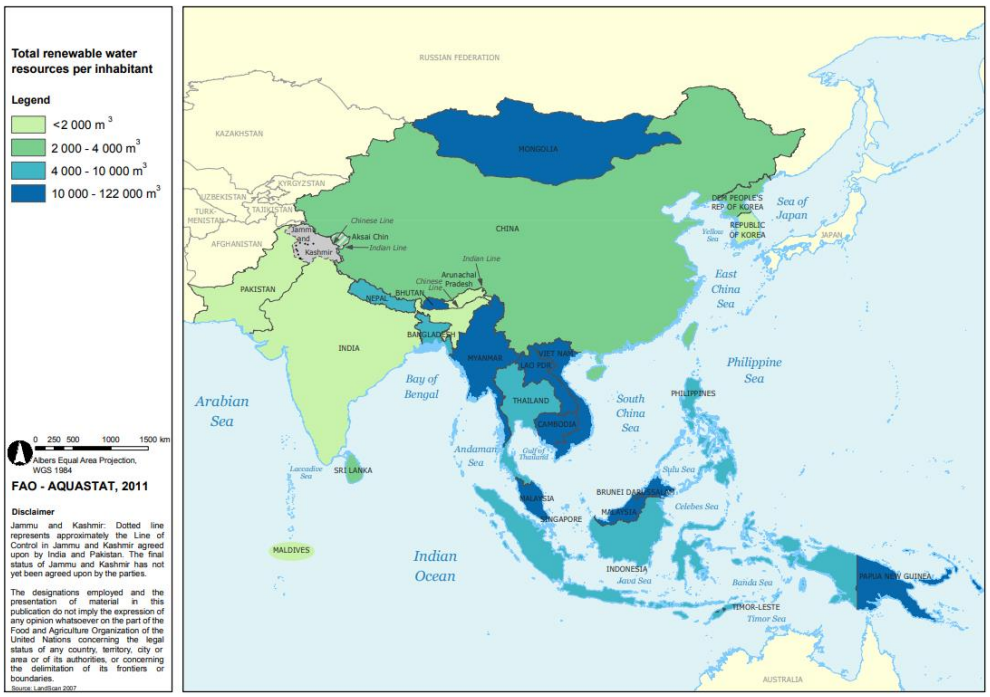

Figure 1-2 Total renewable water resources per inhabitant in Asia (FAO, 2011b).

Water resource distribution in the Southern and Eastern Asia region varies due to the large range of climates (uneven distribution of rainfall, Figure 1-3), which results in different water use conditions. The hydrology of the region is dominated by the typical monsoon climate, which induces large inter-seasonal variations in river flows. Due to the southwest monsoon influence, from May to October is the rainy season in the Southern and Eastern Asia, abundant annual rainfall occurring, and water is mainly produced in this period. Spatial and temporal uneven distribution cause different basins suffering from different water issues. Flood control is the main concern in the humid areas, such as in the Mekong, Red, Brahmaputra and Ganges basins, while water resource assessment is the major problem in the arid areas such as central China. Without flow regulation, water resource is abundant during flood seasons when it is usually less needed. Around 70-90% of the total annual flow occurs during rainy seasons. Therefore, the average annual values of river flows cannot well present the available water resources for use. Water resources available for use should include figures on low flow. The amount of water readily available for use is between 10-20% of the total renewable water resources in the absence of storage (FAO, 2003a). Mekonnen and Hoekstra (2016) assessed global water scarcity on a monthly basis, and from their results, south-east Asian was facing severe water scarcity from January to June when are the irrigation seasons.

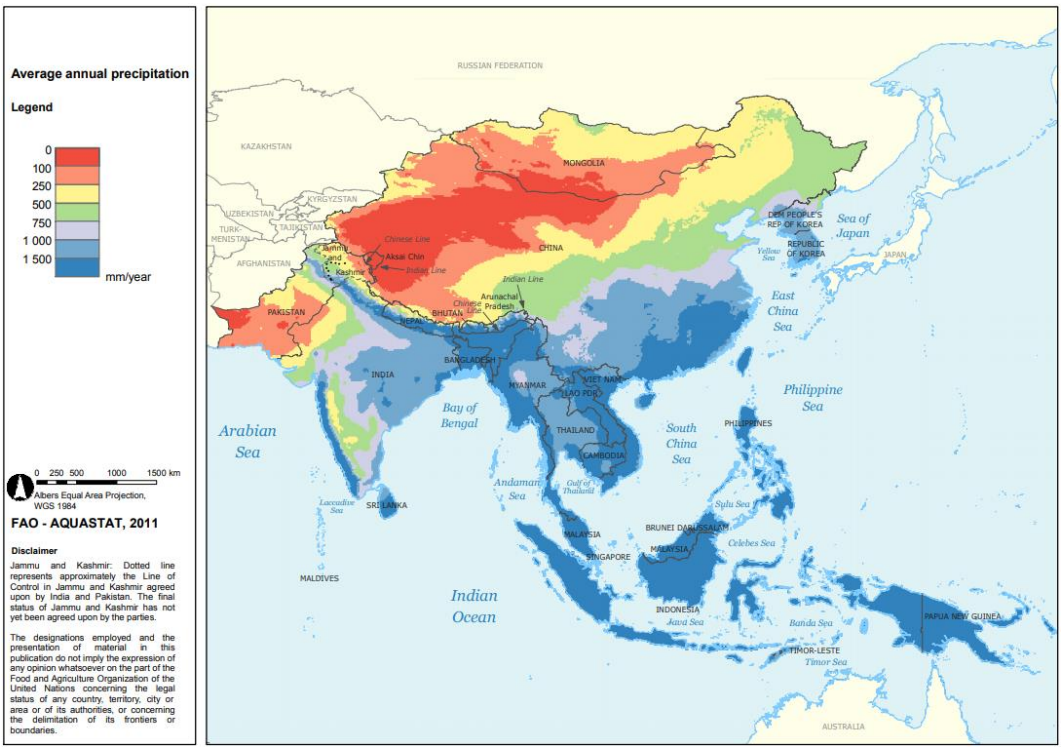

Figure 1-3 Average annual precipitation (FAO, 2011b).

Furthermore, under climate change and variability, impacts on water resource are expected to be significant, with projected increases in water stress already pronounced by 2050 (FAO, 2011a). In South-East Asia, extreme weather events associated with El Niño have been reported to be more frequent and intense in the past years (Bates

et al., 2008). Impacts of climate change on seasonality and amount of water flow from river systems are expected (Bates *et al.*, 2008). Climate change affects water systems by sea-level rise, higher frequency of cyclones (Eastern and Southeast Asia), increased the incidence of floods and low flows (FAO, 2011a). Deltas and coastal areas will be doubly at risk of flooding from sea-level rise and more variable wet-season rainfall.

1.1.3. Water quality in Asia (especially in China and Vietnam)

The growing population, industrialization and agricultural development have altered water quality in Asia, and water quality issue might be exacerbated by climate change in Asia (Park *et al.*, 2010; Evans *et al.*, 2012), though the overall impact of climate change on water quality will be marginal compared to socioeconomic changes (Hanjra and Qureshi, 2010; Evans *et al.*, 2012). In many developing and underdeveloping areas in Asia, inadequate sanitation facilities, sewerage and wastewater treatment result in quantities of wastewater reaching water bodies. 40% of the global death toll due to unsafe or inadequate supply of water, sanitation, and hygiene occurs in Asia (Evans *et al.*, 2012).

Besides, non-point source pollution is also of concern. South and Southeast Asia is predominantly an agrarian society. Agricultural non-point source is considered a significant threat to water quality in this region, especially considering the rise in agrochemical consumption. Three main forms of agricultural nonpoint sources have been identified: sediments; nutrients such as carbon (C), nitrogen (N) and phosphorus (P); pesticides (Valcu, 2013). High sediment loads is a common feature in many Asian basins due to the pronounced topography of the region, especially the basins originating from the Himalayan-Tibetan Plateau, such as the Mekong, the Red, the Yangtze and the Yellow rivers (Milliman and Syvitski, 1992; Ludwig and Probst, 1998; Evans *et al.*, 2012).

Nutrients such as C, N and P are key elements in biogeochemical processes, however, excessive inputs of these nutrients can significantly accelerate the processes of eutrophication, deteriorating water quality. River export of dissolved nutrients to the seas increased considerably in China during 1970-2000, and anthropogenic sources have become increasingly important, in particular nutrients losses from agriculture: more than 50% of the dissolved N and P in Chinese rivers are from agriculture. (Qu and Kroeze, 2012). The main rivers of China exported total N and P into coastal waters in 2012 was 3.1 and 0.3 Mt yr^{-1}, respectively: the Yangtze River was the largest riverine nutrient source for the coastal waters, and its riverine N and P export in 2012 was 2.0 and 0.2 Mt yr^{-1}, respectively; and the Yellow River exported riverine N and P was 0.02 and 0.0013 Mt yr^{-1}, respectively; the Pearl River exported riverine N and P was 0.8 and 0.03 Mt yr^{-1}, respectively (Tong *et al.*, 2015). The total DOC flux exported by the Yangtze, Yellow and Pearl rivers into the China Sea to be approximately 2.73 Mt yr^{-1} (Shi *et al.*, 2016). In Southeast Asia, the population concentrates mostly in large deltas where anthropogenic pressure is very high, leading to N and P pollution by agriculture,

industries, and domestic effluents, most often released with no treatment (Luu *et al.*, 2012). The riverine delivery total N and total P through the Red River was 0.1-0.2 and 0.03-0.05 Mt yr^{-1} (Le et al., 2005; Luu et al., 2012). In China, the food security is a national priority due to the big population and lead to the widespread application of pesticides on farmland (Ouyang *et al.*, 2016), which makes China one of the largest producers and consumers of pesticides in the world today (Grung *et al.*, 2015). Total pesticide loss in China was estimated about 4.39×10^3 t in 2011 (Ouyang *et al.*, 2016). However, China has striven to reduce the reliance on its agricultural production on toxic pesticides (Evans *et al.*, 2012; Hoi *et al.*, 2016). In Vietnam, due to insufficient pesticide management capacity of the government, pesticide types and quantities registered and distributed on the market have substantially increased in Vietnam over the last 10 years (Hoi *et al.*, 2016). Hence, in order to understand the nutrients and pesticide transport, it is necessary to first figure out the suspended sediment transport (Boithias *et al.*, 2014).

Managing the water quality challenges above requires an appropriate monitoring programme, however, surface water quality monitoring in some Asia countries is insufficient due to the cost, remote location or management. In Laos and Vietnam surface water quality monitoring is more limited; besides, in both countries, there are many difficulties, in particular, the unclear definition of responsibilities and competences among different ministries and agencies at national and provincial scales (Evans *et al.*, 2012). Therefore, advanced tools and methods can be applied in these regions combining with limited in-situ data to overcome the deficiency of measurement data.

1.2. Hydrologic Cycling

1.2.1. Global hydrologic cycling

Earth is a huge system, composed of lithosphere, hydrosphere, atmosphere and biosphere. Water plays an important role in this system and makes the interdependence among these circles. And the hydrological cycle is one of the specific signs of this close relationship.

The water form is not only a liquid but also a solid (e.g. hail, snow) and a gas (e.g. water vapor). The total amount of water in the world is constant, but water is continuously changing from one form to another and is continuously moving at different speeds (Shaxson *et al.*, 2003). Driven by solar and atmospheric movements, natural water evaporates or transpires into the atmosphere in the form of water vapor, through the surface of water (stream, lake, sea), land (soil and rock), and plant stem and leaf. Under the appropriate conditions, the water vapor in the atmosphere condenses into water droplets which fall under gravity to the ground surface of the earth in the form of precipitation. A portion of the precipitation infiltrates or percolates into underground under the effect of molecular force, capillary force and gravity; a part forms surface runoff under gravity, flows into the streams and lakes, and finally converges into the

sea; the rest returns to the atmosphere through evapotranspiration and transpiration. The portion that infiltrates into underground becomes soil moisture, and then returns to the atmosphere through evapotranspiration; or replenishes aquifers under the ground, becoming underground water, and then flows into the streams and lakes. This endless and circulatory movement process is called water or hydrologic cycling. Figure 1-4 is the hydrologic cycling process.

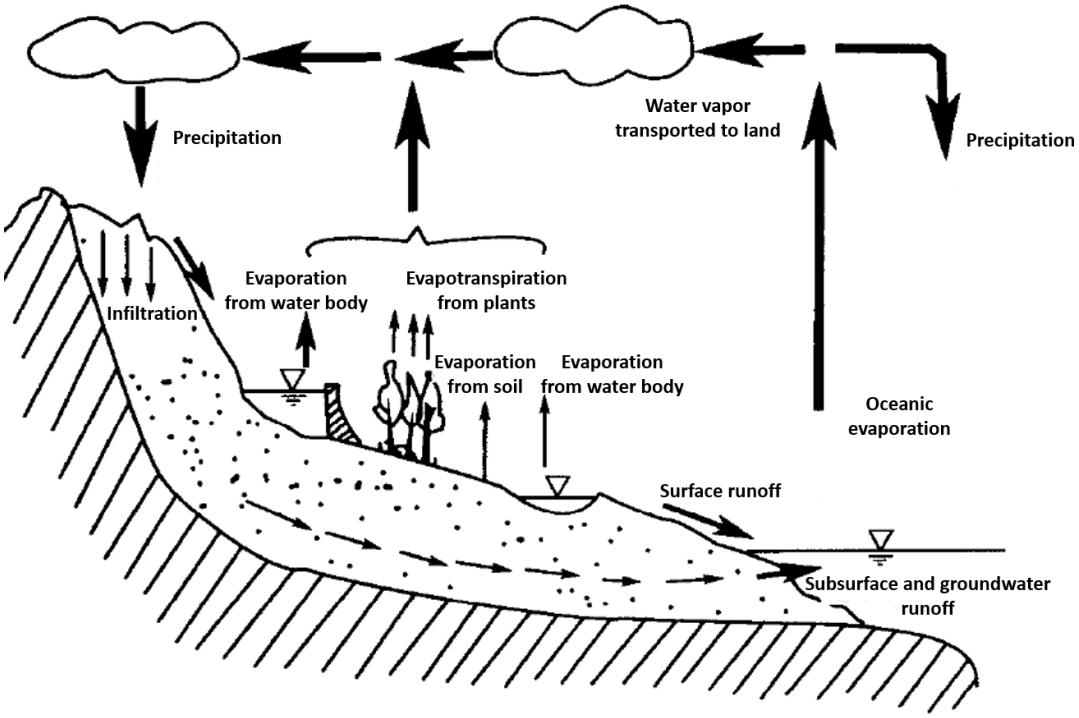

Figure 1-4 Hydrologic cycling process.

1.2.2. Hydrologic cycling at a basin scale

The area surrounded by the ground divide (ridgeline) is called the watershed/basin. Watershed or regional hydrological cycling is actually the formation of regional runoff by rainfall. The rainfall that falls into the basin first meets the requirements of interception, sink filling, and infiltration, and the rest forms the surface runoff, flowing into the drainage network. River network plays a critical role in the hydrological cycle, processing and transporting sediments, nutrients and contaminants to oceans, and river discharge is a result of a suite of processes contributing to the hydrological cycle. Therefore, understanding changes in river discharge under its influence factors is of utmost importance.

There are many large rivers in Asia which are among the largest in the world in terms of length, basin area and annual volume. These large Asian river basins have some special and important features such as monsoon impacts, glacier shrinkage in the headwaters, densely populated mega deltas, and role of Siberian rivers in climate control (Kundzewicz *et al.*, 2009).

River hydrological cycle and water quality are affected by climate variability and

changes, also human disturbance (such as water diversions and withdrawals, and flow regulation via dams). Climate variations, particularly temperature and precipitation, have effects on river systems both at short and long time scales, such as floods and droughts caused by typhoons and El Nino and La Nina, especially in the tropics (Arnell, 1999; Nijssen *et al.*, 2001; Dang *et al.*, 2018). Kundzewicz et al. (2009) addressed that in much of Asia area, the main influence factors affecting river flow is the monsoon precipitation. Precipitation plays a critical role in the hydrological cycle and exerts vital socio-economic impacts. The discharge from the rivers in the Asian monsoon region is sensitive to the seasonal cycle in precipitation. The amount of rainfall varies greatly from year to year depending on the strength of the monsoonal flows and the amount of water vapour transported, which leads to large interannual water flow fluctuations. For years with weaker monsoon rains, water deficits may occur, causing reductions in crop yields and major food supply problems in densely populated areas. Precipitation has decreased in parts of southern Asia, especially since the 1970s, while the linear trend of rainfall decrease in southern Asia region for 1900–2005 was 7.5% (significant at 1% level) (Kundzewicz *et al.*, 2009), while at the end of the twenty-first century, the annual mean precipitation is projected to increase in southern to eastern Asia (Nohara *et al.*, 2006).

To face the challenge of increasing water demand under uncertain variations of climate, dams have been built globally for water storage (Figure 1-5). Globally, at least 45,000 large dams have been built, and nearly half of the world's rivers have at least one large dam (Dams, 2000). At the continental scale, the greatest number of large reservoirs and the greatest summed reservoir capacities are located in Asia (Vörösmarty *et al.*, 1997). From a Global Reservoir and Dam database, approximate 28% dams are located in Asia (Lehner *et al.*, 2011b, 2011a). In addition, future hydropower development is primarily concentrated in developing countries and emerging economies of Southeast Asia (Zarfl *et al.*, 2015). The hydrological, morphological and ecological impact of large dams can be dramatic (Best, 2019). Dams coupled to climate variability have an impact on water regime and fluxes of matters, mainly SS (Vörösmarty *et al.*, 1997; Manh *et al.*, 2015; Yang *et al.*, 2015). Vörösmarty et al. (1997) estimated that more than 40% of global river discharge is intercepted by the large impoundments. Dam implementation can cause a significant reduction in SF. Vörösmarty et al. (2003) estimated greater than 50% of potential sediment trapping by dams in regulated basins. However, reduced sediment transport affects estuarine and coastal communities (Syvitski *et al.*, 2005). For example, as a result of reduced sediment delivery, many river deltas are sinking, thereby increasing the vulnerability of human populations depending on their ecosystem services for survival (Zarfl *et al.*, 2015).

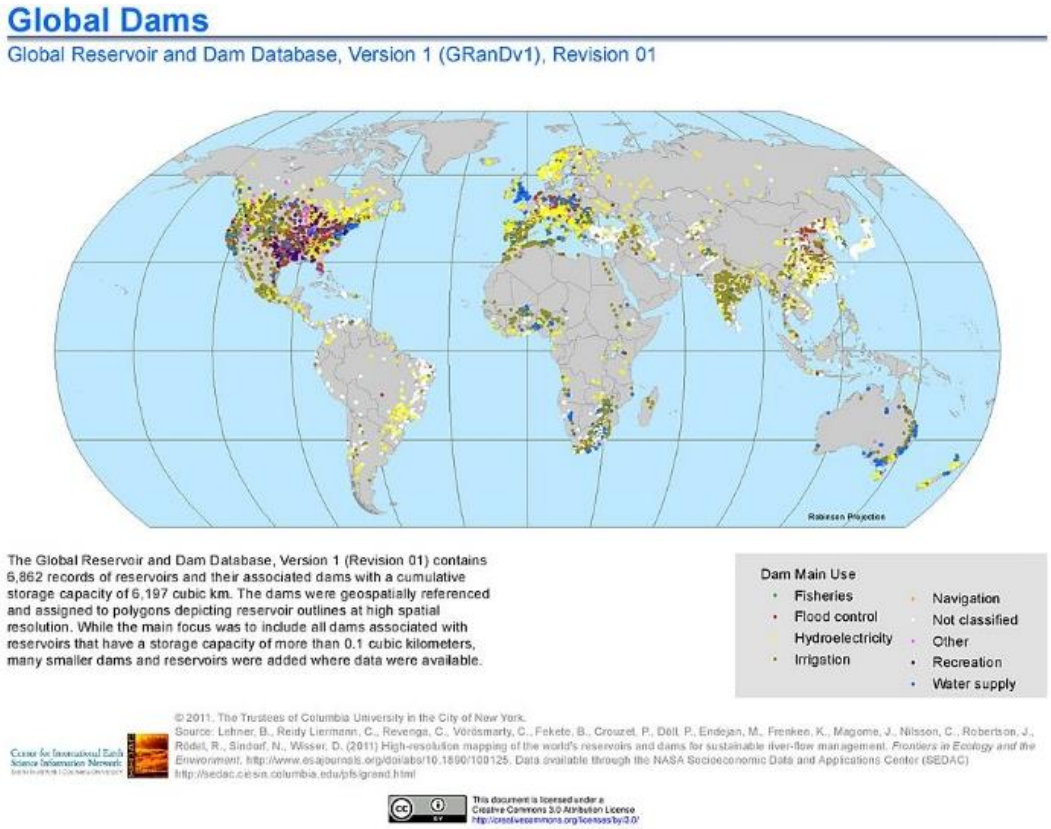

Figure 1-5 The global reservoir and dam distributions, resource from the Socioeconomic Data and Applications Center (SEDAC: https://sedac.ciesin.columbia.edu/data/collection/grand-v1/maps/gallery/search).

1.3. Sediment Fluxes

The suspended sediment (SS) transportation by rivers is a key component of the global denudation system (Walling and Fang, 2003). It can measure the rate of denudation of the continents and the erosion processes. Besides, it is a reflection of land and river degradation and the associated reduction in the global soil resource (Walling and Fang, 2003). A big portion of the sediment transported by rivers represents soil eroded from the landscape, such as agricultural land, and the magnitude of this flux therefore also provides a measure of land degradation.

Sediments play a decisive role for diversification and composition and, hence, the quality of habitats, especially for the mid- to the long-term development of habitat features (Hauer *et al.*, 2018). The transportation process of SS by rivers also drives nutrients (like C and P) and contaminant (such as metals and pesticides) to the seas which is an essential process for marine biogeochemical cycle and diversity (Lal *et al.*, 1995; Syvitski *et al.*, 2005; Kunz *et al.*, 2011; Cohen *et al.*, 2013; Boithias *et al.*, 2014; Garneau *et al.*, 2017). Sediment-associated transport accounted for more than 90% of the total river-borne flux of elements such as nutrients and metals (Martin and Meybeck, 1979), and around 43% of the total transport of organic carbon from the land to the oceans by rivers is in particulate form (Ludwig and Probst, 1996b).

The SS load transported by a stream or a river will commonly represent a mixture of

sediment derived from different locations and from different source types within the contributing catchment (Walling, 2005; Hauer *et al.*, 2018). The SS in the rivers mainly comes from two sources: erosion and weathering from the landscape, and channel degradation and erosion. Figuring out the SS source is important in understanding the SS dynamics and the sediment budget of a basin, also is a key precursor to the design of effective sediment management and control strategies for basin management; besides, it can help to control sediment-associated nutrient and contaminant fluxes (Walling, 2005).

River sediment fluxes are sensitive to many influences, from human activities to natural effects (Walling and Fang, 2003). Human disturbances can come from landscape such as land clearance, land use change, soil and water conservation measures, and from the channel part such as reservoir construction, water abstraction and sand excavation. Humans increase the river transport of sediment through soil erosion activities and decrease this flux to the coastal zone through sediment retention in reservoirs (Syvitski *et al.*, 2005). Natural factors can come from climates such as monsoon, typhoon and rainfall intensity, geological activity such as earthquake and landslide.

From the study of global scale, 50% of the sediment load records showed evidence of statistically significant upward or downward trends, with the majority evidencing declining loads (Walling and Fang, 2003). Therefore, understanding how the influencing factors effecting on different sources would be a base but important work for studying SS load transportation.

1.3.1. Land degradation and soil erosion

Nowadays, with the growing population, the demand for agriculture production is increasing too. Large-scale conversion of forests to agriculture lands is a consequence of increased agriculture production demand, leading to increased soil erosion. High soil erosion must cause high depositions of sediment in rivers and lakes, and this is one of the major reasons for floods and water pollutions (Yang *et al.*, 2003).

Wilkinson and McElroy (2007) indicated that subaerial erosion as a result of human activity, primarily through agricultural practices, had resulted in a sharp increase in net rates of continental denudation; and present farmland denudation is proceeding at a rate of around 75 Gt yr^{-1} and is largely confined to the lower elevations of Earth's land surface. Increased soil erosion led to increased sediment fluxes in most of the rivers across the globe (Gupta *et al.*, 2012). Syvitski et al. (2005) addressed that humans had increased the inland sediment transport by the global rivers through soil erosion by 2.3 ± 0.6 Gt yr^{-1}. Yang et al. (2003) pointed out that nearly 33% of the world's arable land was lost to erosion, with loss continuing at a rate of more than 10 million ha yr^{-1}.

Asia probably has suffered more from soil erosion compared to other continents due to its geomorphology, climate factors and the human activities (Dregne, 1992; Ananda

and Herath, 2003; Lal, 2003; Yang *et al.*, 2003). That natural erosion is primarily confined to drainage headwaters, and around 83% of the global river sediment flux is derived from the highest 10% of Earth's surface (Wilkinson and McElroy, 2007). The Himalayan-Tibetan Plateau is the birthplace of many important rivers including the Indus, the Ganges, the Brahmaputra, the Irrawaddy, the Salween, the Mekong, the Red, the Yangtze and the Yellow rivers, and this area has been recognized as a great SS contributor (Milliman and Syvitski, 1992; Ludwig and Probst, 1998). From Figure 1-6 we can see that the Himalayan-Tibetan Plateau is in high erosion. Active tectonic movements (such as earthquake, debris flow and landslide), steep slopes, freeze-thaw and weathering erosions are the main issues in the riverhead high-elevation areas. Active human activities inside these basins (such as deforestation, agriculture, urbanization, road construction and mining) accelerate the soil erosion processes.

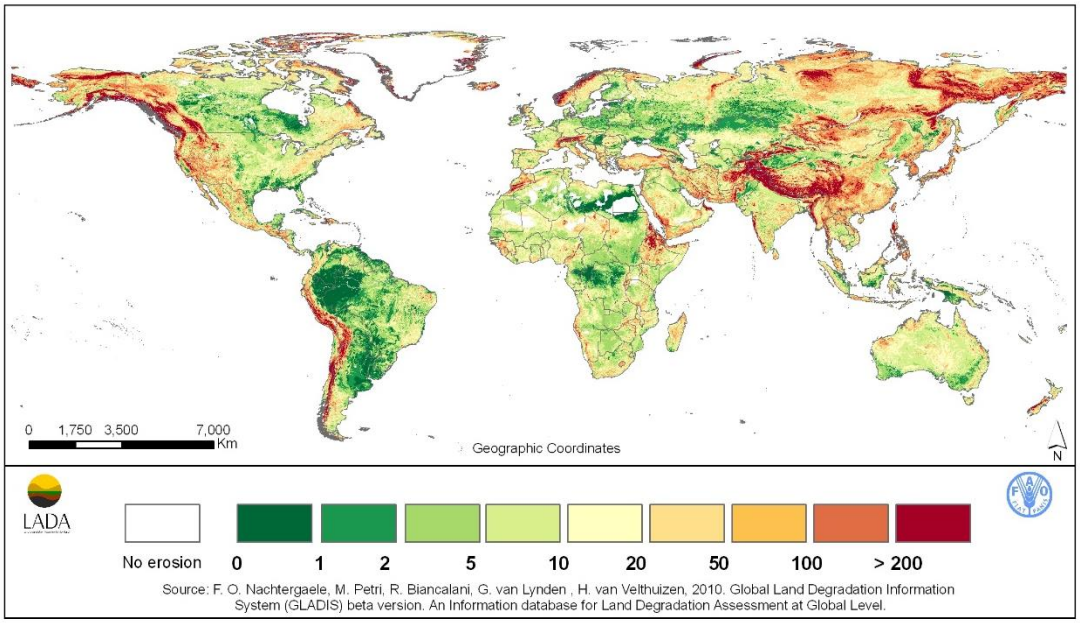

Figure 1-6 Worldwide predicted soil loss (t ha yr^{-1}) (Nachtergaele et al., 2010).

Yang et al. (2003) found that Southeast Asia had the most serious soil erosion problems and hot spots were close mountainous areas located in the tectonic zones and dense croplands of the high population regions where both natural geomorphology and human activity are major factors for inducing soil erosion; and there was an increasing trend found in Asian, and the regions with the largest increases were in the tropic rainforest regions (Southeast Asia), such as Thailand and the lower Mekong basin (Yang *et al.*, 2003). In the Mekong River basin, the soil erosion in the 1980s was 9.6 t ha yr^{-1} and predicted to reach 13.0 t ha yr^{-1} in the 2090s (Yang *et al.*, 2003).

In Vietnam, more than 40% of its steeply sloping lands (62% of the country) suffer severe erosion (Dregne, 1992). From previous studies, the annual soil losses in the Red River basin in Vietnam's part ranged from 0.9 to 174 t ha yr^{-1} (Podwojewski *et al.*, 2008; Nguyen *et al.*, 2011; Mai *et al.*, 2013; Tuan *et al.*, 2014). In the area of the Red River basin in China's part, Gu (2016) found that the average annual soil erosion was 18.4 t ha yr^{-1} (136 Mt yr^{-1}) in 2000 while it was 18.7 t ha yr^{-1} (138 Mt yr^{-1}) in 2010; severe

soil erosion area which was only less than 10% of the total erosion area, however, contributed 57% to 65% of the total erosion amount; farmland was the hot spot of soil erosion, followed by grassland and forest; slope above 15° and elevation between 1000-2000 m a.s.l. were the hot spots of erosion.

1.3.2. Sediment export by rivers

Global sediment flux to the oceans was estimated from 12.6 to 18.5 Gt yr^{-1}, and Asia exported the most sediments (4.8 Gt yr^{-1}) among continents (Syvitski *et al.*, 2005; Gordeev, 2006; Syvitski and Kettner, 2011). High sediment loads is a common feature in many Asian basins due to the pronounced topography of the region, especially the basins originating from the Himalayan-Tibetan Plateau, such as the Mekong, the Red, the Yangtze and the Yellow rivers (Milliman and Syvitski, 1992; Ludwig and Probst, 1998; Evans *et al.*, 2012).

Investigation of global value and the current trend in sediment exports has some constraints and uncertainties (Walling and Fang, 2003; Cohen *et al.*, 2013). Firstly, lack of sediment data in many rivers, especially in the rivers in developing and underdeveloped countries, can cause an underestimation on the global sediment exports. Even the sediment flux data is available, but the measurement only considers suspended sediment flux, not the bed load transport. Secondly, analysis of annual sediment flux temporal trends requires records of enough length data. Long-term sediment monitoring programmes, however, are rare in many areas of the world.

Dam is a key tool for people to exploit the water resource (water supply, electricity generation and flood control) in many areas of the world, especially in the areas with intensive population and agricultural activities (Schmutz and Moog, 2018). Lehner et al. (2011b) estimated that there were 6862 records of reservoirs and their associated dams and about 2.8 million impoundments larger than 0.1 ha worldwide. However, dam constructions can induce associated impacts such as interruption of river continuity, siltation of river bed and clogging of interstitial, downstream river bed incision and downstream flow and water quality alteration (Figure 1-7) (Schmutz and Moog, 2018).

The evidence afforded by the sample of the world's rivers indicates that reservoir construction is probably the most important influence on land-ocean sediment fluxes (Walling and Fang, 2003). Early, Vörösmarty et al. (1997) estimated that more than 40% of global river discharge was intercepted by the large impoundments and that an around 70% proportion of this discharge maintains a theoretical sediment trapping efficiency in excess of 50%; for regulated drainage basins the global, discharge-weighted residence time change was 0.16 years, representing a 30% potential sediment trapping. More recently, Vörösmarty et al. (2003) indicated that greater than 50% of basin-scale sediment flux in regulated basins was potentially trapped in artificial impoundments, with a discharge-weighted sediment trapping due to large reservoirs (≥ 0.5 km^3) of 30%, and an additional contribution of 23% from smaller reservoirs.

Syvitski et al. (2005) addressed that fluvial sediment loads, over 100 Gt of sediment, including carbon (around 1 to 3%), had been sequestered behind reservoirs. With more dam are going to operate, sediment trapping loads and percentage might increase.

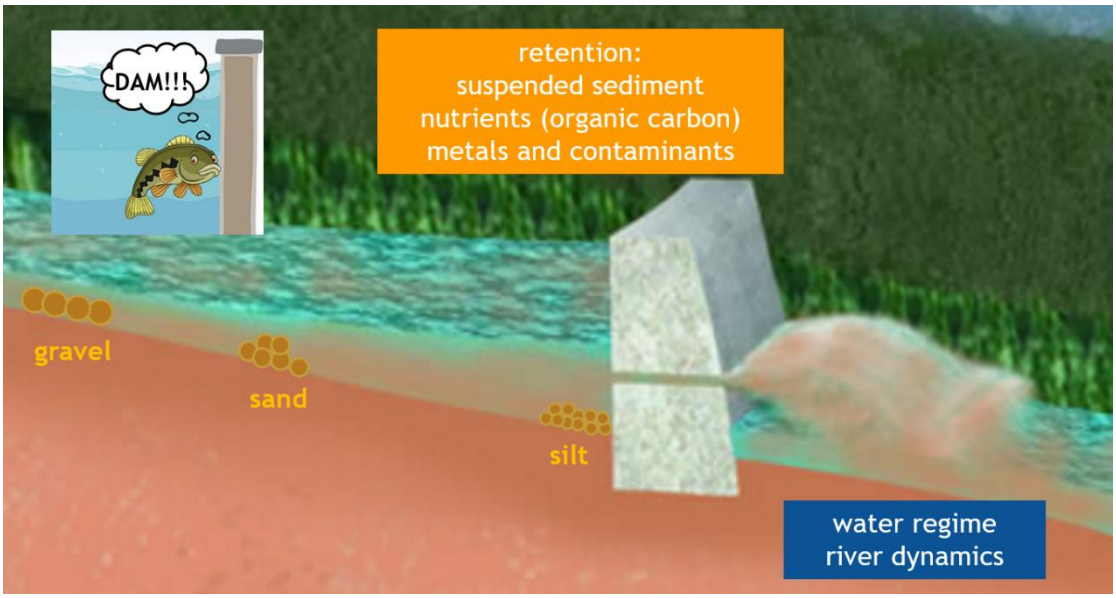

Figure 1-7 Dam construction interrupts the river continuity (such as fish migration, sediment and nutrient transport) and alters the downstream flow and sediment regimes.

Dam and weir constructions can reduce downstream gravel supply and therefore lead to armors, thus increase intensify flushing out heterogeneous sorted sediments. (Hauer *et al.*, 2018). As a consequence, the resultant deficits in bed-load transport may lead to continuous riverbed incision with the risk of channel avulsion and riverbed breakthrough during single flood events. Dam constructions may cause significant alterations of the sediment regime (such as grain size distribution) based on the storage of water and the capture of sediment by dams which cause profound downstream changes in the natural patterns of the hydrologic variation and sediment transport (Hauer *et al.*, 2018). Dam constructions not only retain the sediment, breaking the sediment continuum, but also alter the dynamics of sediment transport processes. Large amounts of retained suspended load in the reservoirs are released in a short period of time during flushing, mostly in conjunction with flood events, resulting in a surplus of sediments in downstream river sections. Consequently, high loads of mostly fine sediments cause high concentrations of turbidity and can be responsible for losses and mortality of aquatic organisms (Espa *et al.*, 2015; Hauer *et al.*, 2018).

Asian rivers were estimated to export 4.8 Gt yr^{-1} sediment to the oceans (Syvitski and Kettner, 2011). However, Africa and Asia showed the largest reduction in sediment flux to the coast in rivers (such as the Nile, Orange, Niger, and Zambezi in Africa and the Yangtze, Indus, and Yellow in Asia), and 31% of the total sediment load retained in reservoirs were indicated in Asia and 25% in Africa (Syvitski *et al.*, 2005).

Since the 1980s, the sediment load of the Yellow River has dropped markedly to <50% of this earlier value in response to reduced precipitation, increased water abstraction and improved sediment control practices in the Loess region of the Middle Yellow River (Walling and Fang, 2003). Mean sediment flux of the Yangtze River decreased by 71% between 1950-1968 and the post-Three Gorge Dam decade, about half of which occurred prior to the pre-Three Gorge Dam decade; approximately 30% of the total decline and 65% of the decline since 2003 can be attributed to the Three Gorge Dam, 5% and 14% of these declines to precipitation change, and the remaining to other dams and soil conservation within the drainage basin (Yang *et al.*, 2015). During 2007-2013, the fluvial sediment supply from the Pearl River to the coast showed a massive 71% decrease compared to period 1954-1979 when the human influences were not significant (Ranasinghe *et al.*, 2019). In the Mekong River basin, the sediment trap efficiency was predicted to increase to 78-81% with all the planned reservoirs being built, and the potential annual sediment trap would be 70-73 Mt (Kummu *et al.*, 2010). In the Ren River basin, due to the construction of the biggest dam, Hoa Binh dam, sediment flux drastically decreased from 100-160 Mt yr^{-1} to around 40 Mt yr^{-1} during 1997-2004, and the mean annual sediment trapping efficiency of Hoa Binh dam was 88% (Vinh *et al.*, 2014). The annual sediment flux of the Ganga River was estimated from 262 to 390 Mt yr^{-1} during 2004-2010 (Rice, 2007; Lupker *et al.*, 2011); and the annual sediment flux of the Brahmaputra River was 387 Mt yr^{-1} in 2006 (Rice, 2007), however, Rahman et al. (2018) found that these two major river systems were following a declining trend, and sediment load was decreasing at a rate of 4-10 Mt yr^{-1}.

Asian rivers export high sediment fluxes to the oceans especially the Himalayan-Tibetan Plateau originating rivers (Milliman and Syvitski, 1992; Ludwig and Probst, 1998; Evans *et al.*, 2012). Most estimations of sediment flux were calculated based on a monthly or an annual scale. However, most sediment export happens during flood events linked to daily discharge variations. Therefore, it would be necessary to study the sediment fluxes in this region on a daily time scale in order to precisely estimate the export of suspended sediment and its associated nutrients and contaminants, and also to understand the transport response to the flood events.

1.4. Fluvial Organic Carbon

Carbon (C) cycling is a cornerstone of ecosystem biogeochemistry as it is a critical element for all biota cellular processes (Kroeze *et al.*, 2012). Carbon can be divided into inorganic carbon (IC) and organic carbon (OC). The most essential pools for carbon in an aquatic environment include dissolved inorganic carbon (DIC), dissolved organic carbon (DOC) and particulate organic carbon (POC) (Göltenboth and Lehmusluoto, 2006).

Inorganic carbon (IC) in the form of DIC is available in water in three forms: CO^2, HCO_3^-, CO_3^{2-}, and their availability depends on the pH values of the water (Göltenboth and Lehmusluoto, 2006); in the atmosphere, IC is primarily in the form of CO_2 (Dodds and Whiles, 2010; Cole, 2013).

Organic carbon (OC) is the base of organic compounds which contain carbon atoms bonded to hydrogen atoms and possibly other elements such as nitrogen or phosphorous. OC provides the materials and energy for metabolism within the ecosystem. Soluble compounds including soil humic substances, polysaccharides, polypeptides and some colloidal materials comprise the DOC; living and dead micro-organisms and carbon in suspended sediments are isolated as particulate organic carbon (POC) (Schlesinger and Melack, 1981).

The OC transport by rivers to the ocean is important to coastal heterotrophic organisms, even though riverine OC represents only a small fraction (0.9%) of net global terrestrial primary production (Zhao and Running, 2010; Huang *et al.*, 2012). Before reaching the ocean, C from land transit through the continuum formed by soil, groundwater, riparian zones, rivers, lakes, estuaries and coastal marine areas, combined with contaminants.

1.4.1. Sources of organic carbon

Riverine OC mainly comes from three sources: the allochthonous source, which is based on terrestrial origins, such as weathering from rocks, leaching from soil and the decomposed products like the tissue of plants on land; the autochthonous source, which derives from primary production within the river itself, such as from algae and phytoplankton. Anthropogenic influences from agricultural, domestic and industrial activities can also be regarded as an allochthonous source (Hope *et al.*, 1994; Huang *et al.*, 2012).

The DOC is a mixture of substances. Besides allochthonous inputs, leaching from the soil is the main sources for DOC while the uptake by bacteria is the most important output (Le, 2005). The POC is mainly composed of the substances bound in the organism and the detritus. The main source for POC is the primary production. POC can be transformed by secretion, excretion and autolysis into DOC and be derived from DOC by physico-chemical and biological processes (Göltenboth and Lehmusluoto, 2006).

Fluvial DOC and POC concentrations are mainly related to the soil organic carbon (Aitkenhead and McDowell, 2000; Huang *et al.*, 2012; Li *et al.*, 2017; Fabre *et al.*, 2019). Soil organic carbon depends on land management and land use, and it can enter the river by washed out by rain and by leaching (Escolano *et al.*, 2018). Soil resources in many Asian countries are being overexploited, degraded, and irreversibly lost due to inappropriate land management practices, industrial activities, and land use changes that lead to soil sealing, erosion, contamination, and loss of organic carbon, which subsequently increase the OC exports to the oceans.

1.4.2. Dissolved and particulate organic carbon exports by rivers

The riverine OC cycle and budget have been paid attention and studied in recent decades. Schlesinger and Melack (1981) used two ways to estimate the global OC flux: the first was by an inventory and extrapolation of data on loss of carbon per unit volume

of river discharge from 12 intermediate and large rivers, and they found an OC export of 0.37 Gt yr^{-1}; the second was using measurements of the fluvial loss of organic carbon per unit area of land in various ecosystem types, and they found the OC flux was 0.41 Gt yr^{-1}. Ludwig and Probst (1996) utilized a database of mean annual DOC and POC fluxes of 32 rivers, respectively, and other ecological factors to calculate DOC and POC fluxes, and found a global annual OC flux of 0.38 Gt yr^{-1} (DOC of 0.21 Gt yr^{-1} and POC of 0.17 Gt yr^{-1}). Aitkenhead and McDowell (2000) examined the relationship between DOC flux and soil C:N ratio on a biome basis; and by using their C:N model, they estimated the total export of riverine DOC from land to the oceans to be 0.36 Gt yr^{-1}. Schlünz and Schneider (2000) re-estimated the modern global riverine OC flux and gave the value of 0.43 Gt yr^{-1}, of which 0.18 Gt yr^{-1} was transported by Asian rivers. More recently, Li et al. (2017) re-evaluated the riverine global OC flux to 0.48 Gt yr^{-1}, of which 0.24 Gt yr^{-1} was DOC and 0.24 Gt yr^{-1} was POC, and Asian rivers exported more DOC and POC than other continents. As presented in Section 1.3.2, Himalayan rivers export high quantity of sediments to the oceans, and it has also been recognized to be a great source of OC (Aucour *et al.*, 2006; Galy *et al.*, 2007).

The humid tropical climate is associated with the highest carbon yield (Ludwig and Probst, 1996b; Aitkenhead and McDowell, 2000; Huang *et al.*, 2012; Carvalhais *et al.*, 2014). The tropical region (30°N–30°S) covers around 43% of the world's land but contributes 66% of global outflow, 73% of sediment load and over 61% of terrestrial net primary production (Milliman and Syvitski, 1992; Syvitski *et al.*, 2005). Therefore, tropical rivers are critical to total global fluvial organic carbon flux. Aitkenhead and McDowell (2000) found the riverine DOC flux from tropical regions were 0.15-0.23 Gt yr^{-1}. Huang et al. (2012) used published and unpublished data, considering 175 tropical rivers, estimated the fluvial carbon fluxes and found that these tropical rivers delivered approximately 0.27 Gt yr^{-1} organic carbon to the estuaries, of which 0.14 Gt was DOC and 0.13 Gt was POC. They found that rivers in the equatorial region between 3°N and 6°S produced high DOC; and the type of soil was a main influencing factor: the pattern of DOC distribution was similar to the distribution of soil OC density. They also pointed out that rivers in mainland Asia have the highest specific export rates in terms of DOC and POC. The tropical rivers in Asia exported 0.05 Gt yr^{-1} of DOC and 0.06 Mt yr^{-1} POC to the oceans (Huang *et al.*, 2012).

From above we can see that Asian rivers export high OC fluxes to the oceans and the tropical region is high-yield of OC. Most estimations were calculated based on a monthly or an annual scale. However, most OC export happens during flood events linked to daily discharge variations. Hardly any study estimated OC fluxes on a daily time step. Therefore, the DOC and POC exported by Asian tropical rivers take a large portion of the whole Asian rivers OC exports, and it would be necessary to study the OC fluxes in this region at a daily time scale.

1.4.3. Influence factors

Riverine DOC concentration and fluxes are mainly influenced by basin soil OC,

hydrogeology and climate conditions. Soil OC condition is related to land cover and land management. High soil OC and riverine DOC concentration are found in the basins with the land cover of the forest, peatland, wetland and agriculture (Schlesinger and Melack, 1981; Bishop and Pettersson, 1996; Coynel *et al.*, 2005; Billett *et al.*, 2010; Ritson *et al.*, 2019). Forest, peatland and wetland are rich in organic matters and active decomposition processes while farmland is with some organic fertilizer and is eroded by agricultural practices. Hydrogeology conditions such as drainage intensity and basin slopes and climate such as rainfall density can cause different erosion and leaching processes which are essential to DOC concentration and fluxes (Ludwig, 1997; Huang *et al.*, 2012).

The main factors that govern riverine POC are suspended sediment (SS), phytoplankton, soil OC (Ludwig, 1997; Huang *et al.*, 2012; Fabre *et al.*, 2019). Some studies indicate an inverse relationship between %POC (which is the percentage of POC concentration in suspended sediment concentration) and the SS (Ludwig, 1997; Dang *et al.*, 2013a; Fabre *et al.*, 2019). POC concentration is high when the SS concentration is low, and autochthonous OC produced by phytoplankton is the main contribution; when POC concentration is low and SS concentration is high, the mineral matter, erosion soil and sedimentary rock are a major source (Ludwig, 1997; Dang *et al.*, 2013a).

Besides the factors mentioned above, human interferences and climate changes have affected the OC transfer and fluxes (Hope *et al.*, 1994; Seitzinger *et al.*, 2010; Escolano *et al.*, 2018). For example, agricultural activities have enhanced the soil erosion which consequently has increased POC input (Ludwig and Probst, 1996b; Ciais *et al.*, 2008; Huang *et al.*, 2012). Dam constructions have sequestered the suspended sediment which consequently decreased POC export, and over 100 Gt of sediment and 1 to 3 Gt of carbon were sequestered in reservoirs constructed largely within the past 50 years (Syvitski *et al.*, 2005); and dam regulation on discharge also affect the DOC transport dynamic and fluxes (Hope *et al.*, 1994; Seitzinger *et al.*, 2010; Hu *et al.*, 2015; Wu *et al.*, 2015; Li and Bush, 2015; Li *et al.*, 2015; Liu *et al.*, 2015, 2019a; Shi *et al.*, 2016; Xia *et al.*, 2016; Huang *et al.*, 2017; Le *et al.*, 2018; Park *et al.*, 2018). Climate variability has been verified to affect OC fluxes (Tian *et al.*, 2013; Wu *et al.*, 2015). Wu et al. (2015) indicated that climate change had influences on POC due to the variations of discharge and sediment load. Tian et al. (2013) compared the DOC in different climate zones in USA and found that temperature was a key variable for DOC export and climate warming would have a greater impact on riverine DOC yields in cooler climate zones than on those in warmer climate zones.

The Red River basin is a basin crossing subtropical and tropical climate zones and shared among China, Laos and Vietnam, combining different land uses and affected by human activities such as intensive agriculture and dam implements. Previous studies, both on using sampling data and modelling, have investigated that human activities have impacts on hydrology and SS (Le et al., 2007; Lu et al., 2015; Vinh et

al., 2014; Wang et al., 2011; Wei et al., 2019, submitted); these studies especially found a strong retention of SS caused by dams. Hence, it would be interesting to understand the OC processes and quantify OC fluxes in this basin at the interannual scale with a daily time step.

1.5. General Approaches and Tools

For assessing the hydrological cycle and suspended sediment, the general method and tools are in-situ field measurements, empirical and simple equations, remote sensing techniques, geographic information systems, and numerical simulations. However, field-collecting data at large spatial and temporal scales is expensive, and often impracticable in some remote areas and underdeveloped regions. Empirical or/and simple equations, such as sediment rating curves are sometimes applied to quantify the sediment flux (SF) (Asselman, 2000; Syvitski *et al.*, 2000; Achite and Ouillon, 2007; Zhang *et al.*, 2018). However, a sediment rating curve requires discharge (Q) as an input, which might not be available for remote and underdeveloped regions, and its parameters can vary a lot among a big drainage basin. Therefore, this method might neither be the best choice for calculating the SF on a daily scale nor in a large basin.

Numerical models combined with other techniques (such as remote sensing) can fill the gap in sediment dynamic measurements (Syvitski *et al.*, 2005; Wilkinson *et al.*, 2009) and offer insight into future and past trends in response to environmental and human changes, such as land use change and climate change. In addition, simulations can be carried out at a large spatial scale and at a daily time scale to quantify, analyze and forecast water resources and quality. In particular, it can realistically represent the spatial variability of the basin, which will provide a global view of the whole basin. Many physically-based hydrological models had been used (Daniel *et al.*, 2011; Islam, 2011; Devia *et al.*, 2015; Fu *et al.*, 2019), such as MIKESHE (Graham and Butts, 2005), HSPF (Bicknell *et al.*, 1997) and Soil and Water Assessment Tool (SWAT) (Arnold *et al.*, 1998). Among these models, SWAT has been proved to obtain good hydrological predictions with a little direct calibration in many different basins around the world (Gassman *et al.*, 2007, 2014; Devia *et al.*, 2015; Fu *et al.*, 2019), and more applications can be found in SWAT literature database: https://www.card.iastate.edu/swat_articles/.

Although SWAT has been applied to many Asian basins, and also to subtropical or/and tropical areas, most of them were at a scale of 77 to 105,000 km^2 (Gassman *et al.*, 2007; Bannwarth *et al.*, 2015; Lweendo *et al.*, 2017; Li *et al.*, 2018; Shrestha *et al.*, 2018; Tan *et al.*, 2019). Tan *et al.* (2019) summarized that a total of 126 articles related to application of SWAT on studying water-related issues (such as climate change, land use change, best management practices, water quality and hydropower) in Southeast Asia, half of which were in Vietnam and Thailand, and the performances of the SWAT model were generally above satisfactory.

The Red River is a typical Asian river system, combining different land uses, affected

by human activities such as intensive dam implementations and agriculture (Le *et al.*, 2007; Nguyen *et al.*, 2011). Recent studies of hydrology and suspended sediment in this basin mainly used data from gauge stations or sampling to do statistical analysis (He *et al.*, 2007; Dang *et al.*, 2010; Lu *et al.*, 2015; Le *et al.*, 2017a), or use modelling to perform simulations at a local scale (Ngo *et al.*, 2015) or in the delta part (Vinh *et al.*, 2014) at a monthly scale; few studies analyzed fluxes at daily scale, but only on a short period (Le *et al.*, 2007), in the delta (Luu *et al.*, 2010). Hiep *et al.* (2018) used SWAT to simulate the discharge at daily scale for four stations (Lao Cai, Yen Bai, Son Tay and Hanoi) on the main Red River during 2005-2009, however, they did not simulate the Da and Lo rivers, nor the suspended sediment. Both Q and SSC can vary greatly from day to day; therefore, it would be more favourable to calculate flux at a daily time step. Also, water quality monitoring is usually carried out during some specific days in a month, and outputs from a model at daily scale can be practical and useful for further studies. In addition, different scenarios of global changes can be considered to help researchers or government administrators to compare different possibilities and set up long-term management plans.

Studies of the nutrients associated with discharge and SS, such as riverine OC, has also been carried out. Most of these researches analysed the concentrations and fluxes of nutrients based on the sampling data (Le *et al.*, 2005, 2010, 2017a; Dang *et al.*, 2013a); few used the modelling way (Le *et al.*, 2017b; Nguyen *et al.*, 2018). At the local or regional scale, in-situ sampling is a direct and accurate way to quantify the riverine C. From sampling data, Le et al. (2017a) estimated that the mean annual TOC yield during 2008-2010 was 270 kt yr^{-1} at Hanoi, of which 142 kt was DOC and 128 kt was POC; Dang et al. (2013) quantified the annual POC flux of 243 kt yr^{-1} at Son Tay during 2006-2009.

However, the same as Q and SS measurement, riverine DOC and POC in-situ field sampling at large spatial and temporal scales is expensive and often impracticable in some remote areas and underdeveloped regions. Using a modelling approach or/and simple equations would overcome these shortages. Le et al. (2017b) and Nguyen et al. (2018) used a modelling approach to identify a seasonal OC variation and to estimate a TOC export of 324 kt yr^{-1} at Son Tay (outlet of the continental basin) during 2013-2014. However, simulation at a seasonal scale might not be precise enough. Hope et al. (1994) indicated that riverine C flux was likely to be underestimated. For most rivers, the OC concentration varies with discharge and season. Discharge is the major factor controlling the output of OC (Hope *et al.*, 1994), and suspended matter and sediment are also the main determinants of POC flux (Ludwig and Probst, 1996b; Huang *et al.*, 2012). Q and SS can vary largely due to the intensive rainfall and storms. Consequently, the concentration of OC may fluctuate greatly. However, sampling is usually taken at fortnightly or monthly intervals which might induce underestimation when there is a storm or intense rainfall during the intervals. Therefore, it would be more precise to assess and calculate OC flux at a daily time step using daily discharge, suspended sediment and OC concentrations, and a modelling coupling remote sensing

and in-situ measurement data would be a good tool.

1.6. Objectives of this Study

With the increasing requirement of fresh water for agriculture, urban and industry, water availability becomes an important concern in the 21st century, it is an indispensable resource for both the environment and human beings. Understanding of the hydrologic cycle, such as water movement processes through the land surface and subsurface, water budget and storage, will help us gain sustainable water supplies. Rivers play a crucial component of the terrestrial hydrological cycle. The water budget of a river will help the administration improve management practices. The sediment transport by rivers from land to the ocean is a key pathway within the global geochemical cycle. The sediment is a carrier of sediment-associated matters, such as nutrients (like C and P), metals and pesticides. Both sediments and these associated matters are important for downstream topography and ecosystem. Besides, the sediment flux is also an indicator of the global denudation system and provides a general measure of the rate of denudation of the continents and of the efficacy of erosion processes in lowering the land surface of the globe. Riverine organic carbon is a basic and essential matter for river and marine ecosystem and its cycle forms a part of the global biogeochemical cycle.

Therefore, assessing water discharge, suspended sediment and riverine organic carbon dynamics and quantifying water budget, sediment and organic carbon fluxes can enable us to use and manage wisely and scientifically the precious water resource, to provide a measure of land degradation and the associated reduction in the global soil resource, to better understand the global biogeochemical cycles and processes.

The Red River is one of the important river basins in Asia. It passes two climate zones (subtropics and tropics) and three countries (China, Vietnam and Laos). The agriculture activities and inhabitants develop along the river, making it an important river for culture and economics. As other Asian rivers, inside this basin, increasing human activities (farming and damming) has changed and degraded the ecosystem and aquatic system. Besides, the south-east Asian is influenced by climate variability. Hence, the Red River basin would be a good example for researchers to study the impacts of human activities and climate variability on hydrological and biogeochemical cycles.

Most of the researches on the Red River basin were implemented by in-situ field work or analysis hydrology data from gauge stations. However, these methods are not suitable and practicable for researchers to carry on a large basin scale and to understand each subbasin. Modelling combined with satellite data and observed data is an efficient role to study the hydrologic and biogeochemical cycling at large spatial scale and long temporal scale. However, most modellings of dynamics and concentrations were carried out at a monthly or annual scale which would not be precise enough for understanding the transfer processes and quantifying the exports.

Hence, the main objective of this thesis is to apply a new tool (modelling method) in the Red River basin to analyze hydrology, suspended sediment and organic carbon transport at a daily time step in order to diagnose impacts of the global changes by separating the effect of climate variability and anthropogenic influences (damming). The specific objectives are: (1) to characterize the hydrology and to quantify the suspended sediment concentration and fluxes of the Red River basin at a daily time step; (2) to assess the impacts of climate variability and dam constructions on discharge and sediment in a separate way; (3) to quantify particulate and dissolved organic carbon at a daily time step and to assesses the impacts of climate variability and dams.

The study is focused on the period of 2000-2013 as depending on the data availability (both remote sensing data and in-situ measurement data).

Chapter 2

Materials and Methods

2. CHAPTER Ⅱ: Materials and Methods

Global Theme of the Materials and Method

Figure 2-1 illustrates the materials and methods for this study.

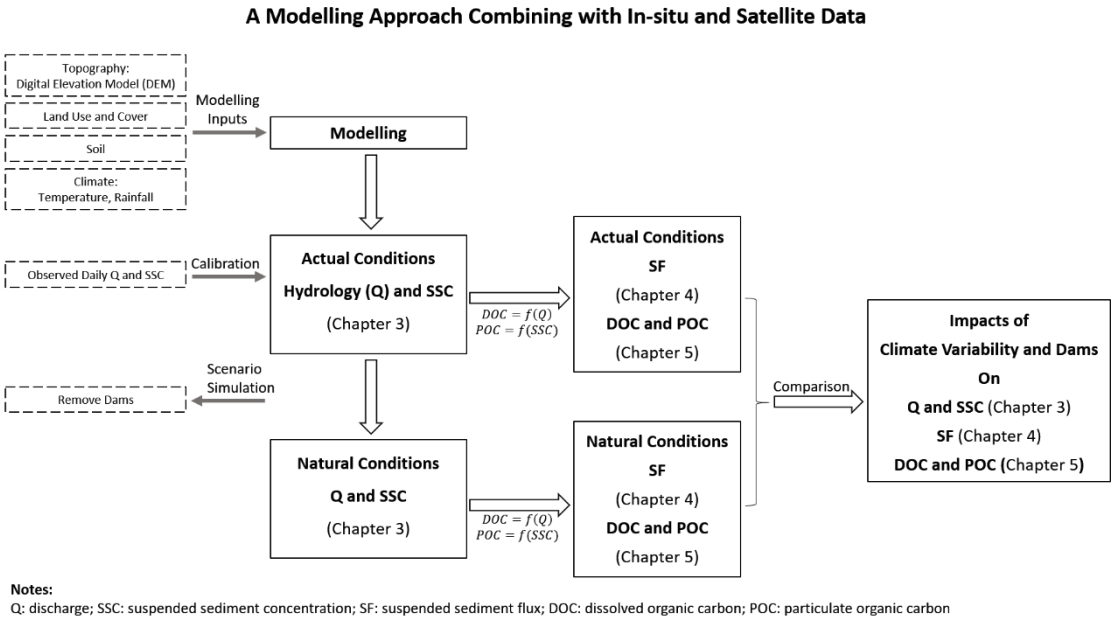

Figure 2-1 Global theme of materials and methods for this study.

2.1. Study Area

2.1.1. General information

The Red River basin located in South-East Asia (Figure 2-2). It is one of the five largest river basins (the Yellow, Yangtze, Pearl, Red and Mekong river basins) in East and Southeast Asia, and is an important contributor of fluvial matters to the western Pacific Ocean (Wang *et al.*, 2011).

The Red River basin is the second largest river in Vietnam and is from the longitude 100.00° to 107.17° East and from the latitude 20.00° to 25.50° North. It is a portion of the international border among China, Laos and Vietnam. The total area of the Red River basin is approximately 159,000 km^2 of which 49% lies in China, 0.9% in Laos and 50.1% in Vietnam (Le, 2005). Numerous inter-linked rivers, estuaries and coastal waters in the Red River basin make it play an important role in economics, culture and politics in both China and Vietnam.

The terrain is generally high in the northwest, dominated by alpine valley regions, and low in the southeast (Figure 2-3). Rocks in this basin are mainly sandy shale in the north and limestone, metamorphic rock and magmatic rock in the middle and in the south. The main soil types are Acrisols, such as latosol, red earth, yellow-brown soil and fluvisol (Le, 2005; Bai et al., 2015).

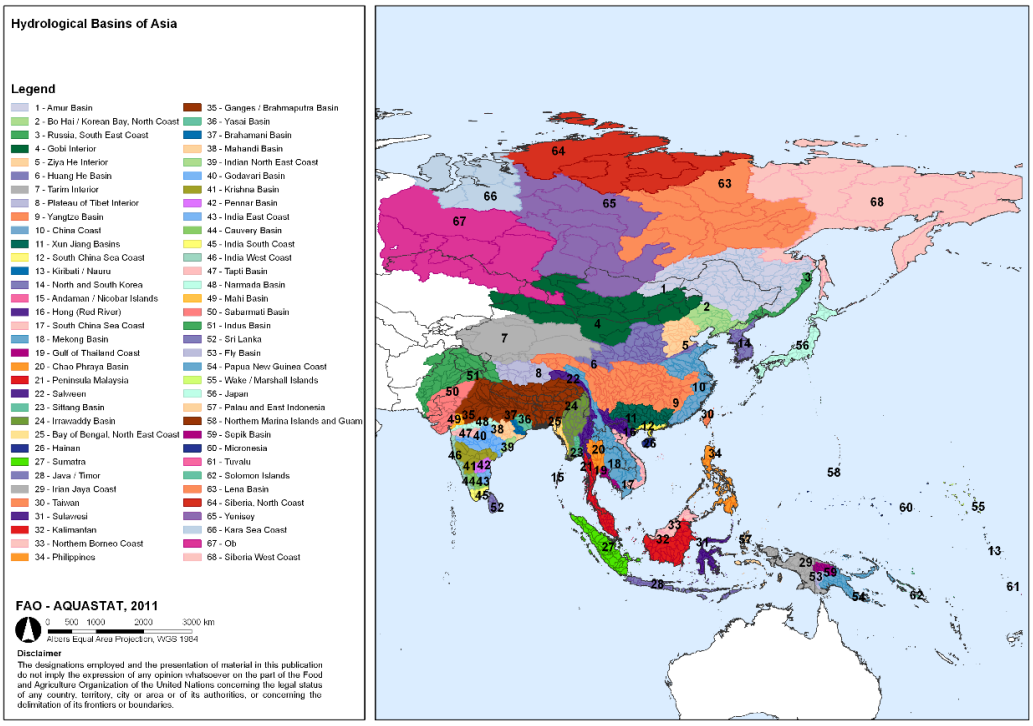

Figure 2-2 Hydrological basins of Asia (AQUASTAT, 2011)

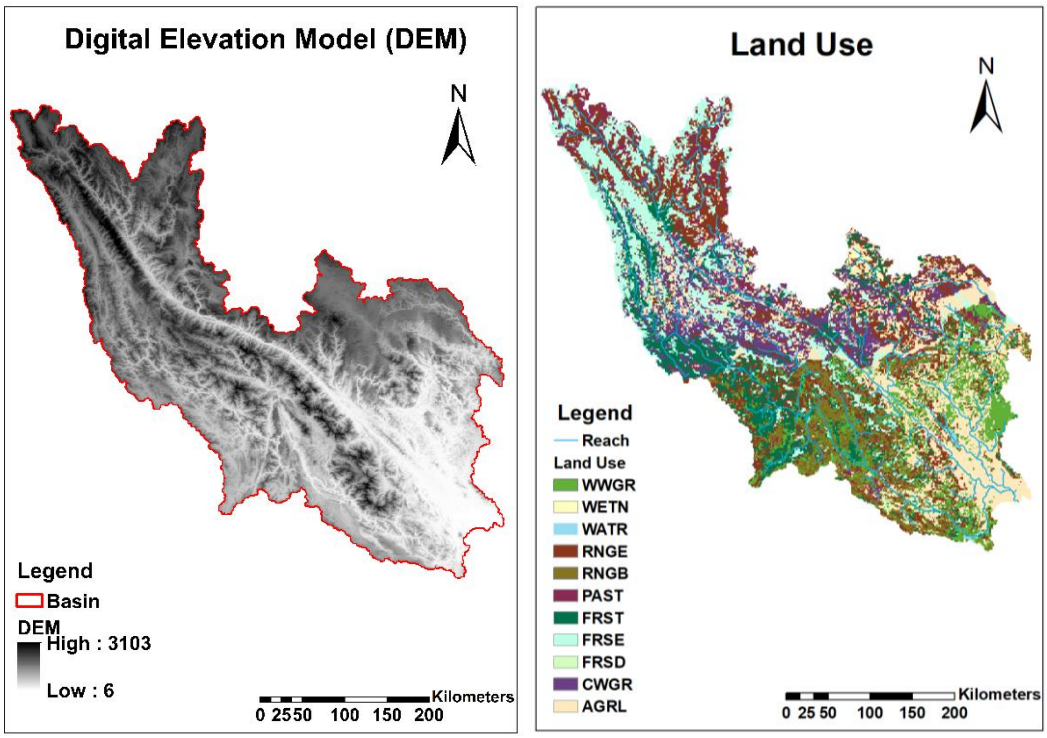

Figure 2-3 Digital Elevation Model (DEM, sourced from SRTM: http://www2.jpl.nasa.gov/srtm) and land use of the Red River basin.

The Red River has three main tributaries (Figure 2-4). The upper part of the main river, before Son Tay, is called the Thao River which named Yuan Jiang or Hong He in China. The tributary on the right bank is the Da River, named Li Xian Jiang in China. The Lo River, named Pan Long Jiang in China, joins the main branch from the left bank. These

three tributaries converge on the Red River 20 km upstream to the Son Tay gauging station.

The Thao River originates in Dali, Yunnan Province (China) which is at the foot of the Himalaya mountains with an elevation of 2650 m. The Red River basin in China is mainly in mountainous regions. The drainage area at Yen Bai station is around 48,500 km^2. The total length of the Thao River is 910 km, of which China shares 692 km (Le, 2005), and the average gradient of the riverbed of this section is 3.9‰ (Zhu *et al.*, 2012). This sub-basin is rich in latosol and red earth, and is vulnerable to soil erosion, therefore, the Thao River is colored into red, which derives the name of the Red River.

The Da River has its source in the Yunnan Province, near to that of the upstream Red River, at an elevation of more than 2000m (Dang *et al.*, 2013b). The Da River basin is also dominated by mountainous areas. Its total length is around 1000 km, 480 km of which is in China's territory. The total drainage area of this sub-basin is approximately 52,780 km^2. The Lo River basin is around 470 km with 275 km in Vietnam. The drainage area of this basin is around 30,370 km^2.

Due to the accessibility of the data and considering the influence of the tide, our study area focused only on the continental basin with a surface of 137,230 km^2 that drained down to Son Tay which is the outlet of the continental basin and the apex of the delta.

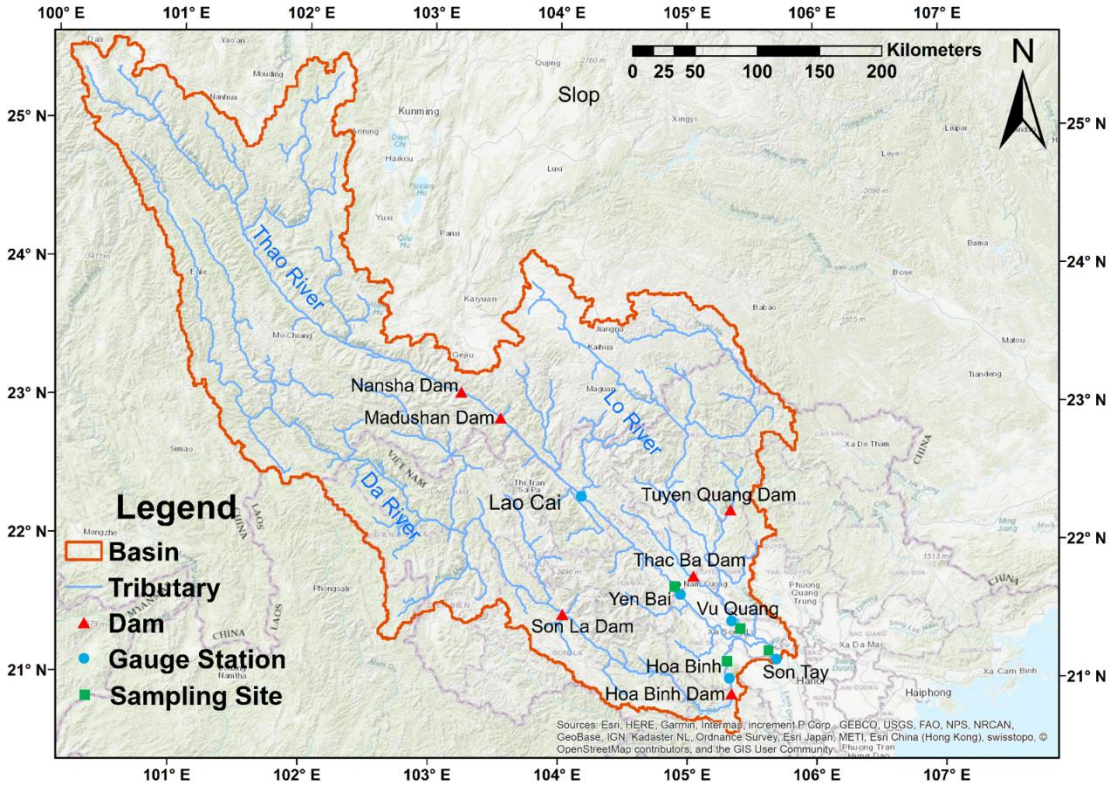

Figure 2-4 The Red River basin: main gauge station (blue point), sampling site (green square) and important dams (red triangle).

2.1.2. Climatic characteristics

The Red River basin is located in low-latitude subtropical and tropical monsoon climate zones. Generally, the south of the basin is more humid and hot than the north part. Mean annual humidity in China's part is around 67-70% and in Vietnam's part is from 82 to 84% (Le, 2005).

The changes of four seasons are not obvious, however rainy and wet seasons are distinctive. Rainy seasons are from May to October due to the southwest monsoon while the wet season from November to April. 80% of the total annual rainfall is coming from the rainy seasons, and intensive rainfall is mainly concentrated in June to August and is unevenly distributed temporally and spatially. The mean annual rainfall is around 1500 mm (Le, 2005).

Due to the big altitude differences in the mountainous regions, the vertical distribution of temperature was significantly different. The mean annual temperature varies from 14 to 16 ℃ in the high mountain regions and it rises above to 24-27 ℃ in the lower part (Le, 2005; Gu, 2016).

Potential evapotranspiration (PET) ranges between 880 and 1150 mm yr^{-1}, and its mean value was 1040 mm yr^{-1} (Le *et al.*, 2007). Simons et al. (2016) who used global satellite-derived data to calculate actual evapotranspiration in the whole watershed, showed values in the range of 860 to 1117 mm yr^{-1}.

2.1.3. Hydrological characteristics and water resources

The water volume of the Red River is rich, the annual water volume is around 130 km^3, among which 48 km^3 is coming from China (Le, 2005; Li, 2017). The water yield of the whole basin is around 810,000 m^3 km^{-2} yr^{-1} (Le, 2005). The water yield in China's part is 647,000 m^3 km^{-2} yr^{-1}, which is the second biggest water yield basin in southwest China after the Brahmaputra basin and following by the Nujiang (Salween) and Lancangjiang (Mekong) basins.

The runoff in this basin is mainly fed by precipitation which makes the hydrology in this region affected by the monsoon climate and results in great inter-seasonal variations in river flows (FAO, 2011b; Li et al., 2016; Li et al., 2008). The spatial distribution of water resource varies according to the distribution of rainfall. Corresponding with temporal precipitation distribution, the runoff is also uneven in intra-annual distribution: flood season occurs from May to October during which time the accumulated runoff accounts for more than 75% of the total annual runoff; low water seasons occur from November to April. The lowest discharge of the upstream in China usually occurs in March, and the minimum discharge observed near the boundary was 28.7 m^3 s^{-1} in 1963 (Ren *et al.*, 2007). The lowest discharge at Son Tay generally showed up in March (Li et al., 2016), and from the discharge data we collected, the minimum daily discharge at Son Tay during 2000-2015 was 493 m^3 s^{-1} (in February 2010). Peak runoff usually occurs in August, and the maximum flood was 8050 m^3 s^{-1} observed at the

gauge station near the boundary in China in 1986 (Xie, 2002), while it was 37,800 m^3 s^{-1} at Son Tay in 1971 (Luu *et al.*, 2010).

Groundwater is abundant and is an important part of water resource in Vietnam, and about 40% of the groundwater resource is north (Le, 2005). The groundwater resource in the Red River basin is abundant too, accounting for around 58% of total streamflow and is a critical component of river flow during winter and spring (Le, 2005; Li, 2017).

The hydrology characteristics of the three main tributaries are different (Figure 2-5). From the hydrology data that we collected from the Vietnam Ministry of Natural Resources and Environment (MONRE) during 2000-2014, the mean annual discharge of the Thao River at Yen Bai station is 655 m^3 s^{-1} and the mean annual suspended sediment concentration is 762 mg L^{-1}. At the Vu Quang station on the Lo River, the mean annual discharge is 894 m^3 s^{-1} and the mean annual suspended sediment concentration is 117 mg L^{-1}. At the outlet of the Da River, the mean annual discharge is 1645 m^3 s^{-1} and the mean annual suspended sediment concentration is 45 mg L^{-1}. The Thao river is the main contributor of suspended sediment to Son Tay station while the Da river is the main contributor of discharge. At Son Tay station, the mean annual discharge is 3136 m^3 s^{-1} and the mean annual suspended sediment concentration is 171 mg L^{-1}.

Due to the influence of the southwest monsoon (from May to October), 75% of the water yield during these seasons, and the maximum discharge and water yield occur from July and August (Figure 2-5). The Da River is the main contributor of the streamflow to the downstream Son Tay station, around half of the water at Son Tay is contributed by the Da River. The Thao and Lo rivers contribute around 21% and 29% of the water volume to Son Tay, respectively.

The average monthly mean SSC from May to October is around 1.6 times higher than the annual mean SSC, and 4.3 times higher than the average monthly mean SSC during dry seasons (November to Aril). On the contrary to the water volume contributions to the Son Tay outlet, the SSC at Lao Cai and Yen Bai stations on the Thao River have much higher SSC than the other two stations on the outlet of Lo and Da rivers.

Water resource in this basin is mainly used for agriculture, industry and domestic supply. Agriculture consumes 76% and 82% of the total water demand in China and Vietnam, respectively; industry use is 12% and 7% in China and Vietnam, respectively; domestic accounts for 12% and 3% in China and Vietnam, respectively (Le, 2005; Li, 2017). The agriculture in this basin in mountain areas is mainly depending on rainfed (Vezina *et al.*, 2006; Phan Ha *et al.*, 2012), therefore irrigation water intake is not taken into account in our study.

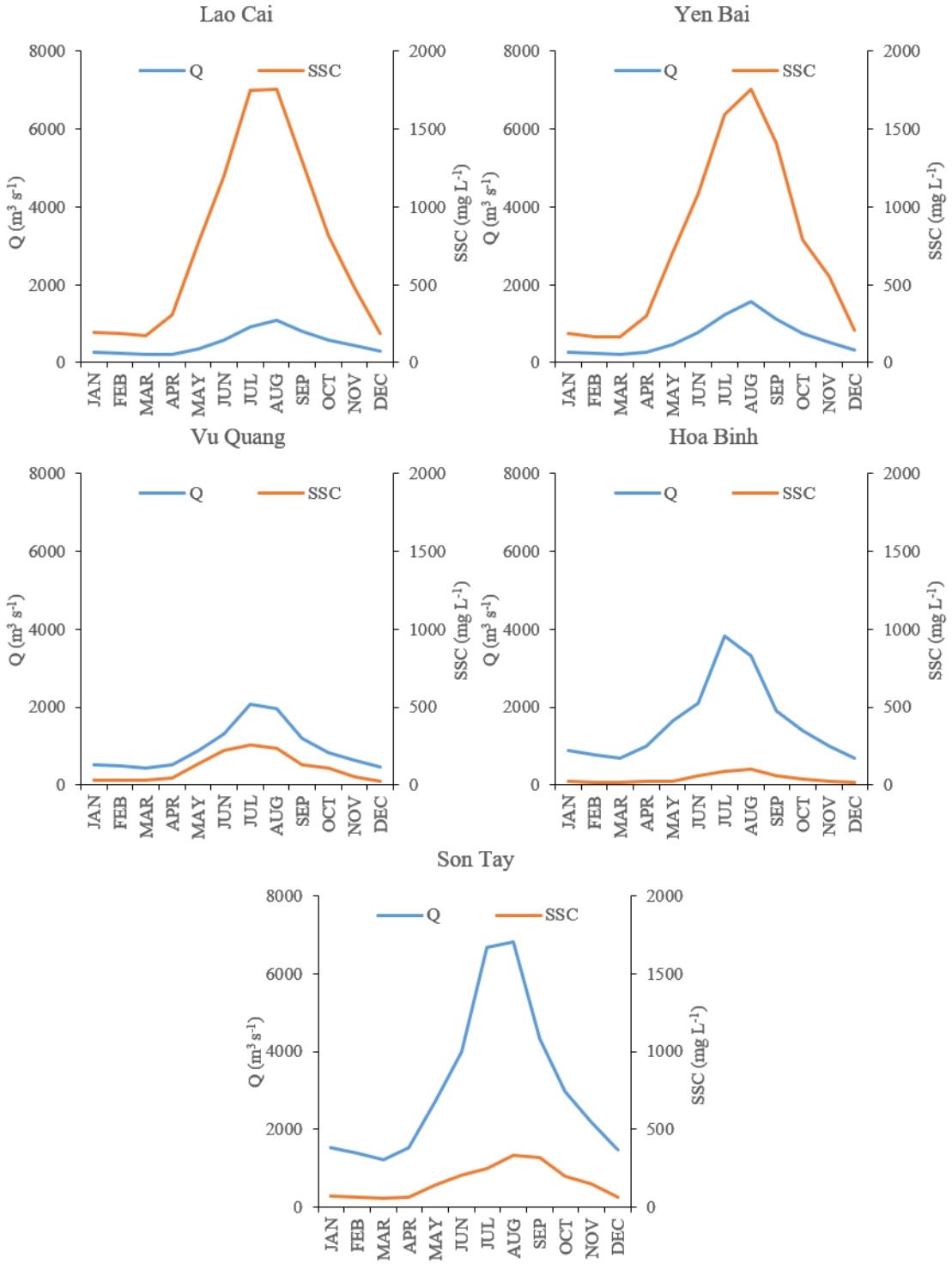

Figure 2-5 Monthly mean discharge (Q) and suspended sediment concentration (SSC) during 2000-2014 at five stations. Data obtained from the Vietnam Ministry of Natural Resources and Environment (MONRE).

2.1.4. Land use and cover

Due to the population and economic growths, the land use and cover have changed within this basin, both in China and Vietnam. Deforestation rate in Southeast Asia has been among the highest in the tropics, and the expansion of agricultural land is the most pervasive anthropogenic land conversion process in Asia (Zhao *et al.*, 2006;

Stibig *et al.*, 2014). By the early 1990s, Vietnam's forest area reached lowest in history, but the two decades later experienced a significant increase in the forest area in both plantation and natural forests (Tan and Hung, 2015). In the study area of this work, during 2000-2010, the land use barely changed: only 6% of the bare land changed to agricultural land (Le *et al.*, 2018), therefore, we hypothesize that the impacts of the land use change during 2000-2013 on discharge, suspended sediment and organic carbon were not significant and were taken into account in this study.

The forest is the main land cover through the whole basin, accounting for 52% of the total area of the basin (Dang, 2006). Forest accounts for different proportions in each sub-basin: 54% in the Thao river basin; 74% in the Da river basin and 23% in the Lo river basin. In the upper part of the Thao basin (in China's part), the forest is dominated by coniferous forest, and the upper part of the Da basin forest is mainly broad-leaved forest (Gu, 2016).

Agriculture shares 20% of the whole basin while industrial plants share 20%. Agriculture accounts for more in the Thao (19%) and Da (13%) basin, and less in the Lo basin (8%). However, the industrial plants are dominated in the Lo basin, accounting 58%, while it accounts for 14% and 3% in the Thao and Da basins, respectively. Urban accounts for 1.4%, 0.3% and 0.6% in the Thao, Da and Lo basins, respectively and 1.2% for the whole basin.

Figure 2-6 showed the photos of the land use taken in the Thao (at Sa Pa, near Lao Cai station) and Da (near Hoa Binh station) basins. Sa Pa is popular tourist place in Vietnam, famous for rice terrace. Contour ploughing is a common cultivate way for rainfed rice farming in the mountainous areas in the Thao basin. Near Hoa Binh where the slope is flatter compared to upstream, the farmers take some bare land to cultivate some industrial plants.


(a) Sa Pa (near Lao Cai in Thao basin)


(b) Sa Pa (near Lao Cai in Thao basin)

Figure 2-6 Land use in the Thao and Da basins. Photos were taken at Sa Pa (a and b) in the Thao basin which is famous for rice terrace and at Hoa Binh (c and d) in the Da basin.

2.1.5. Basin social economy and human activities

The total population of the Red River basin is estimated at 30 million, and population density is low in the upper mountainous region and intensive in the delta part (Le, 2005). The population in China's part is about 15.25 million people, and agricultural communities account for more than 80% of the total population (Gu *et al.*, 2018).

Upper part in China, it is rich in nonferrous metals, such as Stannum and Copper. This area is also an important subtropical and tropical cash crops region. Sugarcane, peanut, banana, pineapple, pomegranate, tobacco and rice are the main cash crops. Therefore, there are some smelters and sugar refineries (Gu, 2016). Down to Vietnam, agriculture structure is similar to China's part. With the decrease of elevation and slope, urban and lowland agriculture are increasing. Important industrial zones are around Son Tay, such as the production of drinks, paper and chemicals (Le, 2005). In the mountainous region of both China and Vietnam, rural people take advantage of the mountains by contour tillage and terrace.

Besides agriculture and industry, dam constructions are another interference for the river systems. Figure 2-7 presented the dams that could be found in the google earth. At least 21 dams can be noticed in China and 21 can be noticed in Vietnam. Dams in the basin are mainly for generating electricity, flood controlling and irrigation (Le, 2005).

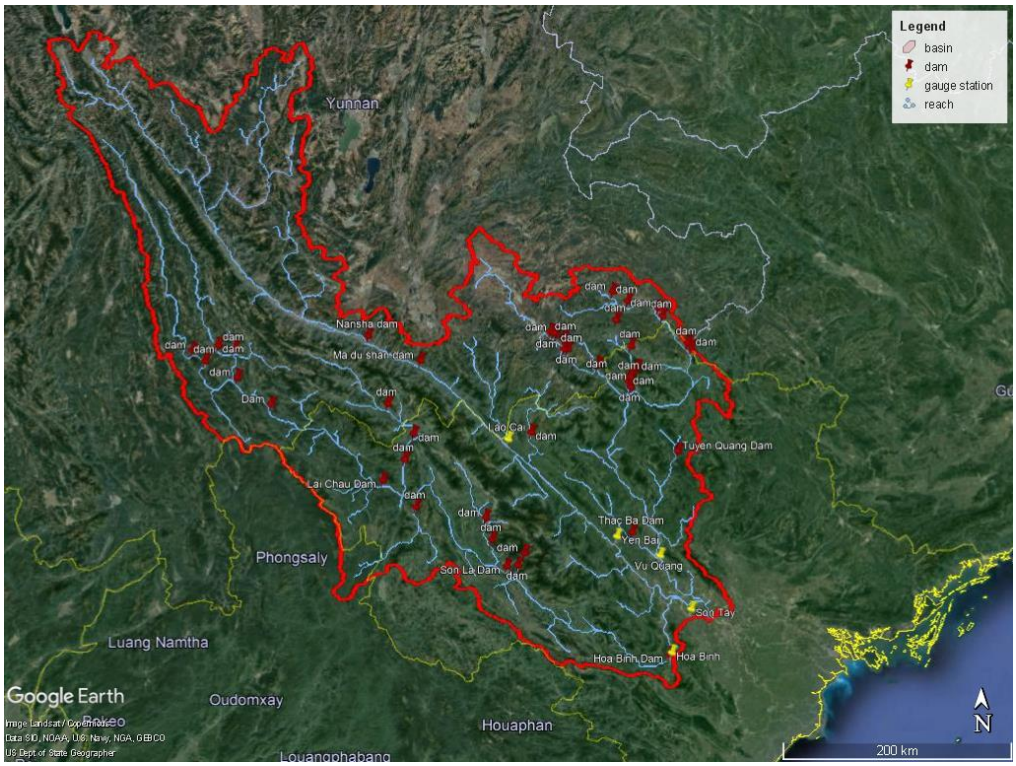

Figure 2-7 The dams that could be found in the Red River basin

On the Thao river, right now there are only Nansha and Madushan dam operated. However, on this tributary, 11-cascade dams are planned including Nansha and Madushan dams in China. On the Da river, there are at least 10 dams have been operated and 6 dams are going to be built in China, and in Vietnam, there are also some dams planned. Hoa Binh and Son La dams are the two biggest dams in Vietnam. Figure 2-8 showed the downstream of the Hoa Binh dam. On the Lo river, there are also many cascade dams. The biggest dam on the Lo river is Thac Ba dam which was built in 1971 and Tuyen Quang dam is also a large-capacity dam which was impounded in March 2008. Table 2-1 presented the main dams impounded in the study period. These 6 dams with large capacity have caused some impacts on the hydrological

system, and more details of the hydrology and suspended sediment transfer will be presented in Chapter 3 and 4.

Figure 2-8 The downstream of the Hoa Binh dam.

Table 2-1 Basic characteristics of the dams that are taken into account in this study.

Name (basin)	**Construction**	**Operation**	**Capacity ($\times 10^9$ m^3)**	**Reservoir surface area (km^2)**	**Mean annual discharge (m^3/s)**	**Maximum discharge (m^3/s)**
Nansha (Thao)	Feb 2006	Nov 2007	0.26	8.7	261	-
Madushan (Thao)	Dec 2008	Dec 2010	0.55	-	302	-
Hoa Binh (Da)	1980	1989	9.50	208	1780	2400
Son La (Da)	Dec 2005	Dec 2010	9.26	224	1530	3438
Thac Ba (Lo)	1965	Oct 1971	2.90	235	190	420
Tuyen Quang (Lo)	Dec 2002	Mar 2008	2.24	81.5	318	750

2.2. Dataset

The observed hydrology and biochemistry data used in this study include:

- daily discharge (Q), daily suspended sediment concentration (SSC) from 2000 to 2014.
- discrete dissolved organic carbon (DOC) and particulate organic carbon (POC) from 2003 to 2013.

2.2.1. Discharge and suspended sediment concentration dataset

The daily Q and SSC data were provided by the Land-Ocean-aTmosphere regional coUpled System study center (LOTUS, http://lotus.usth.edu.vn/), originating from the Vietnam Ministry of Natural Resources and Environment (MONRE). The data period is from 2000 to 2014.

Daily Q and SSC data were provided from 2000 to 2014 at 5 gauge stations: Lao Cai and Yen Bai on the Thao River; Vu Quang at the outlet of the Lo River; Hoa Binh at the outlet of the Da River (Figure 2-4).

2.2.2. Dissolved and particulate organic carbon dataset

POC and DOC data gained from two sources. The first one was provided by the Laboratory of Environmental Chemistry, Institute of Natural Product Chemistry, Vietnam Academy of Science and Technology, detail information of sampling and laboratory measurements can be found in Le et al. (2017a). Samplings were taken generally one to three times per month during 2003-2004, 2008-2010, 2012-2013 at Yen Bai, Vu Quang, Hoa Binh and Son Tay. Due to the sampling difficulties, data during some years and some months are absent. The second source was from Dang (2006) where POC and DOC concentrations at Yen Bai, Vu Quang, Hoa Binh and Son Tay from 2007-2009 can be found. Sampling frequency was generally monthly or bimonthly. Sampling sites are presented in Figure 2-4.

2.3. General Introduction of the Modelling Approach

2.3.1. SWAT general introduction

Soil and Water Assessment Tool (SWAT) is a physically-based, semi-distributed hydrological model developed by Dr. Jeff Arnold for the USDA Agricultural Research Service (ARS) to simulate the quality and quantity of surface and groundwater and predict the environmental impact of land use, land management practices, and climate change, and it requires specific information such as topography, weather, soil properties, land use and land management practices occurring in the basin (Neitsch *et al.*, 2009).

The SWAT model allows us to simulate the water, sediment and agricultural chemical yields in large complex watersheds where there might be no monitoring data with over long periods of time; it can quantify the relative impact of alternative input data, such

as changes in management practices, climate and land cover, etc, on water regime, water quality, suspended sediment, soil erosion and other variables; also, it is a continuous-time model which enables users to study long-term impacts from daily to annual scale. The SWAT has been applied all over the world from small to large basins and performed satisfactorily (Gassman *et al.*, 2007, 2014; Tan *et al.*, 2019).

For modelling, SWAT firstly divides a basin into a number of sub-basins which will enable users to reference different areas of the watershed to one another spatially. Then sub-basins are further subdivided into hydrological response units (HRU) with homogeneous land use, soil type and slope (Figure 2-9).

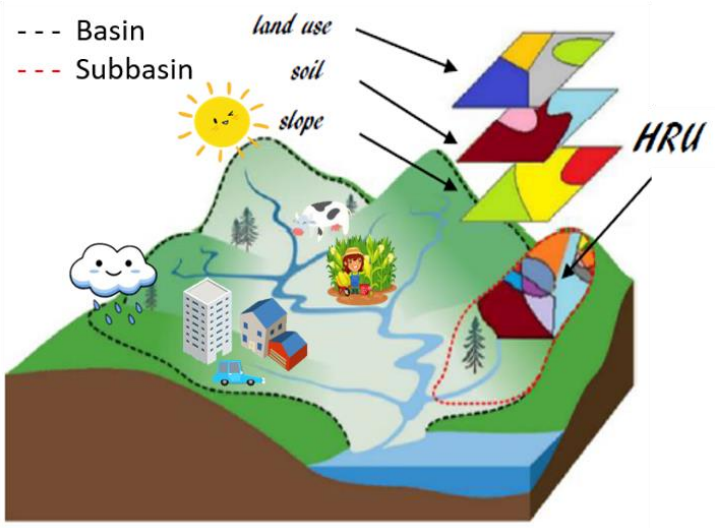

Figure 2-9 Sub-basin and hydrological response units (HRU) partitions in SWAT model.

2.3.2. SWAT application

SWAT is widely used in assessing soil erosion prevention and control, non-point source pollution control and regional management in watersheds. The literature database of SWAT applied in different basins and variables can be found in https://www.card.iastate.edu/swat_articles/.

In Asian basins, SWAT has been applied and presented well performance in various simulations (Gassman *et al.*, 2007, 2014; Piman *et al.*, 2013; Giang *et al.*, 2014; Ma *et al.*, 2015; Shrestha *et al.*, 2018), as well as in some tropical areas (Bannwarth *et al.*, 2014; Fukunaga *et al.*, 2015; Marhaento *et al.*, 2018; Marques da Silva *et al.*, 2018; Rodrigues *et al.*, 2018; Yaduvanshi *et al.*, 2018). In South-East Asia, SWAT was commonly applied to Vietnam and Thailand (Tan *et al.*, 2019), such as Mekong river basin (Piman *et al.*, 2013, 2016; Shrestha *et al.*, 2018) or some local small-scale basins (Vu *et al.*, 2012; Bannwarth *et al.*, 2014; Giang *et al.*, 2014; Le and Sharif, 2015; Ngo *et al.*, 2015; Ha *et al.*, 2018; Marhaento *et al.*, 2018; Nguyen-Tien *et al.*, 2018). This paper applied the SWAT model in a large-scale basin in tropical South-East Asia.

2.3.3. Hydrological modelling component in SWAT

Water balance is the driving force in SWAT regardless of what kind of problems users

want to deal with. Two major divisions are considered in simulating of the hydrology of a watershed: the hydrological cycle over the lands (Figure 2-10), and in the channel network. SWAT simulates the hydrologic cycle based on the water balance equation:

$$SW_t = SW_0 + \sum_{i=1}^{t}\left(R_{day} - Q_{surf} - E_a - W_{seep} - Q_{gw}\right) \quad (1)$$

where SW_t is the final soil water content (mm H_2O), SW_0 is the initial soil water content on day i (mm H_2O), t is the time (days), R_{day} is the amount of precipitation on day i (mm H_2O), Q_{surf} is the amount of surface runoff on day i (mm H_2O), E_a is the amount of evapotranspiration on day i (mm H_2O), W_{seep} is the amount of water entering the vadose zone from the soil profile on day i (mm H_2O), and Q_{gw} is the amount of return flow on day i (mm H_2O).

The land phase of the hydrologic cycle controls the amount of water, sediment, nutrient and pesticide loadings to the main channel in each sub-basin. Over the lands, SWAT simulates surface runoff volumes and peak runoff rates for each HRU using daily or sub-daily rainfall amounts. For computing surface runoff volume, a modification of the Soil Conservation Service (SCS) curve number method (USDA Soil Conservation Service, 1972) is used. Peak runoff rate is predicted with a modification of the rational method which calculates the peak runoff rate as a function of the proportion of daily precipitation that falls during the sub-basin, the daily surface runoff volume, and the sub-basin time of concentration. Lateral flow in the soil profile is calculated simultaneously with redistribution. A kinematic storage model is used to predict lateral flow in each soil layer. The model accounts for variation in conductivity, slope and soil water content. Groundwater is partitioned into two aquifer systems by SWAT: a shallow, unconfined aquifer which contributes return flow to streams within the basin; a deep, confined aquifer which contributes return flow to streams outside the watershed.

The instream routing phase of the hydrologic cycle is the movement of water, sediments, etc. through the channel network of the basin to the outlet. In the routing phase, surface flow is simulated using a variable storage coefficient method developed by Williams (1969) or the Muskingum routing method (Cunge, 1969). In this work, the SCS curve number method and variable storage coefficient method, along with daily climate data, were used for surface runoff and streamflow computations.

Evapotranspiration includes evaporation from rivers and lakes, bare soil, and vegetative surfaces; transpiration from within the leaves of plants; and sublimation from ice and snow surfaces. The model computes evaporation from soils and plants separately. Potential soil water evaporation is estimated as a function of potential evapotranspiration and leaf area index (area of plant leaves relative to the area of the HRU). Actual soil water evaporation is estimated by using exponential functions of soil depth and water content. Plant transpiration is simulated as a linear function of potential evapotranspiration and leaf area index. In this work, the Hargreaves method

(Hargreaves *et al.*, 1985), which requires air temperature only, was chosen to calculate the potential evapotranspiration (PET).

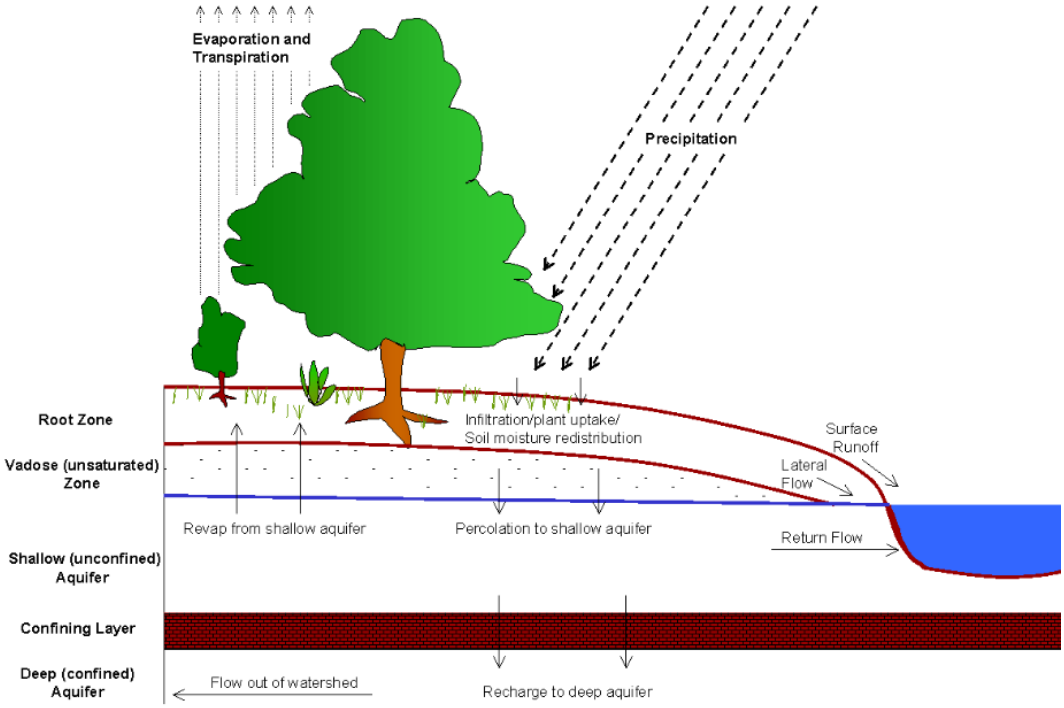

Figure 2-10 The land phase of the hydrologic cycle in SWAT (Neitsch et al., 2009).

2.3.4. Sediment modelling component in SWAT

SWAT considers sediment transport both over the landscape component and in the channel component (Figure 2-11).

In the landscape component, sediment comes from erosion, both geologic erosion and accelerated erosion (induced by human activities). SWAT model tracks particle size distribution of eroded sediments and routes them through ponds, channels, and surface water bodies. Erosion caused by rainfall is calculated with the Modified Universal Soil Loss Equation (MUSLE) for each HRU (Williams, 1975; Neitsch *et al.*, 2009). This equation considers the surface runoff volume, peak runoff rate, soil erodibility, land cover and management, topographic and coarse fragment factor, as following:

$$sed = 11.8 \cdot \left(Q_{surf} \cdot q_{peak} \cdot area_{hru}\right)^{0.56} \cdot K_{USLE} \cdot C_{USLE} \cdot P_{USLE} \cdot LS_{USLE} \cdot CFRG \qquad (2)$$

where sed is the sediment yield on a given day (t), Q_{surf} is the surface runoff volume (mm H_2O ha^{-1}), q_{peak} is the peak runoff rate (m^3 s^{-1}), $area_{hru}$ is the area of the HRU (ha), K_{USLE} is the USLE soil erodibility factor, C_{USLE} is the USLE land cover and management factor, P_{USLE} is the USLE support (agricultural) practice factor, LS_{USLE} is the USLE

topographic factor and CFRG is the coarse fragment factor.

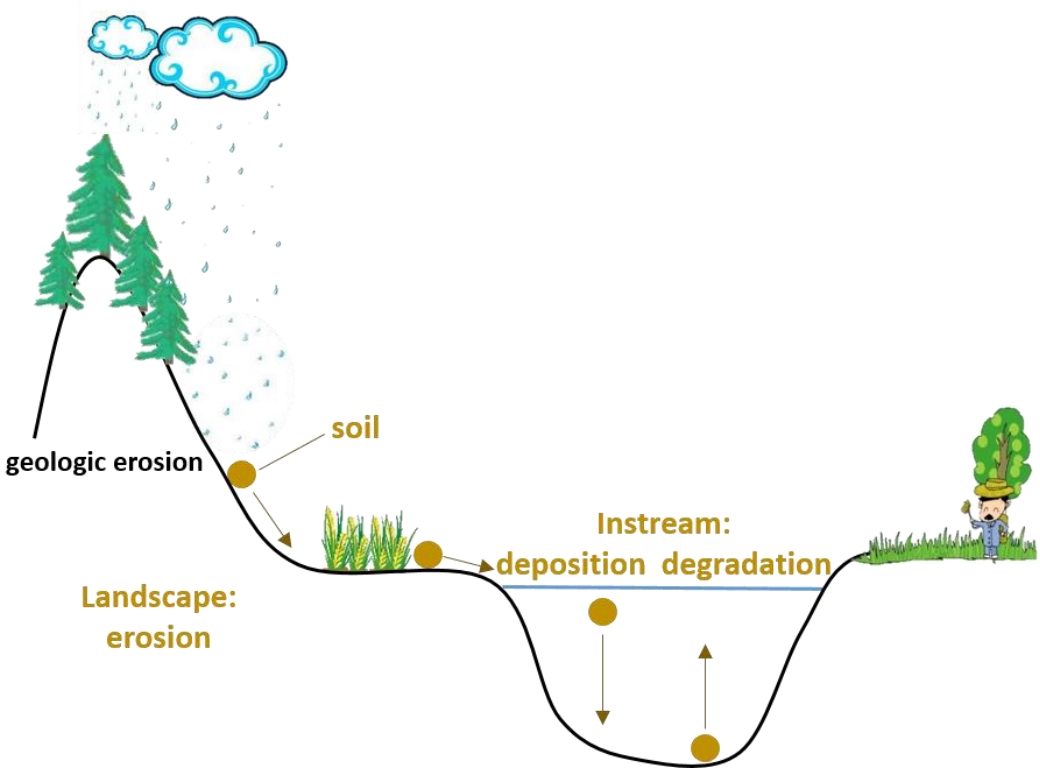

Figure 2-11 Sediment transport in landscape and channel components.

The sediment routing in the channel is a function of two processes: deposition and degradation, operating simultaneously in the reach. SWAT will compute deposition and degradation using the same channel dimensions for the entire simulation. Each subbasin has the main routing reach where sediment from upland subbasins is routed and then added to downstream reaches. The Simplified Bagnold equation (1977) is used as a default method for the sediment routing in stream channels which determines degradation as a function of channel slope and flow velocity. The maximum amount of sediment that can be transported is a function of the peak channel velocity, as following:

$$conc_{sed,ch,mx} = c_{sp} \cdot {v_{ch,pk}}^{spexp} = c_{sp} \cdot \left(\frac{q_{ch,pk}}{A_{ch}}\right)^{spexp} = c_{sp} \cdot \left(\frac{prf \cdot q_{ch}}{A_{ch}}\right)^{spexp} \quad (3)$$

where $conc_{sed,ch,mx}$ is the maximum concentration of sediment that can be transported by the water (t m^{-3}), c_{sp} is a coefficient defined by the user, $v_{ch,pk}$ is the peak channel velocity (m s^{-1}), spexp is an exponent defined by the user, $q_{ch,pk}$ is the peak flow rate (m^3 s^{-1}), A_{ch} is the cross-sectional area of flow in the channel (m^2), prf is the peak rate adjustment factor, and q_{ch} is the average rate of flow (m^3 s^{-1}). More details on these parameters and their usual ranges are reported in chapter 3.

The maximum concentration of sediment calculated with Equation 3 is compared to

the concentration of sediment in the reach at the beginning of the time step ($conc_{sed,ch,i}$, in t m^{-3}). If $conc_{sed,ch,i} > conc_{sed,ch,mx}$, deposition is the dominant process in the reach segment and the net amount of sediment deposited is calculated as:

$$sed_{dep} = \left(conc_{sed,ch,i} - conc_{sed,ch,mx}\right) \cdot V_{ch} \quad (4)$$

where sed_{dep} is the amount of sediment deposited in the reach segment (t), and V_{ch} is the volume of water in the reach segment (m^3).

If $conc_{sed,ch,i} < conc_{sed,ch,mx}$, the available stream power is used to re-entrain loose and deposited material until all of the material is removed. Excess stream power causes bed degradation, and the net amount of sediment re-entrained is adjusted for stream bed erodibility and cover as following:

$$sed_{deg} = \left(conc_{sed,ch,mx} - conc_{sed,ch,i}\right) \cdot V_{ch} \cdot K_{ch} \cdot C_{ch} \quad (5)$$

where sed_{deg} is the amount of sediment re-entrained in the reach segment (t), K_{ch} is the channel erodibility factor, and C_{ch} is the channel cover factor.

2.4. Modelling Setup for Hydrology and Suspended Sediment

2.4.1. Modelling inputs for SWAT

SWAT requires inputs as topography, land cover, soils and meteorological data. Resolutions and download links for DEM, land use and soil can be found in Table 2-2.

Table 2-2 SWAT Inputs Datasets

Data Type	Resolution/Time Scale/Period	Source
Topography (DEM)	1×1 km	Shuttle Radar Topography Mission (SRTM, http://www2.jpl.nasa.gov/srtm)
Land Cover	1×1 km	Global Land Cover 2000 database (https://forobs.jrc.ec.europa.eu/products/glc2000/glc2000.php)
Soil Types	1×1 km	Harmonized World Soil Database (http://webarchive.iiasa.ac.at/Research/LUC)
Temperature	daily scale Jan-1998 to Jul-2014	Climate Forecast System Reanalysis: Global Weather Data for SWAT (https://globalweather.tamu.edu/)
Precipitation	daily scale 0.25° × 0.25° Jan-1998 to Dec-2014	Tropical Rainfall Measuring Mission (TRMM, https://pmm.nasa.gov/TRMM)

A Digital Elevation Model (DEM) was downloaded from the Shuttle Radar Topography Mission (SRTM), which is SRTM is a cooperative project between the National Aeronautics and Space Administration (NASA) and the National Imagery and Mapping Agency (NIMA) of the U.S. Department of Defense (Farr and Kobrick, 2000). This topographic data has been widely used to determine hydrological properties of a landscape, including the extraction of drainage networks and upstream catchment

areas (Farr and Kobrick, 2000). In our study, the landscape slopes were divided into 5 classes by SWAT based on the information from DEM (Figure 2-12a).

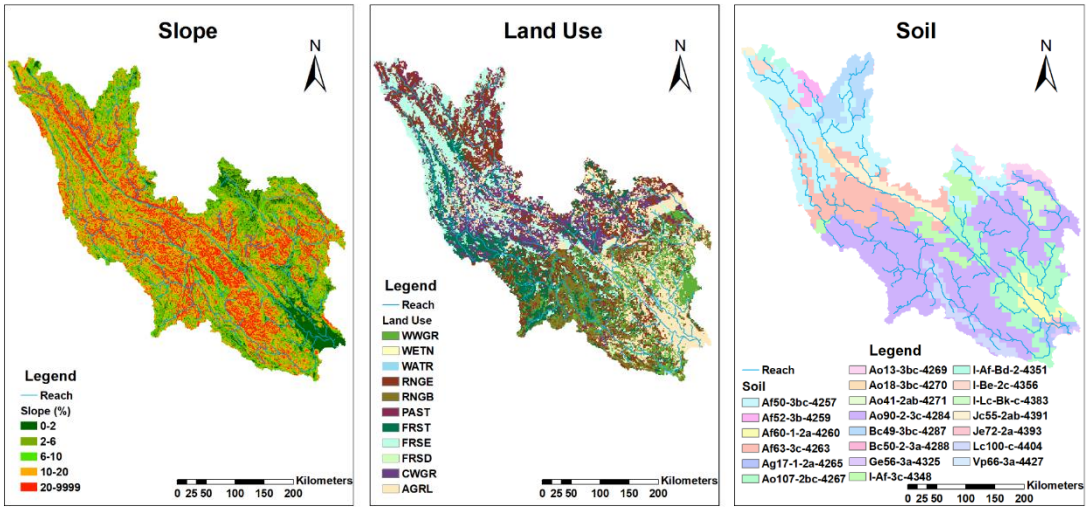

Figure 2-12 SWAT inputs: (a) slop classes; (b) land use map; (c) soil types

Land cover (Figure 2-12b) is from the Global Land Cover 2000 database. The dominant lands are forest (27.56%, with 14.65% of evergreen forest (FRSE in SWAT model); 12.49% of mixed forest (FRST); 0.42% of deciduous forests (FRSD)), agriculture (ARGL, 21.16%), range-grasses (RNGE, 19.94%), wheatgrass (19.57%: with 10.03% of western wheatgrass (WWGR); 9.54% of crested wheatgrass (CWGR)). Land use code and its common name are in Table 2-3.

Table 2-3 Code and its related common name for land use and soil map.

Land Use		Soil Type		
Code	**Common Name**	**Code**	**Common Name**	**Texture**
WWGR	Western wheatgrass	Af50-3bc-4257	Ferric Acrisols	CLAY
WETN	Wetlands-nonforested	Af52-3b-4259		CLAY
WATR	Water	Af60-1-2a-4260		SANDY_LOAM
RNGE	Range-grasses	Af63-3c-4263		CLAY_LOAM
RNGB	Range-brush	Ag17-1-2a-4265	Gleyic Acrisols	SANDY_LOAM
PAST	Pasture	Ao107-2bc-4267	Orthic Acrisols	SANDY_CLAY_LOAM
FRST	Forest-mixed	Ao13-3bc-4269		CLAY_LOAM
FRSE	Forest-evergreen	Ao18-3bc-4270		CLAY_LOAM
FRSD	Forest-deciduous	Ao41-2ab-4271		LOAM
CWGR	Crested wheatgrass	Ao90-2-3c-4284		CLAY_LOAM
AGRL	Agricultural Land	Bc49-3bc-4287	Chromic Cambisols	CLAY_LOAM
		Bc50-2-3a-4288		CLAY_LOAM
		Ge56-3a-4325	Eutric Gleysols	CLAY_LOAM
		I-Af-3c-4348	Lithosols	SANDY_CLAY_LOAM
		I-Af-Bd-2-4351		LOAM
		I-Be-2c-4356		LOAM
		I-Lc-Bk-c-4383		LOAM
		Jc55-2ab-4391	Calcaric Fluvisols	LOAM
		Je72-2a-4393	Eutric Fluvisols	LOAM
		Lc100-c-4404	Chromic Luvisols	LOAM
		Vp66-3a-4427	Pellic Vertisols	CLAY

The soil map (Figure 2-12c) was downloaded from the Harmonized World Soil

Database. 21 soil types are in this study area (Table 2-3), and most of these soils belong to Acrisols, such as Ferric Acrisols in the upper part and Orthic Acrisols in the lower part. Acrisols are characterized by the accumulation of low activity clays in an argic subsurface horizon and by a low base saturation level, and correlate with “Red and Yellow Earths”. Most Acrisols have a thin, brown, ochric surface horizon. The underlying albic subsurface horizon is normally whitish to yellow and overlies a stronger coloured yellow to the red argic subsurface horizon. Acrisols are found on acid rocks, mostly of Pleistocene age or older. They are most extensive in Southeast Asia, the southern fringes of the Amazon Basin, the southeastern USA and in both east and west Africa. Acrisols are easy to degrade and slake to form a hard surface under unprotected land, which is vulnerable to devastating surface erosion under rainfall.

In-situ observed climate data was unable to obtain, therefore, in this study, we took advantage of the satellite data which have been proved to produce good results on hydrology. Daily temperature data were obtained from the Global Weather Data in SWAT file format for a given location and time period. These data come from the Climate Forecast System Reanalysis (CFSR) of the National Centers for Environmental Prediction (NCEP). The CFSR is a reanalysis product. It is a global, high resolution, coupled atmosphere-ocean-land surface-sea ice system designed to provide the best estimate of the state of these coupled domains over this period. CFSR, combining with hydrology models, has been proved to result in similar accuracy results on large river basins (Dile and Srinivasan, 2014; Lauri *et al.*, 2014). Therefore, in this study, we used the temperature from CFSR as modelling inputs for the climate. Temperature stations covered by CFSR for the Red River basin are 624 and their locations were presented in Figure 2-13.

Daily precipitation data was obtained from the Tropical Rainfall Measuring Mission (TRMM, product 3B42 V7) which is a research satellite designed to provide needed information on rainfall by covering the tropical and sub-tropical regions of the Earth. Simons et al. (2016) compared several satellite-based precipitation products (TRMM, the Climate Hazards Group InfraRed Precipitation with Station dataset (CHIRPS), the global rainfall estimate based on the CPC MORPHing technique (CMORPH)) and actual evapotranspiration products in the Red River watershed in order to demonstrate that these datasets can be merged to examine hydrological processes before applying a numerical simulation model, and they found that TRMM rainfall product could provide reliable values in both space and time at this watershed. Rainfall stations covered by TRMM for the Red River basin are 208 and their locations were presented in Figure 2-13.

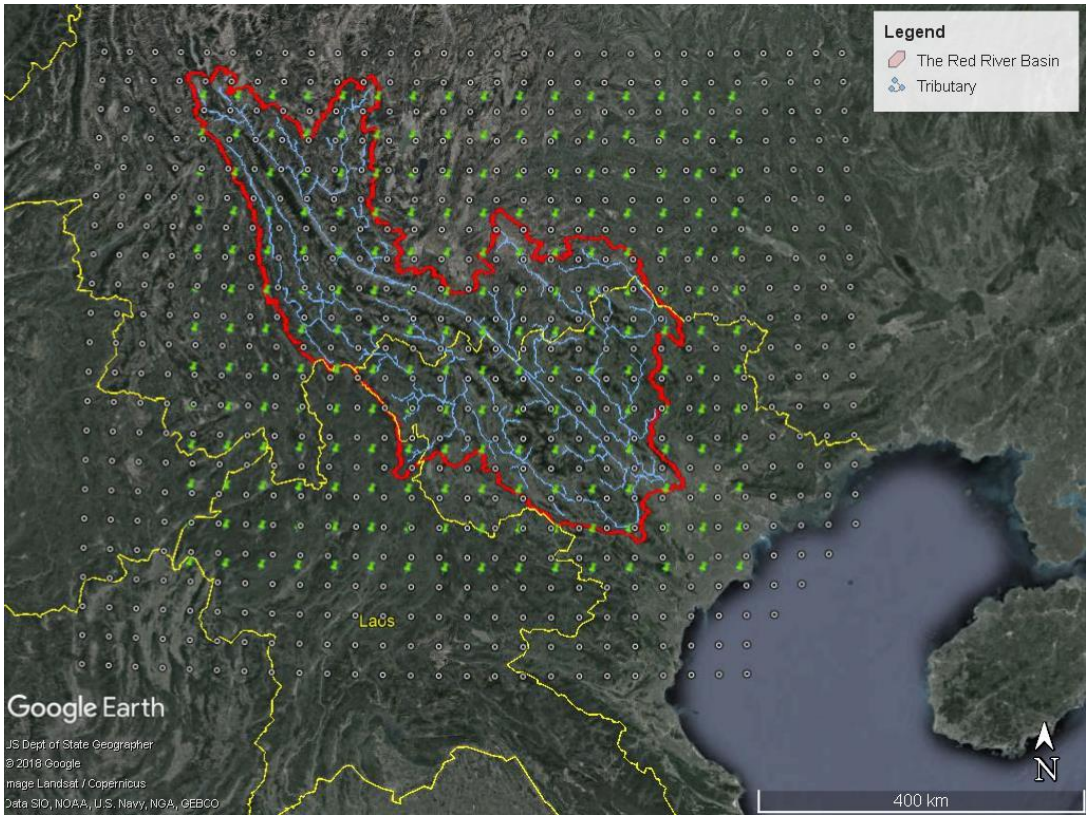

Figure 2-13 Temperature stations (black points) covered by the Climate Forecast System Reanalysis (CFSR) for the Red River basin and rainfall stations (green marks) covered by the Tropical Rainfall Measuring Mission (TRMM) for the Red River basin.

2.4.2. Dam implemented in SWAT

SWAT requires basic information, such as date of impoundment, reservoir surface area, emergency volume, principal volume, initial volume. The volume of outflow can be calculated by one of the following methods: measured daily outflow, measured monthly outflow, average annual release rate, controlled outflow with target release. As it is impossible to get the detailed outflow of dams, and in order to avoid the complex conditions of release operations, and to make the model able to be applied for future hydrology regime prediction, the average annual release rate method which releases the water whenever the dam volume exceeds the principal spillway volume was selected (Neitsch *et al.*, 2009). A minimum and maximum monthly releases were limited for the model according to the Q data we collected and to the release information from reference Le et al. (2007).

As mentioned in Chapter 2.1.5, inside this basin, there are at least 42 dams. Some of them were under construction during the simulation period. In our study, we added 6 important dams into the model, which are with large capacities and whose locations are close to the outlet of each sub-basin (Figure 2-4). Two dams are located on the mainstream of the Thao River, around 150 km and 100 km upstream of Lao Cai respectively; two are on the mainstream of the Da River; the other two are on two branches of the Lo River. Details of each dam were in Table 2-1.

2.5. Fluvial Organic Carbon Computation

2.5.1. Dissolved organic carbon

The equation for calculating the dissolved organic carbon (DOC) was from extracted the work of Fabre et al. (2019) who proposed a prediction of the DOC concentration ([DOC]) with daily discharge (Q). The equation between [DOC] and Q is as followed:

$$[DOC] = \frac{\alpha * Q}{\beta + Q} \quad (6)$$

with [DOC] in mg L^{-1}, Q in mm d^{-1}. This equation underlines the necessity to well simulate Q in order to obtain good results for [DOC]. The parameter α (mg L^{-1}) represents a potential of maximum [DOC] at the outlet of each sub-basin, and parameter β (mm d^{-1}) is the Q when the DOC concentration is half of α.

2.5.2. Particulate organic carbon

The equation for calculating the particulate organic carbon (POC) was proposed by Boithias et al. (2014) who generalized the relation between the POC and suspended sediment concentration (SSC) as followed:

$$\%POC = \frac{9.40}{SSC - a} + b \quad (7)$$

where %POC is the percentage of POC in the suspended sediment, and SSC is in mg L^{-1}, parameters *a* and *b* are linked to environmental variables related to each sub-basin (see details in Chapter 1). The parameter *a* is the vertical asymptote corresponding to the low SSC and the organic matter which is rich in OC, such as phytoplankton and residuals, and it is a basin-specific constant, including an anthropogenic impact in the basin; the parameter *b* is the horizontal asymptote representing the suspended matters with low POC in SS which nearly equals to soil organic carbon content, and it is also a basin-specific constant. (Boithias *et al.*, 2014; Fabre *et al.*, 2019)

A limit maximum %POC was set to avoid the denominator to be negative, i.e. when SSC is smaller than a, %POC is regarded as this maximum value.

2.6. Calibration processes

2.6.1. Discharge and Suspended Sediment Concentration calibration

SWAT2012 and ArcGIS10.4 were used in this study. The whole basin was divided into 242 sub-basins and then subdivided into 3812 different HRUs. The simulation was carried out at three temporal scales (daily, monthly and annually) during an overlapped period, from January 2000 to July 2014.

Data of daily Q and SSC from 2000 to 2014 obtained from the Vietnam Ministry of

Natural Resources and Environment (MONRE) at Lao Cai, Yen Bai, Vu Quang, Hoa Binh and Son Tay stations were used to calibrate the model. Figure 2-4 shows the location of each station. Time series plots and statistical methods were used to evaluate the performance of the model in simulating Q and SSC.

The model was calibrated at daily scale using Q and SSC from January 1998 to July 2014 with a two-year warm-up. Parameters were mainly calibrated manually, and the most sensitive ones were automatically calibrated by using SWAT-CUP (Abbaspour, 2015). SWAT-CUP is a tool that allows SWAT users to perform automatic calibrations (Arnold et al., 2012). Five algorithms are proposed for calibration purpose (Yang *et al.*, 2008; Abbaspour, 2015). The SUFI-2 (Sequential Uncertainty Fitting 2) algorithm (Yang *et al.*, 2008), which can identify appropriate parameters sets in a limited number of iterations, was selected in this study. Calibration of water balance and Q were first carried out, once they were well calibrated then the calibration of SSC was carried out. Values of the calibrated parameters for Q and SSC and their definitions and ranges were detailed in Chapter 3.5.

Sensitive hydrological parameters are chosen by literature reviews (Xu *et al.*, 2009; Cibin *et al.*, 2010; Guse *et al.*, 2014; Fukunaga *et al.*, 2015). Relative change of parameters was controlled within ±20%, and absolute change was done by referring to the aforementioned references and theoretical documents (Arnold et al., 2012; Neitsch et al., 2009). Based on actual information from the MONRE and literatures (Le, 2005; Le *et al.*, 2012), parameters like runoff curve number (CN2), soil evaporation compensation factor (ESCO), available water capacity of the soil layer (SOL_AWC), parameters related to groundwater (GW_REVAP, REVAPMN, RCHGR_DP, GWQMN, GW_DELAY) were calibrated to fit the actual water balance. Compared to the default values, ESCO was decreased and GW_REVAP was increased to increase the ET; SOL_AWC was increased by 20%, CN2 was decreased by 10%, REVAPMN was increased, RCHGR_DP and GWQMN were decreased to decrease the surface flow accordingly increase the groundwater flow. Other parameters related to hydrological processes were calibrated to fit the baseflow and peaks, and they were interpreted in the following sub-section.

Sensitive parameters of sediment were chosen from Equation 2 to 5, based on how the sediment was modelled. The suspended sediment concentrations of these three tributaries are very different due to their differences in topography, dams implements and agriculture activities. Therefore, parameters related to land erosion such as USLE_K, USLE_P and FILTERW, and to in-stream erodibility such as CH_COV1 and CH_COV2 were calibrated based on the characteristics of each sub-basin. Dams on the streams not only retain the sediment in reservoirs but also alter the distribution of the grain size of the sediment downstream. Therefore, the parameter related to suspended sediment routing dynamics (SPCON) was changed before and after new dams impounded. Detail descriptions and explanations can be found in Chapter 3.

2.6.2. Dissolved and particulate organic carbon parameters calibration

First, the four parameters mentioned in Equation 6 and 7 (α, β, *a*, *b*) were manually calibrated based on the DOC and POC discrete sampling data and the observed daily Q and SSC at each station, in order to evaluate different parameters associated with each sub-basin, which would indicate the characteristics of each sub-basin.

2.7. Simulation Performance

In this study, simulations were statistically evaluated by the following indicators.

2.7.1. The coefficient of determination (R^2)

R^2 describes the proportion of the variance in measured data explained by the model. R^2 is calculated as followed:

$$R^2 = \frac{\sum_{i=1}^{n}(O_i - \overline{O})(S_i - \overline{S})}{\sqrt{\sum_{i=1}^{n}(O_i - \overline{O})^2}\sqrt{\sum_{i=1}^{n}\left(S_i - \overline{S}\right)^2}} \quad (8)$$

where O_i and S_i are the observed and simulated values, n is the total number of values, $\overline{O}$ is the mean of observed values and $\overline{S}$ is the mean of simulated values.

R^2 ranges from 0 to 1, with higher values indicating less error variance, and typically values greater than 0.5 are considered acceptable (Moriasi *et al.*, 2007).

2.7.2. The Nash–Sutcliffe efficiency (NSE)

NSE is a normalized statistic that determines the relative magnitude of the residual variance compared to the observed data variance (Nash and Sutcliffe, 1970), calculated as followed:

$$NSE = 1 - \frac{\sum_{i=1}^{n}(O_i - S_i)^2}{\sum_{i=1}^{n}(O_i - \overline{O})^2} \quad (9)$$

NSE ranges from negative infinity to 1.00, with NSE=1 being the optimal value. A negative value indicates that the mean value of the observed time series would have been a better predictor than the model (Krause *et al.*, 2005). NSE values between 0.0 and 1.0 are generally regarded as acceptable levels of performance. Related to the guidelines proposed by Moriasi et al. (2007), NSE values above 0.5 are considered as satisfactory in hydrological modelling. Performance ratings for statistics of monthly scale provided by Moriasi et al. (2007) are reported in Table 2-4.

2.7.3. The Percent bias (PBIAS)

PBIAS provides the information of the average tendency of the simulated data to be larger or smaller than their observed counterparts. The optimal value is 0.0, with low-magnitude values indicating accurate model simulation. Positive values and negative

values indicate model underestimation bias and overestimation bias respectively. The equation is presented:

$$PBIAS = \frac{\sum_{i=1}^{n}(O_i - S_i) \times 100}{\sum_{i=1}^{n} O_i} \quad (10)$$

Table 2-4 General Performance Ratings for NSE and PBIAS of a Monthly Time Scale (Moriasi et al., 2007)

Performance Rating	NSE	PBIAS	
		Q	SSC
Very good	0.75 < NSE ≤ 1.00	PBIAS < ±10	PBIAS < ±15
Good	0.65 < NSE ≤ 0.75	±10 ≤ PBIAS < ±15	±15 ≤ PBIAS < ±30
Satisfactory	0.50 < NSE ≤ 0.65	±15 ≤ PBIAS < ±25	±30 ≤ PBIAS < ±55
Unsatisfactory	NSE ≤ 0.50	PBIAS ≥ ±25	PBIAS ≥ ±55

2.7.4. Dissolved and particulate organic carbon validation

Discrete sampling concentration data was used to calculate DOC and POC fluxes through the Load Estimator (LOADEST) regression model, which was developed by U.S. Geological Survey for estimating constituent loads in rivers (Runkel *et al.*, 2004) and was applied to many studies (McClelland *et al.*, 2007; Sickman *et al.*, 2007; Tamm *et al.*, 2008; Huntington and Aiken, 2013). LOADEST is calibrated through regression based on discrete sampling concentration data and observed daily Q, and the best regression model (Approximate Maximum Likelihood Estimator) is used with LOADEST to estimate daily DOC and POC fluxes respectively.

The outputs of LOADEST were used as observation to validate our simulation of DOC and POC fluxes. The mean annual DOC and POC fluxes from other references in the same basin (Dang, 2006; Le *et al.*, 2017a) were also used as validations.

2.8. Scenarios and Output analysis

2.8.1. Scenarios implementations by SWAT

Two scenarios were simulated (Table 2-5): (1) actual conditions with the existing six dams; (2) natural conditions without these six dams in this basin.

The new dams (Nansha, Madushan, Son La, Tuyen Quang dams) stared to operation since 2008. Therefore, the study period was divided into two periods: 2000-2007 and 2008-2013 in order to be able to quantify the impacts of the dams (old and new).

Under actual conditions, the parameter related to sediment routing (SPCON) was set as 0.008 for the 2000-2007 period and 0.002 for the 2008-2014 period because the new dams altered the sediment dynamics and routing. Other parameters than SPCON were kept the same for two periods. The variation of SPCON amongst two periods, obtained after calibration, is discussed in Chapter 3. The simulation was executed at daily, monthly and annual time scales.

In order to consider the impacts of climate variability and dams, a scenario of natural conditions (without these six dams) in the Red River basin was simulated. This simulation was set up with the same parameters as the period 2000-2007, and was running from 2000 to 2013 without any dam implementation. Previous studies (Dang *et al.*, 2010; Vinh *et al.*, 2014; Lu *et al.*, 2015) estimated the impacts on the sediment fluxes from dams before 2011 based on the measurements. Dang et al. (2010) and Vinh et al. (2014) mainly focused on the effect of the Hoa Binh dam, and Lu et al. (2015) also considered the Thac Ba dam, the Tuyen Quang dam and the Son La dam. We extended the time period to 2013 and took also the dams in China and the climate variability into account. The model outputs would then be compared with the values obtained in these studies as a validation.

By comparing the period of 2000-2007 and 2008-2013 under natural condition, the variation of variables induced by climate variability can be quantified. By comparing the differences between the natural and actual conditions in the same period, the impacts on variables due to the dams can be quantified.

Table 2-5 Scenarios setting: actual conditions (AC) and natural conditions (NC), and the two periods covered by the scenarios.

Scenario	**2000-2007** **(river name: dam name)**	**2008-2013** **(river name: dam name)**
Actual Conditions (AC)	Da: Hoa Binh Lo: Thac Ba	Thao: Nansha; Madushan Da: Hoa Binh; Son La Lo: Thac Ba; Tuyen Quang
Natural Conditions (NC)	no dam	no dam

2.8.2. Identification of the influencing factors for soil erosion

As described in Chapter 2.3.4, the SWAT model can calculate both the SS in the channel component and the soil erosion in the landscape component. Therefore, the output of the soil erosion from SWAT was analyzed in order to figure out its influencing factors and its contribution to the sediment fluxes.

Principal component analysis (PCA) was used in this study to identify the factors influencing soil erosion. More detailed explanations of this method can be seen in Basilevsky (1994), Wold et al. (1987) and Ringnér (2008). Origin 2018, a scientific graphing and data analysis software (https://www.originlab.com/), was used to execute PCA by correlation matrix analyzing. Based on the Equation 2, the following variables of each sub-basin were added into PCA model: soil erosion (SE), precipitation (P), water yield (WY), surface runoff (SR), USLE soil erodibility factor (USLE_K), USLE agricultural practice factor (USLE_P), slope, the percentage of sand (Sand%), silt (Silt%) and clay (Clay%) in soil. The input data was the mean annual values of each variable of 242 sub-basins.

2.8.3. Scenarios outputs for dissolved and particulate organic carbon

The outputs from the model would then be used to help us quantify and understand the transfer and the dynamics of the fluvial organic carbon. Firstly, the simulated Q and SSC under actual conditions would be used to assess and quantify the fluvial DOC and POC concentrations and fluxes. Then simulated Q and SSC under natural condition would be used to help us quantify the impacts of Q and SSC variation due to climate variability and dam constructions on DOC and POC fluxes.

2.8.4. Analysis of the relationships between the parameters for calculating the dissolved and particulate organic carbon and the physical characteristic of each sub-basin

After calibrating the parameters in the equations for calculating the dissolved organic carbon (DOC, Equation 6) and particulate organic carbon (POC, Equation 7) at different stations (Yen Bai, Vu Quang, Hoa Binh and Son Tay), different values of each parameter were gained at each station. The relationships between these parameters values at different stations and the physical characteristics of each station were identified. These relationships allow people to gain the value for each parameter based on soil organic carbon content (for DOC and POC equations), mean annual discharger (for DOC) and Chl-a (for POC).

Chapter 3

Modelling Discharge and Suspended Sediment Concentration

This chapter was published in the journal Water. The work of this chapter is the base of the following works in the following chapters. The aim of this chapter is to apply a modelling method in the Red River basin, in order to help us have a better understanding of the water regime and suspended sediment concentration (SSC) through the whole basin. This chapter is the base work for the following steps to simulate and calculate sediment flux and organic carbon.

Wei, X.; Sauvage, S.; Le, T.P.Q.; Ouillon, S.; Orange, D.; Vinh, V.D.; Sánchez-Pérez, J.-M. A Modeling Approach to Diagnose the Impacts of Global Changes on Discharge and Suspended Sediment Concentration within the Red River Basin. *Water* **2019**, *11*, 958. **https://doi.org/10.3390/w11050958**

3. CHAPTER Ⅲ : Modelling Discharge and Suspended Sediment Concentration

3.1. Scientific Context and Objectives

The Red River basin is a typical Asian river basin which is under strong nature and human influences. It is an international river among China, Vietnam and Laos. However, lacking cooperation and information exchanges among these countries set a barrier in having a comprehensive understanding of the whole basin. Therefore, we applied a model method in this basin, in order to help researchers to be able to: (1) study the whole study without the limitation of the discharge and suspended sediment concentration data access; (2) figure out natural and anthropogenic impacts on hydrology, suspended sediment concentration; (3) apply different scenarios for the future studies.

3.2. Materials and Methods

In this work, we used the SWAT model to characterize the hydrology and SSC of the Red River basin (137,200 km^2) on a daily scale. The model requires topography, soil map, land cover and meteorology (temperature and rainfall) data as inputs. These inputs could be downloaded freely which overcomes the limitation of data access. The simulation of discharge (Q) and SSC was carried out at different temporal scales (daily, monthly and annually) from January 2000 to July 2014 at Lao Cai, Yen Bai, Vu Quang, Hoa Binh and Son Tay stations. Yen Bai, Vu Quang and Hoa Binh stations are at the outlet of the Thao, Lo and Da rivers, and Son Tay is the outlet of the continental basin and the apex of the delta. Six important dams inside this basin were taken into account in the model. The model was calibrated based on in-situ data (daily discharge and suspended sediment concentration provided by Vietnam Ministry and Natural Resources and Environment) and parameter analysis. The well-calibrated model presented the actual conditions of the whole basin. Then, dams in this basin were removed, representing the natural conditions, to able us to quantify the impacts of dams and climate variability separately by comparing natural and actual conditions.

3.3. Main Results and Discussions

After the calibration procedure, the performance of the model was evaluated by statistical indicators (R^2, NSE and PBIAS) and was satisfactory.

In this basin, the mean annual rainfall during the study period was 1494mm, 53% of the total rainfall was taken away by evapotranspiration and 47% fed the streamflow. Water yield of the whole basin was 697 mm, among which the surface runoff accounted for 39%, the lateral flow accounted for 3% and the groundwater accounted for 58%. The annual water volume of the Thao, Lo and Da tributaries was 24, 23 and 43 km^3 respectively, and was 95 km^3 at Son Tay. The Da river is the main volume contributor to the Red River, and its volume equals to the sum of the Thao and Lo rivers.

Q and SSC simulations were acceptable and satisfactory at different temporal scales.

Temporal dynamics processes were well presented by the model. SSC showed a distinct decrease after 2007 when there were some new dams starting operation. Dams not only retain the sediment in the reservoirs but also change the downstream sediment grain size distribution. In addition, dams regulate the discharge which consequently changes the hydraulics downstream. These alter the dynamic processes of the downstream suspended sediment. This was confirmed by the modification of the parameter related to in-stream SS transfer and routing.

By comparing with the Q and SSC under natural conditions, the impacts of dams could be noticed on both Q and SSC. However, the impacts of dams on Q is much gentle than on SSC. The impacts of dams were mainly on base flow and some peak flows, and this is caused by dam water regulation, releasing the water to downstream during wet seasons and contain the flood during flood seasons. There were big differences between SSC under natural and actual conditions, which indicates the huge impacts of dams on suspended sediment transfer. We compared two periods of these two conditions, before new dams (2000-2007) and after new dams (2008-2013). By comparing the two periods of the natural condition, the impacts of climate variability can be quantified. Comparing the natural condition of 2000-2007 with the actual condition of 2008-2013, the total impacts due to both the climate and dams can be quantified. The impacts of dams are the difference between the total impacts and the impacts of climate. The results showed that for Q, the climate affected more than the dams, and it caused a 21% decrease on the Thao river, a 4% increase on the Lo river, an 18% decrease on the Da river and a 13% decrease at Son Tay, while the dams caused a 0.3% decrease, a 2% increase, a 10% decrease and a 9% decrease on the Thao, Lo, Da and Red rivers. On the contrary of Q, the climate was not the major influence factor that caused the variations on SSC. The total decrease of the SSC at Thao, Lo, Da and Son Tay was 68%, 72% 99% and 89% respectively, and the decrease caused by dams was 48%, 64%, 90% and 76% on the Thao, Lo, Da and Son Tay respectively.

3.4. Conclusion and Perspectives

The climate variability during the study period showed that a decreasing tendency on rainfall and evapotranspiration and an increasing tendency on temperature, which resulted in a decreasing tendency on available water for this basin. This caused a decrease of Q on most stations, except Vu Quang. Regional climate variations were different, and the sub-basins showed different responses to these variations. The different responses of each sub-basin to climate variation, especially to the rainfall, caused different impacts on SSC of each tributary. This is because the rainfall variation caused different soil erosion of each sub-basin.

The different impact of dams on Q and SSC of each tributary is related to the capacities of dams and their regulation ability. The Hoa Bind and Son La dams on the Da river are the biggest two dams. They have retained great amount sediment in the reservoirs.

With more dams are going to impound in this basin, sediment retention would consequently increase, which would subsequently influence the transport of associated matters, such as nutrients, metals and pesticide. Based on this study, future studies of transfer of these associated matters can be carried out by using the outputs of this model. What is more, more scenarios of global changes, such as land use changes and climate changes can be executed, and their impacts on hydrology and suspended sediment can be done.

Based on this part of work, the study on sediment flux and organic carbon in the Red River can be carried on.

3.5. Full Article Published in *Water*

water

MDPI

A Modeling Approach to Diagnose the Impacts of Global Changes on Discharge and Suspended Sediment Concentration within the Red River Basin

Xi Wei [1,*], Sabine Sauvage [1,*], Thi Phuong Quynh Le [2], Sylvain Ouillon [3,4], Didier Orange [5], Vu Duy Vinh [6] and José-Miguel Sanchez-Perez [1]

1 ECOLAB, Université de Toulouse, CNRS, INPT, UPS, 31326 Auzeville-Tolosane, France; jose-miguel.sanchez-perez@univ-tlse3.fr
2 Institute of Natural Product Chemistry (INPC), Vietnam Academy of Science and Technology (VAST), 18 Hoang Quoc Viet, Cau Giay, Hanoi 100000, Vietnam; quynhltp@yahoo.com
3 LEGOS, Université de Toulouse, IRD, CNES, CNRS, UPS, 31400 Toulouse, France; sylvain.ouillon@legos.obs-mip.fr
4 USTH, Vietnam Academy of Science and Technology (VAST), 18 Hoang Quoc Viet, Hanoi 100000, Vietnam
5 Eco & Sols, Univ. Montpellier, IRD, CIRAD, INRA, Montpellier SupAgro, 34060 Montpellier, France; didier.orange@ird.fr
6 Institute of Marine Environment and Resources (IMER), VAST, 246 Danang Street, Haiphong City 180000, Vietnam; vinhvd@imer.vast.vn

***** Correspondance: xi.wei@etu.ensat.fr (X.W.); sabine.sauvage@univ-tlse3.fr (S.S.)

Received: 11 April 2019; Accepted: 30 April 2019; Published: 7 May 2019

Abstract: The Red River basin is a typical Asian river system affected by climate and anthropogenic changes. The purpose of this study is to build a tool to separate the effect of climate variability and anthropogenic influences on hydrology and suspended sediments. A modeling method combining in situ and climatic satellite data was used to analyze the discharge (Q) and suspended sediment concentration (SSC) at a daily time scale from 2000 to 2014. Scenarios of natural and actual conditions were implemented to quantify the impacts of climate variability and dams. The modeling gained satisfactory simulation results of water regime and SSC compared to the observations. Under natural conditions, the Q and SSC show decreasing tendencies, and climate variability is the main influence factor reducing the Q. Under actual conditions, SSC is mainly reduced by dams. At the outlet, annual mean Q got reduced by 13% (9% by climate and 4% by dams), and annual mean SSC got reduced to 89% (13% due to climate and 76% due to dams) of that under natural conditions. The climate tendencies are mainly explained by a decrease of 9% on precipitation and 5% on evapotranspiration, which results in a 13% decrease of available water for the whole basin.

Keywords: Red River; SWAT model; hydrology; suspended sediment; dam impacts; climate

1. Introduction

Nowadays, the freshwater scarcity has become a global and local dramatic threat for the sustainable development of the human society [1]. The continuous increasing water demand is growing faster than the demographic increase, bringing the water crises as a major world risk [2]. River network plays a critical role in hydrological cycle, and also in processing and transporting sediments and nutrients to oceans. The suspended sediment (SS) transportation by rivers can be a reflection of land and river degradation, and it drives nutrients to the seas which is an essential process for marine biogeochemical cycle and diversity [3,4].

Hydrological cycle and water quality are affected by climate variability and human disturbance. Climate variations, particularly temperature and precipitation, have effects on river systems both at short and long time scales, such as floods and droughts caused by typhoons and El Nino and La Nina, especially in the tropics [5–7]. In addition, under the disturbance of human activities (such as industrial and agricultural water consumption and dam constructions), water ecosystems are facing severe challenge, like the increase of soil erosion, pollutants and nutrient loads, and changes of hydrology regime and sediment fluxes (SF) [8–13].

To face the challenge of increasing water demand under uncertain variations of climate, dams have been built globally for water storage. Globally, at least 45,000 large dams have been built, and nearly half of the world's rivers have at least one large dam [14]. From a Global Reservoir and Dam database, approximate 28% dams are located in Asia [15]. In addition, future hydropower development is primarily concentrated in developing countries and emerging economies of Southeast Asia [16]. As a consequence, dams coupled to climate variability have an impact on water regime and fluxes of matters, mainly SS [17]. Dam implementation can cause a significant reduction of SF; Vörösmarty et al. (2003) [18] estimated greater than 50% of potential sediment trapping by dams in regulated basins. However, reduced sediment transport affects estuarine and coastal communities [19]. For example, as a result of reduced sediment delivery, many river deltas are sinking, thereby increasing the vulnerability of human populations depending on their ecosystem services for survival [15].

Therefore, understanding and quantifying hydrology, soil and biogeochemical processes, and budgets are essential in managing water resource, in controlling and mitigating soil and pollutant loads. For achieving this, appropriate methods and tools are necessary, such as in-situ field measurements, empirical and simple equations, remote sensing techniques, geographic information systems, and numerical simulations. However, field-collecting data at large spatial and temporal scales is expensive, and often impracticable in some remote areas and underdeveloped regions. Empirical or/and simple equations, such as sediment rating curves are sometimes applied to quantify the SF [20–23]. However, a sediment rating curve requires discharge (Q) as an input, which might not be available for remote and underdeveloped regions, and its parameters can vary a lot among a big drainage basin. Therefore, this

method might neither be the best choice for calculating the SF at a daily basis nor in a large basin. Modeling is a good tool, combined with other techniques (such as remote sensing), to compensate the above shortages. Simulations can be carried out at a large spatial scale and at a daily time scale to quantify, analyze and forecast water resources and quality. In particular, it can realistically represent the spatial variability of the basin, which will provide a global view of the whole basin. Many physically based hydrological models had been used [24–27], such as MIKESHE [28], HSPF [29] and Soil and Water Assessment Tool (SWAT) [30]. Among these models, SWAT has been proved to obtain good hydrological predictions with a little direct calibration in many different basins around the world [26,27,31], and more applications can be found in SWAT literature database: https://www.card.iastate.edu/swat_articles/.

Although SWAT has been applied to many Asian basins, and also to subtropical or/and tropical areas, most of them were at a scale of 77 to 105,000 km^2 [31–35]. The Red River is a typical Asian river system, combining different land uses, affected by human activities such as intensive dam implementations and agriculture [36,37]. Recent studies of hydrology and suspended sediment in this basin mainly used data from gauge stations or sampling to do statistical analysis [38–41], or use modeling to perform simulations at a local scale [42] or in the delta part [43] at a monthly scale; few studies analyzed fluxes at daily scale, but only on a short period [37], in the delta [44] or only for discharge or suspended sediment [45]. Both Q and SSC can vary greatly from day to day; therefore, it would be more favourable to calculate flux at a daily scale. Also, water quality monitoring is usually carried out during some specific days in a month, and outputs from a model at daily scale can be practical and useful for further studies. In addition, different scenarios of global changes can be considered to help researchers or government administrators to compare different possibilities and set up long-term management plans.

Hence, the objective of this paper is to apply a new tool in the Red River basin to analyze hydrology and suspended sediment transport in order to diagnose impacts of the global changes by separating the effect of climate variability and anthropogenic influences. The model was applied: (1) to characterize the hydrology of the basin at daily scale; (2) to quantify the SSC in time and space; (3) to assess the impacts of climate variability and dams in a separate way.

2. Materials and Methods

2.1. Study Area

2.1.1. General Characteristics

The Red River basin, located in Southeastern Asia, is a portion of the international border among China, Laos and Vietnam. Of the total area, 49% lies in China, 0.9% in Laos and 50.1% in Vietnam. The Red River originates in Dali, Yunnan Province (China), which is a mountainous region, at an elevation of 2650 m a.s.l. [46]. Due to the

accessibility of the data and considering the influence of the tide, our study area focused only on the continental basin with a surface of 137,200 km^2 that drained down to Son Tay, which is the outlet of the continental basin and the entrance of the delta (Figure 1).

The upper part of the main river, before Son Tay, is called the Thao River. It receives two main tributaries: the Da River from the right bank, and the Lo River from the left bank. These two tributaries join the Red River just 20 km upstream to the Son Tay gauging station.

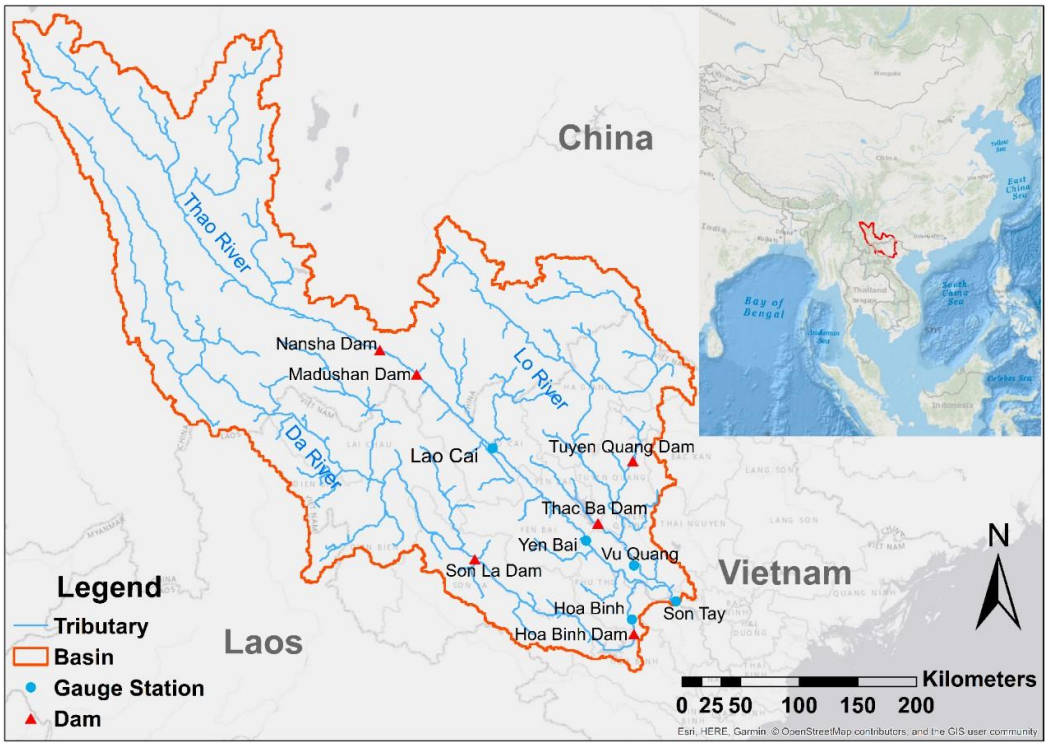

Figure 1. Map of the Red River basin: geographical location of study area in Asia; hydrological gauge stations and dams.

Rapid increase of population and intensive agriculture activities inside the Red River basin require more water supplies for urban, industry and agriculture use, and more and more dams and irrigation channels are built to meet these demands both in China and Vietnam. In the upstream of the Thao River in China, twelve cascade hydropower stations are under construction. The Nansha Dam and the Madushan Dam started impoundment on November 2007 and December 2010, respectively, on the Thao River. On the Da River, the biggest dam named Hoa Binh was put into use in 1989. The Hoa Binh dam has trapped a mass of solid materials, and sedimentation in the reservoir reduces the dam's efficient capacity and life [39]. Therefore, in order to mitigate the siltation of the Hoa Binh dam and to meet the need of economic growth, the Son La dam (upstream) was built and put into use on December 2010. On the Lo River, the Thac Ba dam was implemented in 1972 and the Tuyen Quang dam was carried out on March 2008. More details of these dams can be found in Table 1.

Table 1. Basic Characteristics of the Dams [41].

Name (Basin)	Construction	Operation	Capacity ($\times 10^9$ m^3)	Mean Water Level (m)	Mean Annual Discharge (m^3/s)	Maximum Discharge (m^3/s)
Nansha (Thao)	February 2006	November 2007	0.26	267	261	–
Madushan (Thao)	December 2008	December 2010	0.55	217	302	–
Hoa Binh (Da)	1980	1989	9.50	115	1780	2400
Son La (Da)	December 2005	December 2010	9.26	215	1530	3438
Thac Ba (Lo)	1965	October 1971	2.90	58	190	420
Tuyen Quang (Lo)	December 2002	March 2008	2.24	120	318	750

The upstream part in China is dominated by tectonically active montane areas with steep slopes, usually above 25° [47]. Intensive rainfall and prominent contradiction between human and land make this area vulnerable to high erosion with steep slopes [38,48,49]. The main soil types are Acrisols, such as latosol, red earth, yellow brown soil and fluvisol [48,50]. Therefore, high erosion plus the character of soil types colour the water of the Thao River and the Da River into “red” [50]. In Vietnam, the same Acrisols dominate on the slopes, and grey or alluvial soils dominate in the valleys [41]. Land use in China is mainly forest, accounting for 62% of the area, followed by grassland and cultivated land, accounting for 19% and 18%, respectively [1] (Li et al., 2016). Land use varies in Vietnam in different sub-basins: in the main stream basin (Thao basin), forest is the dominant land use, accounting for 54.2%, followed by rice paddy fields (18.7%) and industrial crops (mainly coffee, rubber, tobacco, etc.) (12.8%); the Lo basin and the Da basin dominate industrial crops (58.1%) and forests (74.4%), respectively [37].

2.1.2. Meteorological and Hydrological General Characteristics

The whole Red River basin passes across two climate zones, from sub-tropical humid monsoon in the upstream basin to tropical humid monsoon in the downstream part. Both zones are marked by a strong seasonality, and controlled by monsoon intensity. The rainy seasons occur from May to October, with precipitation accounting for over 85–90% of the whole year [37,51]. The spatial distribution of precipitation is uneven—in China, it ranges from 700 to 3000 mm $year^{-1}$, averagely around 1000 to 1600 mm $year^{-1}$, and the general trend of regional precipitation distribution increases from upstream to downstream [52,53]; and in the part of basin in Vietnam, the precipitation ranges from 1328 to 2255 mm $year^{-1}$ [37]. The precipitation input used for the model, a product from the Tropical Rainfall Measuring Mission (TRMM), presents a mean value of 1507 mm $year^{-1}$, which is in the range of the precipitation observed in whole basin. More explanations and details about TRMM is presented in Section 2.3.2.

Temperature changes follow a classic orographic pattern: the mean annual temperature upstream in China varies from 15 to 21 °C [52], while in Vietnam it ranges from 14 to 27 °C [50]. Temperature is lower in valley areas.

Potential evapotranspiration (PET) ranges from 880 to 1150 mm $year^{-1}$, and its mean value was 1040 mm $year^{-1}$ [37]. Simons et al. [54] who used global satellite-derived data to calculate actual evapotranspiration in the whole basin showed values in the range of 860 to 1117 mm $year^{-1}$.

The hydrology in this region is affected by the monsoon climate and the runoff is mainly recharged by precipitation, which led to large inter-seasonal variations in river flows [51,53,55]. From the hydrology data that we collected, the mean annual discharge in Son Tay during 2000–2015 was 3082 m^3 s^{-1}. Corresponding to temporal precipitation distribution, the runoff is also uneven in intra-annual distribution: flood season occurs from June to November during which time the accumulated runoff accounts for more than 80% of the total annual runoff; low water seasons occur from December to May. The lowest discharge of the upstream Thao River in China usually occurs in March, and the minimum discharge of the Thao River observed near the border between China and Vietnam was 28.7 m^3 s^{-1} in 1963 [56]. The lowest discharge at Son Tay generally showed up in March, and from the discharge data we collected, the minimum daily discharge at Son Tay during 2000–2015 was 493 m^3 s^{-1} (in February 2010). Peak runoff usually occurs in August, and the maximum flood was 8050 m^3 s^{-1} observed at the gauge station near the boundary in China in 1986 [52], while it was 37,800 m^3 s^{-1} at Son Tay in 1971 [44].

2.2. Modeling Approach

2.2.1. The SWAT Model

The Soil and Water Assessment Tool (SWAT) is a physically based, semi-distributed hydrological model, which requires topography, weather, soil, land use and land management practices, to simulate the water, sediment and agricultural chemical yields in large complex basins where there might be no monitoring data with over long periods of time [57]. For modeling, a basin will be firstly partitioned into sub-basins, or sub-basins which are then further subdivided into hydrological response units (HRU) with homogeneous land use, soil type and slope.

SWAT has been applied in Asian basin and performed well in various simulations [35,58–60], and also in tropical areas [61–66]. In South East Asia, SWAT was commonly applied to Mekong river basin [35,60,67] or some local small-scale basins [42,58,61,65,68–71]. This paper applied the SWAT model in a large-scale basin in the tropical South East Asia.

2.2.2. Hydrological Modeling Component in SWAT

Water balance is the driving force in SWAT regardless of what kind of problems people

want to deal with. Two major divisions are considered in simulating the hydrology of a basin: the hydrological cycle over the lands, and in the channel network.

Over the lands, SWAT simulates surface runoff volumes and peak runoff rates for each HRU using daily or sub-daily rainfall amounts. For computing surface runoff volume, a modification of the Soil Conservation Service (SCS) curve number method [72] is used. Peak runoff rate is predicted based on the water transient time in the sub-basin according to a flood event. In routing phase, surface flow is simulated using a variable storage coefficient method developed by Williams (1969) [73] or the Muskingum routing method [74]. In this work, SCS curve number method and variable storage coefficient method, along with daily climate data, were used for surface runoff and streamflow computations.

The Hargreaves method [75], which required air temperature alone, was chosen to calculate the potential evapotranspiration (PET).

2.2.3. Suspended Sediment Modeling Component in SWAT

SWAT considers sediment transport both over the landscape component and in the channel component.

In landscape component, the model tracks particle size distribution of eroded sediments and routes them through ponds, channels and surface water bodies. Erosion and sediment yield are calculated with the Modified Universal Soil Loss Equation (MUSLE) for each HRU [57,76]. This equation considers the surface runoff volume, peak runoff rate, soil erodibility, land cover and management and topographic and coarse fragment factor as follows:

$$sed = 11.8 \cdot \left(Q_{surf} \cdot q_{peak} \cdot area_{hru}\right)^{0.56} \cdot K_{USLE} \cdot C_{USLE} \cdot P_{USLE} \cdot LS_{USLE} \cdot CFRG \qquad (1)$$

where sed is the sediment yield on a given day (t), Q_{surf} is the surface runoff volume (mm H_2O ha^{-1}), q_{peak} is the peak runoff rate (m^3 s^{-1}), $area_{hru}$ is the area of the HRU (ha), K_{USLE} is the USLE soil erodibility factor (0.013 t m^2 h m^{-3} t^{-1} cm^{-1}), C_{USLE} is the USLE land cover and management factor (dimensionless), P_{USLE} is the USLE support (agricultural) practice factor (dimensionless), LS_{USLE} is the USLE topographic factor (dimensionless) and $CFRG$ is the coarse fragment factor (dimensionless). The sources of data used to determine each parameter are reported in Section 3.3.1.

The sediment routing in the channel is a function of two processes: deposition and degradation, operating simultaneously in the reach. The Simplified Bagnold equation (1977) [77] is used as a default method for the sediment routing in stream channels, which determines degradation as a function of channel slope and flow velocity. The maximum amount of sediment that can be transported is a function of the peak channel velocity, as follows:

$$conc_{sed,ch,mx} = c_{sp} \cdot {v_{ch,pk}}^{spexp} = c_{sp} \cdot \left(\frac{q_{ch,pk}}{A_{ch}}\right)^{spexp} = c_{sp} \cdot \left(\frac{prf \cdot q_{ch}}{A_{ch}}\right)^{spexp} \qquad (2)$$

where $conc_{sed,ch,mx}$ is the maximum concentration of sediment that can be transported by the water (t m^{-3}), c_{sp} is a coefficient defined by the user (dimensionless), $v_{ch,pk}$ is the peak channel velocity (m s^{-1}), spexp is an exponent defined by the user (dimensionless), $q_{ch,pk}$ is the peak flow rate (m^3 s^{-1}), A_{ch} is the cross-sectional area of flow in the channel (m^2), prf is the peak rate adjustment factor, and q_{ch} is the average rate of flow (m^3 s^{-1}). More details on these parameters and their usual ranges are reported in Section 3.3.1.

The maximum concentration of sediment calculated with Equation (2) is compared to the concentration of sediment in the reach at the beginning of the time step ($conc_{sed,ch,i}$, in t m^{-3}). If $conc_{sed,ch,i} > conc_{sed,ch,mx}$, deposition is the dominant process in the reach segment and the net amount of sediment deposited is calculated as:

$$sed_{dep} = \left(conc_{sed,ch,i} - conc_{sed,ch,mx}\right) \cdot V_{ch} \quad (3)$$

where sed_{dep} is the amount of sediment deposited in the reach segment (t), and V_{ch} is the volume of water in the reach segment (m^3).

If $conc_{sed,ch,i} < conc_{sed,ch,mx}$, the available stream power is used to re-entrain loose and deposited material until all of the material is removed. Excess stream power causes bed degradation, and the net amount of sediment re-entrained is adjusted for stream bed erodibility and cover as follow:

$$sed_{deg} = \left(conc_{sed,ch,mx} - conc_{sed,ch,i}\right) \cdot V_{ch} \cdot K_{ch} \cdot C_{ch} \quad (4)$$

where sed_{deg} is the amount of sediment re-entrained in the reach segment (t), K_{ch} is the channel erodibility factor and C_{ch} is the channel cover factor.

2.3. SWAT Data Inputs

SWAT requires inputs as topography, land cover, soils and meteorological data. All the inputs used in this study are listed in Table 2.

2.3.1. Topography, Land Use and Soil

The landscape slopes were divided into 5 classes by SWAT based on the information from DEM (details are shown in Figure 2a). The dominant lands are forest (27.56%, with 14.65% of evergreen forest (FRSE in SWAT model), 12.49% of mixed forest (FRST) and 0.42% of deciduous forests (FRSD)); agriculture (ARGL, 21.16%); range-grasses (RNGE, 19.94%); wheatgrass (19.57%, with 10.03% of western wheatgrass (WWGR) and 9.54% of crested wheatgrass (CWGR)) (Figure 2b).

There are 21 specific soils in study area (Figure 2c); however, most of them are Acrisols [78]. Resolutions and download links can be found in Table 2.

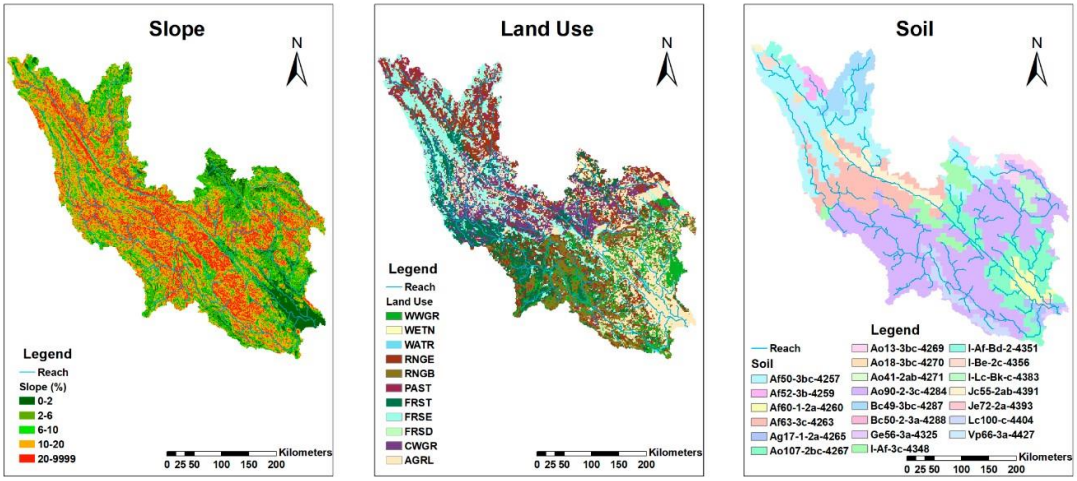

(**a**) (**b**) (**c**)

Figure 2. (**a**) Slop classes; (**b**) land use map; (**c**) soil types.

2.3.2. Meteorological Data

Daily temperature data were obtained from the Global Weather Data in SWAT file format for a given location and time period. These data come from the daily Climate Forecast System Reanalysis (CFSR).

Daily precipitation data was obtained from the Tropical Rainfall Measuring Mission (TRMM, product 3B42 V7), which is a research satellite designed to provide needed information on rainfall by covering the tropical and sub-tropical regions of the Earth. Simons et al. [54] compared several satellite-based precipitation and actual evapotranspiration products in the Red River basin in order to demonstrate that these datasets can be merged to examine hydrological processes before applying a numerical simulation model, and they found that TRMM rainfall product could provide reliable values in both space and time at this basin.

Table 2. SWAT Inputs and Hydrology Datasets.

Data Type	Resolution/Time Scale/Period	Source
Topography (DEM)	1 × 1 km	Shuttle Radar Topography Mission (SRTM30 30 arc-sec, http://www2.jpl.nasa.gov/srtm)
Land cover	1 × 1 km	Global Land Cover 2000 database (https://forobs.jrc.ec.europa.eu/products/glc2000/glc2000.php)
Soil types	1 × 1 km	Harmonized World Soil Database (http://webarchive.iiasa.ac.at/Research/LUC)
Temperature	daily scale Jane 1998 to July 2014	Climate Forecast System Reanalysis: Global Weather Data for SWAT (https://globalweather.tamu.edu/)
Precipitation	daily scale 0.25° × 0.25° Jane 1998 to December 2014	Tropical Rainfall Measuring Mission (TRMM, https://pmm.nasa.gov/TRMM)
Discharge and suspended sediment concentration	5 stations: Lao Cai, Yen Bai, Vu Quang, Hoa Binh, Son Tay daily scale Jane 2000 to December 2014	Vietnam Ministry of Natural Resources and Environment (MONRE)

2.3.3. Dam Implementations

SWAT requires basic information, such as date of impoundment, reservoir surface area, emergency volume, principal volume and initial volume. The volume of outflow can be calculated by one of the following methods: measured daily outflow, measured monthly outflow, average annual release rate and controlled outflow with target release. As it is impossible to get the detailed outflow of dams, and in order to avoid the complex conditions of release operations and to enable the model to be applied for future hydrology regime prediction, the average annual release rate method that releases the water whenever the dam volume exceeds the principal spillway volume [57] was selected. A minimum and a maximum average daily releases for the month were limited for the model according to the Q data we collected and to the release information from reference [37].

The six dams localized in Figure 1 were taken into account in the model. Two dams are located on the main stream of the Thao River, around 150 km and 100 km upstream of Lao Cai, respectively; two are on the Da River; and the other two are on the Lo River. However, inside this basin, there are more dams that were put into use [79], or are under construction during simulation period; and these dams are located more in the upper regions and most are with less capacities. Here, the model only took these six dams with large capacity into account, and also they are located closer to the outlet of each tributary, see Table 1.

2.4. Model Set Up

SWAT2012 and ArcGIS10.4 were used. The whole basin was divided into 242 sub-basins and then subdivided into 3812 different HRUs.

Two scenarios were simulated: (1) actual situation and (2) natural situation. Simulation was carried out at three temporal scale (daily, monthly and annually) during an overlapped period, from January 2000 to July 2014.

2.5. Calibration and Validation Process

The model was calibrated at a daily scale using Q and SSC from 1 January 1998 to 31 July 2014 with a two-year warm-up. Parameters were mainly calibrated manually, and some were automatically calibrated by using SWAT-CUP [80]. SWAT-CUP is a tool that allows SWAT users to perform automatic calibrations [81]. Five algorithms are proposed for calibration purpose [80,82]. The SUFI-2 (Sequential Uncertainty Fitting 2) algorithm [82], which can identify appropriate parameters sets in a limited number of iterations, was selected in this study. Calibration of Q was first carried out, followed by SSC.

Observed data of daily Q and SS concentration from 2000 to 2014, obtained from the Vietnam Ministry of Natural Resources and Environment (MONRE) at Lao Cai, Yen Bai, Vu Quang, Hoa Binh and Son Tay stations, were used to calibrate the model.

Figure 1 shows the location of each gauge station. Time series plots and statistical methods were used to evaluate the performance of model in simulating Q and SSC.

Values from other references [37,39,43,50,51,53,83–85] are used to be validations of the water regime and SSC.

2.6. Model Evaluation

2.6.1. The Coefficient of Determination (R^2)

R^2 describes the proportion of the variance in measured data explained by the model. R^2 is calculated as follows:

$$R^2 = \frac{\sum_{i=1}^{n}(O_i-\overline{O})(S_i-\overline{S})}{\sqrt{\sum_{i=1}^{n}(O_i-\overline{O})^2}\sqrt{\sum_{i=1}^{n}(S_i-\overline{S})^2}} \quad (5)$$

where O and S are the observed and simulated values, n is the total number of values, $\overline{O}$ is the mean of observed values and $\overline{S}$ is the mean of simulated values.

R^2 ranges from 0 to 1, with higher values indicating less error variance, and typically values greater than 0.5 are considered acceptable [86].

2.6.2. The Nash–Sutcliffe Efficiency (NSE)

NSE is a normalized statistic that determines the relative magnitude of the residual variance compared to the observed data variance [87], calculated as follows:

$$\mathrm{NSE} = 1 - \frac{\sum_{i=1}^{n}(O_i-S_i)^2}{\sum_{i=1}^{n}(O_i-\overline{O})^2} \quad (6)$$

NSE ranges from negative infinity to 1.00, with NSE=1 being the optimal value. A negative value indicates that the mean value of the observed time series would have been a better predictor than the model [88]. NSE values between 0.0 and 1.0 are generally regarded as acceptable levels of performance. Related to the guidelines proposed by Moriasi et al. [86], NSE values above 0.5 are considered as satisfactory in hydrological modeling. Performance ratings for statistics of monthly scale provided by Moriasi et al. [86] are reported in Table 3.

2.6.3. The Percent Bias (PBIAS)

PBIAS provides the information of average tendency of the simulated data to be larger or smaller than their observed counterparts. The optimal value is 0.0, with low-magnitude values indicating accurate model simulation. Positive and negative values indicate model underestimation bias and overestimation bias, respectively. Equation is presented as follows:

$$\mathrm{PBIAS} = \frac{\sum_{i=1}^{n}(O_i-S_i)\times 100}{\sum_{i=1}^{n}O_i} \quad (7)$$

Table 3. General Performance Ratings for NSE and PBIAS of a Monthly Time Scale [86].

Performance Rating	NSE	PBIAS	
		Q	SSC
Very good	0.75 < NSE ≤ 1.00	PBIAS < ±10	PBIAS < ±15
Good	0.65 < NSE ≤ 0.75	±10 ≤ PBIAS < ±15	±15 ≤ PBIAS < ±30
Satisfactory	0.50 < NSE ≤ 0.65	±15 ≤ PBIAS < ±25	±30 ≤ PBIAS < ±55
Unsatisfactory	NSE ≤ 0.50	PBIAS ≥ ±25	PBIAS ≥ ±55

According to Moriasi et al. [86], these guidelines should be adjusted based on the quality and quantity of measured data, model calibration procedure and evaluation time step.

3. Results

3.1. Q Simulation and Hydrological Assessment

3.1.1. Hydrological Parameters

Table 4 presents the calibrated parameters for Q and SSC, and their definitions and ranges. Sensitive hydrological parameters are chosen by literature reviews [64,89–91]. Relative change of parameters was controlled within ±20%, and absolute change was done by referring to the aforementioned literatures and theoretical documents [57,81,91,92]. Based on actual information from the MONRE and literatures [50,83], parameters like runoff curve number (CN2), soil evaporation compensation factor (ESCO), available water capacity of the soil layer (SOL_AWC) and parameters related to groundwater (GW_REVAP, REVAPMN, RCHGR_DP, GWQMN, GW_DELAY) were calibrated to fit the actual water balance. Compared to the default values, ESCO was decreased and GW_REVAP was increased to increase the ET; SOL_AWC was increased by 20%; CN2 was decreased by 10%; REVAPMN was increased; and RCHGR_DP and GWQMN were decreased to decrease the surface flow, which accordingly increased the groundwater flow. Other parameters related to hydrological processes were calibrated to fit the baseflow and peaks, and they were interpreted in the following sub-section.

Table 4. Parameters Used to Calibrate Flow and Suspended Sediment Concentration for Different Basins.

Parameter (Name in Equations)	Input File	Definition	Range	Calibrated Value
OV_N	.hru	Manning's "n" value for overland flow	0.01–30	0.4
SLSUBBSN	.hru	Average slope length (m)	10–150	×1.2 (relative change)
HRU_SLP	.hru	Average slope steepness (m/m)	–	×0.8
ESCO	.hru	Soil evaporation compensation factor	0–1	0.7
PRF (*prf*)	.BSN	Peak rate adjustment factor for sediment routing in the main channel	0–2	1
SPCON (*Csp*)	.BSN	Linear parameter for calculating the maximum amount of sediment that can be re-entrained during channel sediment routing	0.0001–0.01	0.008 (Period 2000–2007) 0.002 (Period 2008–2014)
SPEXP (*spexp*)	BSN	Exponent parameter for calculating sediment re-entrained in channel sediment routing	1–2	2
ALPHA_BF	.gw	Baseflow alpha factor	0–1	0.02
GW_REVAP	.gw	Groundwater "revap" coefficient	0.02–0.20	0.03
REVAPMN	.gw	Threshold depth of water in the shallow aquifer for "revap" or percolation to the deep aquifer to occur	0–1000	800
RCHGR_DP	.gw	Deep aquifer percolation fraction	0.0–1.0	0
GWQMN	.gw	Threshold depth of water in the shallow aquifer required for return flow to occur	0–5000	600
GW_DELAY	.gw	Groundwater delay time	0–500	16
SOL_AWC	.sol	Available water capacity of the soil layer	0–1	×1.2
USLE_K (K_{USLE})	.sol	USLE equation soil erodibility (K) factor	0–0.65	Thao River basin 0.3 Lo River basin 0.2 Da River basin 0.3
CH_COV1 (K_{ch})	.rte	The channel erodibility factor	−0.05–0.6	Thao River basin: upstream Yen Bai: 0.23; Yen Bai-Son Tay: 0.013 Lo River basin 0.013 Da River basin 0.026
CH_COV2 (C_{ch})	.rte	Channel cover factor	−0.001–1	1
CH_N2	.rte	Manning's "n" value for the main channel	−0.01–0.3	0.05
USLE_P (P_{USLE})	.mgt	USLE equation agricultural practice factor	0–1	Thao River basin 0.7(agriculture) Lo River basin 0.4(agriculture) Da River basin 0.7(agriculture)
FILTERW	.mgt	Width of edge-of-field filter strip	0–100	Thao River basin 0 Lo River basin 25 Da River basin 0
CN2	.mgt	Initial SCS runoff curve number	35–98	×0.9 (Relative change)
CH_N1	.sub	Manning's "n" value for the tributary channels	0.01–30	1

3.1.2. Q simulations

Daily and monthly evaluation statistics are presented in Table 5. According to the NSE of daily scale Q simulations, results are acceptable (as NSE > 0) for the stations on the Thao, Lo and Da rivers, and is satisfactory (NSE > 0.5) for Son Tay. At monthly scale, the performance of the model is good, except at Vu Quang station where it is satisfactory. PBIAS values indicate that the model underestimated the discharge for

majority stations except for Yen Bai. The absolute values of PBIAS were within 21.3, which is satisfactory. Hence, according to the statistic evaluations, the model performed well simulating Q at both daily and monthly scales.

Table 5. Evaluation Statistics of Observed and Simulated Discharge (Q), Suspended Sediment Concentration (SSC) and Sediment Flux (SF) on Different Time Scales for Each Station.

Constituent	Scale	Statistics	Lao Cai	Yen Bai	Vu Quang	Hoa Binh	Son Tay
Q (m^3/s)	Daily	NSE	0.44	0.35	0.38	0.49	0.61
		R^2	0.57	0.52	0.45	0.53	0.64
		PBIAS	2.8	−11.2	21.2	18.1	6.0
		p-value	<0.01	<0.01	<0.01	<0.01	<0.01
	Monthly	NSE	0.78	0.78	0.58	0.70	0.85
		R^2	0.82	0.88	0.65	0.77	0.86
		PBIAS	2.8	−11.0	21.3	17.9	5.9
		p-value	<0.01	<0.01	<0.01	<0.01	<0.01
SSC (mg/L)	Daily	NSE	0.31	0.23	0.02	0.10	0.19
		R^2	0.34	0.30	0.29	0.36	0.34
		PBIAS	−21.4	−28.7	−46.5	−26.3	−28.0
		p-value	<0.01	<0.01	<0.01	<0.01	<0.01
	Monthly	NSE	0.70	0.64	0.24	0.59	0.52
		R^2	0.73	0.71	0.55	0.67	0.70
		PBIAS	−21.5	−27.3	−46.8	−26.5	−29.5
		p-value	<0.01	<0.01	<0.01	<0.01	<0.01

Figure 3 illustrates the observed and simulated Q comparisons at daily and monthly scale for five stations. Simulated Q shows the same trends as observed Q. At daily scale, the model underestimated base Q at Vu Quang station; and simulated peak Q was underestimated during some floods, especially at Vu Quang and Hoa Binh stations. At Son Tay, at the confluence of the Thao, the Lo and the Da rivers, the simulated Q shows a better agreement with both the base Q and peak Q. At monthly scale, peaks fit well on the Thao River (Lao Cai and Yen Bai) and at Son Tay, while they were underestimated on the Lo (Vu Quang) and the Da River (Hoa Binh); and underestimation on baseflow are only largely noticeable at Vu Quang on a monthly scale.

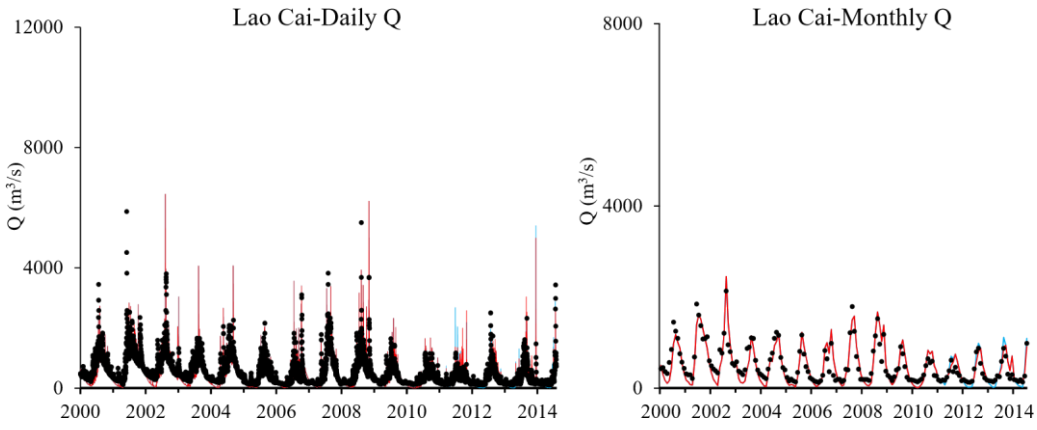

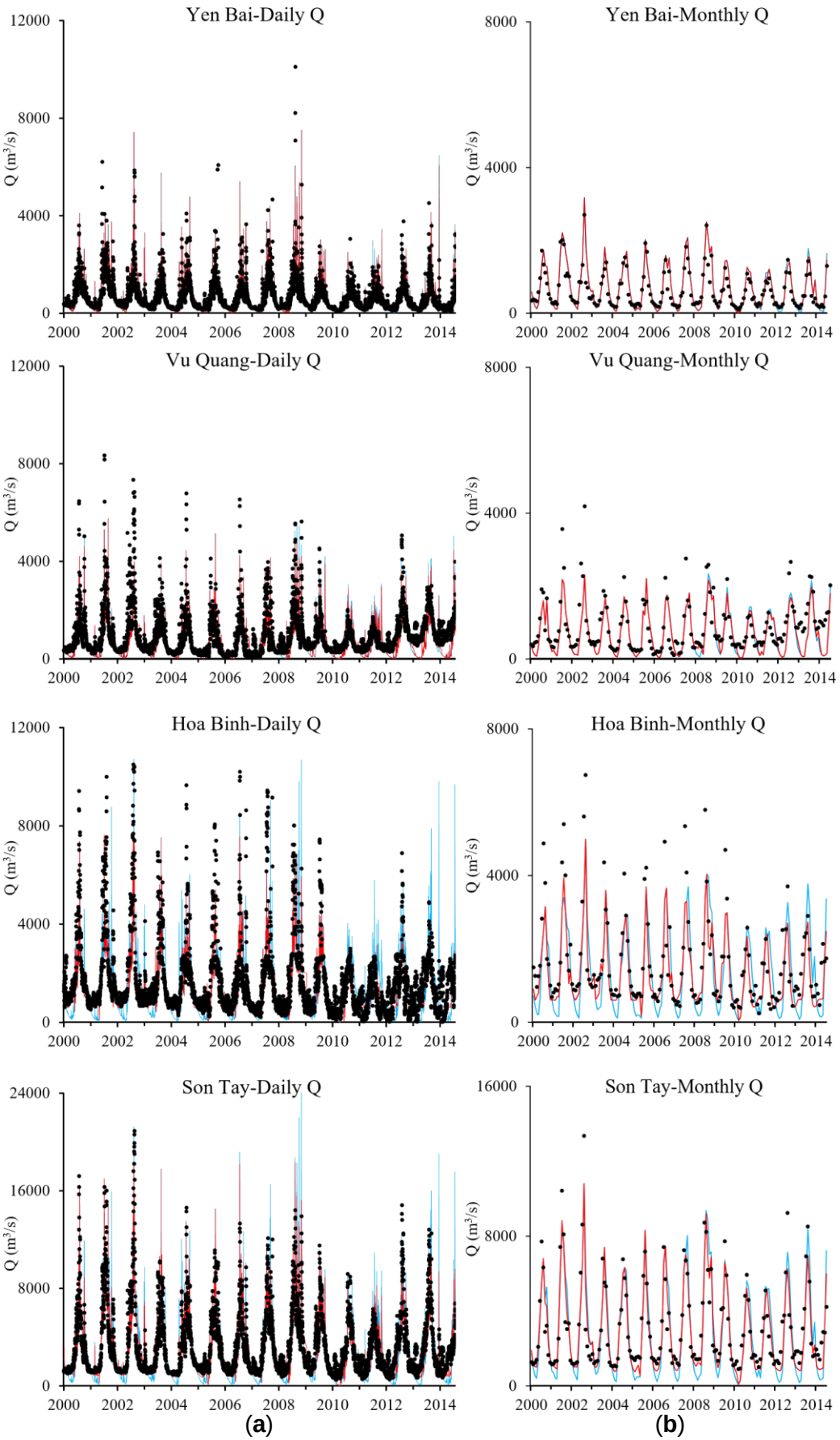

Figure 3. Observed (black dot) and actual simulated (red solid line) daily (**a**) and monthly (**b**) discharge (Q) at five stations from January 2000 to July 2014. Blue solid line represents the scenario simulation of Q under natural conditions.

3.2. SSC Simulation

3.2.1. Calibration of SSC

As shown in Section 2.2.3, two groups of parameters were considered, and their calibrated values are shown in Table 4.

A first group of parameters related to landscape processes are involved in Equation (1). Among these parameters, USLE_K and USLE_P are sensitive to soil erosion. Due to the soil characteristics (poor stability and erosion resistance), the Thao and Da basins are more vulnerable to soil erosion [47]. Therefore, USLE_K of the Thao and Da basins (0.3) were higher than that of the Lo basin (0.2). The agricultural practice factor, USLE_P, is defined as the ratio of soil loss with a specific agricultural practice (such as contour tillage, strip cropping on the contour and terrace systems) to the corresponding loss with up-and-down slope culture [57]. In the Thao and Da basins, contour tillage and terrace are common in mountainous regions, such as in Yuanyang County in China and Sa Pa in Vietnam. In the Lo basin, industrial crops and rice paddy are common because of its lower slope. Therefore, referring to the values in accordance with different slopes, 0.7 was set for USLE_P for the agriculture land use in Thao and Da basins and 0.4 for the agriculture land use in the Lo basin. Sediment yield from landscape can be lagged and trapped routed through grassed waterway and vegetative filter strips before reaching the stream channel. In the Lo basin, edge-of-field filter strips, which could be cultivated lands, grass and bush, are widely distributed along the river, while in the other two sub-basins, there are no such filter strips due to the steep valley. From measurements on Google Earth views, the width can range from 20 m to more than 300 m. Combining filed investigation, expertise from local researchers and calibrations from model, a width edge-of-field filter strips of 25 m was set for FILTERW in the Lo basin, which is considered as an average and approached value.

A second group of parameters, relating to in-stream SS process (deposition and aggradation), is required for Equation (2), which is more familiar with a power function sediment rating curve as:

$$SSC = \alpha Q^{\beta} \quad (8)$$

where α and β are regression coefficients.

SPCON, SPEXP and PRF are the key parameters that control the maximum concentration of sediment that can be transported by the flow. SPCON corresponds to α and it is a proxy to express the river bed erodibility; the PRF parameter modulates the SPCON behavior, and the default value of PRF often equals 1. SPEXP corresponds to β to express the erosive power of the river [39]. According to Asselman [22], a low α-value coupled to a high β-value are characteristic of river sections with little sediment transport at low discharge. During the study period (2000–2014), the Red River basin encompassed large ranges of measured SSC values: 6.9–18,300

mg/L in the Thao River; 0.6–3350 mg/L in the Lo River; 0.4–481 mg/L in the Da River; and 2.1–4100 mg/L in the Red River at Son Tay. The Red River transports little sediment at low discharge, and a low α-value and a high βvalue should be set for this basin. Therefore, SPEXP was set to 2, and SPCON was calibrated after PRF and SPEXP were fixed. A value of 0.008 was set to SPCON before dam implementations, from 2000 to 2007. After dam implementations, the coarser particles were retained by dams, and the particle size distribution was affected downstream, leading to a change in the channel erodibility. Then, the dynamics of downstream suspended sediment transport decreased. Due to the complexity of dam implementations over the study period, we assume that the hydrodynamics of SS transport by the rivers in the Red River changed after 2007. Indeed, the Nansha dam is operational since 2008, and the Madushan dam construction started by the end of 2008; then Tuyen Quang is operational since 2008. Therefore, a lower value of SPCON (0.002) was set for the period from 2008. In Equation (4), two parameters are related to degradation process: CH_COV1 is the channel erodibility factor, and CH_COV2 is the channel cover factor channel. CH_COV1 is a function of properties of the bed or bank materials, and is conceptually similar to the soil erodibility factor used in the USLE equation [57]. CH_COV2 was set to 1, which means there is no vegetative cover on channel.

3.2.2. SSC Simulations

Statistics evaluation of SSC simulations at daily and monthly scales are shown in Table 5. According to the general evaluation of NSE and R^2, SSC simulations at these 5 stations are acceptable (NSE > 0, R^2 > 0). From the general performance ratings at monthly scale recommended by Moriasi et al. [86], Lao Cai, Yen Bai, Hoa Binh, and Son Tay stations presented satisfactory and good performance; and for the Vu Quang station, though the NSE is not satisfactory, PBIAS is within the satisfactory range. PBIAS values indicate that the model overestimated SSC for all stations. Maximum absolute values of PBIAS were 46.8%, which is still satisfactory following the Moriasi criteria (Table 5). Therefore, according to the statistic evaluations, the model simulated SSC at a satisfactory range.

The simulated SSC is in the range of the observed SSC during the simulation period, and showed similar trends to observations at the five stations (Figure 4). However, the magnitude of simulated SSC peaks was either underestimated or overestimated during some periods. For example, daily simulated SSC peaks were generally underestimated before 2009 at Lao Cai, Yen Bai, Hoa Binh, and Son Tay, but monthly SSC peaks fit well with observed monthly peaks. Conversely, some monthly simulated SSC peaks were overestimated, such as in 2011–2014 at Lao Cai, 2012–2014 at Yen Bai, 2006–2007 at Vu Quang, 2005 at Hoa Binh, and 2003–2006 at Son Tay.

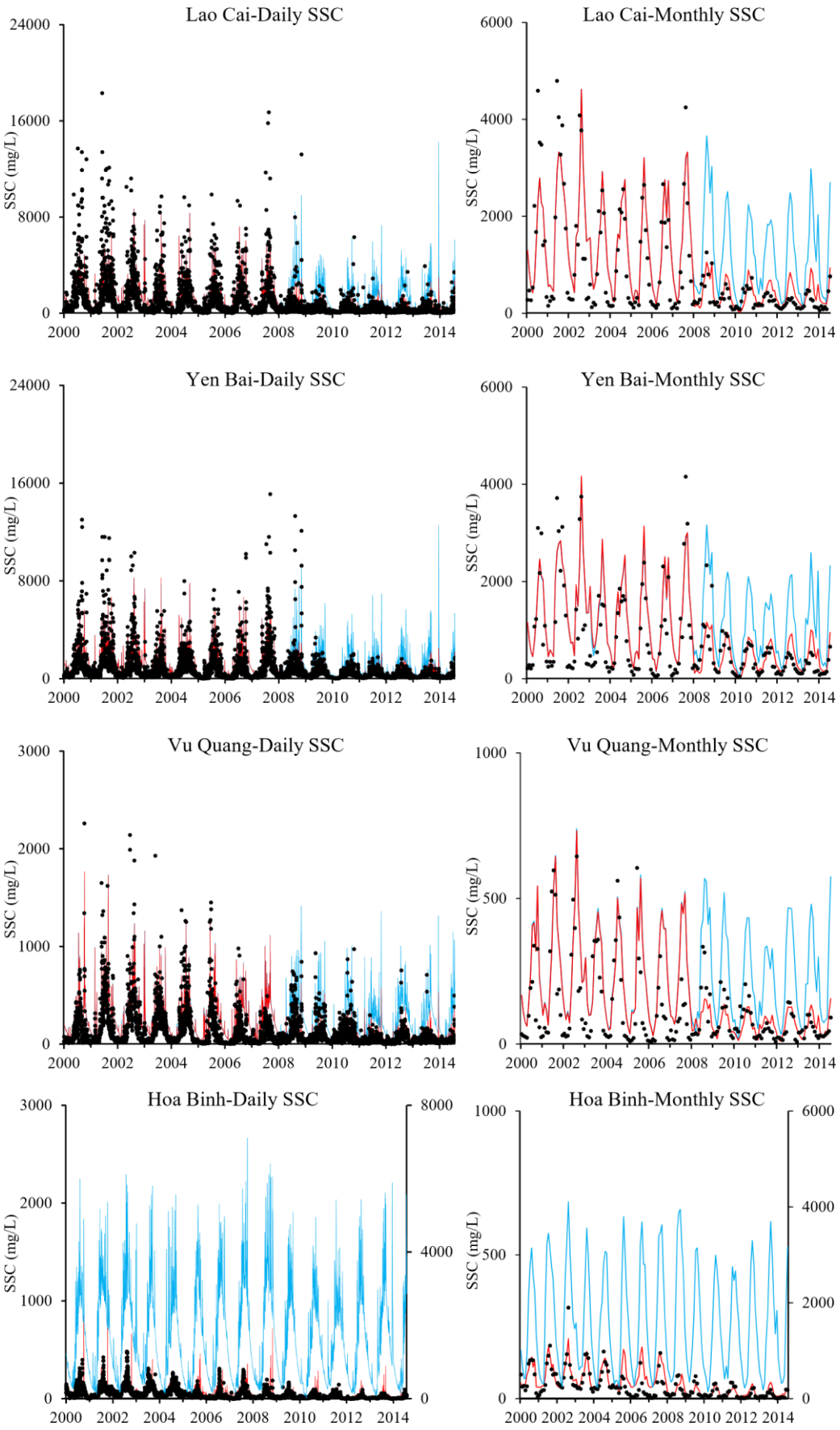
Lao Cai-Daily SSC
Lao Cai-Monthly SSC
Yen Bai-Daily SSC
Yen Bai-Monthly SSC
Vu Quang-Daily SSC
Vu Quang-Monthly SSC
Hoa Binh-Daily SSC
Hoa Binh-Monthly SSC
SSC (mg/L)
2000 2002 2004 2006 2008 2010 2012 2014

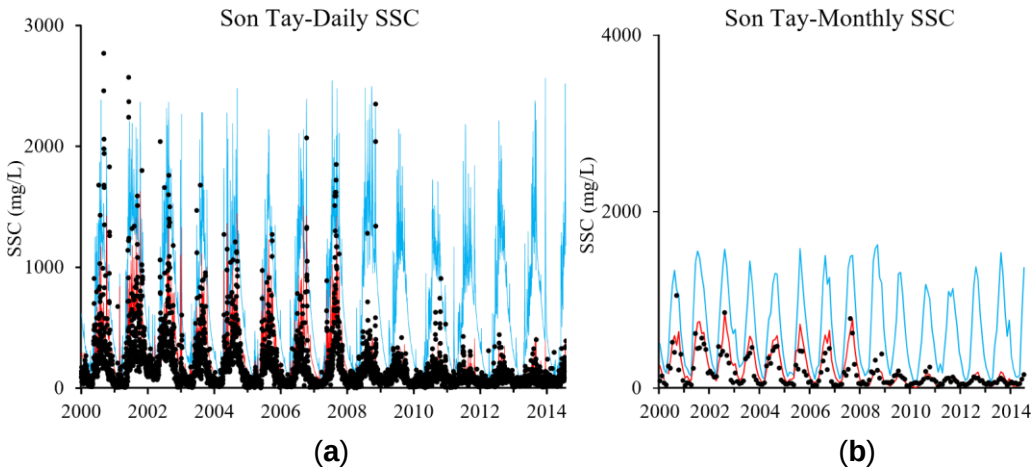

Figure 4. Observed (black dot) and actual simulated (red solid line) daily (**a**) and monthly (**b**) suspended sediment concentration (SSC) at five stations from January 2000 to July 2014. Blue solid line represents the scenario simulation of SSC under natural conditions.

3.3. Impacts of Climate Variability and Dams

In order to identify and separate the impacts of climate variability and dams, analysis was carried out based on the annual mean Q and SSC of natural conditions (without dams) and actual conditions.

3.3.1. Impacts on Q

Table 6 presents the annual mean Q in each year and the variation tendency of each station under different scenarios.

For the whole study period, under natural conditions, the biggest decreasing tendency of Q is at Son Tay station, followed by Yen Bai station, and least decreasing tendency is at Vu Quang station; under actual conditions, the annual mean Q decreased at almost the same degree at most stations compared with those under natural conditions, except at Hoa Binh station and consequently at Son Tay. During 2008–2013, the natural annual mean Q showed bigger decreasing tendencies compared to 2000–2013; actual annual mean Q decreased faster on the Thao River and Da River.

Decreasing rate was calculated from comparison between 2000–2007 and 2008–2013. The actual annual mean Q during 2008–2013 at Son Tay reduced to 13% of that during 2000–2007 under natural conditions; among them 9% was reduced by the climate variability, and 4% was caused by the dams upstream. Among the three tributaries, the Thao River shows little impacts of dams; the Vu Quang station on the Lo River actually shows positive impacts of climate and dams; the Hoa Binh on the Da River shows almost equal impacts of climate and dams.

Table 6. Annual mean discharge (Q) from 2000 to 2013 and the multi-year annual mean Q of 2000– 2007 (before new dams' constructions) and 2008–2013 (after new dams' constructions). Variation tendency of annual mean Q from 2000–2013 and 2008–2013. Impact percentages of climate variability and dams.

Q ($m^3 s^{-1}$)	Lao Cai		Yen Bai		Vu Quang		Hoa Binh		Son Tay	
	NC*	AC*	NC*	AC*	NC*	AC*	NC*	AC*	NC*	AC*
2000	551	551	757	757	694	694	1318	1370	2910	2963
2001	778	778	1013	1013	803	803	1645	1613	3656	3624
2002	741	741	971	971	733	733	1687	1688	3489	3491
2003	796	796	1029	1029	794	794	1677	1619	3696	3637
2004	520	520	745	745	670	670	1373	1364	2936	2928
2005	405	405	644	644	717	717	1217	1198	2713	2694
2006	476	476	666	666	651	651	1455	1456	2920	2921
2007	605	605	793	793	675	675	1521	1523	3123	3125
2008	693	693	995	995	975	1006	1810	1774	4019	4015
2009	406	406	623	623	722	763	1240	1391	2736	2928
2010	348	348	516	516	567	567	1110	849	2304	2043
2011	365	349	574	557	654	656	1221	1034	2603	2401
2012	351	352	566	568	723	717	1203	1093	2669	2556
2013	420	420	646	645	763	760	1452	1101	3066	2712
2000–2007	609	609	827	827	717	717	1487	1479	3180	3173
2008–2013	430	428	653	651	734	745	1339	1207	2900	2776
Tendency 2000–2013 ($m^3 s^{-1} year^{-1}$) (related R**)	−27.4 (0.70)	−27.7 (0.70)	−28.5 (0.66)	−28.8 (0.66)	−2.7 (0.12)	−2.2 (0.09)	−22.2 (0.43)	−40.8 (0.62)	−51.5 (0.44)	−69.9 (0.54)
Tendency 2008–2013 ($m^3 s^{-1} year^{-1}$) (related R**)	−43.1 (0.61)	−43.5 (0.61)	−53.1 (0.57)	−53.5 (0.57)	−27.7 (0.38)	−36.6 (0.46)	−51.1 (0.37)	−116.3 (0.66)	−133.3 (0.42)	−207.8 (0.57)
Impacts of climate and dams	-30%		-21%		+4%		-18%		-13%	
Impacts of climate	-29%		-21%		+2%		-10%		-9%	
Impacts of dams	-0.4%		-0.3%		+2%		-8%		-4%	

*NC, natural conditions; AC, actual conditions; R**, linear regression.

3.3.2. Impacts on SSC

Table 7 presented the annual mean SSC in each year and the variation tendency of each station under different scenarios.

For the whole study period, the SSC under natural conditions showed a biggest decreasing tendency in the Thao River, followed by the Da River, and least decreasing tendency was in the Lo River; under actual conditions, the annual mean SSC decreased more severely at most stations than under natural conditions, except at Hoa Binh station. During 2008–2013, the natural annual mean SSC showed bigger decreasing tendencies compared to 2000–2013; actual annual mean SSC decreased faster on the Thao River, then on the Lo and Da River.

The actual annual mean SSC during 2008–2013 at Son Tay reduced to 89% of that during 2000– 2007 under natural conditions; among the 89%, 13% was reduced because of the climate variability, and 76% was caused by the dams upstream. Among

the three tributaries, Hoa Binh and Vu Quang are influenced more by the dams while the Thao River basin is influenced more by the climate variability.

Table 7. Annual mean suspended sediment concentration (SSC) from 2000 to 2013 and the multi-year annual mean SSC of 2000–2007 (before new dams' constructions) and 2008–2013 (after new dams' constructions). Variation tendency of annual mean SSC from 2000 to 2013 and 2008 to 2013. Impact percentages of climate variability and dams.

SSC	Lao Cai		Yen Bai		Vu Quang		Hoa Binh		Son Tay	
(mg/L)	NC*	AC*	NC*	AC*	NC*	AC*	NC*	AC*	NC*	AC*
2000	1435	1435	1281	1294	241	238	1549	80	682	321
2001	1860	1860	1660	1671	279	276	1809	90	830	396
2002	1815	1815	1669	1686	287	283	1836	88	780	362
2003	1915	1915	1714	1726	277	273	1852	90	848	400
2004	1383	1383	1244	1257	221	216	1586	76	684	307
2005	1196	1196	1141	1166	236	231	1446	71	624	296
2006	1308	1308	1151	1167	225	222	1636	80	679	289
2007	1498	1498	1338	1347	246	244	1717	84	731	320
2008	1727	511	1512	576	286	94	1916	33	800	107
2009	1206	360	1068	438	224	67	1486	22	626	77
2010	1018	342	983	385	208	65	1394	19	554	77
2011	1166	388	1028	428	208	64	1455	18	612	75
2012	1085	381	1005	429	240	69	1384	20	592	78
2013	1243	409	1140	471	227	66	1597	22	655	83
2000–2007	1551	1551	1400	1414	251	248	1679	83	732	336
2008–2013	1241	398	1122	455	232	71	1539	23	640	83
Tendency 2000–2013 ($mg\ L^{-1}\ year^{-1}$) (related R**)	−48.9 (0.68)	−132.9 (0.89)	−42.9 (0.69)	−111.5 (0.89)	−3.5 (0.53)	−19.9 (0.90)	−21.3 (0.49)	−6.7 (0.89)	−13.7 (0.62)	−28.9 (0.90)
Tendency 2008–2013 ($mg\ L^{-1}\ year^{-1}$) (related R**]	−75.3 (0.56)	−11.5 (0.36)	−57.2 (0.54)	−14.5 (0.41)	−7.0 (0.45)	−3.7 (0.62)	−52.6 (0.49)	−1.7 (0.58)	−22.1 (0.48)	−3.5 (0.53)
Impacts of climate and dams	-74%		-68%		-72%		-99%		-89%	
Impacts of climate	-20%		-20%		-8%		-8%		-13%	
Impacts of dams	-54%		-48%		-64%		-90%		-76%	

*NC, natural conditions; AC, actual conditions; R**, linear regression.

4. Discussion

4.1. Uncertainties

4.1.1. Uncertainties of Hydrology Modeling

Base flow alpha factor (ALPHA_BF), which was sensitive for baseflow, was suggested by the Baseflow Filter Program [93,94] to 0.02. Other parameters associated with groundwater and baseflow in Table 4 were calibrated by SWAT-CUP under the range recommended by SWAT theoretical documentation [57]. Hydrological parameters were calibrated at the whole basin, while these three sub-basins are different in hydrogeology, soil and land use. This might cause the deviations on the baseflow estimation at Vu Quang in the Lo sub-basin. In addition, downstream of the Red River system, especially in the Lo River sub-basin, agriculture activities are active and intensive, and there are many complex irrigation systems. Water is extracted for irrigation from the main stream and delivered to ditch and canal, or water can be taken from one river and drainage to another river. This might contribute to uncertainties for the baseflow at the Lo River sub-basin.

The simulation of the peak Q on the Thao River is more satisfactory than on the Lo

and Da Rivers. The underestimation during flood season most probably results from the errors in either precipitation estimates or uncertainties in observed flow. Le et al. [95] indicated that due to the coarse resolution, TRMM rainfall products cannot adequately capture extreme rainfall values. The scatter plots of precipitation from rain gauge stations versus TRMM products from the study of Liu et al. [96] and Simons et al. [54] also showed that high and intensive rainfall is underestimated by TRMM. Discharge of high floods is usually extrapolated by rating curve, which can cause uncertainties.

As shown in Table 1, two dams (the Thac Bac dam and the Hoa Binh dam) were implemented before the beginning of the simulation period (2000), and other dams started to operate since 2008. Upstream of Lao Cai, China has been building cascade power stations, and the first one named Nansha dam started to be built on February 2006 and to work on November 2007, and the second one named Madushan dam began to be constructed downstream in December 2008 and started to work in December 2010. Upstream of the Lo River, the Tuyen Quang dam has been put into function since March 2008. Furthermore, there are at least 10 more smaller dams that can be found on Google Earth in Vietnam; however, when these dams were operated is difficult to figure out. Upstream of Hoa Binh station, the Son La dam was implemented on December 2010, and at least 8 more dams can be seen on Google Earth in Vietnam. Certainly, many dams can be also found in Chinese part for both the Lo and Da River on Google Earth. Liu et al. [97] pointed that hydrological forecasting effectiveness and accuracy would be affected greatly by the construction and operation of the cascade reservoirs. It is difficult for the model to precisely simulate the complex operation of dam discharge, which depends on the arriving water volume, on the downstream water regime, and also on the variation of irrigation storage. Complexities can be seen in the base Q from 2010 to 2014 at Hoa Binh station. Besides, as mentioned before, there are many small dams and irrigation systems that were not taken into account in this model; this also contributed to deviations in simulations. These uncertainties of anthropogenic influences, especially the dams, caused deviation on calibrations, such as the base Q of 2010–2014 at Vu Quang station. Nevertheless, monthly simulated Q at Vu Quang is still satisfactory with NSE of 0.58, R^2 of 0.65, and PBIAS of 21.3.

4.1.2. Uncertainties of Suspended Sediment Modeling

From the daily simulation, we can notice that deviations mainly occur during large floods. Some studies [89,98] showed that modeling might underestimate SSC during high and intensive rainfall. This underestimation can come from the landscape component when using a runoff factor instead of rainfall energy factor, or/and from the channel component where particle-size elements are neither tracked nor considered in the physical processes in floodplains. As already explained, uncertainties can also be related to satellite rainfall estimations from TRMM, or/and from data measurement and sampling strategy.

The SWAT model used a simplified version of Bagnold [77] stream power equation to calculate the maximum amount of sediment that could be transported in a stream segment. However, this algorithm does not keep track of particle size distribution of elements that pass through the channel, and all are assumed to be of silt size. Further, the channel erosion is not partitioned between stream bank and stream bed, and deposition is assumed to occur only in the main channel; flood plain sediment deposition is also not modeled separately [57]. Therefore, this simplification can cause deviations for sediment routing.

4.2. Water Balance and Yield

The average annual rainfall during the simulation period, using the TRMM data of precipitation, was 1493.6 mm, of which 53% (787.7 mm) was taken away through evapotranspiration (ET) and 47% fed the stream flow. The average potential evapotranspiration (ETP) predicted by the model was 1293 mm. Le et al. [83] used different methods to predict the ETP of this basin, and gave a range from 960 to 1289 mm for the period 1964–2008, while the actual evapotranspiration (ETA) was estimated from 771 to 1186 mm. For streamflow, the model estimated a water yield of 696.8 mm, which is close to the real water yield, 669 mm, calculated from the data collected from the Vietnam Ministry of Natural Resources and Environment (MONRE) during the same period. Among the simulated water yield, surface runoff accounted for 39% while the lateral flow accounted for 3% and the groundwater accounted for 58%. This result is in agreement with Le [50] and Bui et al. [84]. Le [50] indicated that the groundwater resource in Vietnam is abundant, accounting for around 58% of total streamflow, and is a critical component river flow during the dry season. Bui et al. [84] underlined on a typical small steep basin of Northern Vietnam that the deep infiltration is a key factor of the hydrological pattern in spite of the strong slope gradient above 30%. Therefore, the model provided a credible simulation for each component.

Simulated mean annual Q during study period at Lao Cai, Yen Bai, Vu Quang, Hoa Binh, and Son Tay are 16.7, 23.7, 23.0, 43.0 and 94.7 km^3, respectively, suggesting that the Thao River and the Lo River account for nearly 54.6% of the total volume of Son Tay, while the Da River accounts for 45.4%. According to the references and data we collected from the MONRE, the mean annual runoff volume upstream in China from 1956–2000 was 14.6 km^3, ranging from 8.4 km^3 in 1980 to 24.6 km^3 in 1971 [53], and the simulation at Lao Cai is within this range; and at Son Tay from 1960 to 2010, the mean annual runoff was 105.7 km^3, with a minimum value of 80.2 km^3 in 2010, and a maximum of 158.4 km^3 in 1971. Other studies indicated that the Da River is the main flow contribution to the Son Tay, accounting for 50–57% of the total discharge [37,39,85]. Simulations are thus in good agreement with other studies and with the observed data.

Hence, combining with the satellite date, the model performed well at both water balance and yield.

4.3. Natural Conditions Effects

In order to find out the driving factors that decrease Q under natural conditions, we analyzed the tendency of the annual mean rainfall, evapotranspiration (ET), and temperature of the whole basin. From Figure 5, we can see that the annual mean rainfall shows decreasing tendencies while temperature shows a contrary tendency. ET can come from the water body, the plants and the soil, and it can be influenced by many factors, such as geomorphology, climate, soil water content, vegetation cover, etc. Ignoring the possible changes of geomorphology and vegetation cover, we checked the variation of soil water content and found that it showed a decreasing tendency though its decreasing rate is smaller than the one of ET (Figure 5b). Not taking into account the runoff loses, the available water yield should theoretically equal the difference between rainfall and ET. We can find in Figure 5a that the difference between rainfall and ET shows a decreasing trend, which might indicate that the average annual water yield decreases. During the study period, the annual mean rainfall reduces by 9%, ET reduces by 5%, and temperature increases by 1%. These changes result a 13% decrease of available water with a 4% decrease of soil water content.

Table 6 shows that the main impact factor is not the same in different sub-basins. This can relate to the regional climate characteristics. From the study of Le et al. [37], among these three sub-basins, the mean annual rainfall was highest for the Thao sub-basin, followed by the Da sub-basin, and then the Lo sub-basin. Therefore, the different Q variation rates of each sub-basin can relate to the distribution of rainfall, and the decrease of the rainfall might affect the Thao basin most, resulting a biggest Q decreasing rate among the three tributaries.

Different SSC decreasing rates relate to the different soil erosion rates under different rainfall intensity of each sub-basin. As described in Section 3.2.1, the Thao and the Da basin are more vulnerable to soil erosion; the possible decrease in rainfall might have much less impacts on soil erosion in these two sub-basins than in the Lo basin.

In our study, it is impossible and difficult for us to get all the information of all the dams in this large-scale basin, and take all of them into account in this model. Therefore, this model cannot strictly represent the natural conditions. However, some of the dams locate quite upstream of the Da and Lo tributaries and are with smaller capacities, and these reasons can make them have much less impact on the SSC at the outlet of each tributary. Hence, removing the 6 dams that we considered in the model might maximally reflect the natural conditions.

Land use changes were not taken into account. However, land use changes have been proved to have effects on soil erosion [99]. Therefore, it would be interesting to take the land use changes into account in the future.

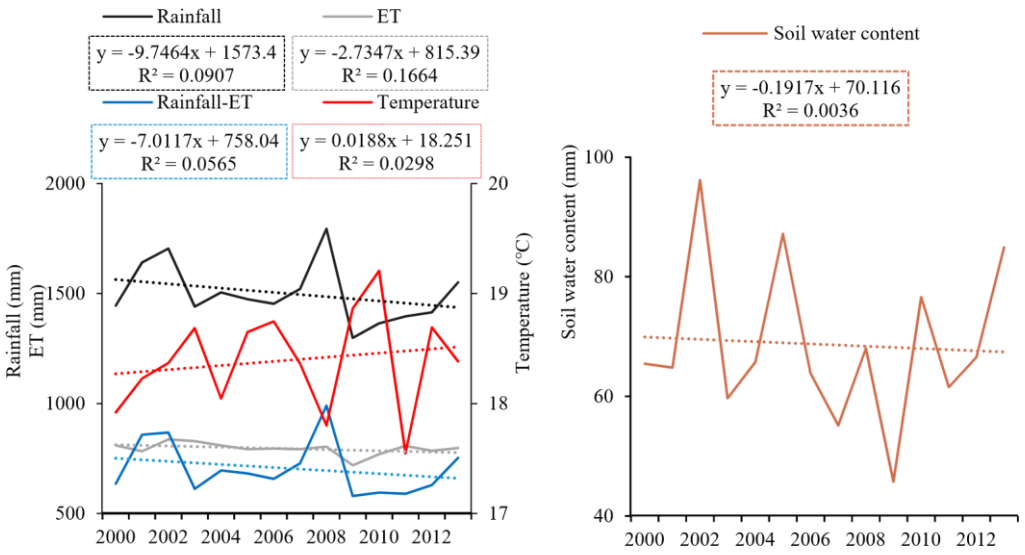

(**a**) (**b**)

Figure 5. (**a**) Annual rainfall (black solid line), actual evapotranspiration (ET) (gray solid line) and temperature (red solid line) of the whole Red River basin from 2000 to 2013. Blue solid line is the difference between rainfall and ET, which theoretically equals to available water. Black, gray, blue and red dash lines are the trendlines of rainfall, ET, the difference between rainfall and ET, and temperature, respectively. Formulas in the black, gray, blue and red rectangles are the linear fit equations of rainfall, ET, the difference between rainfall and ET, and temperature, respectively. (**b**) Mean annual soil water content (brown solid line) of the whole Red River basin from 2000 to 2013. Brown dash line is the trendline of soil water content, and formula in the black the linear fit equation of soil water content.

4.4. Impacts of Dams

Dams show different degrees of impacts on both Q and SSC. Due to the big capacity of Hoa Binh dam, it shows bigger regulating effect on downstream flow than other dams. Liu et al. [97] addressed that the impact of the dam on runoff increased with the dam capacity. However, even though the Hoa Binh dam has a big capacity, its impact on Q is small. This result is in agreement with the study from Dang et al. [39] who found that there was little or no change of Q before and after the Hoa Binh dam.

Previous studies [39,40,43] estimated the impacts on SS from dams before 2011 based on the measurements. Dang et al. [39] and Vinh et al. [43] mainly focused on the effect of the Hoa Binh dam, and Lu et al. [40] also considered the Thac Ba dam, the Tuyen Quang dam, and the Son La dam. We extended the time period to 2013 and also took the dams in China into account. After 2008, at Lao Cao and Yen Bai station, the actual annual mean SSC reduced to 74% and 68% of that during 2000– 2007, among which 54% and 48% are due to the dam effects, respectively. With the accumulation impacts from old dams and new dams, at Vu Quang and Hoa Binh, the actual annual mean SSC reduced to 72% and 99% of that during 2000–2007, among which 64% and 90% are due to the dam effects, respectively. At Son Tay station, the outlet of the continental basin, the annual mean SSC reduced to 89% of that under natural conditions during 2000–2007, and 76% of this 89% was caused by the dams upstream. With more dams to be put into use, the SSC at Son Tay might continue to decrease, and this might influence the downstream water system.

5. Conclusions

This is the first study trying to use a modeling approach to analyze hydrology regime and suspended sediment concentration at a daily scale for a long period in the Red River basin, including considering the successive implementations of dams all along the period. The SWAT model provided some insights on discharge and suspended sediment concentration at daily and monthly scales, respectively, in such a large basin. This study allowed us to understand, characterize, and quantify the discharge and suspended sediment concentration with spatial and temporal variations. What is more, using a modeling approach helped us to separate the impacts from climate variability and anthropogenic impacts. However, some improvements are needed, such as dam information and management, observed rainfall data, discharge and suspended sediment dataset of more stations and longer period, high frequency dataset, to gain a better estimation and understanding of the impacts of climate variability and human interferences.

Under the impacts of both climate variability and dams, the Q and SSC show a decreasing trend. However, climate variability and dams have different influence degrees in different sub-basins. The decrease of Q is more related to climate variability while the decrease of SSC is more related to impacts of dams. The annual mean rainfall of the whole basin decreased 9%, evapotranspiration decreased 5%, and temperature increased 1%; which consequently resulted a 4% decrease on soil water content and a 13% decrease of available water for the whole basin. With the accumulated impacts from three tributaries, at the outlet, Son Tay, from 2008 to 2013, the Q decreased to 13% of that under natural conditions of 2000–2007, and climate variability caused 9% decrease and dams caused 4%; SSC decreased to 89% of that under natural conditions of 2000–2007, and 13% came from the impacts of climate and 76% was decreased by the dams.

With more dams to be implemented in this basin both in Chinese and Vietnamese part, sediment retention would consequently increase, which could subsequently influence the transport of associated matters, such as nutrients, metals, and pesticide, and also the habitats downstream. Based on this study, future studies of nutrients, metal, and pesticide transports and quantification can be carried out by using this new tool. In addition, more scenarios of the global changes, such as land use changes and climate changes in the future and their impacts on hydrology and suspended sediment could be quantified by using the model implemented.

Author Contributions: Conceptualization, X.W. S.S. and J.-M.S.-P.; methodology, X.W., S.S., T.P.Q.L., S.O., D.O., and J.-M.S.-P.; software, X.W. S.S. and J.-M.S.-P.; validation, X.W. S.S. and J.-M.S.-P.; formal analysis, X.W., S.S.,

T.P.Q.L., S.O., D.O., and J.-M.S.-P.; investigation, X.W., S.S., T.P.Q.L., S.O., D.O., and J.-M.S.-P.; resources, X.W., S.S., T.P.Q.L., S.O., V.D.V., D.O., and J.-M.S.-P.; data curation, X.W., J.-M.S.-P., T.P.Q.L., D.O. and V.D.V.; writing—original draft

preparation, X.W.; writing—review and editing, X.W., S.S., T.P.Q.L., S.O., V.D.V., D.O., and J.-M.S.-P.; visualization, X.W.; supervision, S.S. and J.-M.S.-P.; project administration, S.S. and J.-M.S.-P.; funding acquisition, X.W. S.S., J.-M.S.-P., T.P.Q.L., S.O, V.D.V.

Funding: This research was developed under the LOTUS joint laboratory, established with Vietnamese and French research groups (http://lotus.usth.edu.vn/) and funded by L'Institut de recherche pour le développement (IRD). The PhD scholarship of Xi Wei is financially supported by the China Scholarship Council (CSC), grant number 201606240088.

Acknowledgement: We appreciate the LOTUS Int. Joint. Lab for providing the dataset, and also the research travel funds for Xi WEI to collect data and information in Vietnam.

Conflicts of Interest: The authors declare no conflict of interest.

References

1. Mekonnen, M.M.; Hoekstra, A.Y. Four billion people facing severe water scarcity. *Sci. Adv.* **2016**, *2*, e1500323, doi:10.1126/sciadv.1500323.
2. *Global Risks 2015, 10th Edition*; World Economic Forum: Geneva, Switzerland, 2015.
3. Kunz, M.J.; Wüest, A.; Wehrli, B.; Landert, J.; Senn, D.B. Impact of a large tropical reservoir on riverine transport of sediment, carbon, and nutrients to downstream wetlands. *Water Resour. Res.* **2011**, *47*, W12531. 4. Lal, R.; Kimble, J.; Levine, E.; Stewart, B.A. *Soils and Global Change*; CRC Press: Boca Raton, FL, USA, 1995.
5. Nijssen, B.; O'donnell, G.M.; Hamlet, A.F.; Lettenmaier, D.P. Hydrologic sensitivity of global rivers to climate change. *Clim. Chang.* **2001**, *50*, 143–175, doi:10.1023/A:1010616428763.
6. Arnell, N.W. Climate change and global water resources. *Glob. Environ. Chang.* **1999**, *9*, S31–S49, doi:https://doi.org/10.1016/S0959-3780(99)00017-5.
7. Thi Ha, D.; Ouillon, S.; Van Vinh, G. Water and Suspended Sediment Budgets in the Lower Mekong from High-Frequency Measurements (2009–2016). *Water* **2018**, *10*, 846, doi:10.3390/w10070846.
8. Watson, R.T.; Noble, I.R.; Bolin, B.; Ravindranath, N.H.; Verardo, D.J.; Dokken, D.J. *The Intergovernmental Panel on Climate Change (IPCC) Special Report on Land Use, Land-Use Change, and Forestry*; Cambridge University Press: Cambridge, UK, 2000.
9. FAO. *The State of the World's Land and Water Resources for Food and Agriculture (SOLAW)—Managing Systems at Risk*; The Food and Agriculture Organization of the United Nations: Abingdon, UK; Earthscan: New York, NY, USA, 2011; ISBN 9781849713269.
10. Valentin, C.; Agus, F.; Alamban, R.; Boosaner, A.; Bricquet, J.P.; Chaplot, V.; de Guzman, T.; de Rouw, A.; Janeau, J.L.; Orange, D.; et al. Runoff and sediment losses from 27 upland catchments in Southeast Asia: Impact of rapid land use changes and conservation practices. *Agric. Ecosyst. Environ.* **2008**, *128*, 225–238, doi:10.1016/j.agee.2008.06.004.
11. Chen, J.; Shi, H.; Sivakumar, B.; Peart, M.R. Population, water, food, energy and dams. *Renew. Sustain. Energy Rev.* **2016**, *56*, 18–28, doi:10.1016/j.rser.2015.11.043.
12. Zimmerman, J.B.; Mihelcic, J.R.; Smith, J. Global Stressors on Water Quality and Quantity. *Environ. Sci. Technol.* **2008**, *42*, 4247–4254.
13. Hecht, J.S.; Lacombe, G.; Arias, M.E.; Dang, T.D.; Piman, T. Hydropower dams of the Mekong River basin: A review of their hydrological impacts. *J. Hydrol.* **2019**, *568*, 285–300, doi:10.1016/j.jhydrol.2018.10.045.
14. *Dams and Development: A New Framework for Decision-Making*; The World Commission on Dams: London UK, 2000; http://www.dams.org/report/.
15. Lehner, B.; Liermann, C.R.; Revenga, C.; Vörösmarty, C.; Fekete, B.; Crouzet, P.; Döll, P.; Endejan, M.; Frenken, K.; Magome, J.; et al. High-resolution mapping of the world's reservoirs and dams for sustainable river-flow management. *Front. Ecol. Environ.* **2011**, *9*, 494–502, doi:10.1890/100125.
16. Zarfl, C.; Lumsdon, A.E.; Berlekamp, J.; Tydecks, L.; Tockner, K. A global boom in hydropower dam construction. *Aquat. Sci.* **2015**, *77*, 161–170, doi:10.1007/s00027-014-0377-0.
17. Manh, N. Van; Dung, N.V.; Hung, N.N.; Kummu, M.; Merz, B.; Apel, H. Future sediment dynamics in the Mekong Delta floodplains: Impacts of hydropower development, climate change and sea level rise. *Glob. Planet. Chang.* **2015**, *127*, 22–33, doi:10.1016/j.gloplacha.2015.01.001.
18. Vörösmarty, C.J.; Meybeck, M.; Fekete, B.; Sharma, K.; Green, P.; Syvitski, J.P.M. Anthropogenic sediment retention: Major global impact from registered river impoundments. *Glob. Planet. Chang.* **2003**, *39*, 169–190, doi:10.1016/S0921-8181(03)00023-7.
19. Syvitski, J.P.M.; Vörösmarty, C.J.; Kettner, A.J.; Green, P. Impact of humans on the flux of terrestrial sediment to the global coastal ocean. *Science* **2005**, *308*, 376–380, doi:10.1126/science.1109454.
20. Syvitski, J.P.; Morehead, M.D.; Bahr, D.B.; Mulder, T. Estimating fluvial sediment transport: The rating parameters. *Water Resour. Res.* **2000**, *36*, 2747–2760, doi:10.1172/JCI99287.
21. Zhang, S.; Chen, D.; Li, F.; He, L.; Yan, M.; Yan, Y. Evaluating spatial variation of suspended sediment ratingcurves in the middle Yellow River basin, China. *Hydrol. Process.* **2018**, *32*, 1616–1624, doi:https://doi.org/10.1002/hyp.11514.
22. Asselman, N.E. Fitting and interpretation of sediment rating curves. *J. Hydrol.* **2000**, *234*, 228–248.
23. Achite, M.; Ouillon, S. Suspended sediment transport in a semiarid watershed, Wadi Abd, Algeria (1973–1995). *J. Hydrol.* **2007**, *343*, 187–202, doi:10.1016/j.jhydrol.2007.06.026.
24. Daniel, E.B.; Camp, J.V.; LeBoeuf, E.J.; Penrod, J.R.; Dobbins, J.P.; Abkowitz, M.D. Watershed Modeling and its Applications: A State-of-the-Art Review. *Open Hydrol. J.* **2011**, *5*, 26–50, doi:10.2174/1874378101105010026.
25. Islam, Z. *A Review on Physically Based Hydrologic Modeling*; University of Alberta: Edmonton, AB, Canada, 2011; Available online: https://www.researchgate.net/publication/272169378_A_Review_on_Physically_Based_Hydrologic_Modeling (accessed on 3 May 2019).
26. Devia, G.K.; Ganasri, B.P.; Dwarakish, G.S. A Review on Hydrological Models. *Aquat. Procedia* **2015**, *4*, 1001– 1007, doi:10.1016/j.aqpro.2015.02.126.

27. Fu, B.; Merritt, W.S.; Croke, B.F.W.; Weber, T.R.; Jakeman, A J. A review of catchment-scale water quality and erosion models and a synthesis of future prospects. *Environ. Model. Softw.* **2019**, *114*, 75–97, doi:10.1016/j.envsoft.2018.12.008.
28. Graham, D.N.; Butts, M.B. Flexible, Integrated Watershed Modelling with MIKE SHE in Watershed Models. In *Watershed Models*; Singh, V.P., Frevert, D.K., Eds.; CRC Press: Boca Raton, FL, USA, 2005; ISBN 0849336090.
29. Bicknell, B.R.; Imhoff, J.C.; Kittle, J.L.J.; Anthony, S. Donigian, J.; Johanson, R.C. *Hydrological Simulation Program—Frotran: User ' s Manual for Version 11*; AQUA TERRA Consultants: Mountain View, CA, USA, 1997.
30. Arnold, J.G.; Srinivasan, R.; Muttiah, R.S.; Williams, J.R. Large area hydrologic modeling and assesment Part I: Model development. *JAWRA J. Am. Water Resour. Assoc.* **1998**, *34*, 73–89, doi:10.1111/j.17521688.1998.tb05961.x.
31. Gassman, P.W.; Reyes, M.R.; Green, C.H.; Arnold, J.G. The Soil and Water Assessment Tool : Historical development, applications, and future research directions. *Trans. ASAE* **2007**, *50*, 1211–1250, doi:10.1.1.88.6554.
32. Bannwarth, M.A.; Hugenschmidt, C.; Sangchan, W.; Lamers, M.; Ingwersen, J.; Ziegler, A.D.; Streck, T. Simulation of Stream Flow Components in a Mountainous Catchment in Northern Thailand with SWAT, Using the ANSELM Calibration Approach. *Hydrol. Processes* **2015**, *29*, 1340–1352.
33. Lweendo, M.K.; Lu, B.; Wang, M.; Zhang, H.; Xu, W. Characterization of droughts in humid subtropical region, upper kafue river basin (Southern Africa). *Water* **2017**, *9*, 242, doi:10.3390/w9040242.
34. Li, D.; Christakos, G.; Ding, X.; Wu, J. Adequacy of TRMM satellite rainfall data in driving the SWAT modeling of Tiaoxi catchment (Taihu lake basin, China). *J. Hydrol.* **2018**, *556*, 1139–1152, doi:10.1016/j.jhydrol.2017.01.006.
35. Shrestha, B.; Cochrane, T.A.; Caruso, B.S.; Arias, M.E. Land use change uncertainty impacts on streamflow and sediment projections in areas undergoing rapid development: A case study in the Mekong Basin. *Land Degrad. Dev.* **2018**, *29*, 835–848, doi:10.1002/ldr.2831.
36. Thiet, N. Van; Didier, O.; Dominique, L.; Van Cu, P. Consequences of large hydropower dams on erosion budget within hilly agricultural catchments in Northern Vietnam by RUSLE modeling. In proceedings of the International Conference Sediment Transport Modeling in Hydrological Watersheds and Rivers, Istanbul, Turkey, 14–16 November 2012; p. 8.
37. Le, T.P.Q.; Garnier, J.; Gilles, B.; Sylvain, T.; Van Minh, C. The changing flow regime and sediment load of the Red River, Viet Nam. *J. Hydrol.* **2007**, *334*, 199–214, doi:10.1016/j.jhydrol.2006.10.020.
38. He, D.; Ren, J.; Fu, K.; Li, Y. Sediment change under climate changes and human activities in the Yuanjiang Red River Basin. *Chinese Sci. Bull.* **2007**, *52*, 164–171, doi:10.1007/s11434-007-7010-8.
39. Dang, T.H.; Coynel, A.; Orange, D.; Blanc, G.; Etcheber, H.; Le, L. A. Long-term monitoring (1960–2008) of the river-sediment transport in the Red River Watershed (Vietnam): Temporal variability and damreservoir impact. *Sci. Total Environ.* **2010**, *408*, 4654–4664, doi:10.1016/j.scitotenv.2010.07.007.
40. Lu, X.X.; Oeurng, C.; Le, T.P.Q.; Thuy, D.T. Sediment budget as affected by construction of a sequence of dams in the lower Red River, Viet Nam. *Geomorphology* **2015**, *248*, 125–133, doi:10.1016/j.geomorph.2015.06.044.
41. Le, T.P.Q.; Dao, V.N.; Rochelle-Newall, E.; Garnier, J.; Lu, X.; Billen, G.; Duong, T.T.; Ho, C.T.; Etcheber, H.; Nguyen, T.M.H.; et al. Total organic carbon fluxes of the Red River system (Vietnam). *Earth Surf. Processes Landf.* **2017**, *42*, 1329–1341, doi:10.1002/esp.4107.
42. Ngo, T.S.; Nguyen, D.B.; Rajendra, P.S. Effect of land use change on runoff and sediment yield in Da River Basin of Hoa Binh province, Northwest Vietnam. *J. Mt. Sci.* **2015**, *12*, 1051–1064, doi:10.1007/s11629-0132925-9.
43. Vinh, V.D.; Ouillon, S.; Thanh, T.D.; Chu, L.V. Impact of the Hoa Binh dam (Vietnam) on water and sediment budgets in the Red River basin and delta. *Hydrol. Earth Syst. Sci.* **2014**, *18*, 3987–4005, doi:10.5194/hess-18-3987-2014.
44. Luu, T.N.M.; Garnier, J.; Billen, G.; Orange, D.; Némery, J.; Le, T.P.Q.; Tran, H.T.; Le, L.A. Hydrological regime and water budget of the Red River Delta (Northern Vietnam). *J. Asian Earth Sci.* **2010**, *37*, 219–228, doi:10.1016/j.jseaes.2009.08.004.
45. Hiep, N.H.; Luong, N.D.; Viet Nga, T.T.; Hieu, B.T.; Thuy Ha, U.T.; Du Duong, B.; Long, V.D.; Hossain, F.; Lee,H. Hydrological model using ground- and satellite-based data for river flow simulation towards supporting water resource management in the Red River Basin, Vietnam. *J. Environ. Manag.* **2018**, *217*, 346– 355, doi:https://doi.org/10.1016/j.jenvman.2018.03.100.
46. Zhu, Y.; Chen, C.; Jiang, H. Preliminary study on water resources protection in the Yuanjiang dry-hot valley of the Honghe river basin. *Pearl River* **2012**, *1*, 15–17, doi:10.3969/j.issn.1001-9235.2012.01.005. (In Chinese)
47. Zhang, W.; Zhao, Z.; Tan, S.; Li, Y.; Wang, A. Study on the soil erosion in the Yuanjiang–Honghe boundary river areas. *Geol. Surv. China* **2017**, *4*, 64–69, doi:10.19388 /j.zgdzdc.2017. 03.10. (In Chinese)
48. Bai, Z.; Feng, D.; Ding, J.; Duan, X. A study on the variations of soil physico-chemical properties and its environmental impactfactors in the Red River watershed. *Yunnan Geogr. Environ. Res.* **2015**, *27*, 81–90, doi:10.13277/j.cnki.jcwu.2015.04.013. (In Chinese)

49. Barton, A.P.; Fullen, M.A.; Mitchell, D.J.; Hocking, T.J.; Liu, L.; Wu Bo, Z.; Zheng, Y.; Xia, Z.Y. Effects of soil conservation measures on erosion rates and crop productivity on subtropical Ultisols in Yunnan Province, China. *Agric. Ecosyst. Environ.* **2004**, *104*, 343–357, doi:10.1016/j.agee.2004.01.034.
50. Le, T.P.Q. Biogeochemical Functioning of the Red River (North Vietnam): Budgets and Modelling. Ph.D. Thesis, Université Paris VI-Pierre et Marie Curie, Paris, France, 2005.
51. Li, X.; Li, Y.; He, J.; Luo, X. Analysis of variation in runoff and impacts factors in the Yuanjiang-Red River Basin from 1956 to 2013. *Resour. Sci.* **2016**, *38*, 1149–1159, doi:10.18402/resci.2016.06.14. (In Chinese)
52. Xie, S. The Hydrological Characteristics of the Red River Basin. *Hydrology* **2002**, *22*, 57–63, doi:10.3969/j.issn.1000-0852.2002.04.017. (In Chinese)
53. Li, Y.; He, D.; Ye, C. Spatial and temporal variation of runoff of red river basin in yunnan. *J. Geogr. Sci.* **2008**, *18*, 308–318, doi:10.1007/s11442-008-0308-x.
54. Simons, G.; Bastiaanssen, W.; Ngô, L.; Hain, C.; Anderson, M.; Senay, G. Integrating Global SatelliteDerived Data Products as a Pre-Analysis for Hydrological Modelling Studies: A Case Study for the Red River Basin. *Remote Sens.* **2016**, *8*, 279, doi:10.3390/rs8040279.
55. Frenken, K. *Irrigation in Southern and Eastern Asia in Figures*; FAO: Rome, Italy, 2011.
56. Ren, J.; He, D.; Fu, K.; Li, Y. Sediment variation in the Yuanjiang (the Red River Basin) driven by climate change and human activities. *Chin. Sci. Bull.* **2007**, *52*, 142–147, doi:https://doi.org/10.1360/csb2007-52-zkII142. (In Chinese)
57. Neitsch, S.; Arnold, J.; Kiniry, J.; Williams, J. Soil and Water Assessment Tool Theoretical Documentation Version 2009; Texas Water Resources Institute Technical Report No. 406; Texas A&M University System: College Station, TX, USA, 2009.
58. Giang, P.Q.; Toshiki, K.; Sakata, M.; Kunikane, S.; Vinh, T.Q. Modelling climate change impacts on the seasonality of water resources in the upper Ca river watershed in Southeast Asia. *Sci. World J.* **2014**, *2014*, doi:10.1155/2014/279135.
59. Ma, C.; Sun, L.; Liu, S.; Shao, M.; Luo, Y. Impact of climate change on the streamflow in the glacierized Chu River Basin, Central Asia. *J. Arid Land* **2015**, *7*, 501–513, doi:10.1007/s40333-015-0041-0.
60. Piman, T.; Cochrane, T.A.; Arias, M.E.; Green, A.; Dat, N.D. Assessment of Flow Changes from Hydropower Development and Operations in Sekong, Sesan, and Srepok Rivers of the Mekong Basin. *J. Water Resour. Plan. Manag.* **2013**, *139*, 723–732, doi:10.1061/(ASCE)WR.1943-5452.0000286.
61. Bannwarth, M.A.; Sangchan, W.; Hugenschmidt, C.; Lamers, M.; Ingwersen, J.; Ziegler, A.D.; Streck, T. Pesticide transport simulation in a tropical catchment by SWAT. *Environ. Pollut.* **2014**, *191*, 70–79.
62. de Silva, V.P.R.; Silva, M.T.; Singh, V.P.; de Souza, E.P.; Braga, C.C.; de Holanda, R.M.; Almeida, R.S.R.; de Sousa, F.A.S.; Braga, A.C.R. Simulation of stream flow and hydrological response to land-cover changes in a tropical river basin. *Catena* **2018**, *162*, 166–176.
63. da Silva, R.M.; Dantas, J.C.; Beltrão, J.A.; Santos, C.A.G. Hydrological simulation in a tropical humid basin in the Cerrado biome using the SWAT model. *Hydrol. Res.* **2018**, *49*, 908–923, doi:10.2166/nh.2018.222.
64. Fukunaga, D.C.; Cecílio, R.A.; Zanetti, S.S.; Oliveira, L.T.; Caiado, M.A.C. Application of the SWAT hydrologic model to a tropical watershed at Brazil. *Catena* **2015**, *125*, 206–213, doi:10.1016/j.catena.2014.10.032.
65. Marhaento, H.; Booij, M.J.; Hoekstra, A.Y. Hydrological response to future land-use change and climate change in a tropical catchment. *Hydrol. Sci. J.* **2018**, *63*, 1368–1385, doi:10.1080/02626667.2018.1511054.
66. Yaduvanshi, A.; Sharma, R.K.; Kar, S.C.; Sinha, A.K. Rainfall–runoff simulations of extreme monsoon rainfall events in a tropical river basin of India. *Nat. Hazards* **2018**, *90*, 843–861, doi:10.1007/s11069-017-3075-0.
67. Piman, T.; Cochrane, T.A.; Arias, M.E. Effect of Proposed Large Dams on Water Flows and Hydropower Production in the Sekong, Sesan and Srepok Rivers of the Mekong Basin. *River Res. Appl.* **2016**, *32*, 2095– 2108, doi:10.1002/rra.3045.
68. Vu, M.T.; Raghavan, S.V.; Liong, S. Y. SWAT use of gridded observations for simulating runoff—A Vietnam river basin study. *Hydrol. Earth Syst. Sci.* **2012**, *16*, 2801–2811, doi:10.5194/hess-16-2801-2012.
69. Ha, L.T.; Bastiaanssen, W.G.M.; van Griensven, A.; van Dijk, A.I.J.M.; Senay, G.B. Calibration of spatially distributed hydrological processes and model parameters in SWAT using remote sensing data and an autocalibration procedure: A case study in a Vietnamese river basin. *Water* **2018**, *10*, 212.
70. Nguyen-Tien, V.; Elliott, R.J.R.; Strobl, E.A. Hydropower generation, flood control and dam cascades: A national assessment for Vietnam. *J. Hydrol.* **2018**, *560*, 109–126.
71. Le, T.; Sharif, H. Modeling the Projected Changes of River Flow in Central Vietnam under Different Climate Change Scenarios. *Water* **2015**, *7*, 3579–3598, doi:10.3390/w7073579.
72. *National Engineering Handbook-Part 630 Hydrology, Chapter 4–10*; USDA Soil Conservation Service: Washington, DC, USA 1972;
73. Williams, J.R. Flood Routing With Variable Travel Time or Variable Storage Coefficients. *Trans. ASAE* **1969**, *12*, 0100–0103, doi:10.13031/2013.38772.
74. Cunge, J.A. On the subject of a flood propagation computation method (Musklngum method). *J. Hydraul. Res.* **1969**, *7*, 205–230, doi:10.1080/00221686909500264.
75. Hargreaves, G.L.; Hargreaves, G.H.; Riley, J.P. Agricultural Benefits for Senegal River Basin. *J. Irrig. Drain. Eng.* **1985**, *111*, 113–124, doi:10.1061/(ASCE)0733-9437(1985)111:2(113).

76. Williams, J.R. Sediment Routing for Agricultural Watersheds. *JAWRA J. Am. Water Resour. Assoc.* **1975**, *11*, 965–974, doi:10.1111/j.1752-1688.1975.tb01817.x.
77. Bagnold, R.A. Bed load transport by natural rivers. *Water Resour. Res.* **1977**, *13*, 303–312, doi:10.1029/WR013i002p00303.
78. *FAO-Unesco Soil map of the world-Sotheast Asia*; FAO-Unesco: Paris, France, 1979; Volume IX.
79. Dao, N. Dam development in Vietnam: The evolution of dam-induced resettlement policy. *Water Altern.* **2010**, *3*, 324–340.
80. Abbaspour, K.C. *SWAT-CUP: SWAT Calibration and Uncertainty Programs—A User Manual*; Eawag: Dübendorf, Switzerland, 2015; Available online: https://swat.tamu.edu/media/114860/usermanual_swatcup.pdf (accessed on 3 May 2019).
81. Arnold, J.G.; Moriasi, D.N.; Gassman, P.W.; Abbaspour, K.C.; White, M.J.; Srinivasan, R.; Santhi, C.; Harmel, R.D.; van Griensven, A.; Van Liew, M.W.; et al. SWAT: Model Use, Calibration, and Validation. *Trans. ASABE* **2012**, *55*, 1491–1508.
82. Yang, J.; Reichert, P.; Abbaspour, K.C.; Xia, J.; Yang, H. Comparing uncertainty analysis techniques for a SWAT application to the Chaohe Basin in China. *J. Hydrol.* **2008**, *358*, 1–23, doi:10.1016/j.jhydrol.2008.05.012.
83. Le, T.P.Q.; Seidler, C.; Kändler, M.; Tran, T.B.N. Proposed methods for potential evapotranspiration calculation of the Red River basin (North Vietnam). *Hydrol. Process.* **2012**, *26*, 2782–2790, doi:10.1002/hyp.8315.
84. Bui, Y.T.; Orange, D.; Visser, S.M.; Hoanh, C.T.; Laissus, M.; Poortinga, A.; Tran, D.T.; Stroosnijder, L. Lumped surface and sub-surface runoff for erosion modeling within a small hilly watershed in northern Vietnam. *Hydrol. Process.* **2014**, *28*, 2961–2974, doi:10.1002/hyp.9860.
85. Li, Y.; He, J.; Li, X. Hydrological and meteorological droughts in the Red River Basin of Yunnan Province based on SPEI and SDI Indices. *Prog. Geogr.* **2016**, *35*, 758–767. (In Chinese)
86. Moriasi, D.N.; Arnold, J.G.; Van Liew, M.W.; Bingner, R.L.; Harmel, R.D.; Veith, T.L. Model Evaluation Guidelines for Systematic Quantification of Accuracy in Watershed Simulations. *Trans. ASABE* **2007**, *50*, 885–900, doi:10.13031/2013.23153.
87. Nash, J.E.; Sutcliffe, J.V. River Flow Forecasting Through Conceptual Models Part I—A Discussion of Principles. *J. Hydrol.* **1970**, *10*, 282–290, doi:10.1016/0022-1694(70)90255-6.
88. Krause, P.; Boyle, D.P.; Bäse, F. Comparison of different efficiency criteria for hydrological model assessment. *Adv. Geosci.* **2005**, *5*, 89–97, doi:10.5194/adgeo-5-89-2005.
89. Xu, Z.X.; Pang, J.P.; Liu, C.M.; Li, J.Y. Assessment of runoff and sediment yield in the Miyun Reservoir catchment by using SWAT model. *Hydrol. Process.* **2009**, *23*, 3619–3630, doi:10.1002/hyp.7475.
90. Cibin, R.; Sudheer, K.P.; Chaubey, I. Sensitivity and identifiability of stream flow generation parameters of the SWAT model. *Hydrol. Process.* **2010**, *24*, 1133–1148.
91. Guse, B.; Reusser, D.E.; Fohrer, N. How to improve the representation of hydrological processes in SWAT for a lowland catchment—Temporal analysis of parameter sensitivity and model performance. *Hydrol. Process.* **2014**, *28*, 2651–2670, doi:10.1002/hyp.9777.
92. Arnold, J.G.; Kiniry, J.R.; Srinivasan, R.; Williams, J.R.; Haney, E.B.; Neitsch, S.L. *Soil & Water Assessment Tool Input/Output Documentation Version 2012*; Springer US: Austin, TX, USA, 2012.
93. Arnold, J.G.; Allen, P.M.; Muttiah, R.; Bernhardt, G. Automated Base Flow Separation and Recession Analysis Techniques. *Groundwater* **1995**, *33*, 1010–1018, doi:https://doi.org/10.1111/j.17456584.1995.tb00046.x.
94. Arnold, J.G.; Allen, P.M. Automated methods for estimating baseflow and ground water recharge from streamflow records. *J. Am. Water Resour. Assoc.* **1999**, *35*, 411–424, doi:https://doi.org/10.1111/j.17521688.1999.tb03599.x.
95. Le, T.B.; Al-Juaidi, F.H.; Sharif, H. Hydrologic simulations driven by satellite rainfall to study the hydroelectric development impacts on river flow. *Water* **2014**, *6*, 3631–3651, doi:10.3390/w6123631.
96. Liu, J.; Duan, Z.; Jiang, J.; Zhu, A.-X. Evaluation of Three Satellite Precipitation Products TRMM 3B42, CMORPH, and PERSIANN over a Subtropical Watershed in China. *Adv. Meteorol.* **2015**, *2015*, 1–13, doi:10.1155/2015/151239.
97. Liu, X.; Yang, M.; Meng, X.; Wen, F.; Sun, G. Assessing the Impact of Reservoir Parameters on Runoff in the Yalong River Basin using the SWAT Model. *Water* **2019**, *11*, 643, doi:10.3390/w11040643.
98. Oeurng, C.; Sauvage, S.; Sánchez-Pérez, J.M. Assessment of hydrology, sediment and particulate organic carbon yield in a large agricultural catchment using the SWAT model. *J. Hydrol.* **2011**, *401*, 145–153, doi:10.1016/j.jhydrol.2011.02.017.
99. Yang, D.; Kanae, S.; Oki, T.; Koike, T.; Musiake, K. Global potential soil erosion with reference to land use and climate changes. *Hydrol. Process.* **2003**, *17*, 2913–2928, doi:10.1002/hyp.1441.

Chapter 4

Assessing the Sediment Fluxes and Soil Erosion

This chapter was submitted to journal *Hydrological Processes* and is under review. The work of this chapter was extended from the previous chapter. The purpose of this chapter is to characterize and quantify the sediment flux over the basin considering the impacts from climate variability and dam constructions at a daily scale.

Wei, X.; Sauvage, S.; Le, T.P.Q.; Ouillon, S.; Orange, D.; Herrman, M.; Sánchez-Pérez, J.-M. A drastic decrease of suspended sediment fluxes in the Red River related to climate variability and dam constructions. *Hydrological Processes.* Under review.

4. CHAPTER Ⅳ: Assessing the Sediment Fluxes and Soil Erosion

4.1. Scientific Context and Objectives

Asian rivers contribute a large portion of sediment delivering to the seas. However, these river basins in these Asian developing countries are facing severe anthropogenic disturbances, such as intensive farming casing high erosion while intensive damming retaining sediment in reservoir. The Red River is a typical tropical Asian river system under global changes. It plays an important role in agriculture and economy due to its numerous inter-linked rivers, estuaries and coastal waters in this basin. It can be a good representative of the Asian river system and it would be a good example for researchers to study the sediment transfer and fluxes under the natural and anthropogenic impacts. The previous studies on the sediment flux (SF) were mainly focused on the impact of Hoa Bind or/and Thac Ba dams and the exports of the three tributaries based on monthly or annual scale calculations. The purpose of this study is to calculate SF at a daily time step and to diagnose the impacts of climate variability and dam constructions (including new dams). The specific objectives of this work are to: (1) to quantify SF of the Red River basin based on daily Q and SSC; (2) to quantify dam impacts on SF and to identify SF answer to climate variability; (3) to identify the hot spots of soil erosion and SF transfer, and the key parameters that control SF at the scale of the whole basin; (4) to provide rating curves for estimating the SF at the outlets of each sub-basin and of the continental basin, and discuss the variability of their parameters under the influences of climate and anthropogenic changes.

4.2. Materials and Methods

Calibrated SWAT model from previous work was used to calculate the SF at daily scale from 2000 to 2013 at Lao Cai, Yen Bai, Vu Quang, Hoa Binh and Son Tay stations. Two scenarios were carried out: natural condition without dams in this basin; actual condition with six important dams function in this basin. Due to the new dams' operation time, the study period was divided into two periods: before new dams' impoundment (2000-20007) and after new dams' impoundment (2008-2013), to assess the impacts of dams and climate variability. We compared two periods of these two conditions, before new dams (2000-2007) and after new dams (2008-2013). By comparing the two periods of the natural condition, the impacts of climate variability can be quantified. Comparing the natural condition of 2000-2007 with the actual condition of 2008-2013, the total impacts due to both the climate and dams can be quantified. The impacts of dams are the difference between the total impacts and the impacts of climate.

Discharge (Q) and SF simple relations were provided to help researchers have easy access to estimate the monthly mean SF. Rating curves of monthly mean Q and SF for these 5 stations were gained from simulated monthly mean Q and SF, and were evaluated based on the output of the modelling and then validated by the observed dataset.

Hot spots of landscape soil erosion were identified according to the model outputs by

using principal component analysis (PCA), and the main influent factors were figured out through the correlations between them and SF.

4.3. Main Results and Discussions

The monthly and annual SF calculated from daily mean SF gained a satisfactory performance. During the simulation period, the seasonal SF varied from 0.0005 to 34.4 Mt at Lao Cai, from 0.0007 to 39.6 Mt at Yen Bai, from 0.0006 to 4.7 Mt at Vu Quang, from 0.0003 to 3.0 Mt at Hoa Binh, and from 0.0014 to 25.2 Mt at Son Tay. 87-91% of the annual total SF was produced during flood seasons (June to November). Annual SF ranged from 6.8 to 73.6 Mt yr^{-1} at Lao Cai, 11.7 to 85.9 Mt yr^{-1} at Yen Bai, 2.0 to 12.5 Mt yr^{-1} at Vu Quang, and 0.8 to 7.1 Mt yr^{-1} at Hoa Binh. As the confluence of these tributaries, the Red River yields an annual SF at the range of 8.0-69.2 Mt yr^{-1}, with an average specific sediment yield (SSY) of 241 t km^{-2} yr^{-1}.

By comparing the differences between natural and actual conditions at the outlet of the basin, we found a 90% decrease of annual SF during 2008-2013, of which 10% was decreased by climate and 80% was due to the dam retention.

We compared the annual SF and SSY under natural condition of Asian big river basins, and found that though the Red River basin exported less SF than the Yellow River, the Yangtze River and the Mekong River, but its SSY (779 t km^{-2} yr^{-1}) was higher than the Mekong, Pearl River, Yangtze, and was the half of the Yellow River.

The model indicates that the mean annual soil erosion in the whole basin ranged from 0.01 to 43.4 t ha^{-1}, with a mean of 5.5 t ha^{-1} for the whole basin. High erosion areas are identified in the middle part of the Thao River and the downstream of the Da River. Besides, with high precipitation and surface runoff, Lai Chau, Lao Cai, Ha Giang and Son La provinces are the most vulnerable to soil erosion, and their mean annual erosion rate during the study period can be above 20 t ha^{-1}. Precipitation, slope and USLE agricultural practice factor are key influence factors for soil yield in the Red River basin. The soil texture is also a significant factor. Related soil conservation management can be carried out in these hot spots by considering the main influence factors.

The relations of monthly Q and SF resulted from the output of the modelling fit well with the observations of both periods (2000-2007 and 2008-2013). The parameters in the simple Q-SF equation are according to the real sub-basin characteristics. These simple Q-SF equations can be used for the people to estimate the monthly SF without using the SWAT model.

4.4. Conclusion and Perspectives

This study quantified the impacts of climate and dam construction on SF transfer and fluxes separately and found a significant reduction of SF due to the dams. With more dams are going to impound in this basin, the future sediment export might continue to

be reduced. Related sediment regulation in the reservoirs should be executed in order to export enough sediment for downstream ecosystem and delta. Soil conservation management should pay attention in the middle part of the basin. The high advantage of the model is not only that different scenarios can be carried out, but also once it has been calibrated with data from hydrological stations, is that he can serve to estimate and map each term involved in the sediment transport process – including local erosion, local deposition, in-stream sediment discharge – and that it can be used to infer local SF-Q rating curves at any virtual station within the basin from the model simulations, even where there is no true station. This point is of major interest both for scientific applications (e.g., studying spatial variations of SF) and for management purpose, with provinces and other stakeholders.

4.5. Full Article Submitted to *Hydrological Processes*

A drastic decrease of suspended sediment fluxes in the Red River related to climate variability and dam constructions

Xi Wei[1*], Sabine Sauvage[1**], Sylvain Ouillon[2,3], Thi Phuong Quynh Le[4], Didier Orange[5], Marine Herrmann[2,3], José-Miguel Sanchez-Perez[1]

[1]ECOLAB, Université de Toulouse, CNRS, INPT, UPS, Auzeville-Tolosane, France.

[2]LEGOS, Université de Toulouse, IRD, CNES, CNRS, UPS, Toulouse, France.

[3]USTH, Vietnam Academy of Science and Technology (VAST), Hanoi, Vietnam.

[4]Institute of Natural Product Chemistry (INPC), Vietnam Academy of Science and Technology (VAST), Hanoi, Vietnam.

[5]Eco & Sols, Univ. Montpellier, IRD, CIRAD, INRA, Montpellier SupAgro, Montpellier, France.

Correspondence

*Xi Wei, ECOLAB, Université de Toulouse, CNRS, INPT, UPS, Avenue de l'Agrobiopole, 31326 Auzeville-Tolosane, France.

Email: xi.wei_fr@hotmail.com

**Sabine Sauvage, ECOLAB, Université de Toulouse, CNRS, INPT, UPS, Avenue de l'Agrobiopole, 31326 Auzeville-Tolosane, France.

Email: sabine.sauvage@univ-tlse3.fr

Abstract:

The Red River is an Asian river system strongly affected by global changes. This paper aims to characterize and quantify the suspended sediment flux (SF) over the basin under the influences of climate variability and dam constructions. SF was evaluated at the outlets of three main tributaries and along the main course of the Red River from 2000 to 2013 based on daily simulations from a modelling study. Two scenarios under actual and natural (without dams) conditions were carried out to disentangle the impacts of climate and dams. Under natural conditions, the basin would generate 106.9 Mt yr^{-1} of SF to the downstream delta during study period, with a specific sediment yield (SSY) of 778.8 t km^{-2} yr^{-1}. However, under the impacts of climate variability and dams, the mean annual SSY decreased to 84.5 t km^{-2} yr^{-1}. In flood years, without dams, the basin would produce 1.5 times higher SF than in drought years. At the outlet of the basin, the annual mean SF of 2008-2013 (after new dam constructions) got reduced by 90% (10% related to climate and 80% to dam constructions) compared to natural conditions during 2000-2007. The Thao River is the most sensitive to climate variability

while the Da River is mostly affected by the huge-capacity dams. Mean annual retentions of sediment by dams ranged from 7.1 to 111.0 Mt yr^{-1}. Simple rating curves between monthly mean Q and SF were established for estimating SF at the outlet of the tributaries and the Red River. High soil erosion (above 2000 t km^{-2} yr^{-1}) occurred in the middle Thao and the lower Da rivers. Precipitation, slope and agriculture practices are the key influence factors for soil erosion in the basin. Future studies, such as projections under global changes scenarios will be carried out based on this study.

Keywords: Asian river, Red River, modelling, SWAT, scenario, suspended sediment, climate variability, dam, soil erosion.

1. INTRODUCTION

The suspended sediment (SS) transport from continents to oceans by rivers is a crucial process of sediment cycle in the Earth systems: this process drives associated elements to the seas which is essential for marine biogeochemical cycle and diversity; also, it is a reflection of land and river degradation; besides, this process is of great importance in geomorphology, such as downstream delta formation (Lal *et al.*, 1995; Dai *et al.*, 2009; Kunz *et al.*, 2011). Rivers contribute to 95% of the sediment fluxes (SF) to the oceans (Syvitski *et al.*, 2003), which ranged from 15 to 20 billion t yr^{-1} (Milliman and Meade, 1983; Ludwig and Probst, 1996b; Vörösmarty *et al.*, 2003; Beusen *et al.*, 2015; Ouillon, 2018). In particular, Asian rivers such as the Yellow River and the Mekong River contribute to a large part of sediment delivery to the seas (Cohen *et al.*, 2014; Dang *et al.*, 2018). However, climate variability and anthropogenic activities have altered the SF (Dai *et al.*, 2009; Jiang *et al.*, 2009; Dang *et al.*, 2018).

Under anthropogenic disturbances such as intensive agriculture and damming, water ecosystems are facing severe challenges, like the increase of soil erosion, and changes of hydrology regime and SF (IPCC, 2000; Valentin *et al.*, 2008; Zimmerman *et al.*, 2008; FAO, 2011a; Chen *et al.*, 2016). Dam construction is the factor with the strongest influence on land-ocean SF (Walling and Fang, 2003). According to the World Commission on Dams (2000), at least 45,000 large dams have been built globally, and nearly half of the world's rivers have one large dam at least. Lehner et al., (2011) found that around 28% dams are located in Asia. Besides, future hydropower development is primarily concentrated in developing countries and emerging economies of Southeast Asia (Zarfl *et al.*, 2015). Dams cause a significant reduction in SF. Vörösmarty et al. (2003) estimated that the potential sediment trapping by dams in regulated basins was higher than 50%. In some basins, such as the Colorado and Nile, sediment is completely trapped due to the large size of reservoirs and to the flow velocity decreases which weakens the sediment transport ability (Vörösmarty *et al.*, 2003; Walling and Fang, 2003). Reduced sediment transport can induce river deltas sinking, therefore affecting estuarine and coastal human communities (Syvitski *et al.*, 2005; Hauer *et al.*, 2018), and increasing their vulnerability (Lehner *et al.*, 2011b). Asian rivers constitute good indicators of the strong influence of anthropogenic activities on sediment transport (Furuichi *et al.*, 2009; Dang *et al.*, 2010; Arias *et al.*,

2014).

The Red River is a typical Asian river system under the influences of global changes and is the second largest river in Vietnam. It gathers numerous inter-linked rivers, estuaries and coastal waters and plays an important role in agriculture and economy in this basin, which is a major agricultural productions region. Understanding and quantifying the water and soil processes and budgets of this river basin will help to manage soil loads and also to study other Asian rivers. Hence, the objective of this paper is to assess the SS regime in a large Asian basin under the influences of global changes, especially under the impacts of dams. Moreover, it would be more precise to calculate SF at a daily time step as discharge (Q) and suspended sediment concentration (SSC) can vary greatly from day to day. However, few studies analysed fluxes at daily scale in the Red River basin, focusing either on a short period (Le *et al.*, 2007), or only on the delta (Luu *et al.*, 2010), or only on Q or SS (Hiep *et al.*, 2018). Assessing SS regime at a daily time step in the Red River basin will, therefore, contribute to improving our knowledge of the SF across this basin.

For achieving this objective, a modelling approach, combining remote sensing and in-situ data, was used. The hydrology and SSC calibration and validation were described in Wei et al. (2019). The specific objective of the present paper is: 1) to quantify SF of the Red River basin based on daily Q and SSC; 2) to quantify dam impacts on SF and to identify SF answer to climate variability; 3) to identify the hot spots of soil erosion and SF transfer, and the key parameters that control SF at the scale of the whole basin; 4) to provide rating curves for estimating the SF at the outlets of each sub-basin and of the continental basin, and discuss the variability of their parameters under the influences of climate and anthropogenic changes.

2. MATERIALS AND METHODS

2.1 Study area

The study area focuses on the Red River continental basin with a surface of 137,200 km^2 which drains down to Son Tay, the outlet of the continental basin and the entrance of the delta (Figure 4-1).

2.2.1 General characteristics

The Red River basin is located in Southeast Asia, from 20.00° to 25.50° North and from 100.00° to 107.17° East. China occupies 49% of the whole basin, while Vietnam and Laos occupy 50.1% and 0.9% respectively.

Son Tay is a confluence of three main tributaries: the Lo River (named Panlong Jiang in China) on the left bank, the Thao River (named Yuan Jiang in China) upstream of the main river, and the Da River (named Lixian Jiang in China) on the right bank. They join the Red River 20 km upstream to the Son Tay gauging station.

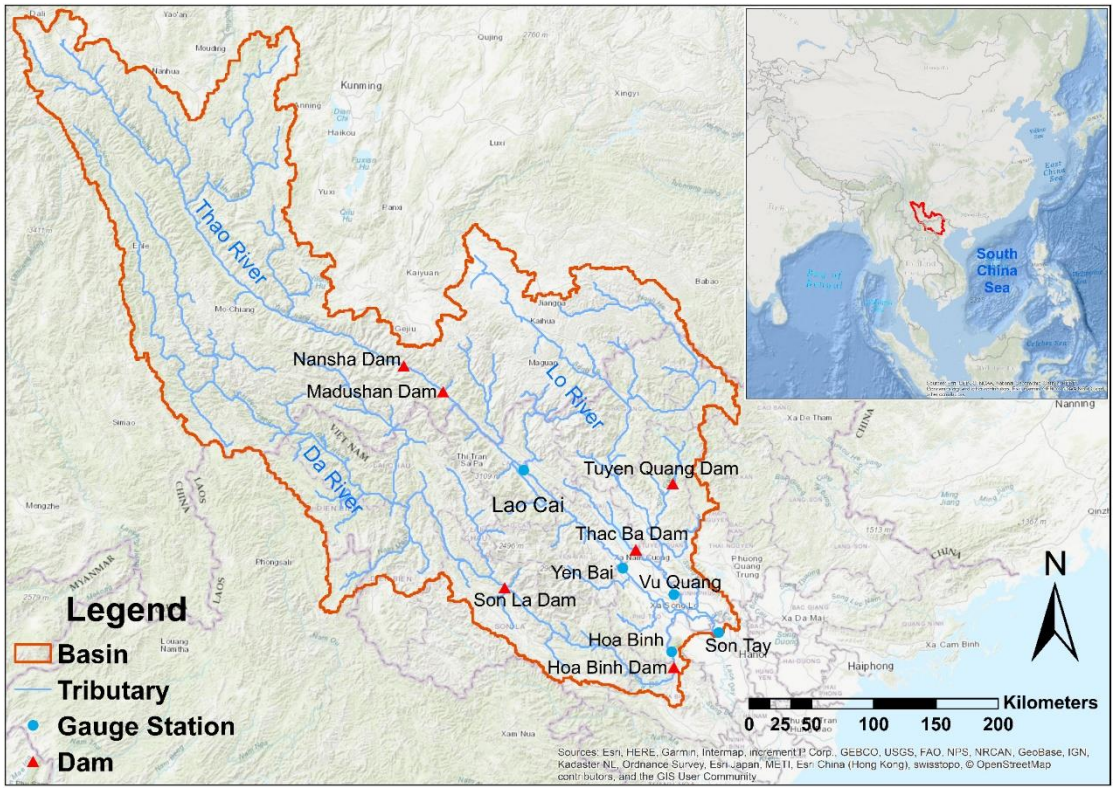

Figure 4-1 The geographical location of the Red River basin in Asia, and locations of the dams and the hydrological gauge stations in the Red River basin.

The part upstream of Lao Cai is mainly formed by tectonically active mountainous areas, with steep slopes, usually above 25° (Zhang *et al.*, 2017) which are vulnerable to soil erosion due to the intensive precipitation and land use changes (Barton *et al.*, 2004; He *et al.*, 2007; Bai *et al.*, 2015). The soil types are mainly Acrisols, such as red earth, yellow-brown soil and fluvisol (Le, 2005; Bai *et al.*, 2015). High erosion plus the character of soil types color the water of the Thao River into “red” (Le, 2005). In Vietnam, the same Acrisols dominate on the slopes while grey or alluvial soils dominate in the valleys (Le *et al.*, 2017a).

In China’s part, the main land cover is forest (62%), followed by grassland (19%) and cultivated land (18%), respectively (Li et al., 2016). In Vietnam’s part, in the Thao basin, forest is dominating, accounting for 54.2%, followed by rice paddy fields (19%) and industrial crops (13%); the Lo and Da basins are dominated by industrial crops (58%) and forests (74%), respectively (Le *et al.*, 2007).

2.1.2 Meteorological characteristics

The whole Red River basin encompasses two different climate zones: humid subtropical climate in the upper part and humid tropical climate in the lower part, and a strong seasonal variability related to the Southeast Asia monsoon system, which alternates between the cold and dry southwestward winter monsoon from November to April and the hot and humid northeastward summer monsoon from May to October. Rainfall during flood seasons contributes to 85-90% of the whole year average (Le et al., 2007; Li et al., 2016). The general trend of regional precipitation distribution

increases from upstream (1000 to 1600 mm yr^{-1} in China) to downstream (1328 to 2255 mm yr^{-1} in Vietnam) (Xie, 2002; Le *et al.*, 2007; Li *et al.*, 2008).

Temperature variations follow a typical orographic pattern. The mean annual temperature varies from 15 to 21 °C in China (Xie, 2002) and from 14 to 27 °C in Vietnam (Le, 2005).

2.1.3 Hydrological characteristics

Runoff is mainly recharged by precipitation which leads to big seasonal variations in river flows (FAO, 2011b; Li et al., 2016; Li et al., 2008). The mean annual discharge during 2000-2015 at Son Tay was 3082 m^3 s^{-1} (Wei *et al.*, 2019a). Corresponding to the distribution of rainfall, the runoff is also unevenly distributed. June to November is the rainy season, and more than 80% of the total annual runoff is produced during these seasons; runoff peaks usually occur in August, and the maximum flood reached 8050 m^3 s^{-1} in 1986 near the bounder in China (Xie, 2002), and 37,800 m^3 s^{-1} at Son Tay in 1971 (Luu *et al.*, 2010). December to May is the dry season, and the minimum discharge occurs in March. The minimum discharge observed near the boundary in China was 28.7 m^3 s^{-1} in 1963 (Ren *et al.*, 2007), and the minimum daily discharge at Son Tay during 2000-2013 was 493 m^3 s^{-1} (Wei *et al.*, 2019a).

2.1.4 Dams implementation

In recent years, both in China and Vietnam, more hydraulic systems, such as irrigation channels and dams, have been built to meet the water demand according to the rapid increase of population and intensive agriculture activities. In this study, we only took into account the dams with big capacity and located on the downstream part, i.e. close to the outlets of each tributary.

On the Thao River, twelve cascade reservoirs were built or are under constructions in China's territory. The impoundment of the first two dams, the Nansha and the Madushan dams, located around 150 km and 100 km upstream of Lao Cai respectively, started on November 2007 and December 2010, respectively.

On the Da River, the biggest dam in Vietnam named Hoa Binh was put into use in 1989. A mass of solid materials has been trapped by this dam, which consequently reduces the dam's efficient capacity and lifetime (Dang *et al.*, 2010). In order to mitigate the siltation of the Hoa Binh dam and to meet the need for economic growth, the Son La dam was built and put into operation in January 2011. On the Lo River, the Thac Ba dam was implemented in 1972 and the Tuyen Quang dam in March 2008 (Table 4-1 and Figure 4-1).

Table 4-1 Basic characteristics of the main dams in the Red River basin (Le et al., 2017a; Wei et al., 2019a)

Dam	Basin	Construction began	Impoundment	Capacity (km^3)
Nansha	Thao	Feb-06	Nov-07	0.26
Madushan	Thao	Dec-08	Dec-10	0.55
Hoa Binh	Da	1980	1989	9.50
Son La	Da	Dec-05	Dec-10	9.26
Thac Ba	Lo	1965	Oct-71	2.90
Tuyen Quang	Lo	Dec-02	Mar-08	2.24

2.2 Data collection

Data of daily Q and SSC from 2000 to 2013 obtained from the Vietnam Ministry of Natural Resources and Environment (MONRE) at Lao Cai, Yen Bai, Vu Quang, Hoa Binh and Son Tay stations. Daily SF, calculated from daily Q and SSC, was used to evaluate the model. Gauge station locations can be found in Figure 4-1.

2.3 Modelling approach

This study expands the work of Wei et al. (2019) where detailed descriptions of the modelling set up and the calibration and validation processes can be found. Here we only present some essential information.

2.3.1 The SWAT model

The Soil and Water Assessment Tool (SWAT) is a physically based, semi-distributed hydrological model. It considers soils, land use and management conditions to predict the impact of land management practices on water and sediment within large complex basins where there might be no monitoring data over long periods of time (Neitsch *et al.*, 2009).

Both hydrological and sediment dynamics in SWAT are simulated in two components: over the land, and in the channel network. More information about SWAT hydrological and sediment modelling can be found in Arnold et al. (1998) and Neitsch et al. (2009).

2.3.2 SWAT data inputs

The topography, land cover and soils maps for the model are presented here to give a better understanding of the characteristic of the Red River basin (Figure 2-12, Wei et al., 2019).

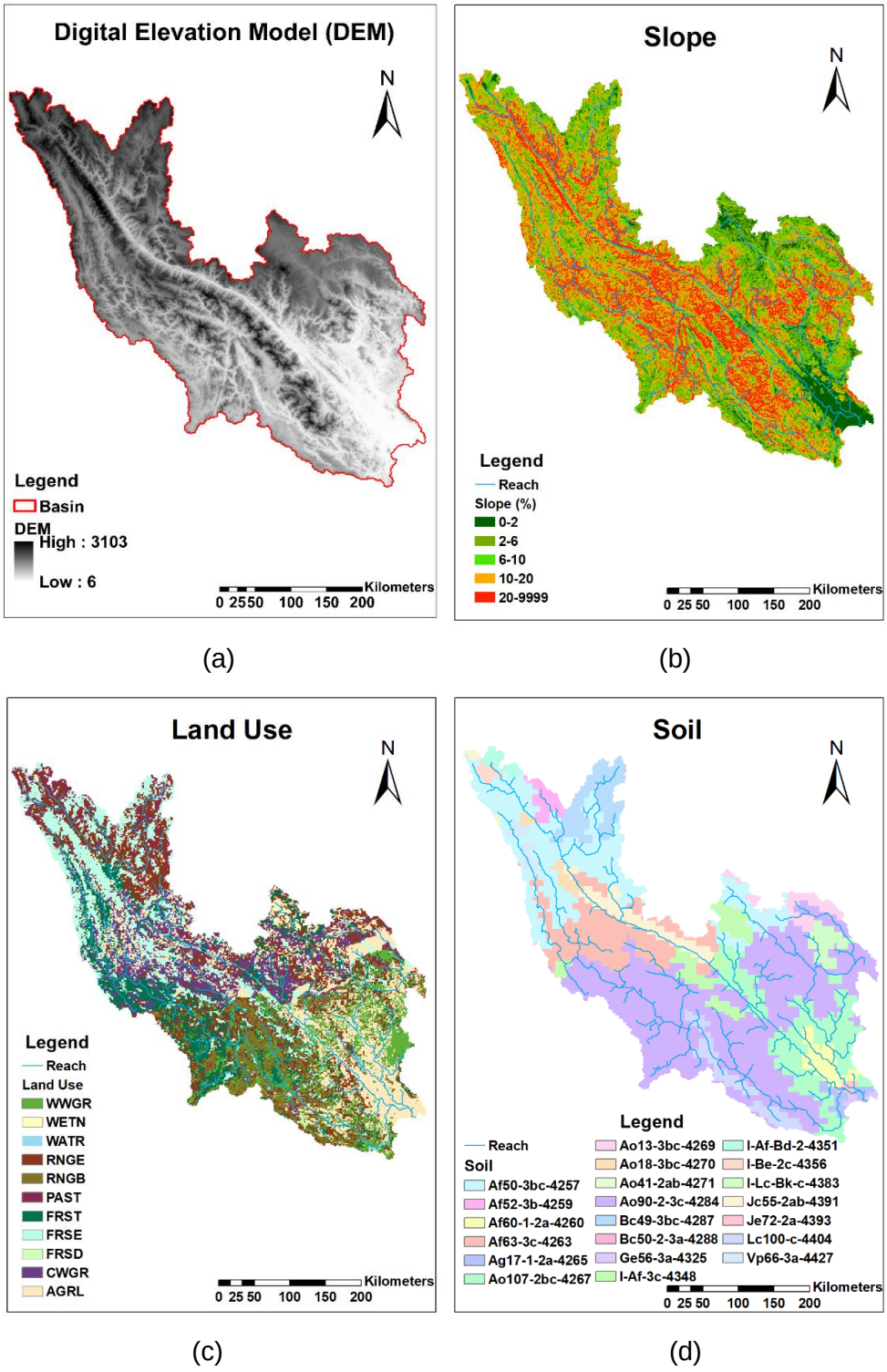

Figure 4-2 (a) digital elevation model (DEM); (b) slop classes: slopes were divided into 5 classes by SWAT based on the (DEM); (c) land use map; (d) soil types. Input data sources can be found in Wei et al. (2019).

2.3.3 Model set up

The whole basin was divided into 242 sub-basins and then subdivided into 3812 different hydrological response units (HRUs) with homogeneous land use, soil type and slope. The daily simulation was carried out and analyzed at different temporal

scales (daily, monthly and annual) from 2000 to 2013.

In order to quantify the impacts of the dams, two scenarios were simulated (Table 4-2): (a) actual conditions with the existing dams; (b) natural conditions without any dams. Parameters were kept the same for actual and natural conditions; the difference between these two scenarios was the dams implementations. New dams mainly started to operate in 2008, therefore, the study period was separated into two periods (2000-2007 and 2008-2013) to evaluate the impact of dams. More detailed descriptions and settings of these two scenarios can be found in Wei et al. (2019).

Table 4-2 Scenarios setting: actual conditions (AC) and natural conditions (NC), and the two periods covered by the scenarios.

Scenario	2000-2007 (river name: dam name)	2008-2013 (river name: dam name)
Actual Conditions (AC)	Da: Hoa Binh Lo: Thac Ba	Thao: Nansha; Madushan Da: Hoa Binh; Son La Lo: Thac Ba; Tuyen Quang
Natural Conditions (NC)	no dam	no dam

2.3.4 Model evaluation and validation

Based on the daily-scale simulation, simulated monthly and annual SF were extracted to compare with observed data for checking the performance of the model. Following the recommendations by Moriasi et al. (2007), coefficient of determination (R^2), Nash–Sutcliffe Efficiency (NSE), and Percent Bias (PBIAS) were used to evaluate the simulations.

2.4 Estimating the impacts of climate variability and dams on SF

By comparing the mean annual SF under natural conditions between 2000-2007 and 2008-2013, the impacts of climate variability can be quantified. By comparing the mean annual SF during 2008-2013 between natural and actual conditions, the impacts of dams can be quantified.

In this study, we hypothesized that the impact of the land use changes during our study period was not significant. Some researchers used a modelling approach to examine the impacts of land use changes on SF in Vietnam and found that an 11-16% decrease in forest land was likely to increase 3.0-3.9% SF (Phan *et al.*, 2010; Khoi and Suetsugi, 2014). In the Red River basin, between 2010 and 2000, the forest percentage stayed the same, and the farmland increased by 8% from bare land (Le *et al.*, 2018), which might cause less than 2% increase of SF according to Khoi & Suetsugi, (2014) and Phan, Wu, & Hsieh, (2010). Therefore, we did not take into account the impacts of land use changes on SF during the study period.

2.5 Q-SF simple relations

The rating curves between monthly mean Q and SF for the 5 gauge stations were established from simulated monthly mean Q and SF, evaluated based on the output of the numerical simulation, and validated through comparison with observed data. Results are presented in Section 3.3.

2.6 Identifying the influencing factors of soil erosion from landscape

Hot spots of land soil erosion were identified according to the model outputs, and the main triggering factors were determined from the correlations between them and SF according to the principal component analysis (PCA) method described below.

PCA was used in this study to identify the factors influencing soil erosion (SE) in this basin. More detailed explanations of this method can be seen in Basilevsky (1994), Lever, Krzywinski, & Altman (2017), Ringnér (2008) and Wold, Esbensen, & Geladi (1987). Based on the parameters analysis in the study of Wei et al. (2019), the following variables of each sub-basin were added into the PCA model to identify the main factor involved in SE in the basing: soil erosion (SE), precipitation (P), water yield (WY), surface runoff (SR), USLE soil erodibility factor (USLE_K), USLE agricultural practice factor (USLE_P), slope, and the percentages of sand (Sand%), silt (Silt%) and clay (Clay%) in soil. The input data to the PCA was the mean annual values of each variable of 242 sub-basins. Results about soil erosion hot spots and triggering factors are presented in Section 3.4.

3. RESULTS

3.1 SF under actual conditions

3.1.3 Monthly variations of actual SF

Monthly and annual SF simulations and observations were plotted in Figure 4-3 and Figure 4-4, and their related statistics evaluations were reported in Table 4-3. From the general performance ratings at monthly scale recommended by Moriasi et al. (2007), Lao Cai, Yen Bai, Hoa Binh and Son Tay stations gained good performance; Vu Quang station gained satisfactory performance. PBIAS values indicate that the model slightly overestimated SF at most stations, and underestimated SF at Hoa Binh station.

Table 4-3 Evaluation statistics of sediment flux (SF) on different time scales for each station from 2000 to 2013

Sediment Flux (Mt)	Statistics	Stations				
		Lao Cai	Yen Bai	Vu Quang	Hoa Binh	Son Tay
Monthly Scale	NSE	0.67	0.66	0.62	0.72	0.71
	R^2	0.68	0.69	0.62	0.75	0.79
	PBIAS	-1.8	-8.7	-0.9	4.6	-24.5
Annual Scale	NSE	0.78	0.60	0.55	0.73	0.54
	R^2	0.78	0.73	0.55	0.77	0.86
	PBIAS	-5.2	-22.6	-0.8	8.6	-24.7

Thanks to the satisfactory calibration of Q and SSC presented in Wei et al. (2019), simulated SF shows similar trends as observed SF and can be considered as satisfactory results (Figure 4-3). Base flow of simulated monthly SF fits well with observations at all stations.

SF show great seasonal variations, especially in the Thao River (see stations of Lao Cai and Yen Bai in Figure 4-3). Maximum flux usually occurs during July to September, and minimum flux generally happens during February and March. 87-91% of the annual total SF was produced during the flood season (June to November). The mean SF for flood season at Lao Cai, Yen Bai, Vu Quang, Hoa Binh and Son Tay were 4.6, 5.9, 1.1, 0.5 and 4.5 Mt month^{-1}, respectively; the mean SF for dry season (December to May) at Lao Cai, Yen Bai, Vu Quang, Hoa Binh and Son Tay were 0.5, 0.7, 0.1, 0.1 and 0.5 Mt month^{-1}, respectively. During the simulation period, the seasonal simulated SF varied from 0.0005 to 34.4 Mt month^{-1} at Lao Cai, from 0.0007 to 39.6 Mt month^{-1} at Yen Bai, from 0.0006 to 4.7 Mt month^{-1} at Vu Quang, from 0.0003 to 3.0 Mt month^{-1} at Hoa Binh, and from 0.0014 to 25.2 Mt month^{-1} at Son Tay.

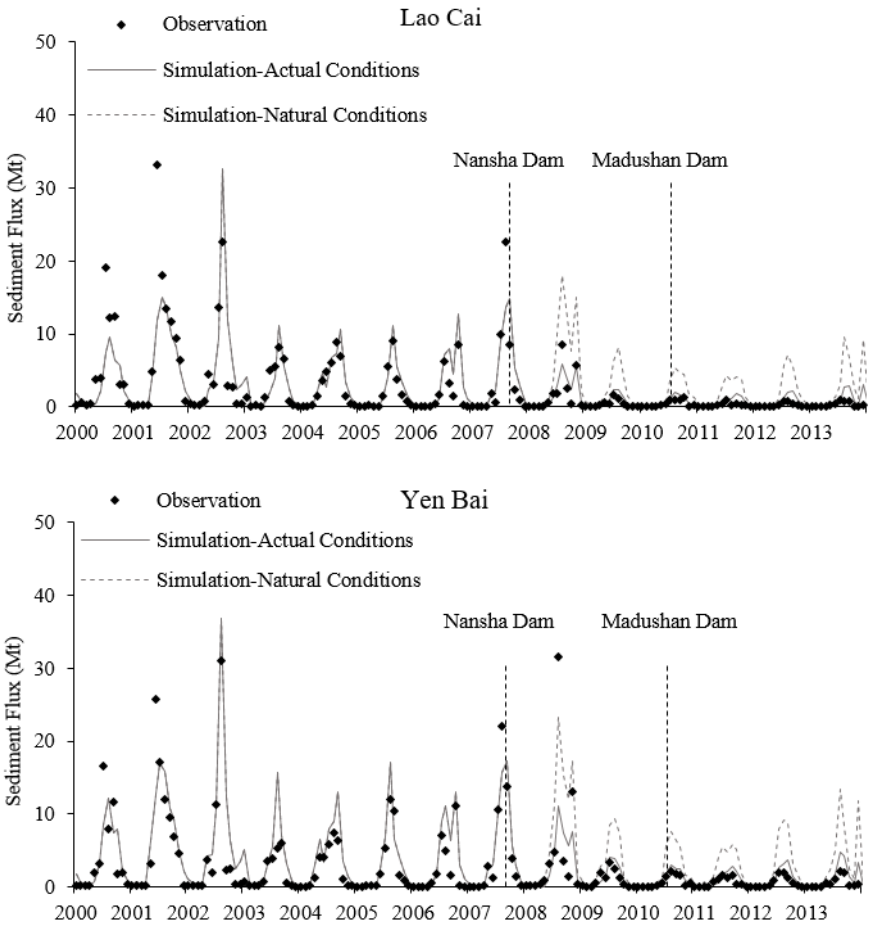

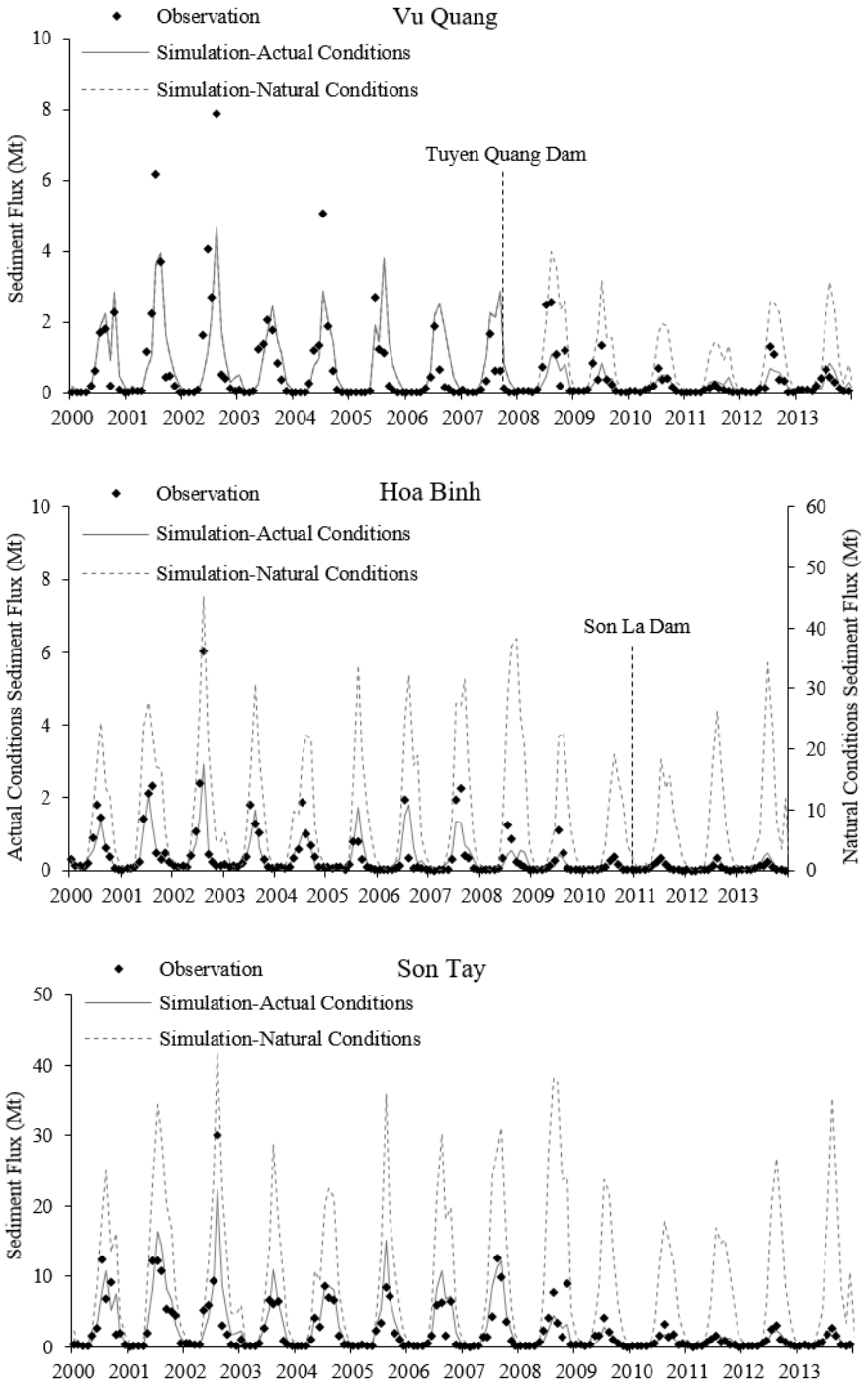

Figure 4-3 Observed (black dot) and simulated (gray solid line) monthly sediment flux, and simulated sediment flux under natural conditions without dams (gray dash line) at five stations from 2000 to 2013.

3.1.2 Annual variations of actual SF

The annual SF exhibits different temporal and spatial variations among the 5 stations (Figure 4-4). For the Thao River, the simulated annual SF ranges from 6.8 to 73.6 Mt yr^{-1} at Lao Cai (with 30.7 Mt yr^{-1} on average during 2000-2013, Table 4-4), and from 11.7 to 85.9 Mt yr^{-1} at Yen Bai (39.8 Mt yr^{-1} on average). The Lo River at Vu Quang is predicted to produce SF ranging from 2.0 to 12.5 Mt yr^{-1} (with 6.6 Mt yr^{-1} on average). On the Da River at Hoa Binh station, the minimum annual SF is 0.8 Mt yr^{-1} and the

maximum is 7.1 Mt yr^{-1} (with 3.6 Mt yr^{-1} on average). Amongst these three tributaries, the Thao River produces the highest SF, followed by the Lo River, and the Da River generates the lowest SF. The Thao River shows higher SF than the other two tributaries due to its high SSC (the annual mean SSC during 2000-2013 at Lao Cai and Yen Bai were 1057 and 1003 mg L^{-1}, respectively, Wei et al., 2019). Even though SSC at Hoa Binh station on the Da River (the annual mean SSC during 2000-2013 was 57 mg L^{-1}, Wei et al., 2019) is much smaller than at Vu Quang on the Lo River (the annual mean SSC during 2000-2013 was 172 mg L^{-1}, Wei et al., 2019), the SF of these two rivers are in the same range. The Da River has a larger runoff (the annual mean Q during 2000-2013 was 1362 m^3 s^{-1}, Wei et al., 2019) with low SSC induced by dam retention, while the Lo River has a lower runoff (the annual mean Q during 2000-2013 was 729 mg/L, Wei et al., 2019) with a higher SSC. As the confluence of these tributaries, the Red River (at Son Tay station) yields an annual SF at the range of 8.0-69.2 Mt yr^{-1}, with an average specific sediment yield (SSY) of 240.5 t km^{-2} yr^{-1}.

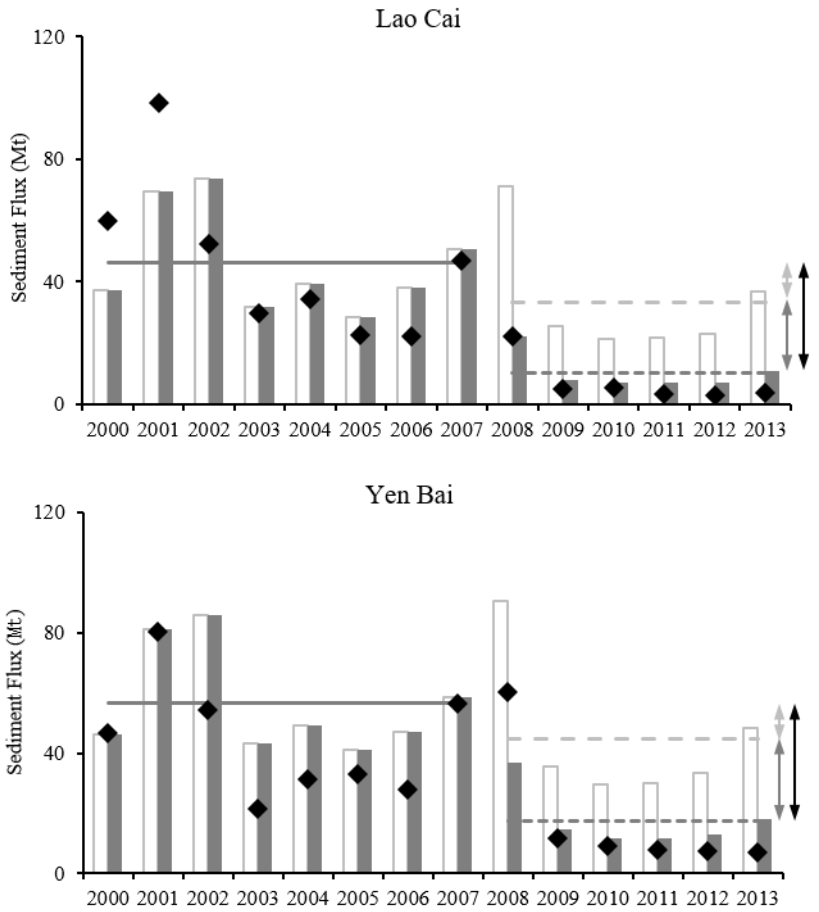

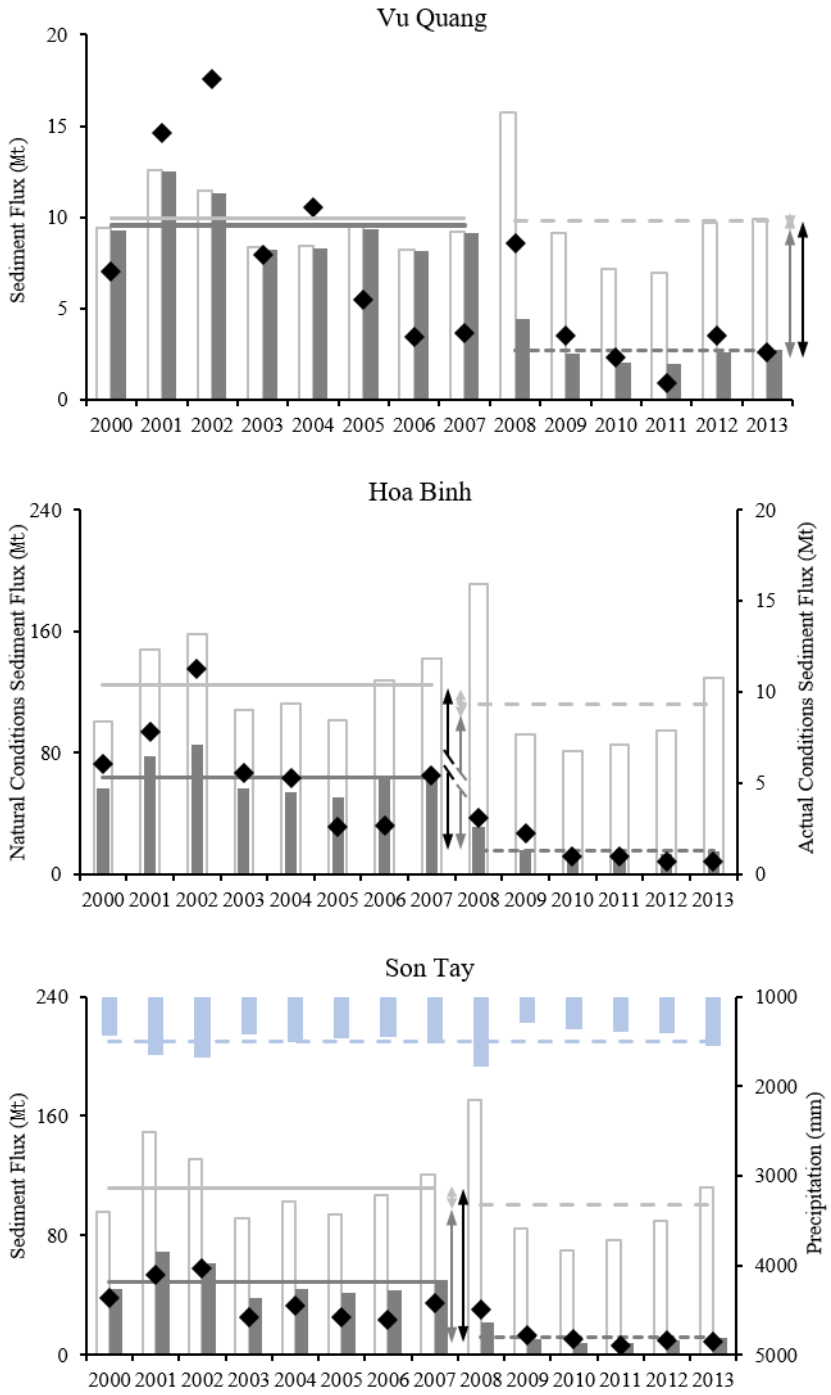

Figure 4-4 Annual sediment flux (SF) from observations (black dot), natural conditions simulations (without dams, gray hollow bar), and actual conditions simulations (gray solid bar) at five stations from 2000 to 2013. Light and dark gray solid lines are the simulated mean annual SF from 2000-2007 of natural and actual conditions, respectively; light and dark gray dash lines are the simulated mean annual SF from 2008-2013 of natural and actual conditions, respectively. The blue bar shows the annual precipitation over the whole basin; blue dash line is the mean annual precipitation of 2000-2013. Black arrow line displays the total SF decrease (caused by both climate variability and dams) which is the difference between the mean annual SF during 2000-2007 under natural conditions and the mean annual SF during 2008-2013 under actual conditions; light gray arrow line displays the difference caused by climate variability which is the differences of the mean annual SF under natural conditions between 2000-2007 and 2008-2013; dark gray arrow line displays the difference caused by dams which is the differences between black arrow and light gray arrow (or between the light and dark dashed lines).

The values of mean annual SF during the study period and sub-periods from references are displayed in Table 4-4. For the whole study period, simulated mean annual SF shows a good match with in-situ data, though slight overestimation at Yen Bai and Son Tay stations. By comparing the mean annual SF of 2008-2013 between natural and actual conditions, the mean annual sediment trapped by the dams during this period range from 7.1 Mt yr^{-1} (Lo River) to 111.0 Mt yr^{-1} (Da River).

Table 4-4 Simulated sediment flux (Mt yr^{-1}) under actual and natural conditions (over the whole period, 2000-2007 period and 2008-2013 period) compared with other studies and in-situ data; values of trapped sediment (calculated as the difference between average values over 2008-2013 in the natural and actual simulations); impacts of climate variability and dams.

Station (River)	1960-1972 (Lu et al., 2015)	1960-1979 (Vinh et al., 2014)	1960-1970 (Dang et al., 2010)	2000-2013			2000-2007			2008-2013			Impact		
				Observed	AC†	NC‡	Observed	AC†	NC‡	Observed	AC†	NC‡	Trapped sediment	Total	Climate Variability	Dams
Lao Cai (Thao)	-	-	-	29.2	30.7	40.5	45.7	46.0	46.0	7.1	10.3	33.3	23.0	-78%	-28%	-50%
Yen Bai (Thao)	44.8	43.4	-	32.5	39.8	51.4	43.9	56.5	56.5	17.2	17.6	44.6	27.0	-69%	-21%	-48%
Vu Quang (Lo)	10.1	9.2	-	6.6	6.6	9.7	8.8	9.6	9.5	3.6	2.7	9.8	7.1	-72%	2%	-74%
Hoa Binh (Da)	71.8	65.0	-	4.0	3.6	119.5	5.8	5.3	124.9	1.5	1.3	112.3	111.0	-99%	-10%	-89%
Son Tay (Red)	120.8	119.3	111.6	26.5	33.0	106.9	36.5	49.1	111.6	13.2	11.6	100.6	89.0	-90%	-10%	-80%

AC†: Actual Conditions
NC‡: Natural Conditions (without dams)

3.2 SF under natural conditions (without any dams)

3.2.1 Inter-annual variations

Like the actual SF (Figure 4-4), interannual SF under natural conditions exhibits high variations. During the study period, results from the simulation under natural conditions suggest that annual SF at Lao Cai, Yen Bai, Vu Quang and Hoa Binh stations should have been from 21.3 to 73.6 Mt yr^{-1}, 29.6 to 90.7 Mt yr^{-1}, 6.9 to 15.8 Mt yr^{-1}, 81.5 to 191.0 Mt yr^{-1}, respectively, thus with a factor of 3 between the highest and the lowest values in the Thao River, and a factor of 2.3 in the Lo and Da rivers. According to the results at the outlet (Son Tay station) the Red River basin should have exported 69.6 to 170.7 Mt yr^{-1} of sediment, with an average SSY of 778.8 t km^{-2} yr^{-1}.

3.2.2 Mean annual SF

Annual SF under natural conditions was compared with observed data from references (Dang et al., 2010; Lu, Oeurng, Le, & Thuy, 2015; Vinh, Ouillon, Thanh, & Chu, 2014, Table 4-4) that covered periods preceding the dams constructions, i.e. before 1979. Despite different time periods, the simulation without dams is close to those in-situ data, though simulations without dams are slightly higher at Yen Bai (~15%) and higher at Hoa Binh (~70%). At Son Tay, the simulation without dams is slightly lower (~10%) than the three reference data. These comparisons show that the model produces a realistic simulation of SF under natural conditions.

3.2.3 SF during flood and drought years

Annual SF at each station in flood and drought years under natural conditions were reported in Table 4-5. During the simulation period, flood years (2001, 2002 and 2008) produce SF 100% higher in the Thao river and 50% higher at Hoa Binh, Vu Quang and Son Tay than drought years (2003-2006 and 2009-2013).

Table 4-5 Sediment fluxes (Mt yr^{-1}) at each station in flood and drought years in the simulation under natural conditions

Station (River)	Flood Years				Drought Years		
	2001	2002	2008	Average	2003-2006	2009-2013	Average
Lao Cai (Thao)	69.5	73.6	71.3	71.5	34.3	25.7	30.0
Yen Bai (Thao)	81.0	85.9	90.7	85.9	45.1	35.4	40.3
Vu Quang (Lo)	12.6	11.4	15.8	13.3	8.6	8.6	8.6
Hoa Binh (Da)	148.0	158.4	191.0	165.8	112.4	96.5	104.5
Son Tay (Red)	149.1	131.6	170.7	150.5	98.7	86.6	92.7

3.3 Simple relation of monthly Q and SF under actual conditions

For both the 2000-07 and 2008-13 periods, monthly simulated SF from the simulation under actual conditions showed a positive power-law relation with monthly simulated Q for the 5 gauge stations as shown by fitted curves in Figure 4-5, with R^2 above 0.95. These 5 stations exported less SF after 2008, which highlights the changes caused by climate variability and by sediment retention of dams. We, therefore, established separately power-law relationships between simulated Q and SF for both periods before and after 2008.

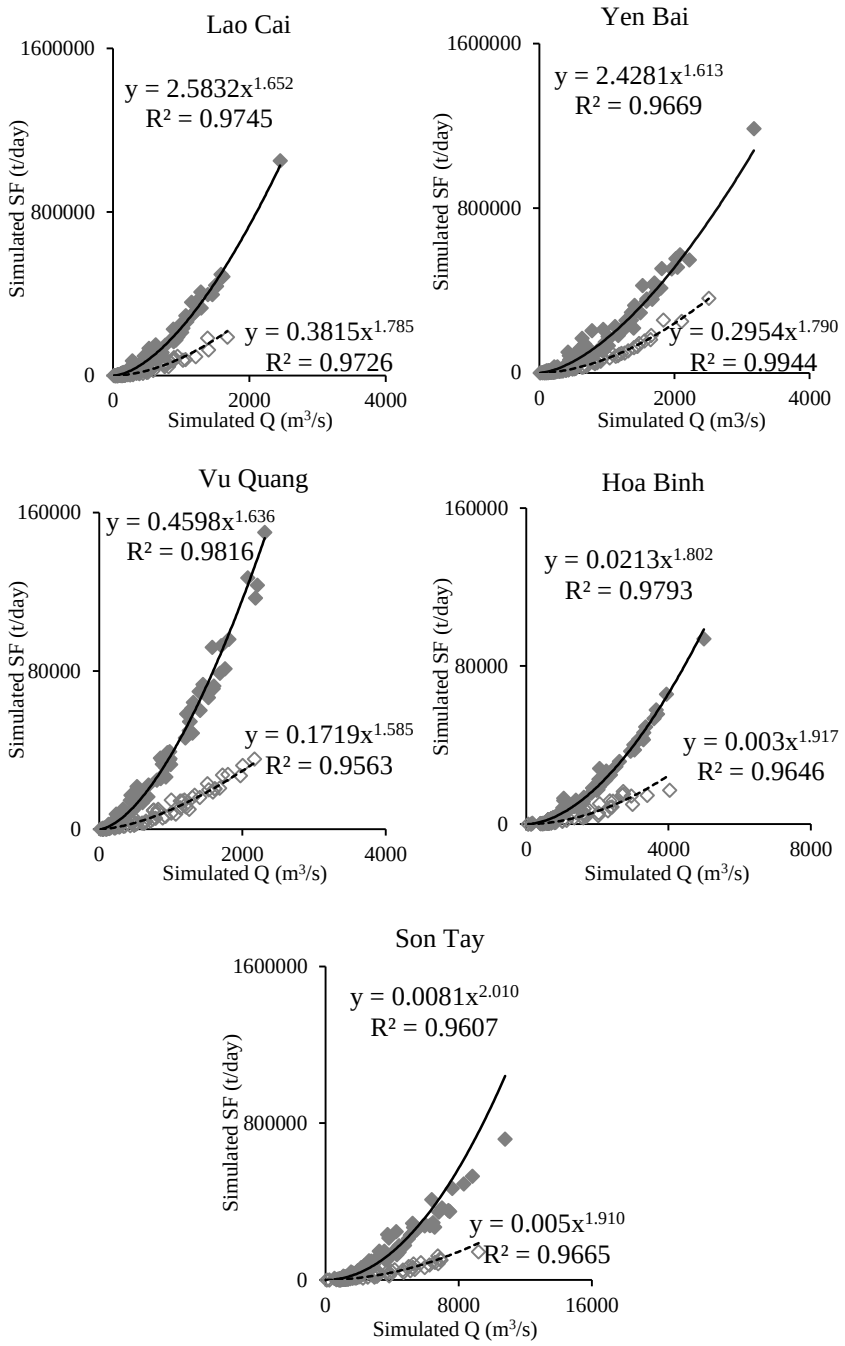

Figure 4-5 Correlation and relations between simulated monthly mean discharge (Q) and simulated monthly mean sediment fluxes (SF) at 5 stations in the simulation under actual conditions. Gray solid squares are of the period 2000-2007; gray hollow squares are of the period 2008-2013. Black solid and dash lines are the fitting curves of period 2000-2007 and 2008-2013, respectively.

The equations established from the monthly simulated Q and SF values were then compared with in-situ observations to be validated (Figure 4-6). For both periods (2000-2007 and 2008-2013), the curves present a good fit with observations, especially when Q is low, with R^2 values generally higher than 0.8. At Vu Quang and Son Tay stations, the points deviations are larger and the values of R^2 of period 2008-2013 (0.73 and 0.75, respectively) are smaller compared with other stations (>0.8), however, the p-value is smaller than 0.001 which indicates that the values obtained from the equation are significantly related to the observations.

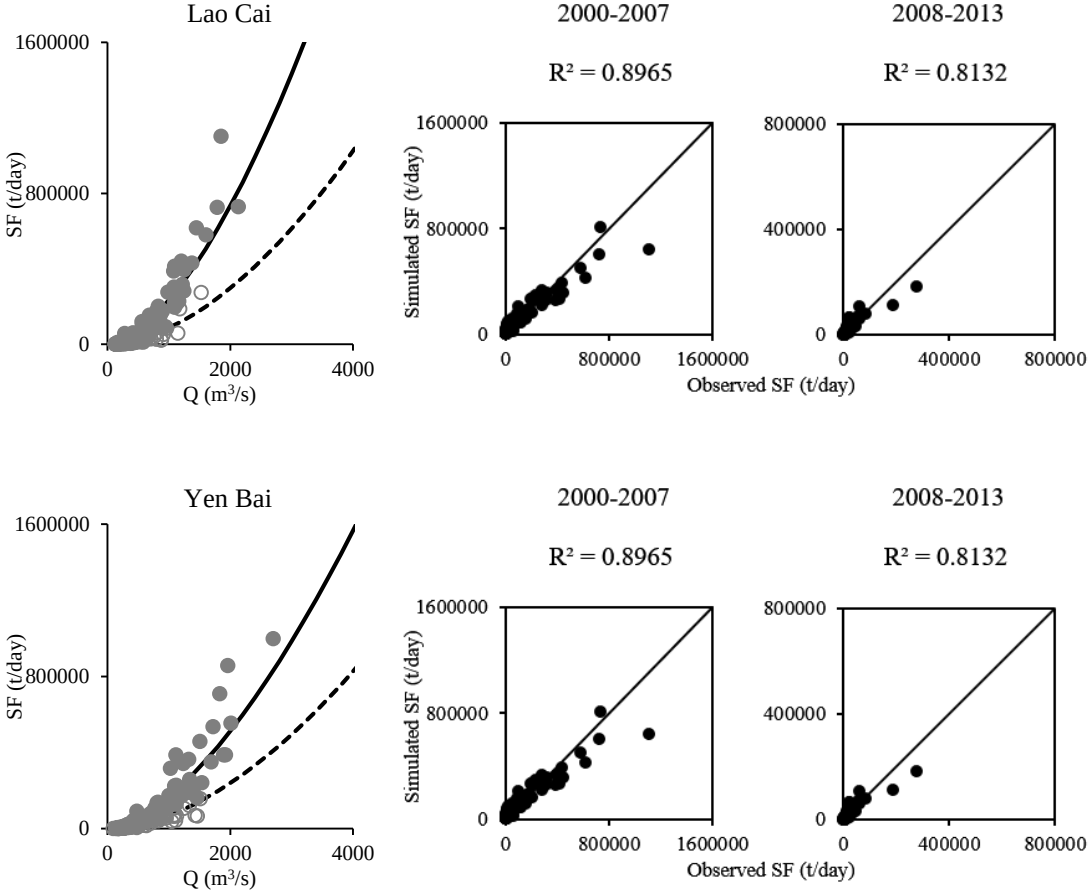

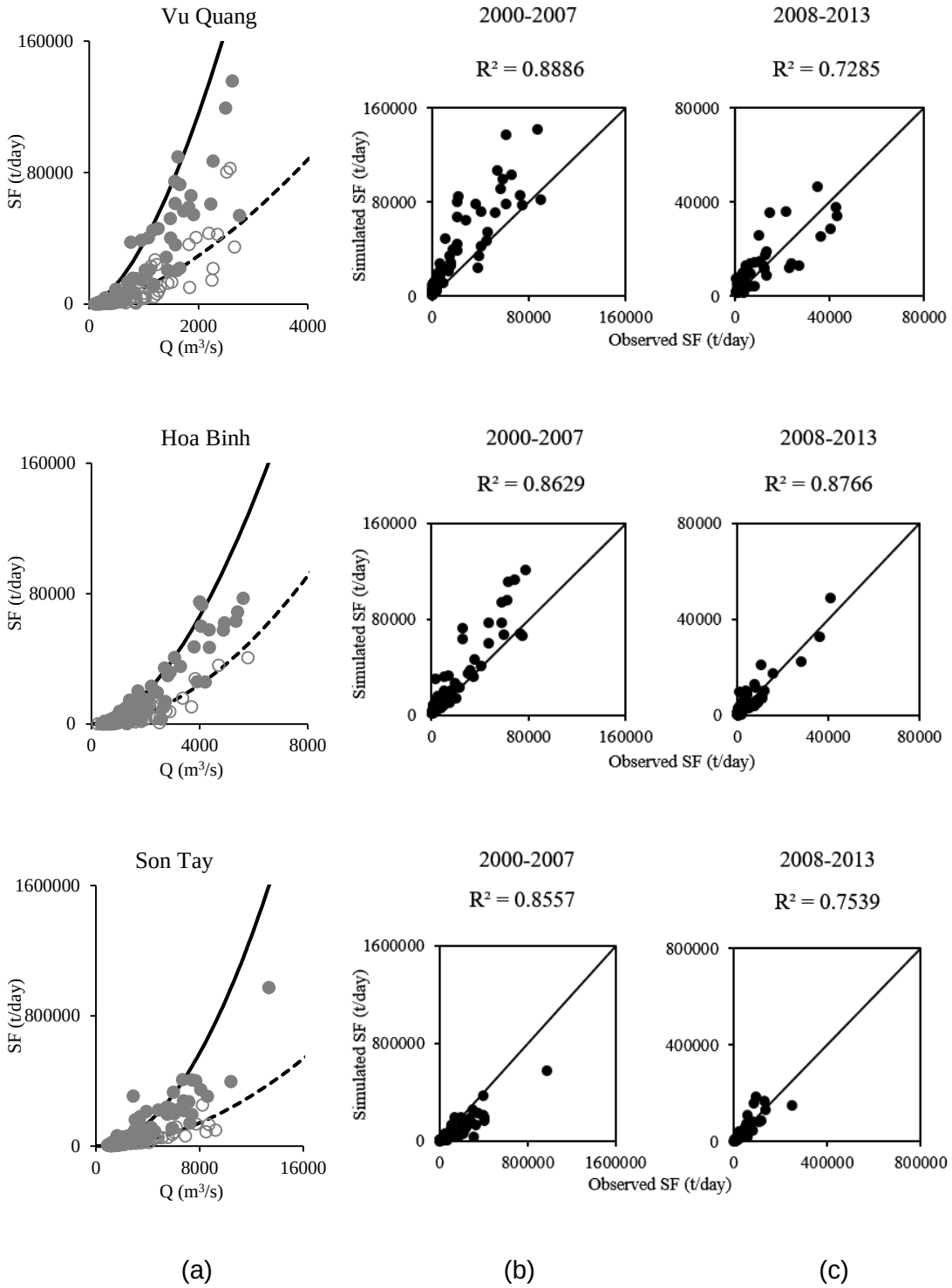

Figure 4-6 (a) Observed data fit with the curve determined from outputs of the simulation under actual conditions. Black solid and dash lines are the rating curves of simulated discharge (Q) and sediment flux (SF) during 2000-2007 and 2008-2013, respectively. Gray dots are the observed data during 2000-2007; gray circles are the observed data during 2008-2013. (b) Comparisons between observed and simulated SF obtained from the Q-SF rating curve of 2000-2007. (c) Comparisons between observed and simulated SF obtained from the Q-SF rating curve of 2008-2013.

3.4 Hot spots of soil erosions

The SWAT model can not only be used to simulate, study and assess the in-stream SF, but also the sediment yield from the land component. Then, based on these simulated mean annual sediment fluxes and soil erosion, hot spots of erosion were identified and presented in Figure 4-7.

The model results indicate that the mean annual soil erosion in the whole basin ranged from 0.01 to 43.4 t ha^{-1} yr^{-1}, with a mean of 5.5 t ha^{-1} yr^{-1} for the whole basin(Figure 4-7c). High erosion areas are identified in the middle part of the Thao River and the downstream of the Da River: with high precipitation (>1500 mm yr^{-1}, Figure 4-7a) and surface runoff (>450 mm yr^{-1}, Figure 4-7b), Lai Chau (sub-basin 173), Lao Cai (sub-basin 116, 117, 135, 148, 149, 157), Ha Giang (sub-basin 119) and Son La (sub-basin 218, 232, 234, 237, 240, 241) provinces are the most vulnerable to soil erosion, and their mean annual erosion rate during the study period can be above 20 t ha^{-1}.

Figure 4-7d presents the in-stream SF spatial variations. High SF can reach locally above 80 t yr^{-1}, with hot spots of high values identified upstream of the Hoa Binh dam, which corresponds with the annual SF values before Hoa Binh dam construction (Table 4-4).

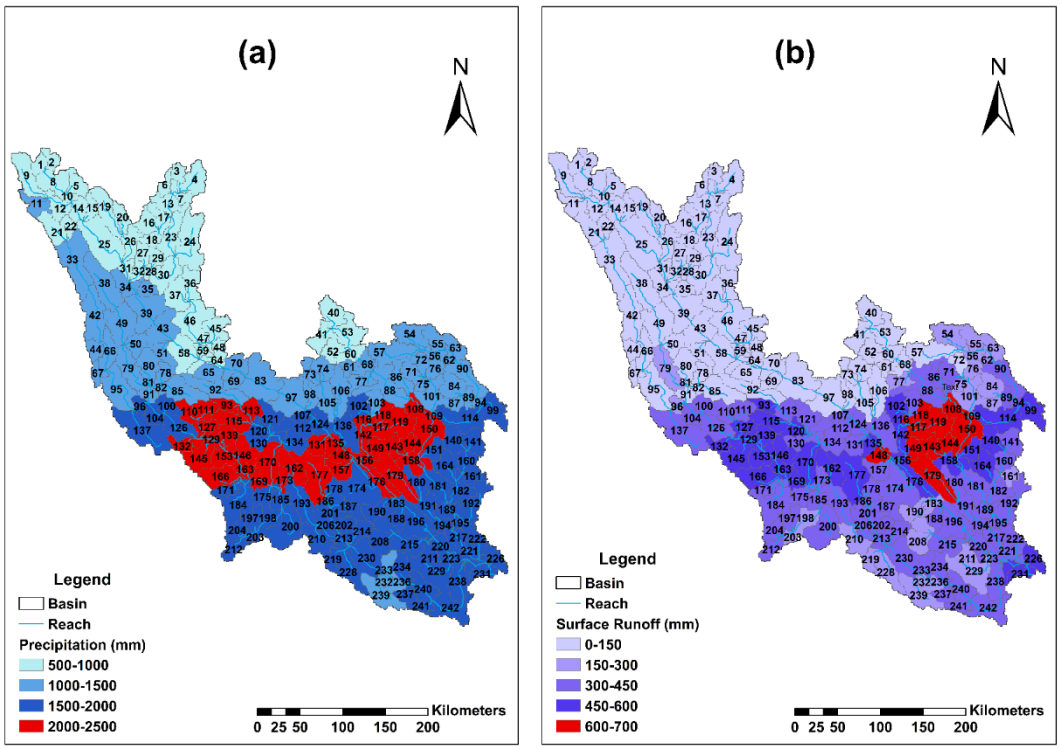

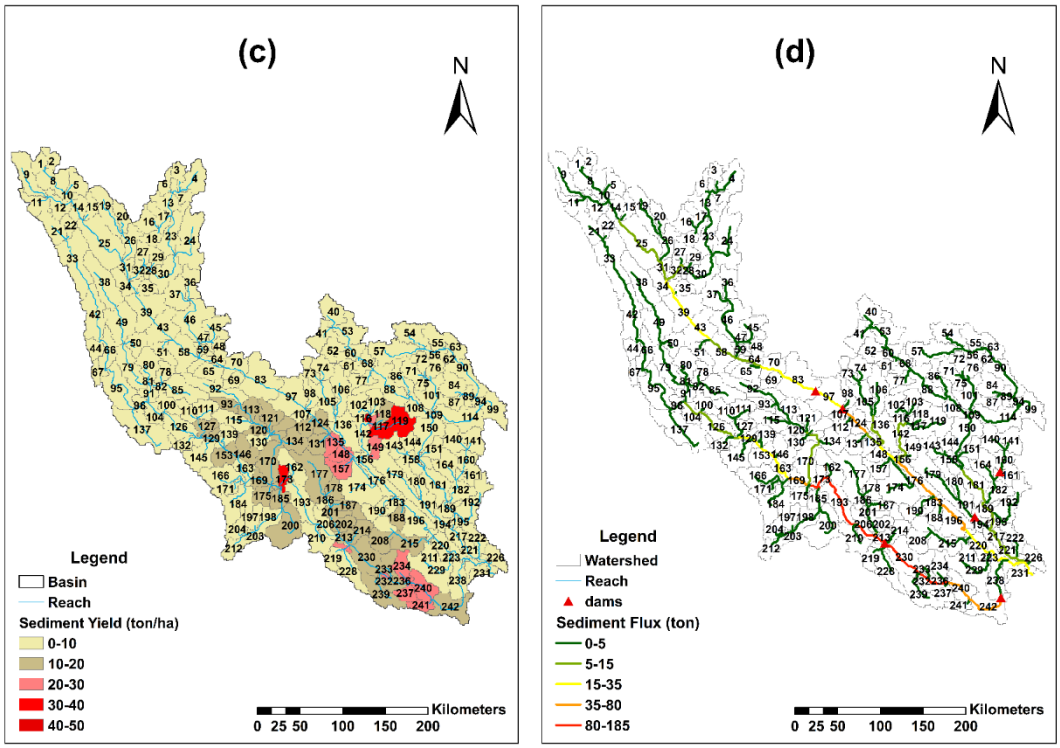

Figure 4-7 Mean annual value of (a) Precipitation distribution (mm yr^{-1}), (b) Surface Runoff (mm yr^{-1}), (c) Soil Erosion (ton ha^{-1} yr^{-1}), (d) In-stream Sediment Flux (ton yr^{-1}) within 242 sub-basins, derived from the actual conditions simulation over the period 2000-2013.

Principal component analysis (PCA) was applied to identify the factors influencing soil erosion (Table 4-6). The PCA results based on the correlation matrix analysis with Varimax rotation produce 3 principal components (PCs) with eigenvalues greater than 1.00, corresponding to an overall cumulative variance of 78.3%, moreover, the 2 first PCs represent a cumulated variance of 67.5%.

Table 4-6 The principal component (PC) loading

Factor	Eigenvectors (percentage of variances %)		
	PC1 (41.6%)	PC2 (25.9%)	PC3 (10.8%)
Soil Erosion (SE)†	0.177	0.399	0.163
Precipitation (P)‡	0.430	0.244	0.101
Water Yield (WY)‡	0.416	0.262	0.095
Surface Runoff (SR)‡	0.446	0.184	-0.033
Slope†	-0.067	0.491	0.125
Clay%†	-0.389	0.117	0.277
Silt%†	0.019	0.243	-0.877
Sand%†	0.346	-0.280	0.256
USLE_P†	-0.246	0.414	0.158
USLE_K†	-0.275	0.340	0.050

†: the simulation from the model

‡: the observation and input data

Notes: underlined values correspond to the first three highest factor loadings in the PC.

4. DISCUSSION

4.1 Uncertainties

Differences between simulations and observations are large on some peaks of SF flow: during these peaks, the SF can be underestimated by a factor >2 (Figure 4-3). Uncertainties can come from three factors: uncertainties associated with rainfall satellite input data; errors due to the numerical simulation approximations; uncertainties associated with in-situ measurement errors on Q and SSC.

The input of a satellite rainfall dataset can cause discrepancy on Q simulation (Wei *et al.*, 2019a). Modelling errors can come from the simplification of algorithms, primarily on SSC simulation. More detailed explanations for uncertainties from the rainfall satellite data and the modelling part are reported in the work of Wei et al. (2019).

In-situ measurements and sampling strategy can also cause errors. For example, a high sampling frequency enables to diminish errors in the estimation of annual SF (Dang *et al.*, 2010). Q and SSC measurements during flood events are usually extrapolated by rating curve. However, the fact that those rating curves may have been established based on non-exceptional conditions might cause deviations on both Q and SSC, and consequently on SF.

4.2 The natural evolution of SF

4.2.1 SF variations caused by climate variability

Comparing the annual SF under natural conditions in 2008-2013 and 2000-2007 shows that climate variability has different impacts on these tributaries, though it induces a decrease at most stations, except at Vu Quang (Table 4-4 and Figure 4-4). The biggest impacts are observed at the two stations on the Thao River (Lao Cai and Yen Bai), causing an average 25% decrease of SF, followed by the Da River (Hoa Binh, ~-10%), with a resulting ~10% decrease on the Red River (Son Tay). On the contrary, at Vu Quang station, the mean annual SF very slightly increased by 2%, in accordance with a similar Q change (2%, Wei et al., 2019).

Our previous study (Wei *et al.*, 2019a) revealed that climate variability had an effect on both Q and SSC in this basin: the rainfall and available water (the difference between rainfall and evapotranspiration) showed decreasing tendencies during the study period, though the decreasing tendencies were not statistically significant through Mann-Kendall method (Mann, 1945; Kendall, 1948), which resulted in a decrease on both Q and SSC. This effect of climate variability on Q and SSC consequently influenced SF. Moreover, the mean annual SF under the natural conditions of the drought years 2009-2013 (86.6 Mt yr^{-1} at Son Tay) is smaller than during the drought years 2003-2006 (98.7 Mt yr^{-1} at Son Tay), except at Vu Quang, as can be seen in Figure 4-4. This might indicate that the annual SF shows a declining tendency under the hydrological regime changes related to climate variability. Previous observations studies indeed suggested

a decrease of rainfall mean and extremes over the last decades over Southeast Asia (Manton *et al.*, 2001). However, longer periods of study are needed to verify this hypothesis and conclude on climate trends and variability. The SF trend of the Red River under the influence of long-term climate variability and hydrology changes will be carried out in future studies.

The annual SF variation caused by climate variability is in fact linked with the Q and SSC variations. The Thao sub-basin is the most sensitive sub-basin to the hydrological regime and to the SSC changes by climate variability (Wei *et al.*, 2019a), likely due to its geomorphology and meteorological characteristics. Li et al. (2016) indicated that hydrological droughts in the Red River basin are much more driven by meteorology than by human activities. Low rainfall induces less landscape soil erosion and less channel erosion than high rainfall. The Thao River basin is sensitive to both landscape erosion and channel erosion due to its steep landscape and channel slopes.

4.2.2 Comparison with other basins

To compare our results with SF and specific sediment yield (SSY) under natural conditions obtained for other Asian rivers, the values provided by Milliman and Syvitski (1992) were considered since they were obtained before 1992 and are less impacted by dams than more recent estimates provided by the literature. From our simulation under natural conditions, the Red River yields an annual SF of 107 Mt yr^{-1}, corresponding to a SSY of 780 t km^{-2} yr^{-1} (Table 4-4). The Yellow River produced 1100 Mt yr^{-1} SF with a SSY of 1400 t km^{-2} yr^{-1}; the Yangtze River caused 480 Mt yr^{-1} SF with a SSY of 250 t km^{-2} yr^{-1}; the Pearl River generated 69 Mt yr^{-1} SF with a SSY of 160 t km^{-2} yr^{-1}; the Mekong River yielded 160 Mt yr^{-1} SF with a SSY of 200 t km^{-2} yr^{-1} (Milliman and Syvitski, 1992). The Red River basin under natural conditions thus exported less SF than the Yellow River (-90%), the Yangtze River (-78%) and the Mekong River (-33%), and 55% more than the Pearl River. However, its SSY was higher than the Mekong (+290%), Pearl River (+388%), Yangtze (+212%), and nearly half of the Yellow River (-44%). When compared to an equivalent surface watershed such as the upper Danube (132,000 km^2), the Red River basin produced almost 3 times higher SSY than that of 265 t km^{-2} yr^{-1} generated by the upper Danube; besides, the upper Danube basin only exported 21.2 t km^{-2} yr^{-1} to the downstream part (Vigiak et al., 2015). These results show that under natural conditions, the Red River basin, though having a smaller surface than other basins in the world, is a very large source of SF from the watershed to the sea.

4.3 Impacts of dams

4.3.1 The reduction caused by dams

Among the three tributaries, dams' impact on the outlet of the Da River (Hoa Binh station) is the most severe, followed by the Lo River; and the dams are less affected on the Thao River (Table 4-4). Two new dams in China caused around 48% reduction

of SF on the Thao River. More cascade dams are under constructions in China, so this value can provide a reference for future studies. The dams on the Lo River reduced around 74% of the annual SF. The large dams on the Da River show an enormous impact on SF, and the trap efficiency is 89% compared to 86-91% from other studies which did not estimate the specific impacts of climate variations of different periods (Dang *et al.*, 2010; Vinh *et al.*, 2014). At the outlet of the Red River basin, the dams upstream caused an 80% decrease of annual SF.

The Son La and Hoa Binh dams on the Da River have large capacities and are located quite downstream to the outlet of the river compared with the dams on the other two tributaries, explaining their higher relative impact. The capacities of the Thac Ba and Tuyen Quang dams are also larger than the two dams on the Thao River. The two dams (Nansha and Madushan) on the Thao River are above 100 km upstream of the Yen Bai station, and along the reach between the dams and Yen Bai station, the impacts of dams on sediment transport are mitigated by the degradation and the soil erosion from the land component. Therefore, the dams show larger impact at the outlet of the Lo River than the Thao River.

Previous studies (Dang *et al.*, 2010; Vinh *et al.*, 2014; Lu *et al.*, 2015) used long-term observed Q and SSC data to analyse the impact of dams on SF. Dang et al. (2010) analysed the observed Q and SSC from 1960-2008, but only at Son Tay station, did not study the Lo and the Da rivers; Vinh et al. (2014) analysed the observed data from 1960-2010 at four stations (not in Lao Cai) and focused the analysis on the impact of the Hoa Binh dam; Lu et al. (2015) also used the observed data from 1960-2010 to assess the impact of a sequence of dams but without considering the dams upstream in China. The present study revisits the impacts of dams by taking into account more dams recently built in the Red River basin. With more dams implemented after 2013 or planned at short/mid-term on these three tributaries, the sediment trap efficiency might still increase and the SF decreases at the outlet of each tributary, consequently at the outlet of the Red River.

4.3.2 Impacts on dynamic processes

From the seasonal variation of SF (Figure 4-3), it can be noticed that the dynamic processes of natural and actual conditions are similar; the impacts of dams are significant on SF peak flow during flood seasons, and dams have much fewer impacts on the base flow of SF.

However, the impacts on the dynamic processes at each station can be different. For example, in 2008, the simulation under natural conditions without dams seems to fit the observations better at Yen Bai and Vu Quang than at other stations. This suggests that, on the same river (Thao), the Nansha dam had weaker impacts at Yen Bai (located more downstream, Figure 4-1) than at Lao Cai for the first year of dam operation, and can be related to the sediment degradation processes between Lao Cai and Yen Bai; also, the Tuyen Quang dam only slightly impacted SF at Vu Quang for

the first year of implementation, presumably because the Lo River has much less SS than the other two tributaries and the sediment retention caused by the new dam at the first year can be relatively lighter. Besides, the Tuyen Quang dam is located on one tributary of the Lo River, whereas the other dams are located directly in the main branch of the Thao and Da rivers. Therefore, the Tuyen Quang dam on the Lo River has fewer impacts on sediment transport.

4.4 Soil erosion

The PCA results identified the factor loadings of each component (Table 4-6): PC1 (consisted of precipitation (P), water yield (WY) and surface runoff (SR)) has the highest weighted variable (41.6%), followed by PC2 (25.9%) which is consisted of soil erosion (SE), slope and USLE agricultural practice factor (USLE_P), and PC3 (10.8%, the percentage of sand (Sand%), silt (Silt%) and clay (Clay%) in soil, i.e. the soil texture). Therefore, precipitation (as water yield and surface runoff are fractions of precipitation), slope and USLE agricultural practice factor (USLE_P) are key influence factors for soil erosion in the Red River basin. The soil texture is also a significant factor. Our results are in agreement with Ranzi *et al.* (2012) who highlighted the major role of rainfall in soil erosion in the Lo basin; Yang et al. (2003) found that the hot spots of soil erosion in Southeast Asia were close mountainous areas located in the tectonic zones and dense croplands regions where both natural geomorphology and human activity are major factors for inducing soil erosion.

Tuan et al. (2014) found annual soil losses from 1.8 to 174 t ha^{-1} yr^{-1} from plot-scale experiment near Son La. Podwojewski et al. (2008) found a soil erosion from 0.86 to 13.5 t ha^{-1} yr^{-1} also in Hoa Binh province on steep slopes, and Phan Ha et al. (2012) demonstrated that the soil loss can be reduced to 0.103 to 1.185 t ha^{-1} yr^{-1} with fodder management. Based on a RUSLE model, Nguyen et al. (2011) simulated a continuous increase of the soil erosion from 1970 to the recent decade 2000, from 4.9 to 5.9 t ha^{-1} yr^{-1}. Mai et al. (2013) found a 1.63 to 17.22 t ha^{-1} yr^{-1} erosion rare near Son Tay. Our simulation is in the range of these references: from 0.01 to 43.4 t ha^{-1} yr^{-1}, with a mean of 5.5 t ha^{-1} yr^{-1} over the whole basin. The soil of the high erosion areas - the middle part of the Thao River and the downstream of the Da River (Figure 4-7c) - is mainly composed of Orthic Acrisols (Ao90-2-3c-4284, Figure 2-12c). This type of soil is acid with sandy-loamy surface soil, and prone to slaking, crusting and erosion. Acrisols form the tropical red soils and red earths, and after eluviation they are subjected to erosion (FAO, 2003b). This result is in agreement with the above conclusion obtained from PCA.

Estimates of annual SF shows that Yen Bai produces more SF than Lao Cai (~30% over the whole period, both under actual and natural conditions, Figure 4-4). This indicates that the soil erosion or/and resuspension likely happens in the part of the basin between Lao Cai and Yen Bai. This can be confirmed by the spatial identification of soil erosion (Figure 4-7c) which also indicates that Lao Cai province is a hot spot of soil erosion.

Before the construction of Hoa Binh dam, sediment input to the Red River mainly originated from the Da River (~120 Mt yr^{-1} in the natural conditions simulations, i.e. more than twice the values estimated for the other tributaries, Table 4-4). The high in-stream SF of the Da River results from both land erosion and channel degradation. Complex dam regulation can cause complex hydraulics compared to the natural channel. Comparison of the natural and actual conditions simulations over the period 2008-2013 suggests a 111 Mt yr^{-1} value of trapped sediment at the Hoa Binh dam. Such a big quantity of sediment from upstream of Hoa Binh should catch the attention of the management because big sedimentation in the reservoir would reduce the capacity and performance of the dam. As explained in Section 2.1.4, this is also a reason why the Son La dam was built.

4.5 Interpretation of Q-SF simple relations

From Figure 4-5 and Figure 4-6, we can see that the relation between monthly Q and SF is a power-law relation of the form:

$$\mathrm{SF} = \mathrm{a}Q^{b} \quad (1)$$

where SF is the monthly mean sediment flux (t day^{-1}), Q is monthly mean water discharge (m^3 s^{-1}), *a* and *b* are regression coefficients.

Equation (1) is formally in accordance with a general sediment rating curve (Asselman, 2000; Syvitski *et al.*, 2000):

$$SSC = a'Q^{b'} \quad (2)$$

where SSC is the suspended sediment concentration (mg L^{-1}), *a'* and *b'* being the regression coefficients. The coefficient *a'* represents the erodibility of the soil, and is equal to SSC when Q is 1 m^3 s^{-1}; a sub-basin with intensively weathered materials which can be eroded and transported easily usually shows a high value of the coefficient *a'*. The coefficient *b'* represents the erosive power of the river and the transport capacity; it is also affected by the grain size distribution of the material available for transport: rivers with sand-sized sediments have higher *b'* values than rivers with silt and clay-sized sediments.

As discussed before, among the three sub-basins, the Thao and Da sub-basins present steep slopes and are vulnerable to soil erosion, therefore their *a*-coefficient should be high. The two stations on the Thao River have the highest *a* values (2.58 and 2.43 for Lao Cai and Yen Bai, respectively, over the 2000-2007 period, Figure 4-5); however, the Hoa Binh station on the Da River has the lowest a value (0.02 over 2000-2007) among these three tributaries because the eroded soil was retained in the Hoa Binh and Son La dams. For each station, the *a*-value decreased between 2000-2007 and 2008-2013 (Figure 4-5): dams retain the SS from upstream soil erosion which induces a decrease of *a* value downstream of the dam.

The average values of the median diameter D_{50} of surface sediment are 0.16, 0.35,

0.175 and 0.2 mm in the Thao, Da , Lo rivers and the reach between the confluence of the Da and Thao rivers at Son Tay, respectively (Vinh *et al.*, 2014), which result in high *b* values at Hoa Binh and Son Tay stations. The *b* values of Lao Cai and Yen Bai on the Thao river and of Vu Quang on the Lo river are similar during 2000-2007 (from 1.61 to 1.65, Figure 4-5) but not during 2008-2013 (1.59 at Vu Quang vs. 1.79 at Lao Cai and Yen Bai). This can indicate that the dams on these two tributaries might change the grain size distributions and transport capacity at these stations.

The relations between monthly Q and SF in Figure 4-5 fit well with the observations of both periods (2000-2007 and 2008-2013, Figure 4-6). The coefficients *a* and *b* in the simple Q-SF equation are in agreement with the real sub-basin characteristics. The curves of two periods also illustrate the differences of the sediment regimes during these two periods: curves of 2008-2013 are more gentle than of 2000-2007 (Figure 4-6), i.e. under the same Q, the SF is lower compared to 2000-2007, which is due to a combined impact of climate and dams. Hence, these simple Q-SF equations can be used by stakeholders to estimate the monthly SF without using the SWAT model.

5. CONCLUSIONS

This study aimed to characterize the suspended sediment flux and the soil erosion of the Red River basin by using the output of a numerical model and in-situ data. Suspended sediment flux was quantified based on daily simulations of discharge and suspended sediment concentration during a long period, taking into account the successive implementations of dams and the climate variability during this period. Furthermore, by implementing a scenario of natural condition without dams in this basin, this study allowed to disentangle the impacts of climate variability and dam constructions at the outlets of each main tributary as well as at the outlet of the continental basin. This provides a reference for future studies on dams' functions and water resource management.

Under the influence of both climate variability and damming, the suspended sediment fluxes showed a drastic decrease during 2008-2013 compared to 2000-2007. These two influencing factors had different effects on each sub-basin. Due to the different climatic and topographical characteristics, such as precipitation distribution and river bed slope, the Thao River is more sensitive to climate variability than the other two tributaries. Conversely, the Da River is the most affected by constructions of huge-capacity dams. At the outlet of the Red River basin, the mean annual sediment fluxes decreased by 90% compared to the value estimated for natural conditions during 2000-2007, of which 10% was due to climate variability and 80% to the dams. A power-law relation between monthly mean discharge and sediment flux was provided at each outlet of the main tributaries and the Red River for stakeholders and decision-makers to have an easy tool to estimate the sediment flux.

The high advantage of the model, once it has been calibrated with data from hydrological stations, is that he can serve to estimate and map each term involved in

the sediment transport process – including local erosion, local deposition, in-stream sediment discharge, etc. – and that it can be used to infer local SF-Q rating curves at any virtual station within the basin from the model simulations, even where there is no true station. This point is of major interest both for scientific applications (e.g., studying spatial variations of SF) and for management purpose, with provinces and other stakeholders.

Land management should pay attention on the high soil erosion areas located in the middle part of the Thao sub-basin and the lower part of the Da sub-basin due to the precipitation distribution, topography and soil texture, and river management should notice the sediment retained in the dams on the Da River.

Some improvements can be done in future research. This study did not take into account the impacts of land use changes on soil erosion and sediment flux. A more precise and higher-frequency in-situ dataset would be useful, such as longer and high-frequency hydrological and meteorological data at more stations, and more information about dam management, in order to have a better estimation and understanding of the impacts of climate variability and human interferences.

With on-going and future climate change and dams constructions in this basin, it would be necessary to pursue further research about the sediment flux variation and its associated contaminant fluxes as well as carbon transfer in order to better manage this basin and protect the downstream coastal areas. In addition, running numerical simulations under scenarios of global changes, such as land use changes and urbanization, would allow to estimate the impacts of these changes on hydrology and suspended sediment fluxes.

ACKNOWLEDGEMENT:

This research was developed in the framework of the Land-Ocean-aTmosphere regional coUpled System study center (LOTUS), an international joint Vietnamese/French laboratory (http://lotus.usth.edu.vn/) funded by the Institut de Recherche pour le Développement (IRD). We thank LOTUS for providing the dataset, and also the research travel funds for Xi Wei to collect data and information in Vietnam. The PhD scholarship of Xi Wei is financially supported by the China Scholarship Council (CSC), grant number 201606240088.

Chapter 5

Assessing Fluvial Organic Carbon Concentration and Fluxes

This chapter is preparing to submit. The work of this chapter was to characterize and quantify the dissolved organic carbon (DOC) and particulate organic carbon (POC) over the basin considering the impacts from climate variability and dam constructions by calculating the DOC and POC at a daily time step.

Wei, X.; Sauvage, S.; Le, T.P.Q.; Fabre C.; Ouillon, S.; Orange, D.; Vinh, V.D.; Sánchez-Pérez, J.-M. A Modelling Approach to Assess Fluvial Organic Carbon Flux and its Response to Climate Variability and Damming on A Large-scale Asian River Basin: Case of the Red River (China and Vietnam). Prepare to submit.

5. CHAPTER Ⅴ: Assessing Fluvial Organic Carbon Concentration and Fluxes

5.1. Scientific Context and Objectives

Tropical humid ecosystems are hot spots of terrestrial organic carbon storage and tropical rivers are critical to total global fluvial organic carbon fluxes. Tropical rivers were estimated to export almost half of the global organic carbon fluxes to the oceans. Asian river basins have also been recognized to produce high organic carbon and export significant organic carbon fluxes to the oceans. Southeast Asian regions are vulnerable to climate changes. Besides, human activities and interferences are strong in developing Asian countries. Therefore, it would be important and interesting to understand the DOC and POC transport dynamics and quantifying DOC and POC fluxes through the tropical Asian river basins at a daily time scale in order to capture the flood events and estimate the organic carbon fluxes preciously. The Red River basin, passing through from subtropical to tropical zone, shared by China, Vietnam and Laos, influenced by strong human activities, would be a great study example. The specific objectives of this paper are: (1) to quantify daily, monthly and annual DOC and POC fluxes through the basin during a long-term period (2003-2013); (2) to quantify the influence of climate variability and dams on DOC and POC transport and fluxes; (3) to propose a new approach to evaluate DOC and POC in different point in the basin without using the SWAT model.

5.2. Materials and Methods

Based on the calibrated daily discharge (Q) and suspended sediment concentration (SSC) from the SWAT model, DOC and POC were calculated through simple equations. First, the equations for calculating the DOC and POC concentrations were calibrated based on DOC and POC discrete sampling data and observed daily Q and SSC data from 2003 to 2013 at Yen Bai, Vu Quang, Hoa Binh and Son Tay stations. Then the outputs of modelled Q and SSC data from previous work were used to calculate the DOC and POC concentrations and then fluxes at a daily time step. Benefitting from the model scenario: actual conditions and natural conditions (without dams), the impacts of the Q due to climate variability and the impacts of dam constructions were able to be quantified.

5.3. Main Results and Discussions

The parameters related to DOC and POC equations well represented the characters of each sub-basin. We found the parameters have relationships with the average soil organic carbon content of the drainage area, the mean annual Q and the Chl-a concentration in the river. Therefore, people are able to use these relationships to evaluate the parameters and then to calculate the DOC and POC concentrations at any point within this basin.

The mean annual export of DOC during 2003-2013 was 222 kt yr^{-1} at Son Tay, which represented 0.26% of the total Asian rivers DOC transport; and the mean annual export

of POC during 2003-2013 was 406 kt yr^{-1} at Son Tay which accounted for 0.37% of the total POC export by the Asian rivers. Compared to some other Asian and tropical rivers, the export of DOC and POC fluxes through the Red River was not high, especially for POC. However, when comparing the specific yields, the Red River basin yielded high DOC and POC values, which is in agreement with some previous studies that indicated that the rivers in mainland Asia have the highest specific export rates worldwide in terms of DOC and POC. High DOC yield of the Red River basin comes from the high leaching from soil and rocks while the high POC yield is contributed from high soil erosion and high suspended sediment concentration.

Under natural conditions (without dams), at the outlet (Son Tay), due to the Q variation induced by climate variability, the DOC flux during 2008-2013 increased 1% compared to 2003-2007, and the flood year 2008 was the main contributor. A 13% reduction of DOC flux was related to dam operations which regulated the discharge during flood seasons. POC fluxes under natural conditions between 2003-2007 and 2008-2013 varied little (-2%) which indicated that climate variability had little impacts on POC fluxes, while the dam constructions caused an 85% decrease in POC flux. At the outlet (Son Tay), the POC flux in 2008 was only 45% of that in 2007 even though 2008 is a flood year. A drastic decrease in SSC and sediment fluxes occurred in the same year. The POC transfer was affected consequently after dam constructions.

At the outlet during 2003-2007, the POC flux accounts averagely 74% of TOC flux, but during 2008-2013, it only accounts 47%. Due to the drop of POC flux, the TOC decreased by 31% at the outlet in 2008 compared to the previous year. With the construction and operation of new dams, the composition ratio of TOC changed, from POC-dominating to DOC-dominating. Besides, the dynamic variations of POC/TOC were also changed by dam regulation. Before new dam constructions, the POC/TOC ratio was low around March and high in flood season. However, after new dams impounded, during June and July, the dams fulfil flood-control functions, retaining water and SS, therefore the POC/TOC ratio became low during the flood season. And around March, dams discharge water for irrigation, SS is released too, which induces high POC/TOC.

5.4. Conclusion and Perspectives

Based on a hydrological model already set up, calibrated and validated over the Red River basin, and on dissolved and particulate organic carbon measurements, a model of organic carbon dynamics was calibrated and validated at a daily time step during a 10-year period (2003-2013) in a large tropical river basin. Intra-annual and inter-annual variations are very difficult to assess from discrete samplings, and only at the hydrometric stations. This method overcomes the shortage of in-situ measurement and allows future studies on different scenarios such as land use and climate changes. This approach could be applied to other basins worldwide and to characterize their corresponding parameters. More intensive sampling during flood season will help to result in more precise parameters. Future studies can keep attention on the fluvial

organic carbon flux and specific yield variations under global changes in order to understand their long-term impacts. Besides discharge and suspended sediment, soil organic carbon content, soil leaching and erosion are the key factors influencing the organic carbon concentration in the Red River basin. Therefore, the link between soil conservation and organic carbon transport can also be carried out.

5.5. Full Article

A Modelling Approach to Assess Fluvial Organic Carbon Flux and its Response to Climate Variability and Damming on A Large-scale Asian River Basin: Case of the Red River (China and Vietnam)

Xi Wei[1], Sabine Sauvage[1], Thi Phuong Quynh Le[2], Clement Fabre[1], Sylvain Ouillon[3,4], Didier Orange[5], Marine Herrmann[3,4], José-Miguel Sánchez-Pérez[1]

[1] ECOLAB, Université de Toulouse, CNRS, INPT, UPS, Auzeville-Tolosane, France.

[2] Institute of Natural Product Chemistry (INPC), Vietnam Academy of Science and Technology (VAST), Hanoi, Vietnam.

[3] LEGOS, Université de Toulouse, IRD, CNES, CNRS, UPS, Toulouse, France.

[4] USTH, Vietnam Academy of Science and Technology (VAST), Hanoi, Vietnam.

[5] Eco&Sols, Univ. Montpellier, IRD, CIRAD, INRA, Montpellier SupAgro, Montpellier, France.

Abstract:

Fluvial organic carbon (OC) transfer is part of the global carbon cycle and is an important resource for downstream ecosystems. However, its transfer process is affected by climate variability and damming. This study chose the Red River basin as a study case, which is located in Southeast Asia and facing the above impacts. This study aims to quantify OC concentrations and fluxes at a daily time step and the impacts of climate variability and damming on OC spatiotemporal transfer processes at a large basin scale for a long time period (2003-2013) by using a new approach based on modelling outputs. Empirical equations for calculating dissolved (DOC) and particulate organic carbon (POC) concentrations were calibrated based on discrete in-situ sampling data. Then simulated daily discharge from the modelling was used to quantify the daily OC fluxes. Results show that the corresponding parameters of the DOC and POC equations well represent the characteristics of each sub-basin, underlining the effects of soil OC content, mean annual discharge and Chlorophyll a. During 2003-2013, at the basin outlet, the exports of DOC and POC were 222 and 406 kt yr-1 respectively, accounting for 0.38% of the total OC (TOC) export by Asian rivers. However, the specific yields of DOC (1.62 t km-2 yr-1) and POC (2.96 t km-2 yr-1) of the Red River basin were ~1.5 times those of other Asian basins. By comparing to a reference scenario (without dams) to actual conditions, we estimated a 12% and 88% decrease in DOC and POC fluxes between 2008-2013 and 2003-2007, respectively, mainly due to damming. Less than 2% of the variations was explained by climate variability. The percentage of POC in TOC decreased from 86% (without dams) to 74% until 2007 then to 47% with new dams. Damming induced a great decrease in POC due to sediment retention, which consequently altered the TOC export and the DOC/POC ratio. This study enables the stakeholders to estimate the OC concentrations with easy-obtained environmental parameters at any point within this basin where sampling is not executable, and the approach used in this basin can be applied over the other basins.

Keywords: the Red River, organic carbon, climate variability, dam, modelling.

1. Introduction

Rivers play an essential role in the global transport of suspended sediment (SS) and associated elements, such as carbon (C), nitrogen and phosphorus. They are a key connection between terrestrial and marine ecosystems. Riverine organic carbon (OC) can be classified into two forms: dissolved organic carbon (DOC) and particulate organic carbon (POC), and is regarded as an indicator of water quality. Moreover, metal ions and pesticides can be adsorbed onto OC and then be carried to the oceans (Boithias *et al.*, 2014; Garneau, 2014). Measuring, quantifying and studying the fate of fluvial OC allows to comprehensively evaluate the degree of organic contamination in water bodies. Riverine OC is mainly derived from the following three pools: 1) an autochthonous pool derived from in-situ biological production, such as phytoplankton, metabolite of animals and plants in rivers; 2) an allochthonous pool derived from terrestrial organic matter, such as soil leaching and erosion; 3) an anthropogenic pool derived from agricultural, industrial and domestic release (Hope *et al.*, 1994; Rizinjirabake *et al.*, 2018).

Long term changes at the basin scale such as climate variability, land use changes and increase damming have altered biogeochemical cycles, including C cycle (Hope *et al.*, 1994; Seitzinger *et al.*, 2010). Therefore, understanding the biogeochemical and dynamical processes involved in riverine OC, and quantifying OC fluxes and their answer to those influence factors are essential to further assess the balance between continental and oceanic fluxes and the impact of those changes.

Riverine C export to the oceans was estimated at 0.9 Gt yr^{-1} (Hope *et al.*, 1994; Cole *et al.*, 2007), of which about 0.38 Gt yr^{-1} was exported as OC (Ludwig and Probst, 1996b). A more recent study from Li et al. (2017) estimated that annual C exported to oceans was approximately 1.06 Gt, including 0.48 Gt of OC. Tropical humid ecosystems are hot spots of terrestrial C storage and tropical rivers strongly contribute to the total global fluvial C flux (Huang *et al.*, 2012; Carvalhais *et al.*, 2014). Ludwig and Probst (1996) indicated that about 45% of the OC exported to the oceans originated from tropical wet areas. The study of Huang et al. (2012) focused on the tropical rivers and indicated that they delivered 0.28 Gt yr^{-1} of OC to the estuaries.

The global annual fluvial flux of DOC to the ocean was from 0.21 to 0.25 Gt yr^{-1}, while Asian rivers contributed by 0.09 to 0.14 Gt yr^{-1} (Ludwig and Probst, 1996b; Huang *et al.*, 2012; Carlson and Hansell, 2015; Li *et al.*, 2017, 2019). The global rivers export of POC was estimated from 0.17 to 0.24 Gt yr^{-1}, and Asia is the major source region, accounting about 50% (0.13 Gt yr^{-1}) (Ludwig and Probst, 1996b; Beusen *et al.*, 2005; Huang *et al.*, 2012; Li *et al.*, 2017). Previous studies also pointed out that the rivers in mainland Asia have the highest specific export rates in terms of DOC and POC (Huang *et al.*, 2012; Li *et al.*, 2019). Most estimations were calculated on a monthly or an

annual scale, and hardly any study estimated OC fluxes on a daily time scale. Sampling and modelling are indeed usually performed at fortnightly or monthly intervals, which might induce underestimation when there is a storm or intense rainfall during the intervals since most OC export happens during flood events. For most rivers, the OC concentration varies with discharge and season (Coynel *et al.*, 2005). Discharge (Q) is the major factor controlling the output of OC (Hope *et al.*, 1994), and suspended sediment concentration (SSC) is also the main determinant of POC flux (Ludwig and Probst, 1996b; Huang *et al.*, 2012). Q and SS can vary largely depending on the seasons but also due to intensive daily rainfall and storms, inducing strong variability of OC concentration and fluxes at the seasonal but also daily scales.

Tropical Asian river basins are key contributors to the OC fluxes export to the oceans, submitted to a wide range of changes. It is therefore essential to develop methods to quantify OC fluxes and their variability in these basins from the interannual to the daily time scales. The Red River basin is an international tropical basin shared among China, Laos and Vietnam, combining different land uses and affected by human activities such as intensive agriculture and dam implementations. Previous studies, based on both in-situ sampling data and modelling, have investigated impacts of human activities on hydrology and SS (Le *et al.*, 2007; Dang *et al.*, 2010; Wang *et al.*, 2011; Vinh *et al.*, 2014; Lu *et al.*, 2015; Wei *et al.*, 2019b); these studies especially found a strong retention of SS (~90% decrease) caused by dams.

Studies about nutrients associated with discharge and SS, such as C, nitrogen, phosphorus, have also been carried out. Most of these researches analysed the concentrations and fluxes of nutrients based on the sampling data (Le *et al.*, 2005, 2010, 2017a; Dang *et al.*, 2013a); few used the numerical modelling (Le *et al.*, 2017b; Nguyen *et al.*, 2018). At the local or regional scale, in-situ sampling is a direct and accurate way to quantify the riverine C. From sampling data, Le et al. (2017a) estimated that the mean annual TOC yield during 2008-2010 was 270 kt yr^{-1} at Hanoi, of which 142 kt was DOC and 128 kt was POC; Dang et al. (2013) quantified the annual POC flux of 243 kt yr^{-1} at Son Tay during 2006-2009.

However, in-situ field sampling at large spatial and temporal scales is expensive and often impracticable in some remote areas and underdeveloped regions. Using a numerical modelling approach, combined with available in-situ data, allows to overcome these shortages. Le et al. (2017b) and Nguyen et al. (2018) used a modelling approach to identify a seasonal OC variation and to estimate a TOC export of 324 kt yr^{-1} at Son Tay during 2013-2014. However, as explained above, such simulations at a seasonal scale do not represent the whole range of OC fluxes variability, and Hope et al. (1994) indicated that riverine C flux was likely to be underestimated when studied only based on seasonal data. Therefore, it would be more precise to assess and calculate OC flux at a daily time step using daily Q, SSC and OC concentrations. Also, it is important to analyse DOC and POC concentrations and dynamics separately.

This work aims at understanding the DOC and POC transport dynamics and quantifying DOC and POC fluxes and their variability through the whole Red River basin. The specific objectives of this paper are: (1) to quantify daily, monthly and annual DOC and POC fluxes through the basin during a long-term period (2003-2013); (2) to quantify the influence of climate variability and dams on DOC and POC transport and fluxes; (3) to propose a new approach to evaluate DOC and POC at different points in the basin.

2. Materials and Methods

2.1 Study area

2.1.2 Geographical characteristics

The Red River basin covers a total area of approximately 159,000 km^2 shared by China (49%), Vietnam (50.1%) and Laos (0.9%). Our study area focuses on the continental drainage catchment at Son Tay which is also the apex of the delta, with a surface of 137,200 km^2 (Figure 5-1).

The Red River is comprised of three main tributaries: the upper part of the main river before the confluence, 20 km upstream to the Son Tay station, is called the Thao River, and it is now the main sediment load contributor (~80%) to Son Tay (Le et al., 2007; Wei et al., submitted); the Da River, on the right river bank, contributes to 50-57% of total discharge at Son Tay (Le *et al.*, 2007; Li *et al.*, 2016a); the Lo River is on the left riverbank, and its annual mean Q and SSC at its outlet are between the Thao and the Da rivers (Lu *et al.*, 2015; Wei *et al.*, 2019a).

The topography within this basin varies greatly, from an elevation of around 3000 to 2000 m in the headwater region in China to 20 m in the delta near the outlet. Most areas are mainly mountainous with slopes mainly above 6%. The Thao and Da sub-basins are much steeper than the Lo sub-basin (Wei *et al.*, 2019a). The upper part of the Red River basin before Yen Bai (Figure 5-1) is formed by tectonically active mountains vulnerable to high erosion with intensive rainfall (Barton *et al.*, 2004; He *et al.*, 2007; Bai *et al.*, 2015; Wei *et al.*, 2019a). The main soil types in the upper part are red earth, yellow-brown soils and fluvisols also known as acrisols (Le, 2005; Bai *et al.*, 2015). The origin of the name of the Red River is due to the soil characteristics and the high erosion, which make the river muddy and red (Le, 2005).

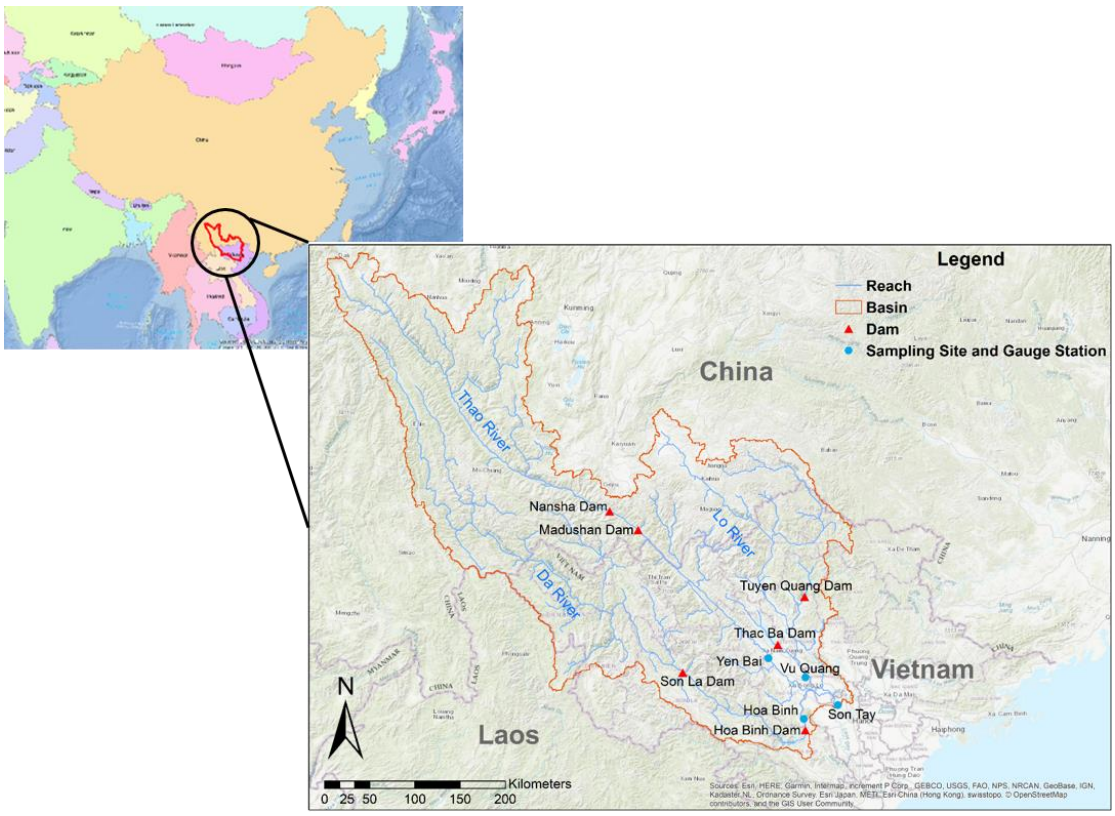

Figure 5-1 The Red River watershed (red outline), with its three main tributaries (the Thao River, the Da River and the Lo River), and sampling sites and gauge stations (blue points). Six large dams were built in this basin (red triangles).

2.1.2 Meteorological characteristics

The whole Red River basin is influenced by the monsoon system, from the subtropical humid monsoon in the upstream basin to tropical humid monsoon in the downstream part, and associated with strong seasonality. The mean annual rainfall was 1590 mm in the whole Red River basin, and over 85-90% of the whole year rainfall happens in the rainy season (May to October) (Le *et al.*, 2007; Li *et al.*, 2016a). The rainfall is also unevenly spatial distributed, and the general trend of regional precipitation distribution increases from upstream to downstream (Xie, 2002; Li *et al.*, 2008). Temperatures differ from the upper mountain region to the lower part through the basin, and the mean annual temperature ranges from 15 to 24 °C (Xie, 2002; Le, 2005).

2.1.3 Hydrological characteristics

The runoff shows high inter-seasonal variations as it is mainly fed by rainfall (Li *et al.*, 2008, 2016a; FAO, 2011b). The flood season occurs from June to November and produces more than 80% of the total annual runoff.

From the discharge data covering the 2003-2013 period and obtained from the Vietnam Ministry of Natural Resources and Environment (MONRE), the mean annual discharge at Son Tay during this period was 3052 m^3 s^{-1}; the lowest daily discharge

observed was 493 m^3 s^{-1} in February 2010, and the maximum daily flood reached 14,800 m^3 s^{-1} in August 2012. Annual water volume at Yen Bai, Vu Quang, Hoa Binh and Son Tay stations were 20.7, 28.2, 51.9 and 99.0 km^3 yr^{-1}, respectively.

2.1.4 Suspended sediment

The sediment fluxes were strongly affected by the constructions of dams in this basin (Le et al., 2007; Lu et al., 2015; Vinh et al., 2014; Wei et al., 2019, submitted). Inside this basin, there are six important dams with large capacity (Figure 5-1). Two dams are located on the Thao River, the Nansha and Madushan dams, which started operating in 2008 and 2011, respectively. The Thac Ba and Tuyen Quang dams on the Lo River were impounded in 1972 and 2008, respectively. Two largest dams, the Hoa Binh and Son La dams on the Da River, started to operate in 1989 and 2011, respectively. More details about these dams can be found in Wei et al. (2019). After new dams impoundment since 2008, the mean annual sediment flux during 2008-2013 was 17.2 Mt yr^{-1} at Yen Bai station (Thao River), 3.6 Mt yr^{-1} at Vu Quang station (Lo River), 1.3 Mt yr^{-1} at Hoa Binh station (Da River) and 13.2 Mt yr^{-1} while at Son Tay station at the Red River delta apex (Wei et al., submitted).

2.1.5 Land use and population

In the Chinese part of the basin, forest accounts for 62%, followed by grassland and cultivated land, accounting for 19% and 18% respectively (Li et al., 2016). In the Vietnamese part, land use varies from different sub-basins, however forest and agriculture account for the larger portion of the land use in the Red River basin: in the Thao basin, forest is the dominant land use, accounting for 54.2%, followed by cultivated land (31.5%); in the Lo and Da basins dominate cultivated land (58.1%) and forests (74.4%), respectively (Le *et al.*, 2007).

The total population of the basin was about 42 million in 2012 of which 11 million was in China and 31 million in Vietnam (Li et al., 2016). Gu et al. (2018) recently revised this number to 15.25 million inhabitants in China's part. The population density in the different sub-basins varies significantly with 101, 132 and 150 inhabitants km^{-2} in the Da, Lo and Thao sub-basins, respectively, and with the densest part around Son Tay (Le et al., 2007). The rural population accounts for 70 to 80% of the whole population (Le *et al.*, 2017a; Gu *et al.*, 2018).

2.2 Data sources

Daily discharge (Q) and suspended sediment concentration (SSC) data were obtained from the Vietnam Ministry of Natural Resources and Environment (MONRE) at Yen Bai, Vu Quang, Hoa Binh and Son Tay stations from 2003 to 2013 (see Figure 5-1). Yen Bai, Vu Quang and Hoa Binh stations are the outlets of the Thao, Lo and Da rivers, respectively.

Inputs such as topography (digital elevation model), land use, soil map, rainfall and temperature were used to simulate daily Q and SSC using the SWAT model (Neitsch

et al., 2009), as detailed in the previous work of Wei et al. (2019). Soil map is presented in Figure 5-2.

POC and DOC data were obtained from two sources. The first one was provided by the Laboratory of Environmental Chemistry, Institute of Natural Product Chemistry, Vietnam Academy of Science and Technology. Detail information about these sampling and laboratory measurements can be found in Le et al. (2017a). Samplings were taken generally one to three times per month from 2003-2004, 2008-2010, 2012-2013 at Yen Bai, Vu Quang, Hoa Binh and Son Tay. Due to the sampling difficulties, data are missing for some years or months. The second source was from Dang (2006) who provided POC and DOC concentrations at Yen Bai, Vu Quang, Hoa Binh and Son Tay during 2008-2009, with sampling frequency generally monthly or bimonthly.

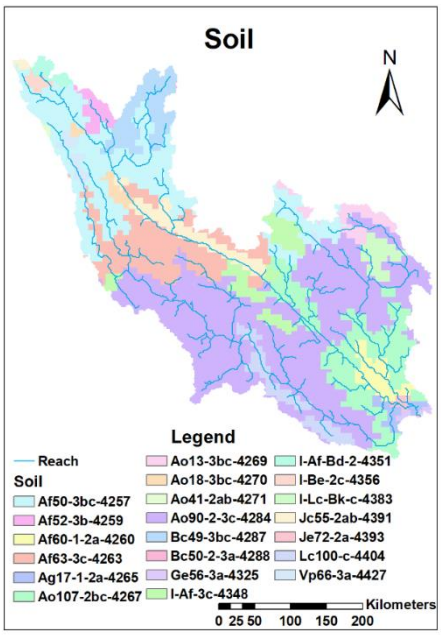

Figure 5-2 Soil map of the Red River basin (Wei et al., 2019a).

2.3 Organic carbon calculation

2.3.1 DOC equation

The equation for calculating the DOC concentration [DOC] from daily Q was taken from the work of Fabre et al. (2019):

$$[\mathrm{DOC}] = \frac{\alpha * \mathrm{Q}}{\beta + \mathrm{Q}} \quad (1)$$

where [DOC] is in mg L^{-1}, Q in mm d^{-1}; the parameter α (mg L^{-1}) represents a potential of maximum [DOC] at the outlet of each sub-basin, and the parameter β (mm d^{-1}) is the Q when [DOC] is half of α.

2.3.2 POC equation

The equation for calculating the POC concentration was proposed by Boithias et al. (2014) who generalized the relation between the POC and suspended sediment concentration (SSC) as followed:

$$\%POC = \frac{9.40}{\mathrm{SSC}-a} + b \text{ (if SSC > a)}$$

$$\%POC = \%POC_{max} \text{ (if SSC ≤ a)} \quad (2)$$

where %POC is the percentage of POC in the suspended sediment, $\%POC_{max}$ is the maximum value over the basin, SSC is in mg L^{-1}, and parameters *a* and *b* are linked to environmental variables related to each sub-basin (see details in Section 3.1.4). The parameter *a* (in mg L^{-1}) is the vertical asymptote corresponding to a low SSC with organic matter rich in OC, such as phytoplankton and residuals; this basin-specific constant includes an anthropogenic impact over the basin. The parameter *b* (in %) is the horizontal asymptote representing the SSC with low POC, nearly equals to soil organic carbon content, and it is also a basin-specific constant (Boithias *et al.*, 2014; Fabre *et al.*, 2019). When SSC is smaller than *a*, %POC is equal to as its maximum value, $\%POC_{max}$.

2.4 Modelling strategy

2.4.1 Parameters calibration for DOC and POC

The five parameters (α, β, *a*, *b*) in Equation 1 and 2 were manually calibrated based on the OC sampling data and the observed daily Q and SSC at each station. This allowed to determine values of specific parameters associated with each sub-basin, which are representative of the characteristics of each sub-basin. The values of each parameter were calibrated separately in order to obtain simulation as close as possible to the observed values. The maximum value of %POC was set by considering covering 99.9% of the dataset.

2.4.2 Scenarios settings

The SWAT is a physically-based model used to simulate the quality and quantity of Q, SSC and nutrients over river basin, and to predict the environmental impacts of human activities and climate variability (Neitsch et al., 2009). However, the SWAT model cannot compute the DOC and POC concentrations. Wei et al. (2019) applied the SWAT model on the Red River, obtaining simulated daily Q and SSC from 2000 to 2013 in good agreement with in-situ measurements (scenario of actual conditions, with dams). A reference scenario (without dams) was also implemented in their study to assess separately the impacts of climate variability and dams on Q and SSC, respectively. Actual conditions and reference scenario settings are presented in **Error! Reference source not found.**. More detailed information on simulated Q and SSC can be found in Wei et al. (2019).

The idea of this study is to apply the simulated daily Q and SSC of actual conditions and reference scenario from modelling to Equation 1 and 2 to calculate the simulated DOC and POC concentrations and fluxes under those two conditions (Figure 5-3).

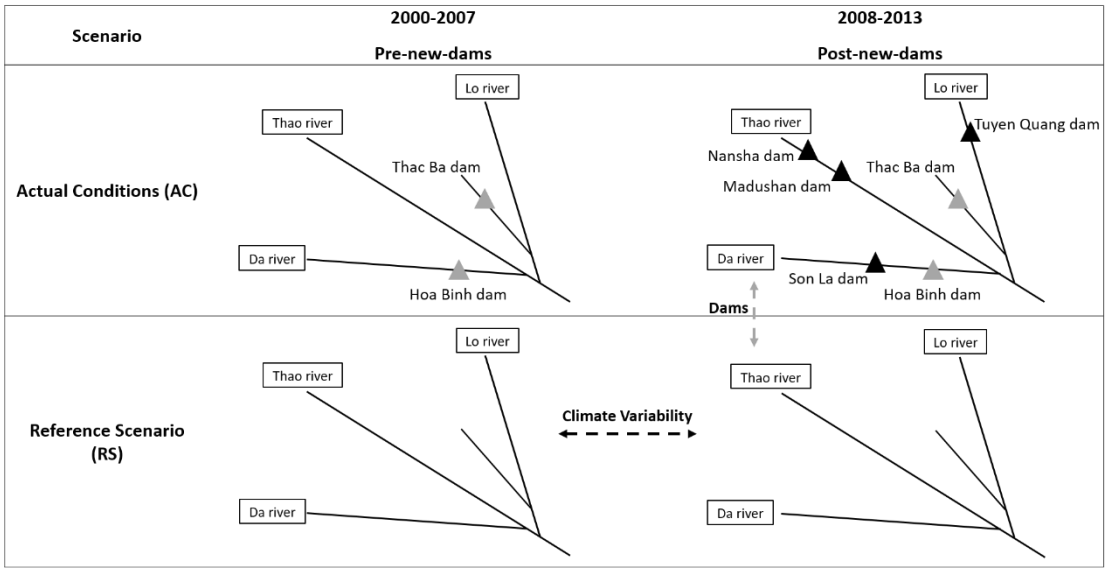

Figure 5-3 The setting for Actual Conditions and Reference Scenario: gray triangles are the old dams impounded before the study period and black triangles are the new dams impounded since 2008. By comparing actual conditions to reference scenario during 2008-2013, the impacts of these dams can be quantified; by comparing the period 2008-2013 to 2003-2007 under reference scenario, the impacts of climate variability can be quantified.

2.5 Model evaluation and validation for DOC and POC

Discrete sampling was first used to calculate OC fluxes from observed data through the Load Estimator (LOADEST) regression model, which was developed by U.S. Geological Survey for estimating constituent loads in rivers (Runkel *et al.*, 2004) and had been applied to many studies (McClelland *et al.*, 2007; Sickman *et al.*, 2007; Tamm *et al.*, 2008; Huntington and Aiken, 2013): LOADEST model is calibrated through regression analysis based on discrete sampling data of OC and observed daily Q, and the best regression model (Approximate Maximum Likelihood Estimator) is used with LOADEST to estimate daily DOC and POC fluxes respectively. The outputs of LOADEST were then used as a reference to validate our calculations. The mean annual DOC and POC fluxes from other studies in the same basin (Dang, 2006; Le *et al.*, 2017a) were also used as references for validations.

The coefficient of determination (R^2) and the Nash–Sutcliffe efficiency (NSE) were used as statistical tests to evaluate the quality of our calculation by comparing the results from LOADEST with ours (Nash and Sutcliffe, 1970; Moriasi *et al.*, 2007). R^2 values greater than 0.5 are considered acceptable; NSE values greater than 0 are generally regarded as acceptable levels of performance (Moriasi *et al.*, 2007).

3. Results

3.1 DOC and POC concentrations

3.1.1 DOC equation application

The parameters α and β in Equation 1 obtained for each station and the number of measured DOC values between 2003 and 2013 used to infer them are listed in Table 5-1. The values of parameter α vary from 4.5 to 5.5; parameter β varies from 0.7 to 2.5, geographically increasing from the upstream to the downstream.

Table 5-1 Values of the parameters α and β for dissolved organic carbon (DOC, Equation 1) and of the parameters a, b and $\%POC_{max}$ for particulate organic carbon (POC, Equation 2) at different stations, and number (N) of sampling data (DOC and POC) used to calibrate the parameters.

Variables	Parameter	Yen Bai	Vu Quang	Hoa Binh	Son Tay
DOC	N (DOC)	94	94	96	73
	α	4.5	5.0	5.5	5.0
	β	0.7	0.8	1.7	2.5
POC	N (POC)	63	58	54	49
	a	40.0	7.0	5.0	20.0
	b	1.0	1.5	1.7	1.5
	$\%POC_{max}$	10	15	40	15

3.1.2 DOC concentrations temporal variations

The daily variations of observed and simulated DOC concentrations at four stations from 2000 to 2013 are presented in Figure 5-4. The observed DOC concentrations were measured over some short periods and did not show clear seasonal variations. The simulated DOC concentrations are in the range of the observations (values of the range are presented in the following sub-section), with most sampling points captured by our calculations. Generally, simulated DOC concentration varies in accordance with Q variations, increasing from May to July, staying high during the highest floods in August and September, and decreasing from October to April.

Simulated mean annual DOC concentrations increase in the following order: Yen Bai (1.39 mg L^{-1}) < Vu Quang (1.50 mg L^{-1}) < Hoa Binh (1.60 mg L^{-1}) < Son Tay (1.81 mg L^{-1}).

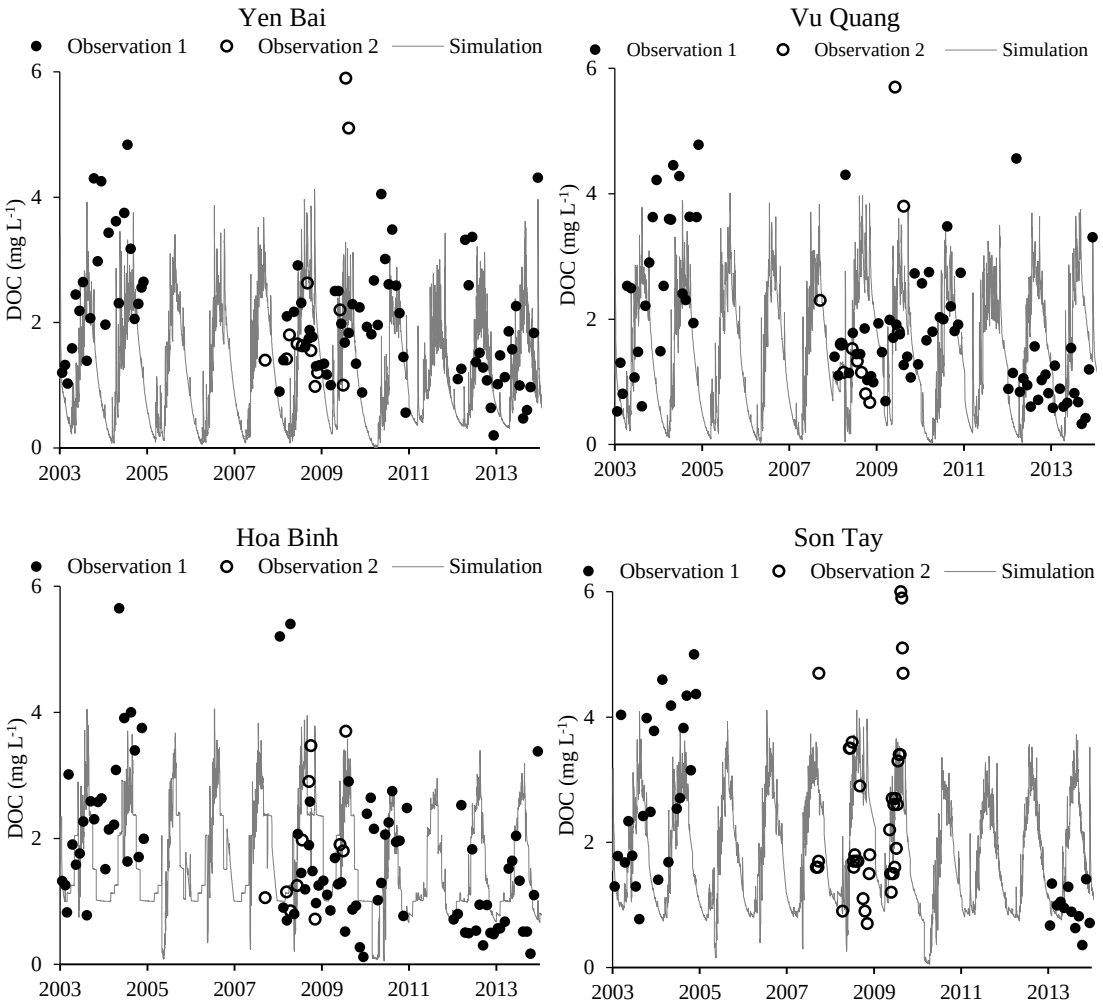

Figure 5-4 Daily variations of dissolved organic carbon (DOC) concentration (mg L^{-1}) at four stations from 2003 to 2013. Observation 1 (black dot) shows the DOC measured by Le et al. (2017a); observation 2 (white dot) shows the DOC measured by Dang (2006); calculations from Equation 1 based on the simulated discharge (Q, m^3 s^{-1}) from Wei et al. (2019) with the values of the parameters given in Table 2 are the gray solid line.

3.1.3 DOC concentrations ranges and spatial variations

Simulated DOC concentrations at four stations varied slightly (Figure 5-5a). At Yen Bai station, DOC concentration was from 0.01 to 4.13 mg L^{-1} with an average of 1.25 mg L^{-1} (observations from 0.20 to 5.90 mg L^{-1}); at Vu Quang, DOC was in the range of 0.03 to 4.01 mg L^{-1} with an average of 1.50 mg L^{-1} (observations from 0.33 to 5.70 mg L^{-1}); at Hoa Binh, DOC concentration varied from 0.05 to 4.05 mg L^{-1} with an average of 1.60 mg L^{-1} (observations from 0.12 to 5.65 mg L^{-1}); at Son Tay, DOC shifted from 0.05 to 4.11 mg L^{-1} with an average of 1.81 mg L^{-1} (observations from 0.36 to 6.00 mg L^{-1}).

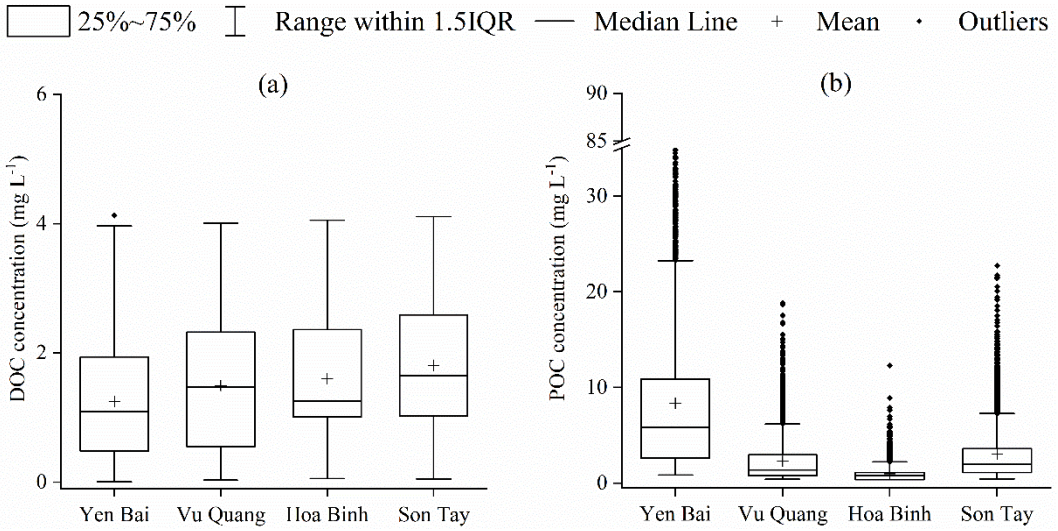

Figure 5-5 Box plot of daily simulated dissolved organic carbon (DOC) and daily particulate organic carbon (POC) concentration (mg L^{-1}) at four stations during 2003-2013 in the Red River basin. IQR represents the interquartile range.

3.1.4 POC equation application

Figure 5-6 shows the percentage of POC in suspended sediment (%POC) against the suspended sediment concentration (SSC) computed from available measurements in the period 2003-2013. %POC shows a significant and negative relationship with SSC, following well Equation 2.

We obtained different values of parameters *a*, *b*, and $\%POC_{max}$ for the four stations (Table 5-1). The values of parameter *a* vary largely, with a maximum value of 40.0 mg L^{-1} at Yen Bai and a minimum of 5.0 mg L^{-1} at Hoa Binh. Parameter *b* varies from 1.0 to 1.7%, with a maximum at Hoa Binh and a minimum at Yen Bai. The maximum value of %POC was set by considering covering 99.9% of the dataset. $\%POC_{max}$ varies strongly with a minimum of 10 mg L^{-1} at Yen Bai and a maximum of 40 mg L^{-1} at Hoa Binh.

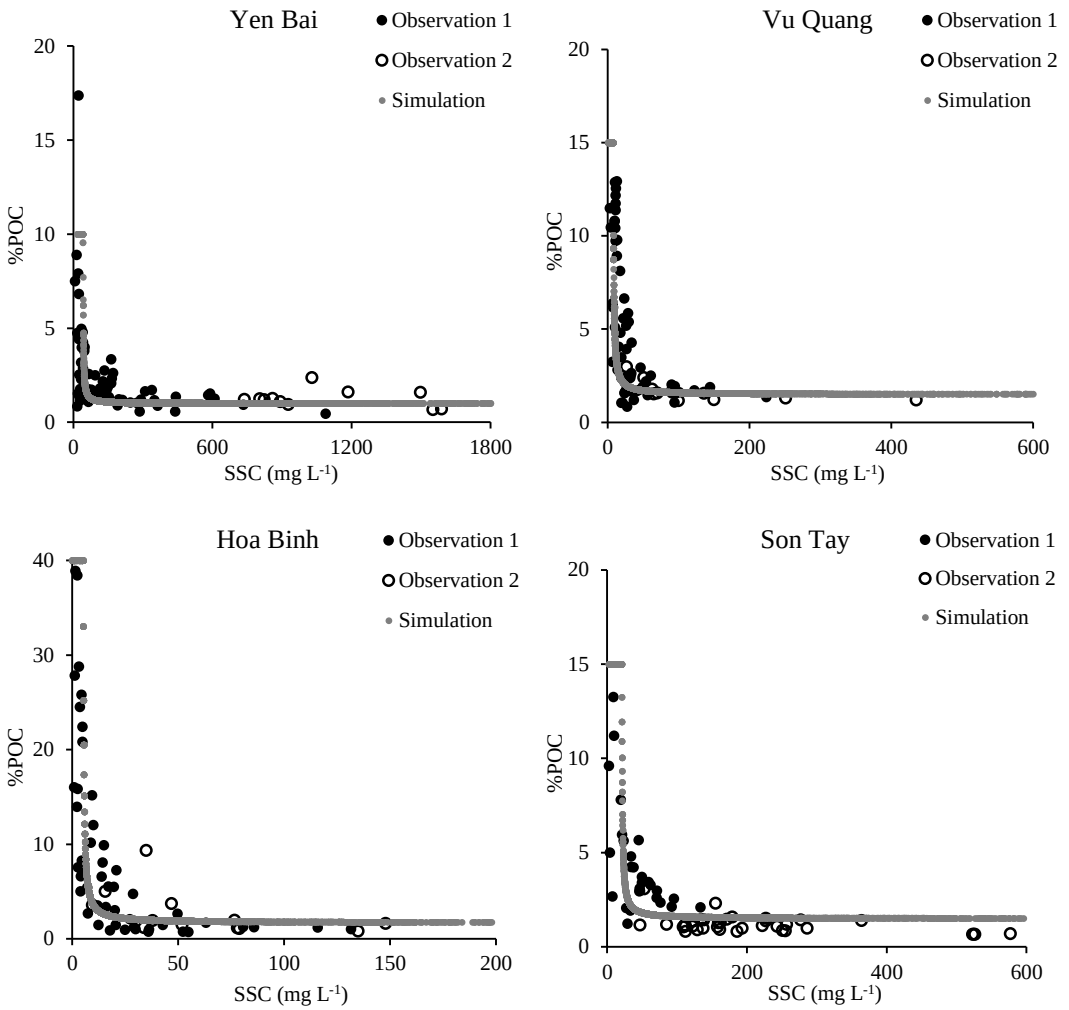

Figure 5-6 Relationship between the percentage of POC concentration (%POC) in the suspended sediment concentration (SSC, mg L^{-1}) and observed SSC (mg L^{-1}). Observation 1 (black dot) corresponds to the measurements from Le et al. (2017a); observation 2 (white dot) corresponds to the measurements from Dang (2006); gray solid dots were the calculations from Equation 2 based on the observed SSC data collected from the Vietnam Ministry of Natural Resources and Environment (MONRE). $\%POC_{max}$, the maximum limit of %POC, was set as 10%, 15%, 40% and 15% for Yen Bai, Vu Quang, Hoa Binh and Son Tay, respectively.

3.1.5 POC concentrations temporal variations

Figure 5-7 illustrates the daily variations of simulated and observed POC concentrations at four stations from 2003 to 2013. POC concentrations showed great seasonal and inter-annual variations. POC peak flows occurred from May to October. Seasonal variations strongly weakened during more recent years (2008-2013), and the POC peak flows decreased. For Yen Bai, Vu Quang, Hoa Binh and Son Tay stations, the standard deviation is 10.11, 2.75, 0.84, 3.55 mg L^{-1} respectively over 2003-2007, and 3.76, 0.83, 0.53, 0.96 mg L^{-1} respectively over 2008-2013; and the maximum POC concentration is 82.77, 18.86, 7.91, 22.72 mg L^{-1} respectively during 2003-2007, 30.12, 9.50, 12.31, 6.52 mg L^{-1} respectively during 2008-2013.

Calculations are in the same range as discrete samplings (values of the range are presented in the following sub-section) and produced acceptable results. Comparing the simulated POC concentrations to the observations, simulated POC peaks can be underestimated for some years. Simulated POC base values are generally in good agreement with in-situ observations.

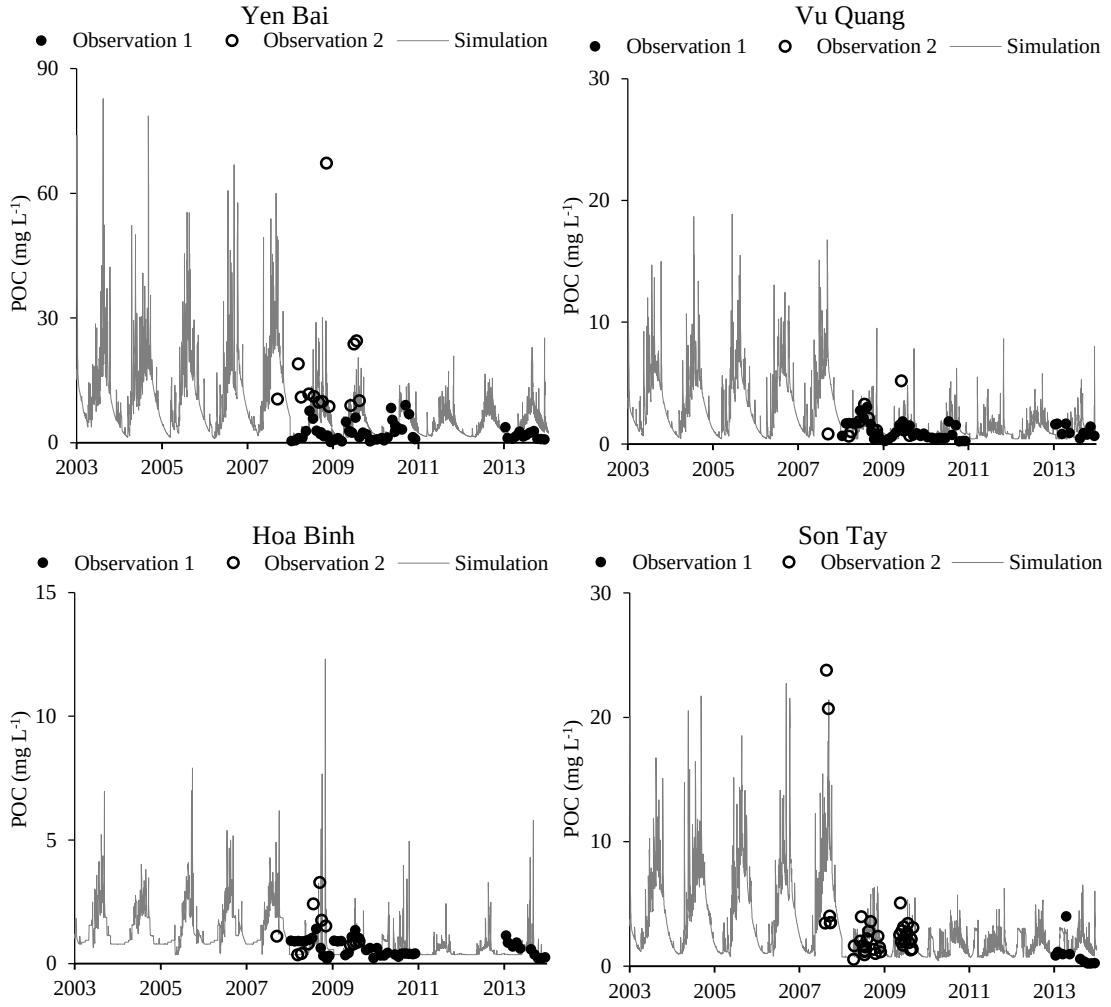

Figure 5-7 Daily variation of particulate organic carbon (POC) concentration (mg L^{-1}) at four stations from 2003 to 2013. Observation 1 (black dot) was observed POC from Le et al. (2017a); observation 2 (white dot) was the observed POC from Dang (2006); simulation (gray solid line) was simulated from Equation 2 based on the simulated suspended sediment concentration (SSC, mg L^{-1}) from Wei et al. (2019).

3.1.6 POC concentration ranges and spatial variations

Figure 5-5b presents the POC concentrations ranges at the four stations. From the calculations, POC concentrations vary from 0.85 to 82.77 mg L^{-1} with an average of 8.35 mg L^{-1} at Yen Bai (observations from 0.14 to 67.20 mg L^{-1}), from 0.40 to 18.86 mg L^{-1} with an average of 2.30 mg L^{-1} at Vu Quang (observations from 0.20 to 5.17 mg L^{-1}), from 0.36 to 12.31 mg L^{-1} with an average of 0.96 mg L^{-1} at Hoa Binh (observations from 0.18 to 3.27 mg L^{-1}) and from 0.43 to 22.72 mg L^{-1} with an average of 3.03 mg L^{-1} at Son Tay (observations from 0.20 to 23.78 mg L^{-1}). Our calculations have larger

ranges compared to observations because our calculations period covers the years before when the POC concentrations were high. The POC low concentrations at these four stations do not differ much, but significant differences occur at POC peak fluxes.

3.2 Fluxes of DOC and POC

3.2.1 DOC flux variations

Daily variations of DOC fluxes at four stations are presented in Figure 5-8a. Simulated DOC fluxes fit well with the observations during low flow periods. Daily calculations represent realistically the DOC flux fluctuations during flood seasons.

As described in Section 2.5, the results from the LOADEST model are used as references to validate our calculations, and Figure 5-8b shows the DOC fluxes from LOADEST and our calculations at a monthly scale. Compared to the results from LOADEST, the simulated base DOC flux is lower and the peak DOC flux was higher for some years; the R^2 at these four stations varied from 0.65 to 0.74 and the NSE is in the range of 0.02-0.56, which indicates that our calculations of DOC fluxes at monthly scale are acceptable.

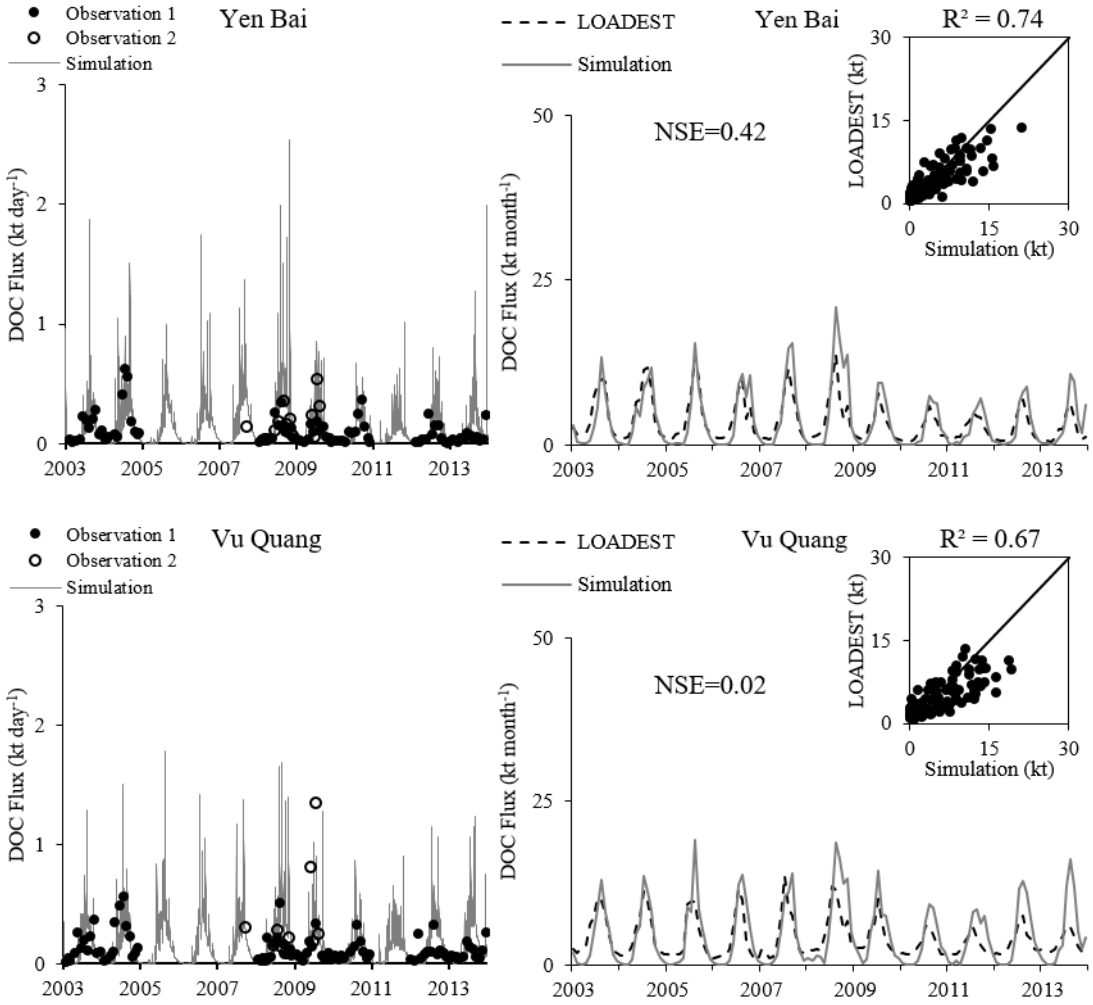

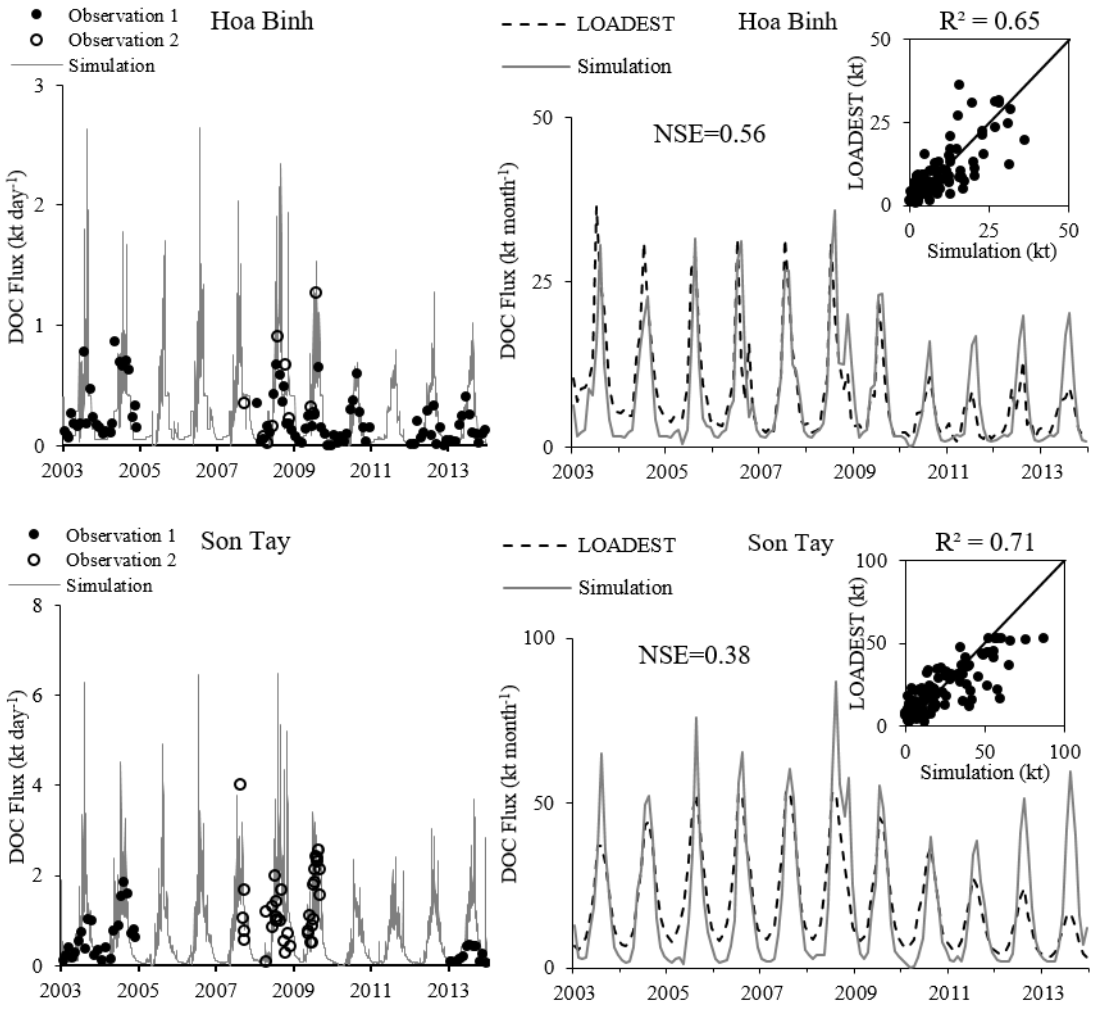

Figure 5-8 (a)Mean daily variation of dissolved organic carbon (DOC) fluxes (kt day^{-1}) at four stations from 2003 to 2013. Observation 1 (black dot) was calculated from the measured DOC concentration from Le et al. (2017a); observation 2 (white dot) was calculated from the measured DOC concentration from Dang (2006); the gray solid line was the simulated DOC fluxes (kt day^{-1}) calculated based on the DOC concentrations from Equation 1 and the Q from SWAT model. (b) Mean monthly DOC fluxes (kt month^{-1}) comparison between results from LOADEST and our calculations.

Annual DOC fluxes variations are presented in Figure 5-9. The mean annual DOC flux during the study period at Yen Bai, Vu Quang, Hoa Binh and Son Tay stations are 44, 53, 88 and 222 kt yr^{-1}, respectively. Spatially, annual DOC flux increased in the following order: Yen Bai < Vu Quang < Hoa Binh < Son Tay. The maximum annual DOC flux occurs in 2008 which is the maximum flood year during the study period and minimum annual DOC flux occurred in 2010 which is the maximum dry year during the study period.

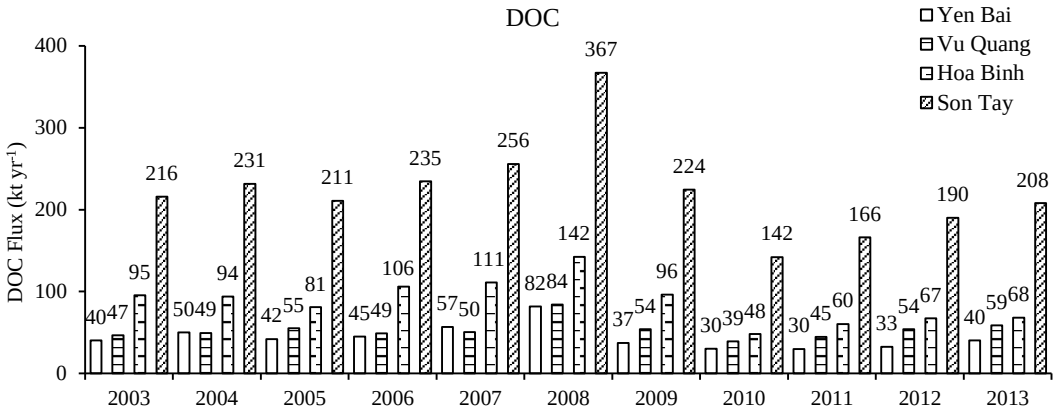

Figure 5-9 Simulated annual dissolved organic carbon (DOC) fluxes (kt yr^{-1}) at four stations from 2003 to 2013.

3.2.2 POC flux variations

Figure 5-10a illustrates the daily variations of POC fluxes at four stations. Like for daily DOC fluxes, simulated POC fluxes are in the range of the observations.

The observed data were sampled after 2007, and some dams (the Nansha, Madushan, Tuyen Quang and Son La dams) were under constructions during the 2003-2007 period and operating since 2008. The POC conditions before and after 2008 were hence different because of the impacts of dam constructions on suspended sediment. The POC sampling concentrations before are few. Here we thus only compared the POC fluxes from LOADEST and from our simulation over the 2008-2013 period, and our calculation results during 2003-2007 were plotted to provide an insight of POC fluxes during this period (Figure 5-10b). Generally, the results from LOADEST and our simulation fit well on both POC peak and base fluxes: R^2 is in the range of 0.50-0.59 while the NSE varies from 0.34 to 0.56, indicating an acceptable performance.

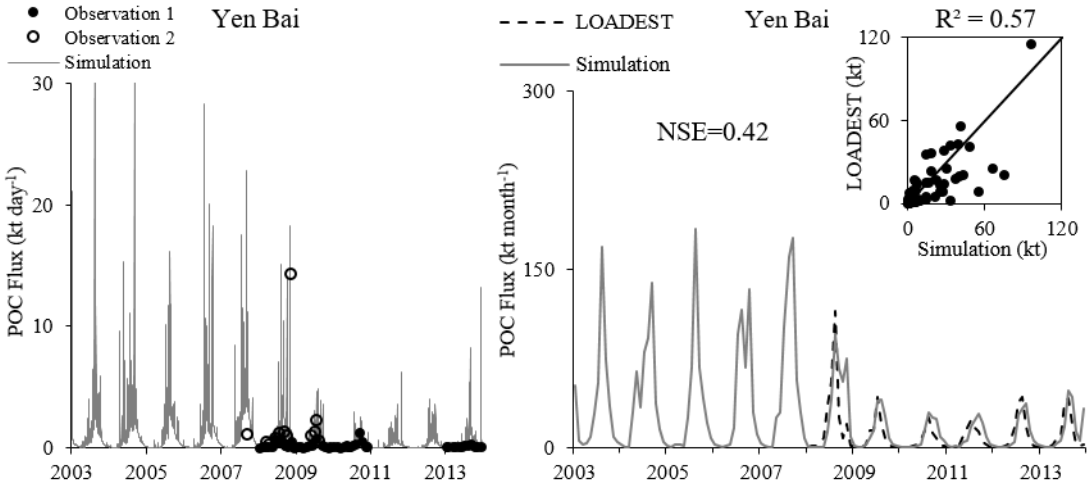

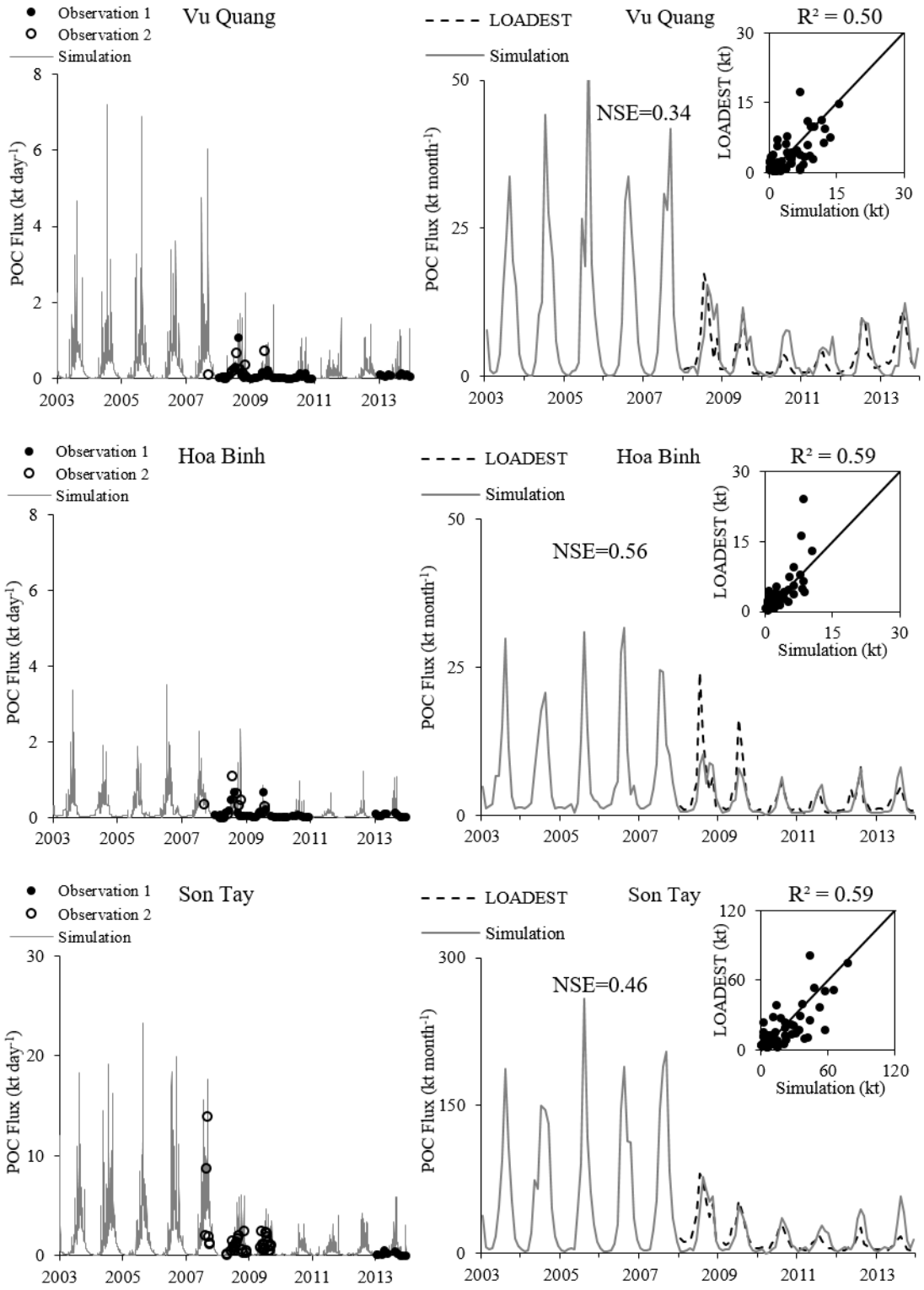

(a) **(b)**

Figure 5-10 (a) Mean daily variation of particulate organic carbon (POC) flux (kt day^{-1}) at four stations from 2003 to 2013. Observation 1 (black dot) was calculated from the measured POC concentration from Le et al. (2017a); observation 2 (white dot) was calculated from the measured POC concentration from Dang (2006); the gray solid line was the simulated POC flux (kt day^{-1}) based on the POC concentrations from Equation 2 and the Q from SWAT model. (b) Mean monthly POC flux (kt month^{-1}) comparison between results from LOADEST and our calculations during 2008-2013.

Figure 5-11 shows the calculated annual POC flux variations for the four stations between 2003-2013. The mean annual POC fluxes of Yen Bai, Vu Quang, Hoa Binh and Son Tay stations are 318, 83, 55 and 406 kt yr^{-1}, respectively. Among the three tributaries, the Thao River exported the highest POC loads, followed by the Lo River. The contrary to what obtained for the DOC export, the Da River exported the smallest POC flux. The POC flux was the highest at the confluence (Son Tay station). The maximum annual POC flux generally occurred in 2007 while the minimum annual POC flux occurred in 2011.

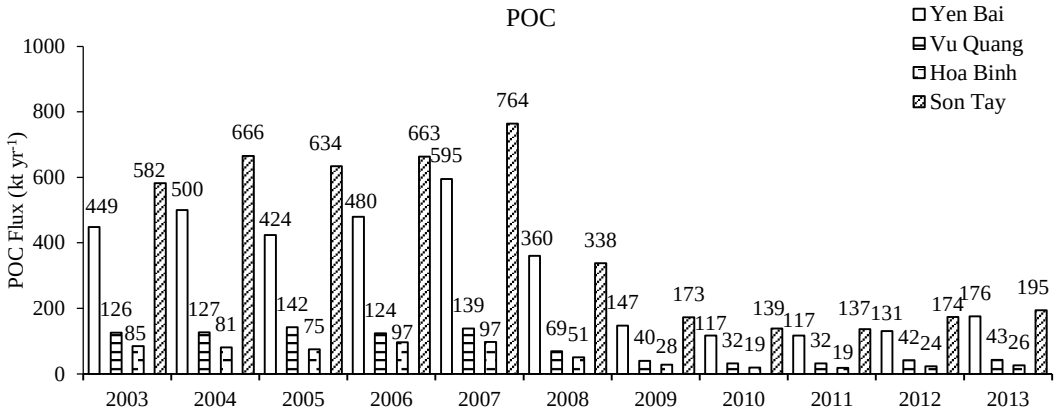

Figure 5-11 Simulated annual particulate organic carbon (POC) fluxes (kt yr^{-1}) at four stations from 2003 to 2013.

3.2.3 TOC flux variations

Annual TOC fluxes showed great inter-annual variations (Figure 5-12). The mean annual TOC flux for the whole study period were 350, 136, 143 and 628 kt yr^{-1} at Yen Bai, Vu Quang, Hoa Binh and Son Tay stations, respectively. Comparing the TOC export among the three tributaries, TOC fluxes exported by the Lo and Da rivers were of the same order, and the Thao River exported around 2.5 times higher TOC than the Lo and Da rivers. The highest TOC fluxes were generated in 2007 and the lowest in 2010.

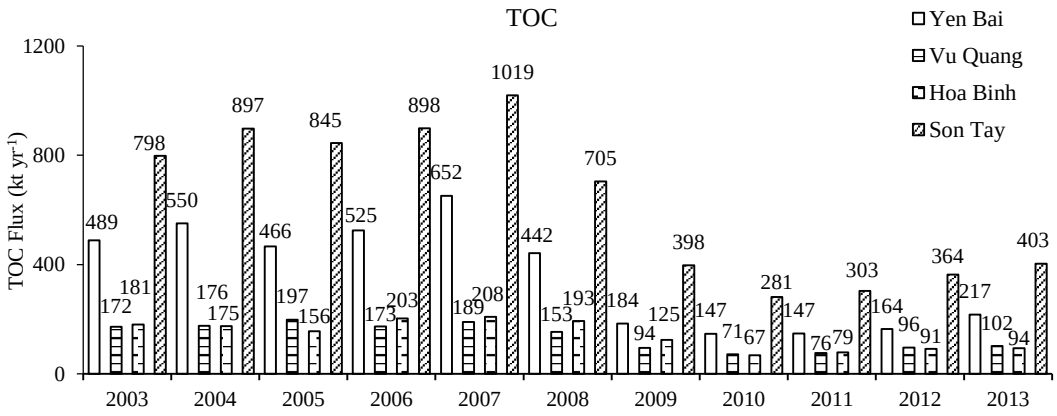

Figure 5-12 Simulated annual total organic carbon flux (kt yr^{-1}) at four stations from 2003 to 2013.

3.3 TOC fluxes variations under natural condition

Figure 5-13(a) presents simulated monthly TOC fluxes variations under natural and actual conditions at Son Tay station. The differences between under natural and actual conditions for monthly DOC fluxes are small (p=0.5) while for monthly POC fluxes are significant (p<0.001). The differences in the dynamic processes between natural and actual conditions occur during the flood seasons, and are much larger for POC than DOC: the average monthly fluxes during June and August under natural and actual conditions for DOC are 42.0 and 40.3 kt month^{-1}, respectively, and for POC are 271.5 and 72.4 kt month^{-1}, respectively.

The annual fluxes of POC under natural and actual conditions also differ a lot compared to the DOC fluxes (Figure 5-13b). When comparing the period after new dams (2008-2013) to the previous period (2003-2007), the annual DOC flux under actual conditions got reduced by 12%: 1% increased due to Q change induced by climate variability and 13% decreased due to dam constructions; the annual POC flux decreased by 87%, of which 2% was due to Q variation caused by climate variability and 85% due to dam constructions.

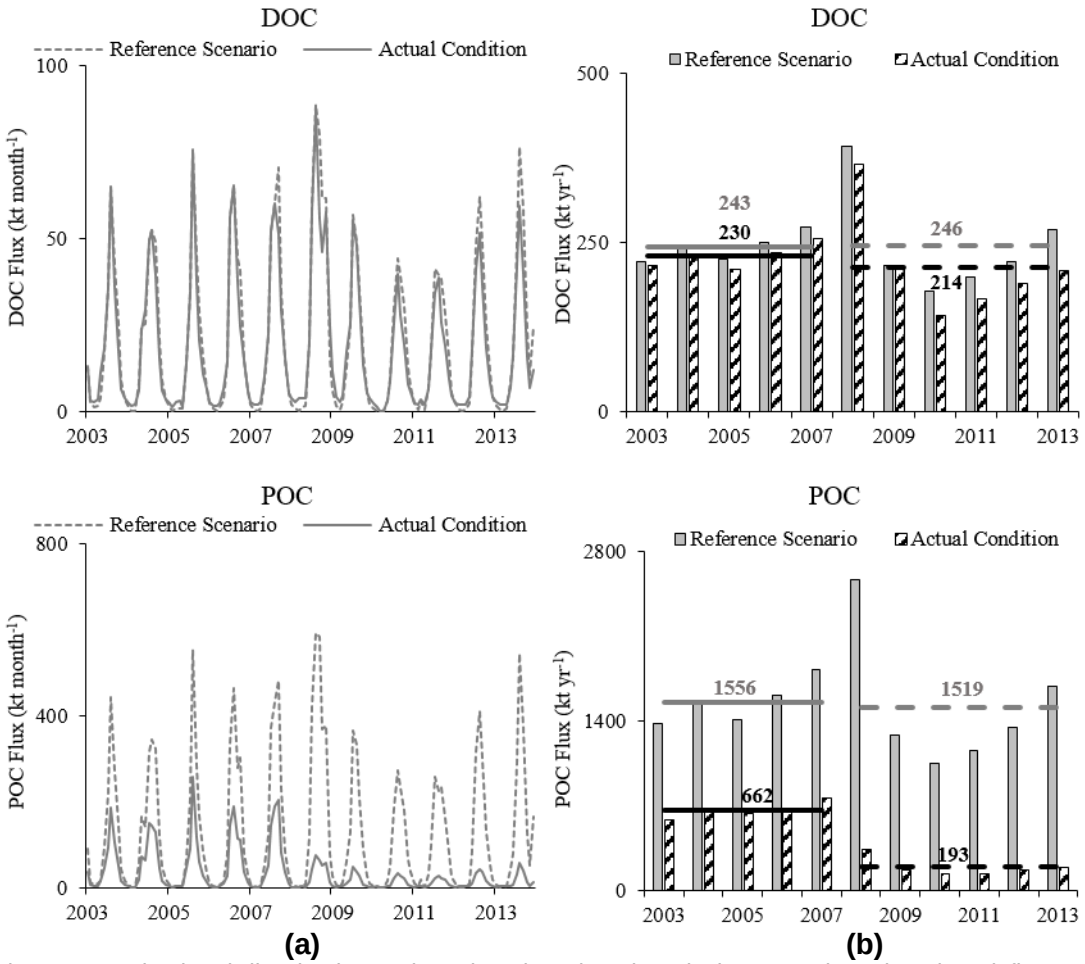

Figure 5-13 Simulated dissolved organic carbon (DOC) and particulate organic carbon (POC) fluxes at Son Tay station under reference scenario and actual conditions: (a) Monthly variations; (b) Annual budgets. The black solid arrow displays the total decrease caused by climate variability and dams between 2003-2007 and 2008-2013; the gray dash arrow displays the decrease related to climate variability and the black dash arrow displays the decreased caused by dams.

The variations of POC resulted in the variations of POC percentage in TOC (POC/TOC) at Son Tay station (Figure 5-14).

The POC/TOC ratio under natural conditions is higher (from 81 to 89% with an averaged value of 85%, standard deviation=1.7%) than that under actual conditions (from 33 to 90% with an averaged value of 58%, standard deviation=13.6%); moreover the POC/TOC ratio under natural conditions show a weaker seasonal variability than under actual conditions (Figure 5-14a).

The ratio POC/TOC under actual condition decreased after 2007 and its seasonal variability also changed afterwards (Figure 5-14a). During 2003-2007, the maximum POC/TOC generally occurred in September and October whereas the minimum POC/TOC showed up during February and March. During 2008-2013, the maximum POC/TOC showed up generally in February and March and the minimum in December, January or June.

There is a clear negative shift of POC/TOC ratio in 2008 under actual conditions (Figure 5-14). The mean annual POC/TOC ratio under natural conditions stayed the same (86%) during 2003-2007 and 2008-2013, while under actual conditions it decreased from 74% during 2003-2007 to 47% during 2008-2013.

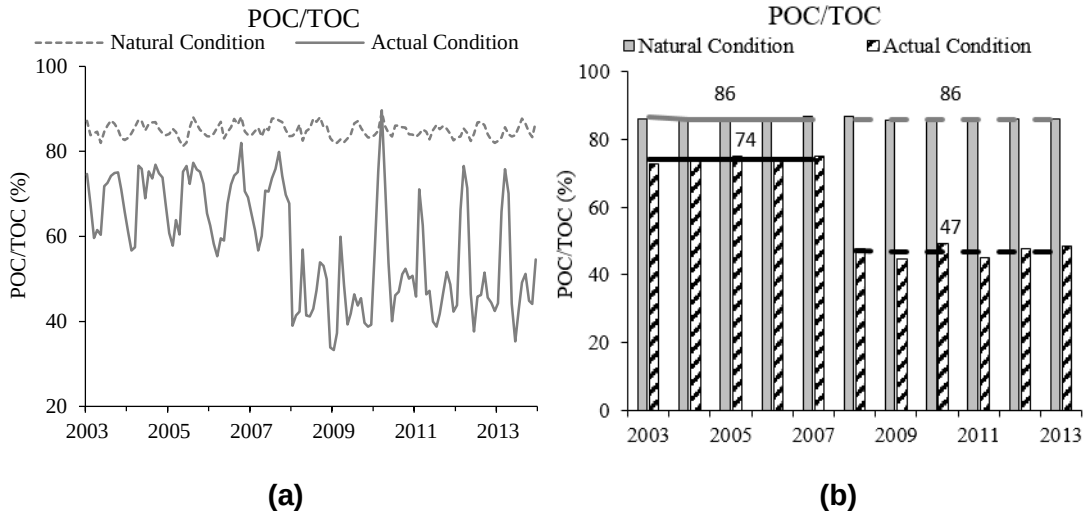

Figure 5-14 Simulated particulate organic carbon (POC) percentage in total organic carbon (TOC) during 2003-2013 under natural and actual conditions: (a) mean monthly variations; (b) mean annual values.

4. Discussion

4.1 Parameter analysis

4.1.1 Parameters of DOC

The parameter α is the potential maximum riverine DOC concentration at each station, and it can be related to its sources. Previous studies indicated that DOC increased with increasing soil carbon content (Manninen *et al.*, 2018), and the soil organic matter through soil erosion and leaching were the main source for fluvial DOC (Dang, 2006;

Lloret *et al.*, 2016; Le *et al.*, 2017a). Figure 5-15 presents the soil organic carbon content and soil erosion through the Red River basin. The average soil organic carbon contents (% soil weight) of the drainage area of Yen Bai, Vu Quang, Hoa Binh and Son Tay are 1.60%, 1.79%, 1.92% and 1.77%, respectively. Figure 5-15 shows that the relationship between the parameter α and the average soil organic carbon content of the drainage area of each station is significant, showing a positive correlation. The increasing order of mean annual DOC concentration during 2003-2013 at the outlet of each river is consistent with the increasing order of the average soil organic carbon content: Yen Bai < Son Tay< Vu Quang < Hoa Binh.

The parameter β corresponds to the discharge Q when the DOC concentration is half of α, so it is linked to α. In addition, β increases in the following order: Yen Bai < Vu Quang < Hoa Binh < Son Tay (Table 5-1), and the annual mean Q for these four stations (Yen Bai: 608 m^3 s^{-1}, Vu Quang: 848 m^3 s^{-1}, Hoa Binh: 1529 m^3 s^{-1}, Son Tay: 3052 m^3 s^{-1}) increase in the same order. We assume that within the same basin the parameter β can be positively correlated with Q, however, this needs to be further studied and confirmed from other basins worldwide.

Equation 1 was also applied at the outlet of the Yenisei River basin, located in the Arctic region with a watershed surface of 2,540,000 km^2, and the parameter α and β were 15.0 and 1.29, respectively (Fabre *et al.*, 2019). The α at the outlet of the Yenisei River basin is higher than at the outlet of the Red River basin due to the high soil OC of the permafrost in the Yenisei basin. This is in agreement with the relationship we found between parameter α and soil organic carbon content (% soil weight).

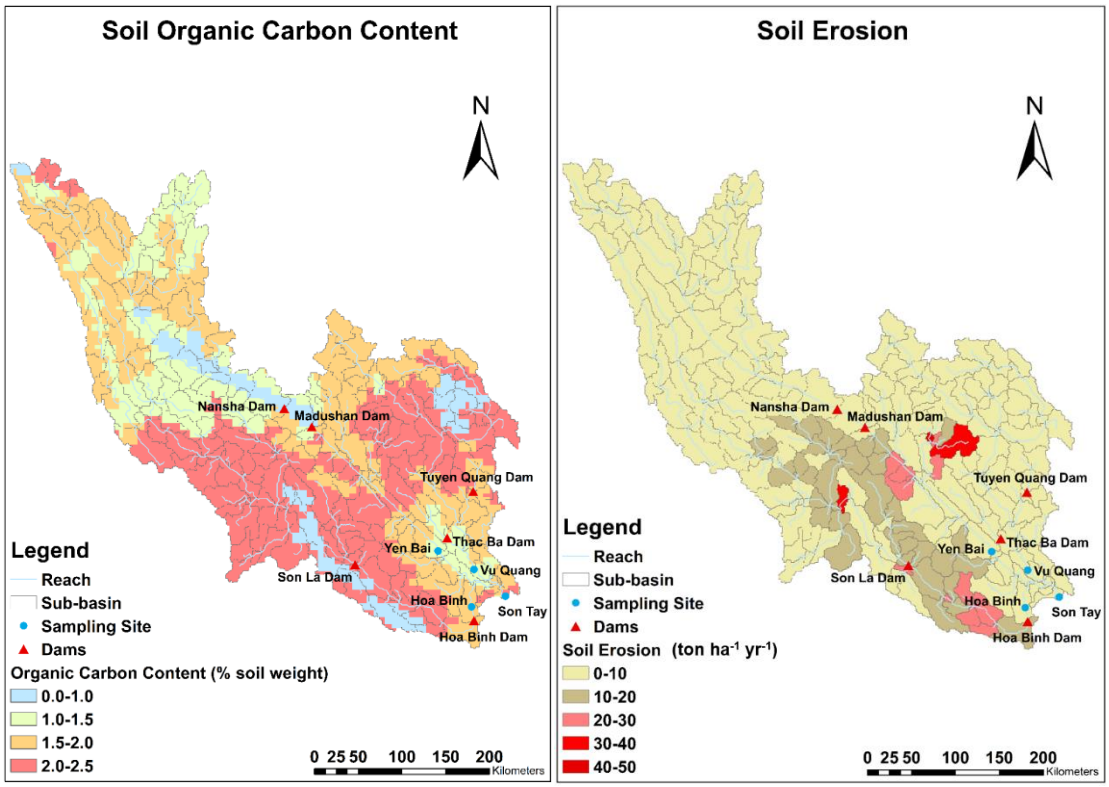

(a) **(b)**

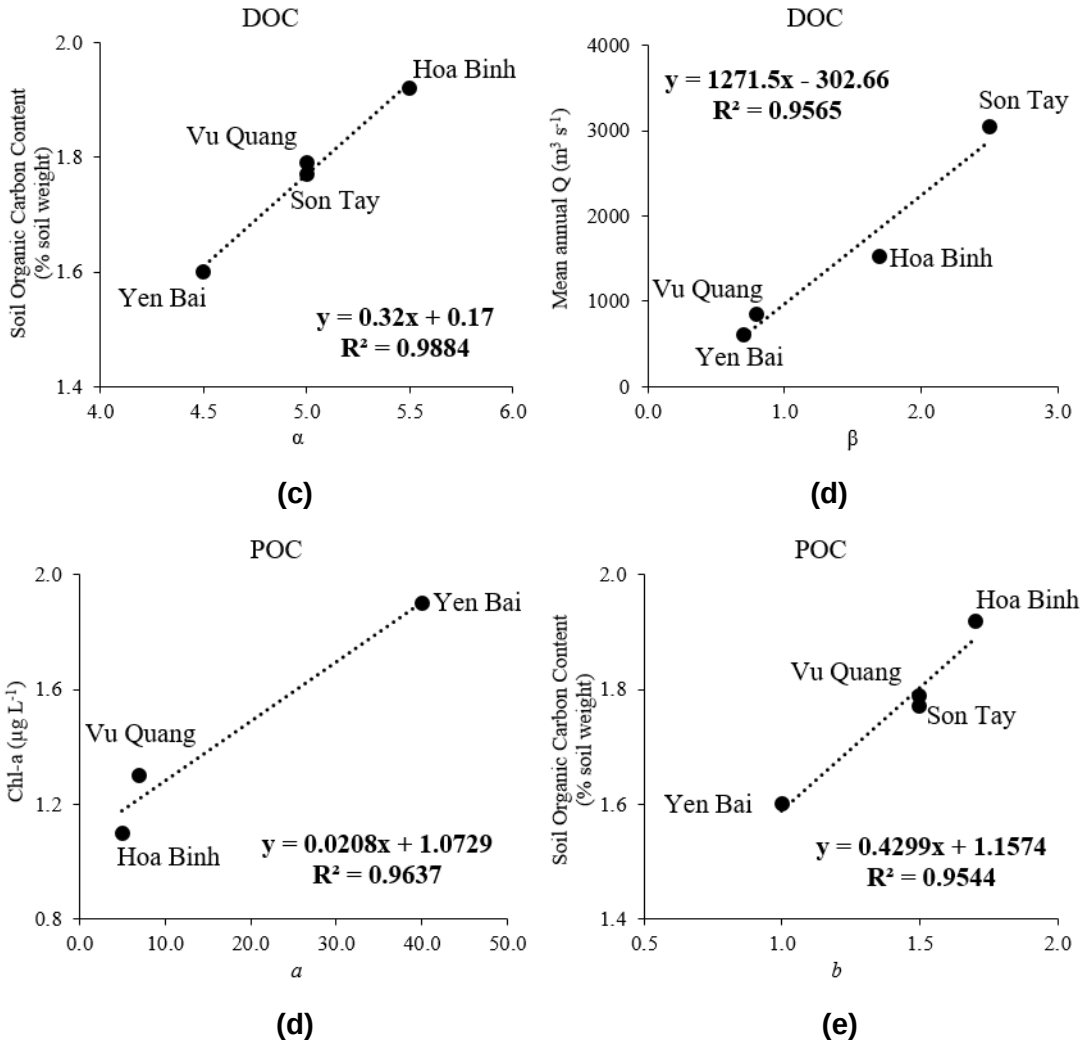

Figure 5-15 (a) Soil organic carbon content (% soil weight) within each sub-basin; (b) annual soil erosion of the Red River basin (ton ha^{-1} yr^{-1}) (Wei et al., 2019a); (c) relation between the parameter α in DOC equation (Equation 1) and the average soil organic carbon content of the drainage area of each station; (d) relation between the parameter β in DOC equation (Equation 1) and the mean annual discharge (Q) of each station; (e) relation between the parameter a in POC equation (Equation 2) and Chl-a (µg L^{-1}) (Le et al., 2017a); (f) relation between the parameter b in POC equation (Equation 2) and the average soil organic carbon content of the drainage area of each station.

4.1.2 Parameters of POC

The maximum of %POC decreases in the following order (Table 5-1): Hoa Binh (40) >= Son Tay and Vu Quang (15) > Yen Bai (10). The SSC at Hoa Binh station was the lowest (annual mean during 2003-2013 is 34 mg L^{-1}) compared to other stations (annual mean SSC for Yen Bai, Vu Quang and Son Tay is 631, 99 and 137 mg L^{-1}, respectively) due to the retention by the dams, especially by the Hoa Binh dam (Dang *et al.*, 2010; Wei *et al.*, 2019a). Besides, algae and phytoplankton in the reservoir can contribute to high particulate organic carbon. Therefore, these two factors induce a high maximum %POC at Hoa Binh station. On the contrary, at Yen Bai station, the SSC is the highest with low autochthonous organic production compared to other

stations (Dang, 2006; Dang *et al.*, 2010; Nguyen *et al.*, 2018), therefore, the maximum %POC is small.

The parameter a is a basin-specific constant which includes anthropogenic impacts and corresponds to low SSC values and organic matter that is rich in OC, such as phytoplankton and residuals. Comparing the minimum SSC values of the three tributaries, the Thao River presents the highest one (15.2 mg L^{-1}) while at Hoa Binh station on the Da River the lowest one (0.6 mg L^{-1}) is observed, which explains the corresponding values of a - high at Yen Bai (40, Table 5-1) and low at Hoa Binh (5). Besides, thanks to the constructions of the Nansha and Madushan dams, local villagers have entered into extensive fish farming (Rousseau, 2014). The fish feed and fish feces are rich in organic matters (Beristain, 2005). Moreover, near the Nansha dam, there is a sugarcane processing plant that often releases chemicals and wastes into the Red River (Rousseau, 2014). These factors make the water quality downstream of the Madushan dam very bad (Rousseau, 2014), which contributes to explain the high parameter a value at Yen Bai. In addition, the concentrations of Chl-a of these three tributaries from large to small was in the following order: Yen Bai (1.9 µg L^{-1}) > Vu Quang (1.3 µg L^{-1}) > Hoa Binh (1.1 µg L^{-1}) (no data for Son Tay in Le et al., 2017a), which is in the same order as the values of parameter a (Figure 5-15d). Therefore, the parameter a accurately expresses the characteristics of each tributary in this study.

As described in Section 2.3.2, the parameter *b* is the horizontal asymptote representing the suspended matters with low OC concentration which is near soil content. From Figure 5-15e we can see that the parameter *b* shows a positive and significant correlation with the average soil organic carbon content of the drainage area of each station. Hence, the values of the parameter *b* well represent the actual characteristics of each sub-basin.

The parameters *a* and *b* were set to 5 mg L^{-1} and 2.1%, respectively, in an agricultural basin in south-east France (Boithias *et al.*, 2014); and to 0.95 mg L^{-1} and 3.9%, respectively in an Arctic basin (Fabre *et al.*, 2019). The minimum SSC observed in the study river of Boithias et al. (2014) is 5 mg L^{-1} while it is around 1 mg L^{-1} of Fabre et al. (2019) hence, they set the parameter *a* to 5 mg L^{-1} and 0.95 mg L^{-1}. In our study, the parameter *a* is higher than the minimum SSC observed at each station, which indicates the contributions from phytoplankton and residuals in the Red River that were not observed in the study rivers of Boithias et al. (2014) and Fabre et al. (2019). In the study area of Boithias et al. (2014), the top soil organic matter content is about 2%, which is higher than our basin (1.6-1.9%). In the study case of Fabre et al. (2019), the permafrost stores abundant soil OC, thus, the parameter *b* is high in that basin. Therefore, the parameter *b* from their studies are higher than from ours (from 1.0% to 1.7%). From the above, the parameters *a* and *b* obtained from Boithias et al. (2014), Fabre et al. (2019) and this study seem to represent well the specific characteristics of each basin worldwide.

4.1.3 Application: a new method to evaluate the DOC and POC concentrations

Our results also enable us to propose a new method to evaluate the DOC and POC concentrations at any point within the Red River basin. If one knows the values of average soil organic carbon content of the drainage area, mean annual discharge and the Chl-a concentration in the river, using the relationships in Figure 5-15 indeed allows to determine α, β, a and b; Equation 1 and 2 can then be used to evaluate the DOC and POC concentrations.

4.2 Comparison of the OC contents

4.2.1 Comparison with other studies for the Red River

We first compared our simulations with results from other studies based on sampling in the Red River basin (Table 5-2). To make things comparable, we perform our comparison over the common 2008-2009 period.

For the mean annual DOC concentration, our simulated results are slightly lower (averagely -17%) compared to the other two studies (Dang, 2006; Le *et al.*, 2017a). In both studies, discrete samplings were just taken once or twice per month and at dry seasons the frequency was even lower, while our results were calculated based on a daily time step simulation. Those different temporal scales can induce differences in the estimations of mean annual DOC concentration. The mean annual DOC flux of 2008-2009 at Vu Quang and Hoa Binh stations estimated by Dang (2006) is around 60% higher than that from Le et al. (2017a). Note that results from the LOADEST are close to the ones of Le et al. (2017a) (Table 5-2) as a large proportion of sampling data used by the LOADEST comes from their dataset. Comparing our results to the LOADEST, the DOC fluxes are 17-28% higher at the three tributaries, and 3% higher at the outlet Son Tay station. Hope et al. (1994) indicated that low-frequency sampling led to an underestimation of the riverine C flux due to the under-representation of storm flow conditions. Finally, our study produces an estimation of 222 kt yr^{-1} of DOC flux at Son Tay (Table 5-2) over 2003-2013, which accounts for 0.26% of the total DOC export by Asian rivers to the seas, estimated to 85.45 Mt yr^{-1} by Li et al. (2019).

Significant differences in mean annual POC concentration during 2008-2009 can be found between Dang (2006) and Le et al. (2017a): POC concentrations from Le et al. (2017a) is only averagely 31% of that from Dang (2006); our results are between theirs (Table 5-2). POC concentration is strongly linked to SSC which can vary greatly from sampling location and time. The POC fluxes estimated by Le et al. (2017a) are averagely 59% of the values estimated by Dang (2006), especially at Yen Bai station where the SSC is very high. Comparing our results to the LOADEST, our estimations are 10-31% lower on the three tributaries and 34% lower at Son Tay. Since POC fluxes transported by the Asian rivers are 76.90 Mt yr^{-1} (Li *et al.*, 2017), the export of POC at Son Tay (406 kt yr^{-1} over 2003-2013 in our study) accounts for 0.37% of the total POC export by the Asian rivers.

The estimated TOC flux during 2003-2013 at Son Tay is equal to 628 kt yr^{-1}. Regardless of the time period, the mean annual TOC at Son Tay was estimated from 324 to 506 kt yr^{-1} (Dang, 2006; Nguyen *et al.*, 2018), and our calculation is higher than theirs (94% higher than Nguyen et al. (2018) and 24% higher than Dang (2006), again due to the difference of calculation time step: our calculations at a daily time step take all flood events into consideration. Finally, our results suggested that the Red River exported 628 kt yr^{-1} of TOC over 2003-2013, i.e. contributed approximately 0.38% of TOC exported by the Asian rivers (164 Mt yr^{-1}, Li et al., 2017).

Table 5-2 Comparisons of organic carbon concentrations and fluxes between the present study and other studies in the Red River and in other rivers

River	Station	Drain Area (10^3 km^2)	Period	DOC			POC			Reference
				Concentration (mg L^{-1})	Flux (kt yr^{-1})	Specific Yield (kg km^2 yr^{-1})	Concentration (mg L^{-1})	Flux (kt yr^{-1})	Specific Yield (kg km^2 yr^{-1})	
Red	Yen Bai	48.50	2008-2009	1.9	47	969	24.7	274	5649	Dang, 2006
				2.2	44	866	2.6	59	1258	Le et al., 2017a
				-	46	-	-	197	-	LOADEST (this study)
				1.51	59	1216	5.21	253	5216	This study
			2003-2013	1.39	44	907	8.35	318	6557	This study
	Vu Quang	30.37	2008-2009	2.4	78	2568	1.8	84	2766	Dang, 2006
				1.9	49	1613	0.8	47	1218	Le et al., 2017a
				-	59	-	-	50	-	LOADEST(this study)
				1.77	69	2272	1.33	55	1811	This study
			2003-2013	1.50	53	1745	2.30	83	2733	This study
	Hoa Binh	52.78	2008-2009	2.3	131	2482	1.3	55	1042	Dang, 2006
				1.7	82	1497	0.5	54	758	Le et al., 2017a
				-	98	-	-	58	-	LOADEST(this study)
				1.84	119	2255	0.62	40	758	This study
			2003-2013	1.60	88	1667	0.96	55	1042	This study
	Son Tay	137.23	2008-2009	2.5	263	1916	3.95	243	1771	Dang, 2006
				-	286	-	-	259	-	LOADEST(this study)
				2.03	296	2157	1.66	255	1858	This study
			2003-2013	1.81	222	1618	3.03	406	2959	This study
Mekong	My Thuan (DOC) Phnom Penh (POC)	795	1972-1998 (DOC) 2006 (POC)	n.a.	2200	2767	2.01	1670	2100	Li et al., 2013 Ellis et al., 2012
Pearl	n.a.	452	2005-2006	1.7	380	840	1.5	540	1195	Ni et al., 2008
Yangtze	Datong	1830	2009	2.03	1580	863	n.a.	1520	831	Wang et al., 2012
Godavari	Rajahmundry	313	2003-2005	1.24	130	415	n.a.	756	2414	Balakrishna et al., 2006
Yellow	Lijin	752	2008-2012	3.3	60	80	1.39	410	545	Ran et al., 2013
Amazon	Obidos	6000	1994-2000	7.18	26900	4483	0.85	5800	967	Moreira-Turcq et al., 2003
Congo	Kinshasa-Brazzaville	3700	2009-2010	9.2	12480	3373	1.46	1960	530	Spencer et al., 2016

4.2.2 Comparison with other rivers

Compared with some other Asian and tropical rivers, the export of DOC and POC fluxes through the Red River is not that large, especially for POC (Table 5-2). However, when comparing specific yields, the Red River basin yields high DOC and POC values, in agreement with some previous studies which indicated that the rivers in mainland Asia have the highest specific export rates worldwide in terms of DOC and POC (Huang *et al.*, 2012; Li *et al.*, 2019).

The DOC flux of the Red River is 58% and 10% of that of the Pearl and Mekong rivers respectively, which are geographically close to the Red River; 14%, 171% and 370% of that of the Yangtze, Godavari and Yellow rivers; around 1% and 2% of that of the Amazon and Congo rivers (Table 5-2). However, the DOC yield of the Red River basin (1618 kg km^{-2} yr^{-1}) is about twice of those of the Pearl and Yangtze basins and is around half of those of the Mekong and Congo basins. Though the DOC flux of the Red River is smaller than those of Pearl and Yangtze rivers, its specific DOC yield is higher than theirs. The high DOC yield of the Red River basin comes from the high leaching from soil and rocks. Previous studies pointed out that the main source of DOC in the Red River basin is from the allochthonous origin, such as diffuse sources (leaching from the soil) during rainy seasons and point sources (industrial and domestic wastewater) during dry seasons (Dang, 2006; Le *et al.*, 2017a). Infiltration is a key factor of the hydrological pattern in this basin (Bui *et al.*, 2014), which accelerates leaching processes. Wei et al. (submitted) found a high erosion, with a mean of 5.5 t ha^{-1} yr^{-1} and hot spots above 20 t ha^{-1} yr^{-1}, in the Red River basin due to the precipitation, slope, agricultural practice and soil texture. These features accelerate the loss of soil organic carbon from land to river.

Though the POC flux of the Red River is quite low compared to other Asian rivers (from -1% for the Yellow River to -76% for the Mekong River, Table 5-2), its specific yield (2959 kg km^{-2} yr^{-1}) is quite high compared to the Mekong (41%) and the Pearl River (+148%) basins which are two basins close by. Le et al. (2017a) emphasized that the main source of the POC was the soil leaching and erosion, not the phytoplankton. The soil erosion in this basin is high, especially in the middle part (Wei et al., submitted). Besides, POC is related to SSC, and the SSC in the Thao River is very high, with an annual mean of 631 mg L^{-1} at Yen Bai station during 2003 to 2013, and 137 mg L^{-1} at Son Tay station.

4.3 Controls and influences on OC fluxes

Figure 5-9, Figure 5-11 and Figure 5-12 show the annual evolution of simulated DOC, POC and TOC fluxes at four stations. The interannual variability of DOC flux is significant but not huge (standard deviations equal to 14, 11, 26, 55 kt yr^{-1} for Yen Bai, Vu Quang, Hoa Binh and Son Tay respectively). The DOC flux was the highest in 2008 (Figure 5-9) which is the flood year and was quite low during 2010-2013 (averagely 33, 49, 61 and 176 kt yr^{-1} for Yen Bai, Vu Quang, Hoa Binh and Son Tay respectively)

which are the drought years. Comparing DOC fluxes under natural and actual conditions allows quantifying the impacts of Q variations associated with climate variability and dam constructions, respectively (Figure 5-13). Under natural conditions, due to the Q variation associated with climate variability, the DOC flux during 2008-2013 only increased by 1% compared to 2003-2007, and the flood year 2008 was the main contributor. Under actual conditions, a 13% reduction of DOC flux was induced by dams which allowed regulation of peak flow during flood seasons. Previous studies also revealed that climate variability and dam constructions within the Red River basin had impacts on Q, however, they showed that Q was more influenced by climate variability than dams (Wei *et al.*, 2019a): they found that at the Son Tay outlet, the annual mean Q was reduced by 13% from 2000-2007 to 2008-2013, with 9% due to climate variability and 4% due to the dams.

A distinct decrease of POC flux can be noticed after 2007 at all four stations (Figure 5-11) when some new dams started to operate. At the outlet (Son Tay), the POC flux in 2008 was only 45% of that in 2007 even though 2008 is a flood year, and the average POC fluxes decreased by 88% in 208-2013 compared to 2003-2007. These dams have trapped the suspended sediment and changed the grain size distribution of downstream sediment (Wei *et al.*, 2019a), which consequently affected the POC transfer. In 2008, a drastic decrease of SSC and sediment fluxes indeed occurred: the SSC at Son Tay decreased by 67% and the sediment flux decreased by 58% in 2008 compared to 2007 (Wei et al., 2019, submitted). Similarly, to DOC fluxes, POC fluxes under natural conditions varied little (2%) between 2003-2007 and 2008-2013. Dams caused an 85% decrease in POC flux. Our study reveals that in the Red River basin, dams induced severe sequestration of POC fluxes due to suspended sediment retention.

Dams in this basin have therefore different degrees of influence on DOC and POC fluxes. Our conclusions are in agreement with other studies in other basins, showing that: the water-sediment regulation of dams had no significant influence on DOC fluxes (Xia *et al.*, 2016), but a significant impact on the POC fluxes (Li *et al.*, 2015; Xia *et al.*, 2016).

Due to the drop of POC flux, the TOC flux decreased by 31% at the outlet in 2008 compared to the previous year (Figure 5-12). At Son Tay outlet, the POC flux accounted for 74% of the TOC flux during 2003-2007, while it only accounted for 47% during 2008-2013 with the main part of organic carbon in the dissolved phase. Previous studies indicated that the Asian rivers draining erosion-prone mountainous terrain deliver more POC than DOC, particularly during the rainy seasons (Ludwig and Probst, 1996b; Park *et al.*, 2018). However, with the construction and operation of new dams, the composition ratio of TOC changed, from POC-dominating to DOC-dominating (Table 5-3). Besides, the dynamic variations of POC/TOC were also modified by dam regulation (Figure 5-14a). Before new dam constructions, the POC/TOC ratio was low around March and high in flood season. However, after impoundment of new dams, the dams fulfil flood-control functions during June and July, retaining water and SS,

therefore the POC/TOC ratio became also low during the flood season. And around March, dams discharge water for irrigation, also releasing SS, which induces high POC/TOC.

A fundamental change of POC/TOC was observed in 2008. Two new dams (Nansha on the Thao river and Tuyen Quang on the Lo river) started operation in 2008 and two new dams (Madushan on the Thao river and Son La on the Da river) impounded in 2011. Compared to the other two tributaries, the POC/TOC ratio at Yen Bai on the Thao River did not decrease that sharply (Table 5-3). The Madushan and Nansha dams are located around 230 km upstream to Yen Bai station, therefore, the suspended sediment and POC over this distance can be regulated by the terrestrial inputs as well as the river bed degradation. At Hoa Binh station, before the new Son La dam became operational, the POC/TOC percentage was already low because of the Hoa Binh dam which was impounded in 1989. Therefore, the biggest impact on the POC/TOC ratio at Son Tay is due to the change of the POC/TOC from the Lo river, i.e. Tuyen Quang dam contributes most to the decrease of POC/TOC at Son Tay.

Table 5-3 The percentage of particulate organic carbon (POC) in total organic carbon (TOC) in two periods (before and after the new dam constructions) at each station

Variables	Period	Yen Bai	Vu Quang	Hoa Binh	Son Tay
POC/TOC	2003-2007	91%	72%	47%	74%
	2008-2013	81%	44%	26%	47%

4.4 Errors and uncertainties in the estimation

Parameters in Equation 1 and 2 were calculated based on discrete sampling data, however, sampling is impossible to be carried out when discharge was very high. Therefore, sampling DOC and POC concentrations at high discharge were lacking. More intensive sampling during flood season helps to obtain more precise parameters. During low discharge periods, some DOC sampling data can be scattered due to the uncertainty source such as industrial and urban discharge. Along the Red River, the inhabitants are mainly farmers and villagers who might discharge the waste into the river. Moreover, %POC can vary greatly even on the same day due to the instantaneous suspended sediment concentration. Hence, the data from Le et al. (2017a) and Dang (2006) can be different even under a similar SSC concentration.

Errors in estimating OC concentration and flux can also come from the simulated Q and SSC. However, the errors of simulated Q and SSC are within acceptable limits (Wei *et al.*, 2019a). Moreover LOADEST was used as a validation for our simulation, however, it was found to produce high biases when calculating long term loading (Stenback *et al.*, 2011; Hirsch, 2014).

As mentioned in Section 3.1.5, POC parameters calibration was based on the data sampled since 2008 when new dams started operating. Therefore, the POC concentration and flux before 2008 were an insight to roughly estimate the potential

retention of POC in the reservoirs. According to Wei et al. (2019, submitted), the dynamic transfer processes and fluxes of SS before and after new dam constructions were different. Therefore, POC dynamic transfer processes and fluxes would be different before and after the new dam constructions. Hence, the parameter *b* related to POC (Equation 2) should be different before 2008.

5. Conclusions

Based on a hydrological model already set up, calibrated and validated over the Red River basin, and on dissolved and particulate organic carbon in-situ measurements, a model of organic carbon dynamics was calibrated and validated at a daily time step during a 10-year period (2003-2013) in the large tropical Red River basin. Intra-annual and inter-annual variations are very difficult to assess from discrete in-situ samplings and only possible at the hydrometric stations. Based on the daily simulated organic concentration, discharge and suspended sediment from a modelling study, daily organic carbon fluxes were able to be simulated considering all short term events not only at hydrometric stations but also anywhere within the basin. This allows for understanding the spatio-temporal variations of organic carbon in this basin.

Discharge and suspended sediment are crucial factors for fluvial organic carbon fluxes. However, the organic carbon fluxes and specific yield have been altered by climate variability and intensive human activities in this basin. Especially, dam impoundments had a clear effect on trapping particulate organic carbon, inducing a decrease in total organic carbon export and a different organic carbon composition ratio.

This study demonstrates the advantages of using a calibrated model in combination with available discrete in-situ data when continuous field measurements are not available. It reveals that during 2003-2013, at the outlet of the Red River basin, the export of dissolved and particulate organic carbon were 222 and 406 kt yr^{-1} respectively, accounting for 0.38% of the total organic carbon export by Asian rivers. However, the specific yields of dissolved organic carbon (1618 kg km^2 yr^{-1}) and particulate organic carbon (2959 kg km^2 yr^{-1}) of the Red River basin were high (more than double) compared to other Asian basins such as the Yellow, Yangtze and Pearl. By comparing the scenario of natural conditions (without dams) to actual conditions, we found a 12% and an 88% decrease in dissolved and particulate organic carbon fluxes, respectively, mainly due to dams regulations (less than 2% of variations was explained by climate variability). The percentage of particulate organic carbon in total organic carbon decreased from 86% to 74% until 2007 then to 47% with new dams. Dam constructions altered the total organic carbon yield and its constituent ratio.

The corresponding parameters of dissolved and particulate organic carbon equations well represented the characteristics of each sub-basin, showing the effect of soil OC and Chlorophyll a. Hence, once people have the values of average soil organic carbon content of the drainage area and the Chl-a concentration, they can evaluate the dissolved and particulate organic carbon at any point within the Red River basin.

This study allows future studies on different scenarios such as land use and climate changes. This approach could be applied to other basins worldwide to characterize their corresponding parameters. Future studies should focus on the fluvial organic carbon flux and specific yield variations under global changes in order to understand their long-term evolutions. Besides discharge and suspended sediment, soil organic carbon content, soil leaching and erosion are the key factors influencing the organic carbon concentration in the Red River basin. Therefore, the link between soil conservation and organic carbon transport can also be carried out.

Acknowledgement:

This research was developed in the framework of the Land-Ocean-aTmosphere regional coUpled System study center (LOTUS), an international joint Vietnamese/French laboratory funded by the Institut de Recherche pour le Développement (IRD). We thank LOTUS for providing the hydrological dataset, and also the research travel funds for Xi Wei to collect data and information in Vietnam. We also appreciate the Vietnam Academy of Science and Technology (VAST) to provide organic carbon sampling data. The PhD scholarship of Xi Wei is financially supported by the China Scholarship Council (CSC), grant number 201606240088.

Chapter 6

General Discussion

6. CHAPTER Ⅵ: General Discussion

6.1. Water Regime

6.1.1. Hydrological cycle and water yield

In the Red River basin, the mean annual rainfall from TRMM was 1494 mm yr^{-1} from 2000 to 2013 (Table 6-1), of which 53% was consumed by evapotranspiration and 47% by streamflow. Rainfall is an important determinant of the fluxes and states of the land surface hydrological system, and its spatial and temporal patterns, intensity and duration of significantly affect the hydrological cycles (Nijssen, 2004; Yang *et al.*, 2015; Wang *et al.*, 2016). The Mekong and Pearl river basins are geographically located close to the Red River (Figure 2-2), and these three rivers originate from Himalayan-Tibetan Plateau. The mean annual rainfall for the Mekong and Pearl river basins is 1470 (during 1983-2016 period) and 1525 (during 1960-2005 period) mm yr^{-1}, respectively (Zhang *et al.*, 2012; Chen *et al.*, 2019), and the annual rainfall of the Red River basin is around theirs. The Red River basin has a higher annual rainfall compared to the Yangtze (1086 mm yr^{-1} during 1980-2015, Cui *et al.*, 2017) and Yellow (466 mm during 1981-2013, Wu *et al.*, 2016) river basins. In Asia, the annual rainfall of the tropical river basins is higher than others in the subtropical and temperate zones. Compared to other large tropical river basins, the mean annual rainfall of the Red River basin is 29% lower than Amazon (2095 mm yr^{-1} during 1973-2013, Almeida *et al.*, 2017), and is slightly lower (4%) than the Congo (1560 mm yr^{-1} during 1951-1989, Alsdorf *et al.*, 2016).

Table 6-1 Mean annual values of rainfall and hydrology for some big Asian and tropical rivers.

River	Basin Area (10^3 km^2)	Rainfall		Hydrology				Reference
		Period	rainfall (mm yr^{-1})	Period	Yield (km^3 yr^{-1})	Discharge (m^3 s^{-1})	Depth (mm yr^{-1})	
Red	137	2000-2013	1494	2000-2013	95	3003	697	This study
Mekong	795	1983-2016	1470	2009-2016	400	12684	503	Dang et al., 2018
Pearl	452	2000-2009	1650	2000-2009	268	8498	593	Wu et al., 2012
Yangtze	1830	1980-2015	1086	2003-2013	838	26573	466	Yang et al., 2015
Yellow	752	1981-2013	466	n.a.	58	1839	77	Wu et al., 2016
Irrawaddy	413	n.a.	n.a.	1991-2012	380	12054	1057	Sirisena er al., 2018
Congo	3500	1951-1989	1560	2000-2010	1282	40662	347	Alsdorf et al., 2016
Amazon	5960	1973-2013	2095	n.a.	6591	209000	1099	Moreira-Turcq et al., 2003

For streamflow, the model estimated a mean annual water yield of 95 km^3 yr^{-1} (with a mean annual water depth of 697 mm yr^{-1} and mean annual discharge of 3003 m^3 s^{-1}, Table 6-1), of which 58% was the groundwater, 39% was surface runoff accounted and 3% was the lateral flow. The groundwater is the main component for the river flow in the Red River basin, especially during the dry season. The mean water yield of the Mekong, Pearl, Yangtze, Yellow and Irrawaddy rivers is 400 km^3 yr^{-1} (with a mean annual water depth of 503 mm yr^{-1} and mean annual discharge of 12,684 m^3 s^{-1} during 2009-2016, Dang *et al.*, 2018), 268 km^3 yr^{-1} (with a mean annual water depth of 593

mm yr^{-1} and mean annual discharge of 8498 m^3 s^{-1} during 2000-2009, Wu *et al.,* 2012), 838 km^3 yr^{-1} (with a mean annual water depth of 466 mm yr^{-1} and mean annual discharge of 26,573 m^3 s^{-1} during 2003-2012, Yang *et al.*, 2015), 58 km^3 yr^{-1} (with a mean annual water depth of 77 mm yr^{-1} and mean annual discharge of 1839 m^3 s^{-1}, period not mentioned in Wu *et al.*, 2016), 380 km^3 yr^{-1} (with a mean annual water depth of 1057 mm yr^{-1} and mean annual discharge of 12,054 m^3 s^{-1} during 1991-2010, Sirisena *et al.*, 2018), respectively; and the mean annual water yield for the Congo and Amazon river is 1282 km^3 yr^{-1} (with a mean annual water depth of 347 mm yr^{-1} and mean annual discharge of 40,662 m^3 s^{-1} during 2000-2010, Alsdorf *et al.*, 2016) and 6591 km^3 yr^{-1} (with a mean annual water depth of 1099 mm yr^{-1} and mean annual discharge of 209,000 m^3 s^{-1}, period not mentioned in Moreira-Turcq *et al.*, 2003). Though the annual water discharge and yield of the Red River basin are lower than the Mekong, Pearl, Yangtze and Congo, its annual water depth is the highest among these rivers. According to the ratio of the annual water depth to the annual rainfall of each basin, the Amazon and Red River basins have the highest ratio values with 52% and 47%, respectively, compared to the the Mekong (34%), Pearl (36%), Yangtze (43%) and Congo (22%), i.e. rainfall of the Red River and Amazon basin produces the most streamflow per unit area.

The groundwater accounts for a big portion of the annual water yield in the Red River basin. This can be contributed by the Karst landform (also known as carbonate rock) in this basin. The water-yielding properties of carbonate rocks vary widely; some yield almost no water and are considered to be confining units, whereas others are among the most productive aquifers known (Ford and Williams, 2007; Carbonate-rock aquifers, 2016). Most karst rocks are fissured because of the presence of joints, faults and bedding planes, and these interconnected fissures provide routes for water flow (Ford and Williams, 2007). The joints in Yunnan province (the part of the Red River in China) are wide and aquifers in this area are mainly associated with fractures, and strong leaching from carbonate rocks is discovered (Ford and Williams, 2007; Le *et al.*, 2018). Groundwater is mainly recharged by vertical infiltration from precipitation and during the flood time and wet season by the lateral flow from rivers. The groundwater of the nearby Pearl River basin is also abundant (Hou *et al.*, 2018).

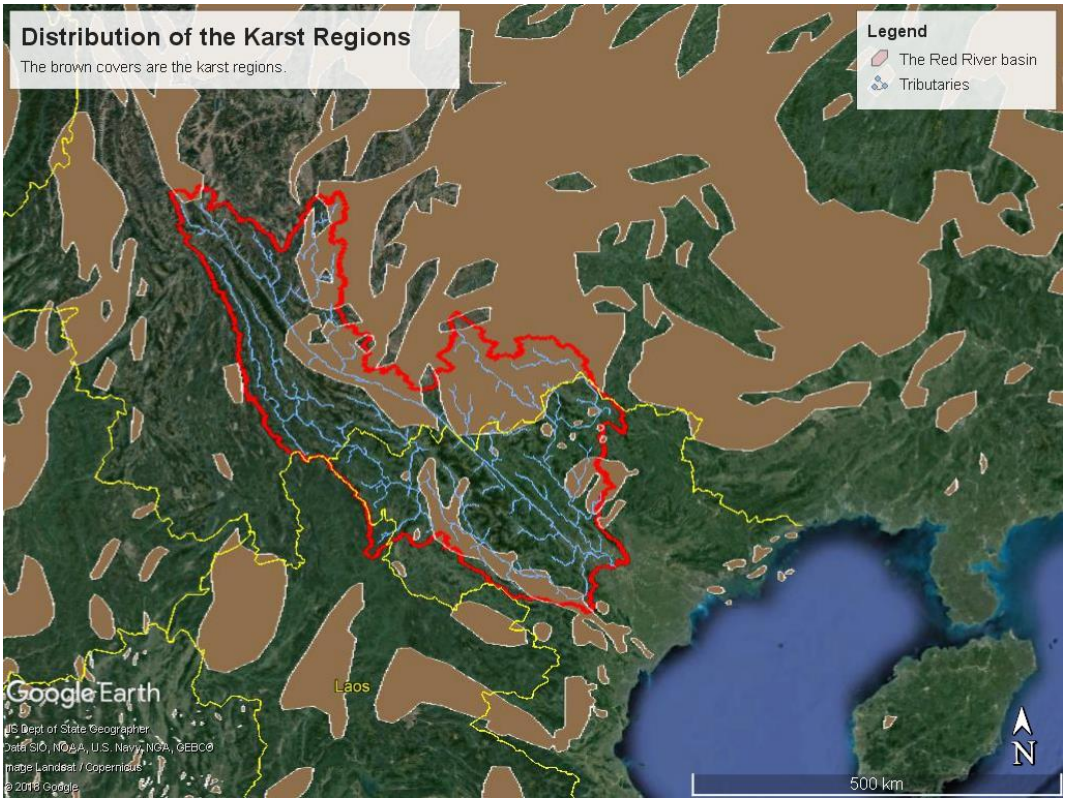

Figure 6-1 Distribution of the Karst regions, resource from World Map of Carbonate Rock Outcrops v3.0 (https://www.fos.auckland.ac.nz/our_research/karst/)

6.1.2. Impacts of dams on discharge

Vörösmarty et al. (1997) estimated that more than 40% of global river discharge is intercepted by the large impoundments. In the Red River, with the new dams implementations after 2008, the cumulative impacts of dams (comparison between 2008-2013 and 2000-2007, i.e. pre-new-dams and post-new-dams) on Q at Lao Cai, Yen Bai, Vu Quang, Hoa Binh and Son Tay is -0.4% (p=0.97), -0.3% (p=0.98), -2% (p=0.90) and -8% (p=0.45), respectively, and at Son Tay is -4% (p=0.74).

The impacts of dams on Q at different sub-basins are different: the impacts on the Da basin (-8%) is greater than the other two sub-basins (the Thao -0.3% and Lo 2%). The different impacts are mainly influenced by the capacity and location of dams. The two dams located on the Da river have bigger capacities (>9 km^3, Table 1 in Chapter 4) than the others on the Thao (~0.5 km^3) and Lo (~2.9 km^3) rivers. Dams with bigger capacity have larger effects on discharger regulation: weakening the flood peaks during flood seasons and replenishing the runoff for irrigation during dry seasons (Liu *et al.*, 2019b). Besides, the Hoa Binh dam is located downstream close to the Hoa Binh gauge station (outlet of the Da River), without the mitigation or regulation from the rainfall in the area between the dam and the gauge station.

Though the dams on the Red River showed impacts on annual mean Q, the impacts are less than 8% and are not significant. Our results are in agreement with Dang *et al.* (2010) who found that there was no significant difference in the Q before and after Hoa Binh dam construction. By comparing the mean annual discharge of the pre- (1993-

2002) and post- (2003-2012) the Three Gorges Dam decades, Yang *et al.* (2015) found a 13% decrease in the mean annual discharge among which the relative impacts of dams was 8%. Along the Mekong River, no significant changes between pre-dam and post-dam periods were observed in annual mean discharge (Lu and Siew, 2006; Lu *et al.*, 2014). The anthropogenic impact (the construction of dams) in the Pearl Basin had little influence on water discharge, i.e. has therefore been insignificant (Zhang *et al.*, 2008; Wu *et al.*, 2012). For the above Asian rivers, dams mainly regulate the seasonal Q and have no significant influence on annual mean Q, which is in agreement with Biemans *et al.* (2011) who demonstrated that dams would not necessarily significantly reduce water discharge at a yearly time scale.

6.1.3. Impacts of climate variability on discharge

Compared to the impacts of dam constructions on annual mean Q of the Asian rivers, the impacts of climate variability (precipitation, evapotranspiration and temperature) is larger (Wang *et al.*, 2006; Zhang *et al.*, 2008; Lu *et al.*, 2014; Yang *et al.*, 2015). Li et al. (2016) indicated that hydrological droughts in the Red River basin are much more driven by meteorology than by human activities.

In the Red River basin, the impacts of climate variability on different sub-basins varied from +2% (at the Lo basin, p=0.76) to -29% (at the Lao Cai station in the Thao basin, p=0.04; the other station in the Thao river showed a decrease of 21% with p=0.07); the impacts of climate variability at Hoa Bind (in the Da river) and Son Tay stations was -10% (p=0.23) and -9% (p=0.30). The decrease caused by climate variability is only significant at Lai Cai station, which might indicate that the upper part of Lao Cai station, i.e. the part in China, might be more sensitive and susceptible to the climate variability than the basin in Vietnamese part. Regional climate variations induced different impacts. Among these three sub-basins, the mean annual rainfall was highest for the Thao sub-basin, followed by the Da and then the Lo (Le *et al.*, 2007). Therefore, the different Q variation rates of each sub-basin can relate to the distribution of rainfall, and the decrease of the rainfall might affect the Thao basin most, resulting in the biggest Q decreasing rate among the three tributaries. Precipitation and evapotranspiration (as reflected by temperature change) are the most obvious natural changes to the environment (Yang *et al.*, 2015). For the entire basin, during the study period (2000-2013), the annual mean rainfall reduces by 9% ($p>0.05$), evapotranspiration reduces by 5% ($p>0.05$), and temperature increases by 1% ($p>0.05$). These changes result in a 13% decrease in available water ($p>0.05$) with a 4% ($p>0.05$) decrease in soil water content.

Over the past 50 years (1950-2000), due to the regional precipitation variations (~10% decrease) in the Yellow River basin induced by global El Niño/Southern Oscillation (ENSO) events, the water discharge to the sea decreased by approximately 51% (Wang *et al.*, 2006). In the Yangtze River basin, the rainfall during 2003-2012 was 6% lower than during 1993-2002, which contributed to 61% of the Q decrease between these two periods (Yang *et al.*, 2015). Wu *et al.* (2012) found that between 1994 and

2009, the precipitation in the Pearl River basin decreased by 18% (p=0.03) and water discharge decreased by 32% (p<0.01), and indicated that inter-annual fluctuations of water discharge were governed by changes in climate than the anthropogenic impacts. Studies on the Mekong River basin found that the annual total precipitation in this basin fluctuated along the years (1983-2016) with a non-significant trend (p > 0.05) (Chen *et al.*, 2019), but there were significant associations (p < 0.01) between water discharge and rainfall in the upper Mekong Basin (upstream of the Chiang Saen station), indicating predominant controls of precipitation in the upper basin on water discharge (Lu *et al.*, 2014).

However, the effects of climate variability and change on global hydrological cycles are complex and rely on the context of individual river basins, rather than being simply a function of changing precipitation (Immerzeel *et al.*, 2010; Best, 2019). The complexity of such feedbacks between climate and river flow is exemplified in considerations of the great rivers that flow from the mountains of Asia which rely on both monsoonal rainfall and snowmelt (Bookhagen and Burbank, 2010; Immerzeel *et al.*, 2010; Best, 2019). Immerzeel *et al.* (2010) demonstrated that snow and glacial melt were important hydrologic processes for the rivers fed from the Tibetan plateau, however, this area was threatened by climate change, which subsequently affected the meltwater and then streamflow and water availability; the effects in the Indus and Brahmaputra basins were likely to be severe owing to the high dependence on meltwater while the effects in the Yellow River basin might be positive as the low dependence on meltwater and a projected increased upstream precipitation.

From our results and the above studies we can see that even the climate variability (especially the precipitation) might not be significant, it did have impacts on water discharge. Dam constructions in someway can mitigate the impacts of climate variability by regulating and storing water from flood seasons to dry seasons for irrigation.

6.2. Suspended Sediment

6.2.1. Sediment export

The Red River basin exported 33.0 Mt yr^{-1} (with a specific yield of 240 t km^{-2} yr^{-1}) sediments to the downstream delta part during 2000-2013, accounting for 0.7% of the total Asian river sediment (4740 Mt yr^{-1}) delivery to the seas (Syvitski *et al.*, 2005). At Son Tay outlet, 90% of the total sediment export happened during the southwest monsoon seasons (from May to October). There is a big difference in the mean annual sediment fluxes (SF) between 2000-2007 (pre-new-dams) and 2008-2013 (post-new-dams): the SF before new dams implementations was 49.1 Mt yr^{-1} (with a specific yield of 358 t km^{-2} yr^{-1}) and decreased to 11.6 Mt yr^{-1} (with a specific yield of 84 t km^{-2} yr^{-1}).

Global sediment flux to the oceans was estimated from 12.6 to 18.5 Gt yr^{-1}, and Asia exported the most sediments (4.7 Gt yr^{-1}) among continents (Syvitski *et al.*, 2005; Gordeev, 2006; Syvitski and Kettner, 2011). Warm temperate regions have the highest

sediment yield as compared with other climates (Syvitski *et al.*, 2005). The Yangtze River exported 145 Mt yr^{-1} (with a specific yield of 79 t km^{-2} yr^{-1}) during 2003-2012 (Yang *et al.*, 2015). The Yellow River transported 143 Mt yr^{-1} (with a specific yield of 190 t km^{-2} yr^{-1}) downstream to the sea during 2000-2008 (Miao *et al.*, 2011). The SF of the Pear River during 2000-2009 is 36 Mt yr^{-1} with a specific yield of 80 t km^{-2} yr^{-1} (Wu *et al.*, 2012). The Mekong River exported around 37.5 Mt yr^{-1} with a specific yield of 47 t km^{-2} yr^{-1} to the sea during 2009-2016 (Dang *et al.*, 2018). The Congo River delivered 30.7 Mt yr^{-1} with a specific yield of 8.8 t km^{-2} yr^{-1} during 1990-1993 (Coynel *et al.*, 2005). The Amazon River during 1995-2016 exported 60 Mt yr^{-1} (with a specific yield of 8.8 t km^{-2} yr^{-1}) to the Atlantic Ocean (Montanher *et al.*, 2018). Though the sediment export of the Red River is only around 33% of the Mekong, Pearl and Congo rivers, 20% of the Amazon river and 8% of the Yellow and Yangtze rivers, however, the specific yield of the Red River basin is around 8 times higher than the Congo and Amazon basins, double of the Mekong basin, in the same order with the Pearl and Yangtze basins, and half of the Yellow basin.

Under natural conditions (without any dams), the Red River should have yielded an annual SF of 107 Mt yr^{-1} during 2000-2013, corresponding to a specific yield of 780 t km^{-2} yr^{-1}. For comparing the SF and specific yield under natural conditions of the Red River basin with other basins, the values provided by Milliman and Syvitski (1992) were considered since those data were obtained before 1992 and are less impacted by dams than more recent estimations. The Yellow River produced 1100 Mt yr^{-1} SF with a specific yield of 1400 t km^{-2} yr^{-1}; the Yangtze River caused 480 Mt yr^{-1} SF with a specific yield of 250 t km^{-2} yr^{-1}; the Pearl River generated 69 Mt yr^{-1} SF with a specific yield of 160 t km^{-2} yr^{-1}; the Mekong River yielded 160 Mt yr^{-1} SF with a specific yield of 200 t km^{-2} yr^{-1} (Milliman and Syvitski, 1992). The Red River basin under natural conditions thus exported less SF than the Yellow River (-90%), the Yangtze River (-78%) and the Mekong River (-33%), and 55% more than the Pearl River. However, its specific yield was higher than the Mekong (+290%), Pearl River (+388%), Yangtze (+212%), and nearly half of the Yellow River (-44%). When compared to an equivalent surface watershed such as the upper Danube (132,000 km^2), the Red River basin produced almost 3 times higher specific yield than that of 265 t km^{-2} yr^{-1} generated by the upper Danube; besides, the upper Danube basin only exported 21.2 t km^{-2} yr^{-1} to the downstream part (Vigiak et al., 2015). These results show that under natural conditions, the Red River basin, though having a smaller surface than other basins in the world, is a very large source of SF from the watershed to the sea.

From above we can see that under both actual and natural conditions, though with the dams continuously implementations in the Red River basin, its specific sediment yield is high among those Asian river basins. This is due to its soil erosion within the basin.

6.2.2. Soil erosion

Riverine sediment fluxes can come from the landscape (soil erosion) and in-stream process (river degradation and resuspension). The mean annual soil erosion in the

Red River basin ranged from 1 to 4340 t km^{-2} yr^{-1}, with a mean of 550 t km^{-2} yr^{-1} for the whole basin. In Vietnam, more than 40% of its steeply sloping lands (62% of the country) suffer severe erosion (Dregne, 1992). From previous studies, the annual soil losses in the Red River basin in Vietnam's part ranged from 90 to 17,400 t km^{-2} yr^{-1} (Podwojewski *et al.*, 2008; Nguyen *et al.*, 2011; Mai *et al.*, 2013; Tuan *et al.*, 2014). In the area of the Red River basin in China's part, Gu (2016) found that the average annual soil erosion was 1840 t km^{-2} yr^{-1} (136 Mt yr^{-1}) in 2000 while it was 1870 t km^{-2} yr^{-1} (138 Mt yr^{-1}) in 2010; severe soil erosion area which was only less than 10% of the total erosion area, however, contributed 57% to 65% of the total erosion amount; farmland was the hot spot of soil erosion, followed by grassland and forest; slope above 15° and elevation between 1000-2000 m a.s.l. were the hot spots of erosion.

High erosion areas are identified in the middle part of the Thao River and the downstream of the Da River (Figure 4-7): with high precipitation (>1500 mm yr^{-1}) and surface runoff (>450 mm yr^{-1}), Lai Chau (sub-basin 173), Lao Cai (sub-basin 116, 117, 135, 148, 149, 157), Ha Giang (sub-basin 119) and Son La (sub-basin 218, 232, 234, 237, 240, 241) provinces are the most vulnerable to soil erosion, and their mean annual erosion rate during the study period can be above 2000 t km^{-2} yr^{-1}. Precipitation, slope and agricultural practice are key influence factors for soil erosion in the Red River basin. Our results are in agreement with Ranzi *et al.* (2012) who highlighted the major role of rainfall in soil erosion in the Lo basin; Yang et al. (2003) found that the hot spots of soil erosion in Southeast Asia were close mountainous areas located in the tectonic zones and dense croplands of the high population regions where both natural geomorphology and human activity are major factors for inducing soil erosion.

Southeast Asia had the most serious soil erosion problems and hot spots were close mountainous areas located in the tectonic zones and dense croplands of the high population regions where both natural geomorphology and human activity are major factors for inducing soil erosion; and there was an increasing trend found in Asian, and the regions with the largest increases were in the tropic rainforest regions (Southeast Asia), such as Thailand and the lower Mekong basin (Yang *et al.*, 2003). In the Mekong River basin, the soil erosion in the 1980s was 9.6 t ha yr^{-1} and predicted to reach 13.0 t ha yr^{-1} in the 2090s (Yang *et al.*, 2003).

Asia probably has suffered more from human-induced soil erosion than any other continent (Dregne, 1992), and Southeast Asia has the most serious soil erosion problems (Yang *et al.*, 2003). The mean erosion rate of Asia was estimated to 1220 t km^{-2} yr^{-1} in the 1980s and was predicted to be 1440 t km^{-2} yr^{-1} in the 2090s (Yang *et al.*, 2003). The hot spots of erosion (Figure 1-6) including the Himalayan–Tibetan ecosystem in South Asia and the Loess Plateau in China; active tectonic movements (such as earthquake, debris flow and landslide), steep slopes, freeze-thaw and weathering erosions are the main issues in the riverhead high-elevation areas.(Milliman and Syvitski, 1992; Ludwig and Probst, 1998; Lal, 2003). Yang et al. (2003) found that there was an increasing trend of soil erosion in Asian, and the regions

with the largest increases were in the tropic rainforest regions (Southeast Asia), such as Thailand and the lower Mekong basin.

In the middle of the Yellow River basin is the Loess Plateau region from where a large amount of sediments is eroded (Ni *et al.*, 2008b), and the range of soil erosions are 4176-7772 t km^{-2} yr^{-1} in 2000 and 1318-6833 t km^{-2} yr^{-1} in 2010 (Yan *et al.*, 2018). In the upstream part of the Yellow River, the soil erosion in 2000, 2003, 2006 is 728, 110 and 803 t km^{-2} yr^{-1}, respectively (Ouyang *et al.*, 2010). The mean annual soil erosion for the Yellow basin is estimated from 750 t km^{-2} yr^{-1} (in the 1980s, Yang *et al.*, 2003) to 1138 t km^{-2} yr^{-1} (during 2010-2012, Wang *et al.*, 2019). The mean annual soil erosion of the Yangze River basin is 3080 Mt in 2000, with a soil erosion rate at 1683 t km^{-2} yr^{-1} (Kong *et al.*, 2018), and is 776 t km^{-2} yr^{-1} during 2010-2012 (Wang *et al.*, 2019). In the Pearl River basin, the mean annual soil erosion is 845 t km^{-2} yr^{-1} during 2010-2012 (Wang *et al.*, 2019). The mean annual soil erosion during 1987-2000 ranged from 0 to 3220 t km^{-2} yr^{-1} in the Mekong River Basin; the soil erosion range of 0-440 t km^{-2} yr^{-1} occupied 60% of the whole basin (Suif *et al.*, 2016).

6.2.3. Impacts of climate variability on suspended sediment

Changes in rainfall can affect the rate of soil erosion and the sediment transport capacity of a river, which influences the sediment flux in that river (Piman and Shrestha, 2017). In the Red River basin, comparing 2008-2013 to 2000-2007, the impacts of climate variability on suspended sediment concentration (SSC) was from -8% (on the Da and Lo basins, with p=0.16 and 0.22, respectively) to -20% (on the Thao basin, p= 0.04), and was -13% (p=0.06) at Son Tay. The impacts of climate variability on sediment fluxes (SF) was -28% (p=0.22) at Lao Cai and -21% (p=0.30) at Yen Bai on the Thao river, 2% (p=0.93) at Vu Quang on the Lo river, -10% (p=0.48) at Hoa Binh on the Da river and -10% (p=0.50) at the outlet of the continental basin (Son Tay). The responses to climate variability are different for each sub-basin, even though these variations are not significant. The Thao sub-basin is more susceptible to climate variability than other sub-basins, and this is related to its Q which is also more sensitive to climate variability than other sub-basins; another reason is that the Thao River basin is vulnerable to both landscape erosion and channel erosion due to its steep landscape and channel slopes.

In the Mekong River basin, interannual hydrological variation plays an important role in sediment supply to the ocean (Dang *et al.*, 2018); Lu *et al.* (2014) found a significant associations between water discharge and rainfall in the upper Mekong Basin ($p < 0.01$), indicating predominant controls of precipitation in the upper basin on water discharge; Piman and Shrestha (2017) found that in the Mekong River basin the potential impact of climate change on sediment yield is greater than on streamflow. During 1994-2009 in the Pearl River basin, the sediment load decreased by 83% of which 20% was due to climate change (an 18% decrease of the rainfall, Wu *et al.*, 2012). In the Yellow River basin, Miao *et al.* (2011) found that the impact of climate on sediment load was -46% during 1970-2008. Yang *et al.* (2015) found that the sediment

flux of the Yangtze River decrease from 320 Mt yr^{-1} during 1993-2002 to 145 Mt yr^{-1} during 2003-2012 (decreased by 55%), and 14% of this decline was attributed to precipitation change. For the Red, Pearl, Yangtze rivers, the impact of climate variability on sediment fluxes is within 20% (despite the different study periods), while it is higher for the Yellow basin.

6.2.4. Impacts of dams on suspended sediment

Dam constructions not only retain the sediments coming from the upstream but also change the sediment size distribution and the discharge dynamics downstream, which consequently change the in-stream transfer dynamics of SS. Yu *et al.* (2013) demonstrated that after dam implementations on the Yellow River the sediment entering the lower reach showed a different transportation pattern in both spatial and temporal scales during 2000-2010 due to a majority of those coarser sediments are temporally sequestrated within reservoirs. After dam implementations, the coarser particles are retained by dams, and the particle size distribution is affected downstream, leading to a change in the channel erodibility. Then, the dynamics of downstream suspended sediment transport decrease. In our study during the calibration process, we found that keeping the same parameter value of SPCON (the sediment transport coefficient, presenting the maximum amount of sediment that can be transported from a reach segment) with 0.008 (for the period before new dam constructions, see Section 3.5) for sediment routing, it was not possible to simulate the suspended sediment concentrations downstream of the dams for the period after new dam constructions. The sediment routing indeed was changed by dam constructions. Therefore, a lower value of SPCON (0.002) was set for the period after new dam operations. However, the SPCON needs to be modified manually after dam operations and it is only allowed to be modified at an entire basin scale, which means it can not be adjusted on a reach scale. This might need to be improved in the SWAT model.

Compared SF during 2000-20007 to 2008-2013, it decreased from 46.0 to 10.3 Mt yr^{-1} at Lao Cai, from 56.5 to 17.6 Mt yr^{-1} at Yen Bai, from 9.6 to 2.7 Mt yr^{-1} at Vu Quang, from 5.3 to 1.3 Mt yr^{-1} at Hoa Binh and from 49.1 to 11.6 Mt yr^{-1} at Son Tay. The decreases on SF was significantly contributed by dams: -50% at Lao Cai ($p=0.02$), -48% at Yen Bai ($p=0.03$), -74% at Vu Quang ($p<0.01$), -89% at Hoa Binh ($p<0.01$) and -80% at Son Tay ($p<0.01$). Among the three tributaries, dams on the Lo and Da rivers show larger impacts than the Thao river. There are two main reasons induced the different responses: first, the dams on the Thao river are located quite upstream to Lao Cai and Yen Bai stations (>100 km upstream of Lao Cao), which allows the reach over this distance to mitigate the impacts of dam through riverbed degradation and soil erosion from the sub-basin between dams and gauge stations; second, the capacities of the dams on the Thao river (a cumulative capacity < 0.9 km^3) are smaller than the ones on the other two tributaries (a cumulative capacity of 5.1 and 18.8 km^3 on the Lo and Da rivers).

In Asia, the 2000s decade exhibits a decreasing trend in suspended sediment flux

(Cohen *et al.*, 2014). The SF of the Pearl River decreased by 83% from 1994 to 2009, and 80% of the decrease in SF was due to anthropogenic impacts (mainly dam constructions) (Wu *et al.*, 2012). The SF of the Yellow River decreased from 398 Mt yr^{-1} during 1986-1999 to 151 Mt yr^{-1} during 2000-2007 (-62%), and dams contributed 30% to this reduction (Peng *et al.*, 2010). The SF of the Yangtze River decreased by 55% between 1993-2002 (320 Mt yr^{-1}) and 2003-2012 (145 Mt yr^{-1}), of which 75% was related to the dams (Yang *et al.*, 2015). For the Mekong River, the SF decreased from pre-dam period (1962-1992) 133 Mt yr^{-1} to post-dam period (1993-2002) 106 Mt yr^{-1} (Kummu and Varis, 2007). Though the SF observed at lower Mekong River only decreased by 20% between pre- and post-dam period, the SF observed at the upper Mekong decreased by 56% (Kummu and Varis, 2007).

6.3. Organic Carbon

6.3.1. Dissolved organic carbon export

Based on the daily-step calculation, the mean annual export of DOC during 2003-2013 was 222 kt yr^{-1} at Son Tay, which accounts for 0.26% of the total DOC export by Asian rivers to the seas, estimated to 85.45 Mt yr^{-1} by Li et al. (2019).

The DOC flux of the Red River is 58% and 10% of that of the Pearl (380 kt yr^{-1}, Ni et al., 2008) and Mekong (2200 kt yr^{-1}, Li et al., 2013) rivers respectively, which are geographically close to the Red River; 14%, 171% and 370% of that of the Yangtze (1580 kt yr^{-1}, Wang et al., 2012), Godavari (130 kt yr^{-1}, Balakrishna et al., 2006) and Yellow (60 kt yr^{-1}, Ran et al., 2013) rivers; around 1% and 2% of that of the Amazon (26900 kt yr^{-1}, Moreira-Turcq et al., 2003) and Congo (12480 kt yr^{-1}, Spencer et al., 2016) rivers (Table 5-2). Compared with some other Asian and tropical rivers, the export of DOC fluxes through the Red River is not that large, however, the DOC yield of the Red River basin (1618 kg km^{-2} yr^{-1}) is about twice of those of the Pearl (840 kg km^{-2} yr^{-1}) and Yangtze (863 kg km^{-2} yr^{-1}) basins and is around half of those of the Mekong (2767 kg km^{-2} yr^{-1}) and Congo (3373 kg km^{-2} yr^{-1}) basins. Though the DOC flux of the Red River is smaller than those of Pearl and Yangtze rivers, its specific DOC yield is higher than theirs. The high DOC yield of the Red River basin comes from the high leaching from soil and rocks. Previous studies pointed out that the main source of DOC in the Red River basin is from the allochthonous origin, such as diffuse sources (leaching from the soil) during rainy seasons and point sources (industrial and domestic wastewater) during dry seasons (Dang, 2006; Le *et al.*, 2017a). Infiltration is a key factor of the hydrological pattern in this basin (Bui *et al.*, 2014), which accelerates leaching processes. Wei et al. (submitted) found a high erosion, with a mean of 5.5 t ha^{-1} yr^{-1} and hot spots above 20 t ha^{-1} yr^{-1}, in the Red River basin due to the precipitation, slope, agricultural practice and soil texture. These features accelerate the loss of soil organic carbon from land to river.

Comparing DOC fluxes under natural and actual conditions allows quantifying the impacts of Q variations associated with climate variability and dam constructions,

respectively (Figure 5-13). Under natural conditions, due to the Q variation associated with climate variability, the DOC flux during 2008-2013 only increased by 1% compared to 2003-2007, and the flood year 2008 was the main contributor. Under actual conditions, a 13% reduction of DOC flux was induced by dams which allowed regulation of peak flow during flood seasons. Previous studies also revealed that climate variability and dam constructions within the Red River basin had impacts on Q, however, they showed that Q was more influenced by climate variability than dams (Wei *et al.*, 2019a): they found that at the Son Tay outlet, the annual mean Q was reduced by 13% from 2000-2007 to 2008-2013, with 9% due to climate variability and 4% due to the dams.

The studies on other Asian river basins, such as the Yangtze, Yellow and Pearl, also found correlations between DOC concentration, flux and precipitation (Shi *et al.*, 2016). In South-east Asia, increases in the frequency and intensity of extreme precipitation events had been observed (Min *et al.*, 2011), and Park *et al.* (2018) indicated that potential changes in monsoon rainfall regimes as a consequence of climate change would amplify seasonal and interannual variations in the transport of carbon. Soil organic carbon is the main source for riverine DOC, and soil erosion and leaching induced by rainfall have a strong impact on the global carbon cycle (Lal, 2003). The impact of dam construction on DOC transport mainly due to water regulation, however, this impact is not significant in our study. In the study of Xia *et al.* (2016) who observed that though the DOC flux in 2013 had decreased by 45 % compared to the period before Xiaolangdi dam operation on the Yellow River, the impact of both water and sediment regulation on DOC concentration was insignificant.

6.3.2. Particulate organic carbon export

The mean annual export of POC during 2003-2013 was 406 kt yr^{-1} at Son Tay which accounted for 0.37% of the total POC export by the Asian rivers (76.9 Mt yr^{-1}, Li et al., 2017).

Though the POC flux of the Red River is quite low compared to other Asian rivers (from -1% for the Yellow River to -76% for the Mekong River, Table 5-2), its specific yield (2959 kg km^{-2} yr^{-1}) is quite high compared to the Mekong (41%) and the Pearl River (+148%) basins which are two basins close by. Le et al. (2017a) emphasized that the main source of the POC was the soil leaching and erosion in the Red River basin, not the phytoplankton. The soil erosion in this basin is high, especially in the middle part (Wei et al., submitted). Besides, POC is related to SSC, and the SSC in the Thao River is very high, with an annual mean of 631 mg L^{-1} at Yen Bai station during 2003 to 2013, and 137 mg L^{-1} at Son Tay station.

A distinct decrease of POC flux can be noticed after 2007 at all four stations (Figure 5-11) when some new dams started to operate. At the Son Tay outlet, the POC flux in 2008 was only 45% of that in 2007 even though 2008 is a flood year, and the average POC fluxes decreased by 88% in 208-2013 compared to 2003-2007. These dams have

trapped the suspended sediment and changed the grain size distribution of downstream sediment (Wei *et al.*, 2019a), which consequently affected the POC transfer. In 2008, a drastic decrease of SSC and sediment fluxes indeed occurred: the SSC at Son Tay decreased by 67% and the sediment flux decreased by 58% in 2008 compared to 2007 (Wei et al., 2019, submitted). Similarly to DOC fluxes, POC fluxes under natural conditions varied little (2%) between 2003-2007 and 2008-2013. Dams caused an 85% decrease in POC flux. Our study reveals that in the Red River basin, dams induced severe sequestration of POC fluxes due to suspended sediment retention.

Studies on POC in other Asian rivers also underlined the significant impacts of dams on POC transport. The annual POC trapping in the dams on the Yellow River can amount to 3.3-4.3 Mt yr^{-1}, which is similar in magnitude to the TOC export to the Bohai Sea (Zhang *et al.*, 2013; Ran *et al.*, 2014). The dams on the Yangtze River affected both the seasonal and interannual variability of terrigenous POC fluxes (Li *et al.*, 2015; Wu *et al.*, 2015): high preservation of POC was observed in reservoirs on the Yangtze River and dam buildings had sequestered around 5 Mt yr^{-1} biospheric POC since 2003, approximately 10% of the global riverine POC burial flux to the oceans. In the late 1990s, the decrease of POC was observed due to the interception of large amounts of sediment load and suspended particulate matter caused by the extensive construction of dams in the Pearl River basin (Guo *et al.*, 2015). Dam constructions, on the one hand, retain the sediment in the reservoir, affecting the POC flux; on the other hand, dam increases water temperature and retention time, which stimulate phytoplankton (a great source of the organic matter) growing in the impounded water (Park *et al.*, 2018). For example, Li *et al.* (2013a) found that a great increase in the abundance of the phytoplankton assemblages in 1997 after the first dam began operation on the upper Mekong River, and then after the cascading dams began operations in 2011, the abundance of the phytoplankton assemblages sharply increased in reservoir impoundment areas. However, in the rivers with high sediment concentrations, the contribution from phytoplankton in the reservoirs to POC are limited. For example, the phytoplankton growth is limited due to the high sediment concentration that reduces the light for algae on the Thao and Da rivers, tributaries of the Red River (Dang, 2006; Le *et al.*, 2017a).

6.3.3. Total organic carbon export and evolution

The Red River exported 628 kt yr^{-1} of TOC over 2003-2013, i.e. contributed approximately 0.38% of TOC exported by the Asian rivers (164 Mt yr^{-1}, Li et al., 2017). Due to the drop of POC flux, the TOC flux decreased by 31% at the outlet in 2008 compared to the previous year (Figure 5-12). At Son Tay outlet, the POC flux accounted for 74% of the TOC flux during 2003-2007, while it only accounted for 47% during 2008-2013 with the main part of organic carbon in the dissolved phase. Previous studies indicated that the Asian rivers draining erosion-prone mountainous terrain deliver more POC than DOC, particularly during the rainy seasons (Ludwig and Probst, 1996b; Park *et al.*, 2018). However, with the construction and operation of new dams,

the composition ratio of TOC changed, from POC-dominating to DOC-dominating (Table 5-3). Zhang *et al.* (2009) found the similar results for a tributary of the Pearl River and indicated that the dominance of DOC flux over POC flux was expected because of the decreasing sediment flux in the recent decade due to reforestation and reservoir construction. Besides, the dynamic variations of POC/TOC were also modified by dam regulation (Figure 5-14a). Before new dam constructions, the POC/TOC ratio was low around March and high in flood season. However, after impoundment of new dams, the dams fulfil flood-control functions during June and July, retaining water and SS, therefore the POC/TOC ratio became also low during the flood season. And around March, dams discharge water for irrigation, also releasing SS, which induces high POC/TOC.

A fundamental change of POC/TOC was observed in 2008. Two new dams (Nansha on the Thao river and Tuyen Quang on the Lo river) started operation in 2008 and two new dams (Madushan on the Thao river and Son La on the Da river) impounded in 2011. Compared to the other two tributaries, the POC/TOC ratio at Yen Bai on the Thao River did not decrease that sharply (Table 5-3). The Madushan and Nansha dams are located around 230 km upstream to Yen Bai station, therefore, the suspended sediment and POC over this distance can be regulated by the terrestrial inputs as well as the river bed degradation. At Hoa Binh station, before the new Son La dam became operational, the POC/TOC percentage was already low because of the Hoa Binh dam which was impounded in 1989. Therefore, the biggest impact on the POC/TOC ratio at Son Tay is due to the change of the POC/TOC from the Lo river, i.e. Tuyen Quang dam contributes most to the decrease of POC/TOC at Son Tay.

Chapter 7

Conclusions and Perspectives

7. CHAPTER Ⅶ: Conclusions and Perspectives

7.1. General Conclusions

This study on hydrology, suspended sediment and organic carbon transport in an Asian tropical basin under global changes provides the understanding of the transport dynamics processes and its key influencing factors. This work confirmed the significant impacts of dam constructions on suspended sediment and organic carbon transport.

7.1.1. Water regime

The rainfall (1494 mm yr^{-1} during 2000-2013 from TRMM) was abundant in the Red River basin among other Asian basins. 47% of the rainfall was fed into the streamflow, which was a high utilization ratio of rainfall compared to other Asian rivers. Though the annual mean discharge of the Red River (3003 m^3 s^{-1}) was low (24% of the Mekong River and 11% of the Yangtze River), its specific water yield was high (697 mm yr^{-1}). The water yield during the southwest monsoon period (from May to October) accounted for 76% of the total water yield in a year.

The impacts of dam constructions on the discharge of the Red River during the study period was insignificant and was -4% at the Son Tay outlet. Dams mainly regulated the discharge at seasonal scale (weakened the flood peaks and increased the flow during dry seasons) but had no significant influence on annual mean discharge. Climate variability had a larger impact on this basin, and the impact for the whole basin was -9%, ranging from -29% for Lao Cai on the Thao river to +2% for Vu Quang on the Lo river. The annual rainfall for the whole basin during the study period showed a decreasing trend though it was not significant. The impact of climate variability was severer on the upper basin with lower mean annual rainfall.

7.1.2. Suspended sediment

The sediment fluxes of the Red River during 2000-2013 was 33 Mt yr^{-1} based on daily-scale model calculation, accounting for 0.7% of the total Asian river sediment (4740 Mt yr^{-1}) delivery to the seas (Syvitski *et al.*, 2005). Around 90% of the annual sediment flux was exported during monsoon seasons (May-October). The sediment export of the Red River was in the same range as the Mekong and Pearl rivers and was around 23% of the Yangtze River, however, the specific sediment yield of the Red River basin was at least 3 times higher than above basins. High suspended sediment concentration (~1500 mg L^{-1}) of the Thao River and high erosion (hot spots above 20 t ha^{-1} yr^{-1}) in the middle basin were the main contributors. Precipitation, slope and agricultural practice are the key influence factors for soil erosion in the Red River basin.

Since 2008, new dams started operating continuously, the sediment export decreased from 49 Mt yr^{-1} during 2000-2007 to 12 Mt yr^{-1} during 2008-2013. Dam constructions were the main factor reducing the sediment export, contributing an 80% decrease on sediment flux. On the contrary, the impact of climate variability was -13%.

7.1.3. Organic carbon

Based on the daily time-step calculation, during 2003-2013, the mean annual export of DOC and POC at Son Tay was 222 and 406 kt yr^{-1}, respectively, which represented 0.26% and 0.37% of the total Asian rivers DOC and POC transport, respectively. During a year, 85% of the total DOC and 88% of the total POC were exported to the delta during the southwest monsoon seasons (May to October). Compared to some other Asian and tropical rivers, the export of DOC and POC fluxes through the Red River was not high. However, its specific DOC and POC yields were high, which is in agreement with some previous studies that indicated that the rivers in mainland Asia have the highest specific export rates worldwide in terms of DOC and POC.

At the Son Tay outlet, due to the Q variation induced by climate variability, the DOC flux during 2008-2013 increased 1% compared to 2003-2007, and the flood year 2008 was the main contributor for the DOC flux during 2008-2013. A 13% reduction of DOC flux was related to dam operations which regulated the discharge during flood seasons. POC fluxes during 2008-2013 decreased by 88% compared to 2003-2007: climate variability had little impacts on POC fluxes (-2%), while the dam constructions caused an 85% decrease. POC transfer was affected consequently after dam constructions.

At the outlet during 2003-2007, the POC flux accounted for averagely 74% of total organic carbon (TOC) flux, but during 2008-2013, it only accounted for 47%. With the constructions and operations of new dams, the POC/TOC ratio changed, from POC-dominating to DOC-dominating. Besides, the dynamic variations of POC/TOC were also changed by dam regulation. Before new dam constructions, the POC/TOC ratio was low around March and high in flood season. However, after new dams impounded, during June and July, the dams fulfil flood-control functions, retaining water and sediment, therefore the POC/TOC ratio became low during the flood season. And around March, dams discharge water for irrigation, suspended sediment is released too, which induces high POC/TOC.

7.1.4. Simple relationships proposed from this study

Firstly, simple relationships between monthly discharge and sediment fluxes at five stations in the Red River basin were established based on the outputs of the modelling, which allows the people to estimate the sediment flux with only monthly discharge data and without using complex models. Second, simple relationships related the parameters in Equation 6 and 7 to the soil organic carbon content (for calculating both DOC and POC), the mean annual discharge (for DOC) and the Chl-a concentration (for POC) enable people to calculate the DOC and POC concentrations within the Red River basin.

7.2. Perspectives

From the above results, we can see that during a decade year (2000-2013) the Red River had changed due to the natural and anthropogenic influences.

For better understanding the effects of climate variability and changes on water balance and availability in this basin, longer time-series data (hydrology and climate) on some key points (such as before and after the important dams, the border between China and Vietnam, and the outlets of the big tributaries) are necessary. This will help decision-makers to optimize the water intake and distribution, especially for intensive irrigation in the delta part of the Red River basin. Besides, climate variability showed some impacts on this basin, especially on the area with low average rainfall (the Thao basin). With longer time-series data on both climate and hydrology will help us have a deeper understanding of the climate effects.

The Red River exported large SS and POC to the downstream delta part. However, with the successive dam constructions in this basin, both SS and POC showed sharp declines by retained in the reservoir. On the one hand, dam management should pay great attention to the sedimentation in the reservoirs in order to guarantee their capacity of the reservoirs and economic effectiveness, especially to the dams on the high SSC rivers (the Thao and Da rivers). Also, for the downstream biogeochemical requirements (nutrients supply and delta form), dam management should release enough discharge in order the water can carry enough sediment and associated nutrients to the downstream. On the other hand, sediment from the landscape should be controlled. Soil erosion in the middle part of the basin and in the low part of the Da sub-basin are high. Appropriate and scientific soil conservation practices should be implemented in these areas, such as terrace and contour strip intercropping can reduce the slopes, afforestation can help protect the land from high and intensive rainfall erosion.

Due to the retention of SS by dams, the POC decreased a lot too. Even though, the specific yield of DOC and POC in the Red River basin are high among Asian river basins. High organic carbon in this basin is mainly coming from soil erosion and leaching. Therefore, for controlling the concentration of organic carbon, soil conservation should be carried out.

For improving the modelling to gain more precise simulations, more dam regulation and management information, more hydrology data from more stations and longer and high-frequency dataset, longer time-series data will be helpful. The Q, SSC and organic carbon sampling data were only gained from Vietnam part. it would be also good to have some data from upstream China's part. Also, the sediment routing parameters in the model (PRF, SPCON and SPEXP) now can only be applied to the whole basin scale, however, each tributary might have different sediment routing conditions. Such sensitive parameters should be applied at a sub-basin or reach scale. In this study, land use during this decade was not taken into account. Some human activities, such as mining and sand excavation were not able to be added into the model. We did not have the dataset for the POC before 2008 when the new dams started to operate, therefore, the impacts of dams on POC was an insight for a possible impact.

Future studies of nitrogen, phosphorus and pesticide can be carried on based on this model. Also, scenarios of global changes, such as climate changes, land use changes, new dam implementations, can be done by this model. Furthermore, this model can be coupled with a delta model, and then with sea model to investigate the impacts of global changes on the biochemical function in the coast.

Conclusions Générales et Perspectives

Cette étude sur l'hydrologie, les matières en suspension et le transport de carbone organique dans un bassin tropical asiatique soumis à des changements globaux permet de comprendre les processus dynamiques du transport et ses facteurs déterminants. Ces travaux ont confirmé les impacts importants des constructions de barrages sur le transport de matières en suspension et de carbone organique associé ainsi que les tendances sur l'impact climatique.

Régime de l'hydrologique

Les précipitations (1494 mm an^{-1} entre 2000 et 2013 provenant du TRMM) ont été abondantes dans le bassin du Fleuve Rouge en comparaison avec les autres bassins asiatiques. 47% des précipitations correspondent au débit, ce qui représente une fraction élevée de la pluie par rapport aux autres fleuves asiatiques. Bien que le débit moyen annuel du Fleuve Rouge (3003 m^3 s^{-1}) soit faible (24% du Mékong et 11% du Yangtsé), son apport spécifique en flux d'eau reste élevé (697 mm an^{-1}). Le débit au cours de la mousson du sud-ouest (de mai à octobre) représente 76% du débit total au cours d'une année.

Les impacts de la construction de barrages sur le débit du Fleuve Rouge au cours de la période d'étude sont quasi négligeables et s'élèvent à -4% du débit à Son Tay. Les barrages régulent principalement les débits à l'échelle saisonnière (atténuent les pics de crue et augmentent le débit pendant les saisons sèches) mais n'ont pas d'influence significative sur les débits moyens annuels. La variabilité climatique a un impact plus important sur ce bassin, et l'impact pour l'ensemble du bassin est de -9%, allant de -29% pour Lao Cai sur la rivière Thao à + 2% pour le Vu Quang sur la rivière Lo durant la période d'étude. Les précipitations annuelles pour l'ensemble du bassin au cours de la période d'étude ont montré une tendance à la baisse, même si elle n'est pas significative. L'impact de la variabilité climatique a été plus sévère sur le haut bassin avec des précipitations annuelles moyennes plus faibles.

Les sédiments en suspension

Les flux sédimentaires du Fleuve Rouge en 2000-2013 sont de 33 Mt^{-1} sur la base d'une simulation journalière, représentant 0,7% du total des matières en suspension des fleuves d'Asie (4740 Mt^{-1}) vers l'Océan (Syvitski *et al.*, 2005). Environ 90% du flux annuel de matières en suspension a été exporté pendant la saison de la mousson (mai à octobre). L'exportation de matières en suspension du Fleuve Rouge se site dans la même gamme que les fleuves du Mékong et du Pearl et représente environ 23% de celle du Yangtze; toutefois, le flux spécifique du Fleuve Rouge est au moins trois fois supérieur à celui des bassins supérieurs. La concentration élevée de matières en suspension (~1500 mg L^{-1}) dans le fleuve Thao et une érosion importante (supérieure à 20 t ha^{-1} an^{-1}) dans le bassin central sont les principaux contributeurs. Les précipitations, la pente et les pratiques agricoles sont les principaux facteurs

d'influence de l'érosion des sols dans le bassin du Fleuve Rouge.

Depuis 2008, de nouveaux barrages ont été mis en service de manière continue. Les exportations de matières en suspension ont diminué, passant de 49 Mt^{-1} en 2000-2007 à 12 Mt^{-1} en 2008-2013 à Son Tay. La construction de barrages a été le principal facteur de réduction des exportations de matières en suspension, contribuant à une réduction de 80% du flux. A l'inverse, l'impact de la variabilité climatique est de -13% à Son Tay.

Le carbone organique

Sur la base des simulations au pas de temps journalier, entre 2003 et 2013, les exportations annuelles moyennes de COD et de COP à Son Tay sont respectivement de 222 et de 406 $kt.an^{-1}$, ce qui représente 0,26% et 0,37% du total des fleuves asiatiques pour le transfert de COD et du COP, respectivement. Au cours d'une année, 85% du COD total et 88% du COP total sont exportés vers le delta pendant la saison de la mousson du sud-ouest (de mai à octobre). Comparés à d'autres fleuves asiatiques et tropicaux, les flux de COD et de COP exportés par le Fleuve Rouge sont plus faibles. Cependant, les flux spécifiques de COD et de COP sont plus élevés, ce qui est en accord avec certaines études antérieures indiquant que les fleuves d'Asie continentale présentent les taux d'exportation spécifiques les plus élevés au monde en termes de COD et de COP.

À Son Tay, en raison de la variation de Q induite par la variabilité climatique, le flux de COD, entre 2008 et 2013 a augmenté de 1% par rapport à 2003-2007, et l'année très pluvieuse de 2008 a été la principale contributrice au flux de COD sur la période de 2008 à 2013. Une réduction de 13% des flux de COD est liée aux activités des barrages qui régulent les flux vers l'aval pendant les saisons des pluies. Les flux de COP ont diminué de 88% en 2008-2013 par rapport à 2003-2007 à Son Tay: la variabilité du climat n'a eu que peu d'impacts sur les flux de COP (-2%), tandis que la construction de barrages a entraîné une diminution de 85%. Le transfert de COP a été affecté de manière importante en conséquence après la construction des barrages.

Pendant la période de 2003-2007, le flux de COP représente en moyenne 74% du flux de carbone organique total (COT), mais en 2008-2013, il ne représente que 47%. Avec la construction et l'exploitation de nouveaux barrages, le rapport COP/COT a été modifié, passant de dominante COP à dominante COD. En outre, les variations dynamiques du COP/COT ont également été modifiées par la mise en place des barrages. Le rapport COP/COT a diminué pendant la saison des crues. Aux alentours du mois de Mars, les barrages rejettent de l'eau pour l'irrigation, des matières en suspension sont également rejetés, ce qui induit une teneur élevée en COP/COT.

Relations simples proposées à partir de cette étude

Premièrement, des relations simples entre les débits mensuels et les flux de sédiments à cinq stations du bassin du Fleuve Rouge ont été établies sur la base des résultats

des simulations, ce qui permet aux gestionnaires et/ou scientifiques d'estimer le flux de matières en suspension avec seulement des données de débits mensuels et sans utiliser de modèles complexes. Deuxièmement, des relations simples reliant les paramètres des équations précédentes à la teneur en carbone organique du sol (pour calculer à la fois le COD et le COP), le débit annuel moyen (pour le COD) et la concentration en Chlorophylle-a (pour le COP) permettent de simuler de manière simple et directe la concentration de COD et de COP dans le bassin du Fleuve Rouge en différents points.

Perspectives

Enfin, cette étude ouvre un certain nombre de perspectives. Ce travail pose tout d'abord les bases sur des études futures sur les transferts de contaminants tels que les métaux et les pesticides. L'outil de modélisation tel que mis en place peut d'ores et déjà être utilisé pour simuler des scénarios de changement d'occupation du sol, d'implémentation de nouveaux barrages et des scénarios de changement climatique. Ce modèle peut aussi d'ores et déjà être couplé de manière externe à un modèle de circulation marine incluant le delta du Fleuve Rouge pour permettre de comprendre l'impact d'un fonctionnement amont-aval dans les dynamiques côtières.

References

References:

Abbaspour KC. 2015. SWAT-CUP: SWAT Calibration and Uncertainty Programs – A User Manual DOI: 10.1007/s00402-009-1032-4

Achite M, Ouillon S. 2007. Suspended sediment transport in a semiarid watershed, Wadi Abd, Algeria (1973–1995). *Journal of Hydrology* **343** (3–4): 187–202 DOI: 10.1016/j.jhydrol.2007.06.026

Aitkenhead JA, McDowell WH. 2000. Soil C:N ratio as a predictor of annual riverine DOC flux at local and global scales. *Global Biogeochemical Cycles* **14** (1): 127–138 DOI: 10.1029/1999GB900083

Almeida CT, Oliveira-Júnior JF, Delgado RC, Cubo P, Ramos MC. 2017. Spatiotemporal rainfall and temperature trends throughout the Brazilian Legal Amazon, 1973-2013. *International Journal of Climatology* **37** (4): 2013–2026 DOI: 10.1002/joc.4831

Alsdorf D, Beighley E, Laraque A, Lee H, Tshimanga R, O'Loughlin F, Mahé G, Dinga B, Moukandi G, Spencer RGM. 2016. Opportunities for hydrologic research in the Congo Basin. *Reviews of Geophysics* **54** (2): 378–409 DOI: 10.1002/2016RG000517

Ananda J, Herath G. 2003. Soil erosion in developing countries: a socio-economic appraisal. *Journal of Environmental Management* **68** (4): 343–353 DOI: 10.1016/S0301-4797(03)00082-3

AQUASTAT. 2011. Hydrological Basins of Asia. *Food and Agriculture Organization of the United Nations (FAO)* Available at: http://www.fao.org/nr/water/aquastat/maps/print1.stm

Arias ME, Cochrane TA, Kummu M, Lauri H, Holtgrieve GW, Koponen J, Piman T. 2014. Impacts of hydropower and climate change on drivers of ecological productivity of Southeast Asia's most important wetland. *Ecological Modelling* **272**: 252–263 DOI: 10.1016/j.ecolmodel.2013.10.015

Arnell NW. 1999. Climate change and global water resources. *Global Environmental Change* **9**: S31–S49 DOI: https://doi.org/10.1016/S0959-3780(99)00017-5

Arnold JG, Kiniry JR, Srinivasan R, Williams JR, Haney EB, Neitsch SL. 2012a. Soil & Water Assessment Tool Input/Output Documentation Version 2012. Springer US.

Arnold JG, Moriasi DN, Gassman PW, Abbaspour KC, White MJ, Srinivasan R, Santhi C, Harmel RD, Griensven A van, Van Liew MW, et al. 2012b. SWAT: MODEL USE, CALIBRATION, AND VALIDATION. *ASABE* **55**: 1491–1508 DOI: 10.13031/2013.42256

Arnold JG, Srinivasan R, Muttiah RS, Williams JR. 1998. Large area hydrologic modeling and assesment Part I: Model development. *JAWRA Journal of the American Water Resources Association* **34** (1): 73–89 DOI: 10.1111/j.1752-1688.1998.tb05961.x

Asselman NE. 2000. Fitting and interpretation of sediment rating curves. *Journal of Hydrology* **234** (3–4): 228–248 DOI: 10.1016/S0022-1694(00)00253-5

Aucour A-M, France-Lanord C, Pedoja K, Pierson-Wickmann A-C, Sheppard SMF. 2006. Fluxes and sources of particulate organic carbon in the Ganga-

Brahmaputra river system. *Global Biogeochemical Cycles* **20** (2): 12 DOI: 10.1029/2004GB002324

Bagnold RA. 1977. Bed load transport by natural rivers. *Water Resources Research* **13** (2): 303–312 DOI: 10.1029/WR013i002p00303

Bai Z, Feng D, Ding J, Duan X. 2015. A study on the variations of soil physico-chemical properties and its environmental impact factors in the Red River watershed (in Chinese). *Yunnan Geographic Environment Research* **27** (4): 81–90 DOI: 10.13277/j.cnki.jcwu.2015.04.013

Balakrishna K, Kumar IA, Srinikethan G, Mugeraya G. 2006. Natural and Anthropogenic Factors Controlling the Dissolved Organic Carbon Concentrations and Fluxes in a Large Tropical River, India. *Environmental Monitoring and Assessment* **122** (1–3): 355–364 DOI: 10.1007/s10661-006-9188-7

Bannwarth MA, Hugenschmidt C, Sangchan W, Lamers M, Ingwersen J, Ziegler AD, Streck T. 2015. Simulation of stream flow components in a mountainous catchment in northern Thailand with SWAT, using the ANSELM calibration approach. *Hydrological Processes* **29** (6): 1340–1352 DOI: 10.1002/hyp.10268

Bannwarth MA, Sangchan W, Hugenschmidt C, Lamers M, Ingwersen J, Ziegler AD, Streck T. 2014. Pesticide transport simulation in a tropical catchment by SWAT. *Environmental Pollution* **191**: 70–79 DOI: 10.1016/j.envpol.2014.04.011

Barton AP, Fullen MA, Mitchell DJ, Hocking TJ, Liu L, Wu Bo Z, Zheng Y, Xia Z. 2004. Effects of soil conservation measures on erosion rates and crop productivity on subtropical Ultisols in Yunnan Province, China. *Agriculture, Ecosystems & Environment* **104** (2): 343–357 DOI: 10.1016/j.agee.2004.01.034

Basilevsky A. 1994. *Statistical Factor Analysis and Related Methods-Capter 3: The Ordinary Principal Components Model*. John Wiley & Sons, Inc.: Hoboken, NJ, USA. DOI: 10.1002/9780470316894

Bates BC, Kundzewicz ZW, Wu S, Palutikof JP. 2008. Climate Change and Water. IPCC Secretariat, Geneva. DOI: 10.1016/j.jmb.2010.08.039

Beristain BT. 2005. Organic matter decomposition in simulated aquaculture ponds.Wageningen University, Netherlands.

Best J. 2019. Anthropogenic stresses on the world's big rivers. *Nature Geoscience* **12** (1): 7–21 DOI: 10.1038/s41561-018-0262-x

Beusen AHW, Van Beek LPH, Bouwman AF, Mogollón JM, Middelburg JJ. 2015. Coupling global models for hydrology and nutrient loading to simulate nitrogen and phosphorus retention in surface water - Description of IMAGE-GNM and analysis of performance. *Geoscientific Model Development* **8** (12): 4045–4067 DOI: 10.5194/gmd-8-4045-2015

Beusen AHW, Dekkers ALM, Bouwman AF, Ludwig W, Harrison J. 2005. Estimation of global river transport of sediments and associated particulate C, N, and P. *Global Biogeochemical Cycles* **19** (4) DOI: 10.1029/2005GB002453

Bicknell BR, Imhoff JC, Kittle JLJ, Anthony S. Donigian J, Johanson RC. 1997. Hydrological Simulation Program--FORTRAN: User ' s Manual for Version 11

Biemans H, Haddeland I, Kabat P, Ludwig F, Hutjes RWA, Heinke J, Von Bloh W, Gerten D. 2011. Impact of reservoirs on river discharge and irrigation water supply

during the 20th century. *Water Resources Research* **47** (3) DOI: 10.1029/2009WR008929

Billett M, Charman D, Clark J, Evans C, Evans M, Ostle N, Worrall F, Burden A, Dinsmore K, Jones T, et al. 2010. Carbon balance of UK peatlands: current state of knowledge and future research challenges. *Climate Research* **45** (1): 13–29 DOI: 10.3354/cr00903

Bishop K, Pettersson C. 1996. Organic carbon in the boreal spring flood from adjacent subcatchments. *Environment International* **22** (5): 535–540 DOI: 10.1016/0160-4120(96)00036-0

Boithias L, Sauvage S, Merlina G, Jean S, Probst JL, Sánchez Pérez JM. 2014. New insight into pesticide partition coefficient Kdfor modelling pesticide fluvial transport: Application to an agricultural catchment in south-western France. *Chemosphere* **99**: 134–142 DOI: 10.1016/j.chemosphere.2013.10.050

Bookhagen B, Burbank DW. 2010. Toward a complete Himalayan hydrological budget: Spatiotemporal distribution of snowmelt and rainfall and their impact on river discharge. *Journal of Geophysical Research* **115** (F3): F03019 DOI: 10.1029/2009JF001426

Bui YT, Orange D, Visser SM, Hoanh CT, Laissus M, Poortinga A, Tran DT, Stroosnijder L. 2014. Lumped surface and sub-surface runoff for erosion modeling within a small hilly watershed in northern Vietnam. *Hydrological Processes* **28**: 2961–2974 DOI: 10.1002/hyp.9860

Carbonate-rock aquifers. 2016. *U.S. Geological Survey* Available at: https://water.usgs.gov/ogw/aquiferbasics/carbrock.html

Carlson CA, Hansell DA. 2015. *Biogeochemistry of Marine Dissolved Organic Matter* (DA Hansell and CA Carlson, eds). Academic Press: San Diego, California, USA. DOI: 10.1016/C2012-0-02714-7

Carvalhais N, Forkel M, Khomik M, Bellarby J, Jung M, Migliavacca M, Mu M, Saatchi S, Santoro M, Thurner M, et al. 2014. Global covariation of carbon turnover times with climate in terrestrial ecosystems. *Nature* **514** (7521): 213–217 DOI: 10.1038/nature13731

Chen A, Ho C-H, Chen D, Azorin-Molina C. 2019. Tropical cyclone rainfall in the Mekong River Basin for 1983–2016. *Atmospheric Research* **226**: 66–75 DOI: 10.1016/j.atmosres.2019.04.012

Chen J, Shi H, Sivakumar B, Peart MR. 2016. Population, water, food, energy and dams. *Renewable and Sustainable Energy Reviews* **56**: 18–28 DOI: 10.1016/j.rser.2015.11.043

Ciais P, Borges A V., Abril G, Meybeck M, Folberth G, Hauglustaine D, Janssens IA. 2008. The impact of lateral carbon fluxes on the European carbon balance. *Biogeosciences* **5** (5): 1259–1271 DOI: 10.5194/bg-5-1259-2008

Cibin R, Sudheer KP, Chaubey I. 2010. Sensitivity and identifiability of stream flow generation parameters of the SWAT model. *Hydrological Processes* **24** (9): 1133–1148 DOI: 10.1002/hyp.7568

Cohen S, Kettner AJ, Syvitski JPM. 2014. Global suspended sediment and water discharge dynamics between 1960 and 2010: Continental trends and intra-basin

sensitivity. *Global and Planetary Change* **115**: 44–58 DOI: 10.1016/j.gloplacha.2014.01.011

Cohen S, Kettner AJ, Syvitski JPM, Fekete BM. 2013. WBMsed, a distributed global-scale riverine sediment flux model: Model description and validation. *Computers and Geosciences* **53**: 80–93 DOI: 10.1016/j.cageo.2011.08.011

Cole JJ. 2013. The Carbon Cycle. In *Fundamentals of Ecosystem Science*Elsevier; 109–135. DOI: 10.1016/B978-0-08-091680-4.00006-8

Cole JJ, Prairie YT, Caraco NF, McDowell WH, Tranvik LJ, Striegl RG, Duarte CM, Kortelainen P, Downing JA, Middelburg JJ, et al. 2007. Plumbing the global carbon cycle: Integrating inland waters into the terrestrial carbon budget. *Ecosystems* **10** (1): 171–184 DOI: 10.1007/s10021-006-9013-8

Coynel A, Seyler P, Etcheber H, Meybeck M, Orange D. 2005. Spatial and seasonal dynamics of total suspended sediment and organic carbon species in the Congo River. *Global Biogeochemical Cycles* **19** (4): n/a-n/a DOI: 10.1029/2004GB002335

Cui L, Wang L, Lai Z, Tian Q, Liu W, Li J. 2017. Innovative trend analysis of annual and seasonal air temperature and rainfall in the Yangtze River Basin, China during 1960–2015. *Journal of Atmospheric and Solar-Terrestrial Physics* **164**: 48–59 DOI: 10.1016/j.jastp.2017.08.001

Cunge JA. 1969. On the subject of a flood propagation computation method (musklngum method). *Journal of Hydraulic Research* **7** (2): 205–230 DOI: 10.1080/00221686909500264

Dai SB, Yang SL, Li M. 2009. The sharp decrease in suspended sediment supply from China's rivers to the sea: Anthropogenic and natural causes. *Hydrological Sciences Journal* **54** (1): 135–146 DOI: 10.1623/hysj.54.1.135

Dams WC on. 2000. Dams and Development: A new framework for decision-making. *The Report of the World Commission on Dams* **23** (November): 58–63 DOI: 10.1097/GCO.0b013e3283432017

Dang TH. 2006. Erosion et transferts de Matières En Suspension, carbone et métaux dans le bassin versant du fleuve Rouge depuis la frontière sino-vietnamienne jusqu'à l'entrée du delta.L'Universite Bordeaux 1, France.

Dang TH, Coynel A, Etcheber H, Orange D, Ngoc P, Tu A, Company D. 2013a. Seasonal Variability of Particulate Organic Carbon (Poc) in a Large Asian Tropical River : the Red River (China / Vietnam). *Journal of Science and Technology* **51** (3): 315–326 DOI: 10.15625/0866-708X/51/3/9592

Dang TH, Coynel A, Etcheber H, Orange D, Pham NAT. 2013b. Seasonal Variability of Particulate Organic Carbon (Poc) in a Large Asian Tropical River : the Red River (China / Vietnam). *Vietnam Academy of Science and Technology* **51** (3): 315–326 DOI: 10.15625/0866-708X/51/3/9592

Dang TH, Coynel A, Orange D, Blanc G, Etcheber H, Le LA. 2010. Long-term monitoring (1960-2008) of the river-sediment transport in the Red River Watershed (Vietnam): Temporal variability and dam-reservoir impact. *Science of the Total Environment* **408** (20): 4654–4664 DOI: 10.1016/j.scitotenv.2010.07.007

Dang TH, Ouillon S, Van Vinh G. 2018. Water and Suspended Sediment Budgets in the Lower Mekong from High-Frequency Measurements (2009–2016). *Water* **10** (7): 846 DOI: 10.3390/w10070846

Daniel EB, Camp J V., LeBoeuf EJ, Penrod JR, Dobbins JP, Abkowitz MD. 2011. Watershed Modeling and its Applications: A State-of-the-Art Review. *The Open Hydrology Journal* **5** (1): 26–50 DOI: 10.2174/1874378101105010026

Devia GK, Ganasri BP, Dwarakish GS. 2015. A Review on Hydrological Models. *Aquatic Procedia* **4** (Icwrcoe): 1001–1007 DOI: 10.1016/j.aqpro.2015.02.126

Dile YT, Srinivasan R. 2014. Evaluation of CFSR climate data for hydrologic prediction in data-scarce watersheds: an application in the Blue Nile River Basin. *JAWRA Journal of the American Water Resources Association* **50** (5): 1226–1241 DOI: 10.1111/jawr.12182

Dodds WK, Whiles MR. 2010. Chapter 13 - Carbon. In *Freshwater Ecology (Second Edition)*, Dodds WK, , Whiles MR (eds).Academic Press: London; 323–343. DOI: https://doi.org/10.1016/B978-0-12-374724-2.00013-1

Dregne HE. 1992. Erosion and soil productivity in Asia. *Journal of Soil & Water Conservation* **47** (1): 8–13

Ellis EE, Keil RG, Ingalls AE, Richey JE, Alin SR. 2012. Seasonal variability in the sources of particulate organic matter of the Mekong River as discerned by elemental and lignin analyses. *Journal of Geophysical Research: Biogeosciences* **117** (G1) DOI: 10.1029/2011JG001816

Ercin AE, Hoekstra AY. 2014. Water footprint scenarios for 2050: A global analysis. *Environment International* **64**: 71–82 DOI: 10.1016/j.envint.2013.11.019

Escolano JJ, Pedreño JN, Lucas IG, Almendro Candel MB, Zorpas AA. 2018. Decreased Organic Carbon Associated With Land Management in Mediterranean Environments. In *Soil Management and Climate Change*Elsevier; 1–13. DOI: 10.1016/B978-0-12-812128-3.00001-X

Espa P, Crosa G, Gentili G, Quadroni S, Petts G. 2015. Downstream Ecological Impacts of Controlled Sediment Flushing in an Alpine Valley River: A Case Study. *River Research and Applications* **31** (8): 931–942 DOI: 10.1002/rra.2788

Evans AE V., Hanjra MA, Jiang Y, Qadir M, Drechsel P. 2012. Water Quality: Assessment of the Current Situation in Asia. *International Journal of Water Resources Development* **28** (2): 195–216 DOI: 10.1080/07900627.2012.669520

Fabre C, Sauvage S, Tananaev N, Noël GE, Teisserenc R, Probst JL, Sánchez-Pérez JM. 2019. Assessment of sediment and organic carbon exports into the Arctic ocean: The case of the Yenisei River basin. *Water Research* **158**: 118–135 DOI: 10.1016/j.watres.2019.04.018

FAO. 2003a. Review of world water resources by country. Rome, Italy. Available at: http://www.fao.org/tempref/agl/AGLW/ESPIM/CD-ROM/documents/5C_e.pdf

FAO. 2003b. Multilingual Thesaurus on Land Tenure (Chinese version) Available at: http://www.fao.org/docrep/005/x2038e/x2038e00.htm

FAO. 2011a. *The state of the world's land and water resources for food and agriculture (SOLAW) – Managing systems at risk*. Food and Agriculture Organization of the United Nations, Rome and Earthscan, London.

FAO. 2011b. Irrigation in Southern and Eastern Asia in figures Available at: http://www.fao.org/docrep/016/i2809e/i2809e.pdf

Farr TG, Kobrick M. 2000. Shuttle radar topography mission produces a wealth of data. *Eos, Transactions American Geophysical Union* **81** (48): 583 DOI: 10.1029/EO081i048p00583

Ford D, Williams P. 2007. *Karst Hydrogeology and Geomorphology*. John Wiley & Sons Ltd,.: West Sussex, England. DOI: 10.1002/9781118684986

Fu B, Merritt WS, Croke BFW, Weber TR, Jakeman AJ. 2019. A review of catchment-scale water quality and erosion models and a synthesis of future prospects. *Environmental Modelling & Software* **114**: 75–97 DOI: 10.1016/j.envsoft.2018.12.008

Fukunaga DC, Cecílio RA, Zanetti SS, Oliveira LT, Caiado MAC. 2015. Application of the SWAT hydrologic model to a tropical watershed at Brazil. *CATENA* **125**: 206–213 DOI: 10.1016/j.catena.2014.10.032

Furuichi T, Win Z, Wasson RJ. 2009. Discharge and suspended sediment transport in the Ayeyarwady River, Myanmar: centennial and decadal changes. *Hydrological Processes* **23** (11): 1631–1641 DOI: 10.1002/hyp.7295

Galy V, Bouchez J, France-Lanord C. 2007. Determination of Total Organic Carbon Content and δ 13 C in Carbonate-Rich Detrital Sediments. *Geostandards and Geoanalytical Research* **31** (3): 199–207 DOI: 10.1111/j.1751-908X.2007.00864.x

Garneau C. 2014. Modélisation du transfert des éléments traces métalliques dans les eaux de surface.Univercite Toulouse III Paul Sabatier, France. Available at: http://thesesups.ups-tlse.fr/2711/

Garneau C, Sauvage S, Sánchez-Pérez J-M, Lofts S, Brito D, Neves R, Probst A. 2017. Modelling trace metal transfer in large rivers under dynamic hydrology: A coupled hydrodynamic and chemical equilibrium model. *Environmental Modelling & Software* **89**: 77–96 DOI: 10.1016/j.envsoft.2016.11.018

Gassman PW, Reyes MR, Green CH, Arnold JG. 2007. The Soil and Water Assessment Tool : historical development, applications, and future research directions. *Transactions of the ASAE* **50** (4): 1211–1250 DOI: 10.1.1.88.6554

Gassman PW, Sadeghi AM, Srinivasan R. 2014. Applications of the SWAT Model Special Section: Overview and Insights. *Journal of Environment Quality* **43** (1): 1 DOI: 10.2134/jeq2013.11.0466

Giang PQ, Toshiki K, Sakata M, Kunikane S, Vinh TQ. 2014. Modelling climate change impacts on the seasonality of water resources in the upper Ca river watershed in Southeast Asia. *Scientific World Journal* **2014** DOI: 10.1155/2014/279135

Göltenboth F, Lehmusluoto P. 2006. LAKES. In *Ecology of Insular Southeast Asia*, Göltenboth F, , Timotius KH, , Milan PP, , Margraf J (eds).Elsevier: Amsterdam, Netherlands; 95–138. DOI: 10.1016/B978-044452739-4/50008-5

Gordeev VV. 2006. Fluvial sediment flux to the Arctic Ocean. *Geomorphology* **80** (1–2): 94–104 DOI: 10.1016/j.geomorph.2005.09.008

Graham DN, Butts MB. 2005. *Flexible, integrated watershed modelling with MIKE SHE in Watershed Models* (DKF V.P. Singh, ed.). DOI: 10.1201/9781420037432.ch10

Grung M, Lin Y, Zhang H, Steen AO, Huang J, Zhang G, Larssen T. 2015. Pesticide levels and environmental risk in aquatic environments in China — A review. *Environment International* **81**: 87–97 DOI: 10.1016/j.envint.2015.04.013

Gu Z. 2016. Spatiotemporal Variation of Soil Erosion in Red River Bain, China (in Chinese).Yunnan University, China.

Gu Z, Duan X, Shi Y, Li Y, Pan X. 2018. Spatiotemporal variation in vegetation coverage and its response to climatic factors in the Red River Basin, China. *Ecological Indicators* **93** (November 2017): 54–64 DOI: 10.1016/j.ecolind.2018.04.033

Guo W, Ye F, Xu S, Jia G. 2015. Seasonal variation in sources and processing of particulate organic carbon in the Pearl River estuary, South China. *Estuarine, Coastal and Shelf Science* **167**: 540–548 DOI: 10.1016/j.ecss.2015.11.004

Gupta H, Kao S-J, Dai M. 2012. The role of mega dams in reducing sediment fluxes: A case study of large Asian rivers. *Journal of Hydrology* **464**–**465**: 447–458 DOI: 10.1016/j.jhydrol.2012.07.038

Guse B, Reusser DE, Fohrer N. 2014. How to improve the representation of hydrological processes in SWAT for a lowland catchment - temporal analysis of parameter sensitivity and model performance. *Hydrological Processes* **28** (4): 2651–2670 DOI: 10.1002/hyp.9777

Ha LT, Bastiaanssen WGM, van Griensven A, van Dijk AIJM, Senay GB. 2018. Calibration of spatially distributed hydrological processes and model parameters in SWAT using remote sensing data and an auto-calibration procedure: A case study in a Vietnamese river basin. *Water (Switzerland)* **10** (2) DOI: 10.3390/w10020212

Hanjra MA, Qureshi ME. 2010. Global water crisis and future food security in an era of climate change. *Food Policy* **35** (5): 365–377 DOI: 10.1016/j.foodpol.2010.05.006

Hargreaves GL, Hargreaves GH, Riley JP. 1985. Agricultural Benefits for Senegal River Basin. *Journal of Irrigation and Drainage Engineering* **111** (2): 113–124 DOI: 10.1061/(ASCE)0733-9437(1985)111:2(113)

Hauer C, Leitner P, Unfer G, Pulg U, Habersack H, Graf W. 2018. The Role of Sediment and Sediment Dynamics in the Aquatic Environment. In *Riverine Ecosystem Management*Springer International Publishing: Cham; 151–169. DOI: 10.1007/978-3-319-73250-3_8

He D, Ren J, Fu K, Li Y. 2007. Sediment change under climate changes and human activities in the Yuanjiang-Red River Basin. *Chinese Science Bulletin* **52** (S2): 164–171 DOI: 10.1007/s11434-007-7010-8

Hiep NH, Luong ND, Viet Nga TT, Hieu BT, Thuy Ha UT, Du Duong B, Long VD, Hossain F, Lee H. 2018. Hydrological model using ground- and satellite-based data for river flow simulation towards supporting water resource management in the Red River Basin, Vietnam. *Journal of Environmental Management* **217**: 346–355 DOI: https://doi.org/10.1016/j.jenvman.2018.03.100

Hirsch RM. 2014. Large Biases in Regression-Based Constituent Flux Estimates: Causes and Diagnostic Tools. *JAWRA Journal of the American Water Resources Association* **50** (6): 1401–1424 DOI: 10.1111/jawr.12195

Hoi P V., Mol APJ, Oosterveer P, van den Brink PJ, Huong PTM. 2016. Pesticide use in Vietnamese vegetable production: a 10-year study. *International Journal of Agricultural Sustainability* **14** (3): 325–338 DOI: 10.1080/14735903.2015.1134395

Hope D, Billett MF, Cresser MS. 1994. A review of the export of carbon in river water: Fluxes and processes. *Environmental Pollution* **84** (3): 301–324 DOI: 10.1016/0269-7491(94)90142-2

Hou Q, Sun J, Jing J, Liu C, Zhang Y, Liu J, Hua M. 2018. A Regional Scale Investigation on Groundwater Arsenic in Different Types of Aquifers in the Pearl River Delta, China. *Geofluids* **2018**: 1–9 DOI: 10.1155/2018/3471295

Hu B, Li J, Bi N, Wang H, Wei H, Zhao J, Xie L, Zou L, Cui R, Li S, et al. 2015. Effect of human-controlled hydrological regime on the source, transport, and flux of particulate organic carbon from the lower Huanghe (Yellow River). *Earth Surface Processes and Landforms* **40** (8): 1029–1042 DOI: 10.1002/esp.3702

Huang TH, Chen CTA, Tseng HC, Lou JY, Wang SL, Yang L, Kandasamy S, Gao X, Wang JT, Aldrian E, et al. 2017. Riverine carbon fluxes to the South China Sea. *Journal of Geophysical Research: Biogeosciences* **122** (5): 1239–1259 DOI: 10.1002/2016JG003701

Huang TH, Fu YH, Pan PY, Chen CTA. 2012. Fluvial carbon fluxes in tropical rivers. *Current Opinion in Environmental Sustainability* **4** (2): 162–169 DOI: 10.1016/j.cosust.2012.02.004

Huntington TG, Aiken GR. 2013. Export of dissolved organic carbon from the Penobscot River basin in north-central Maine. *Journal of Hydrology* **476**: 244–256 DOI: 10.1016/j.jhydrol.2012.10.039

Immerzeel WW, van Beek LPH, Bierkens MFP. 2010. Climate Change Will Affect the Asian Water Towers. *Science* **328** (5984): 1382–1385 DOI: 10.1126/science.1183188

IPCC. 2000. the Intergovernmental Panel on Climate Change: Land Use, Land-Use Change, and Forestry DOI: DOI: 10.2277/0521800838

Islam Z. 2011. A Review on Physically Based Hydrologic Modeling. Alberta, Canada. DOI: 10.13140/2.1.4544.5924

Jiang T, Fischer T, Lu X. 2009. Larger Asian rivers: Climate change, river flow, and watershed management. *Quaternary International* **208**: 1–3 DOI: 10.1016/j.quaint.2010.06.011

Jimmy R. Williams. 1969. Flood Routing With Variable Travel Time or Variable Storage Coefficients. *Transactions of the ASAE* **12** (1): 0100–0103 DOI: 10.13031/2013.38772

Kendall MG. 1948. *Rank correlation methods*. Oxford, England: Griffin.

Khoi DN, Suetsugi T. 2014. The responses of hydrological processes and sediment yield to land-use and climate change in the Be River Catchment, Vietnam. *Hydrological Processes* **28** (3): 640–652 DOI: 10.1002/hyp.9620

Kong L, Zheng H, Rao E, Xiao Y, Ouyang Z, Li C. 2018. Evaluating indirect and direct effects of eco-restoration policy on soil conservation service in Yangtze River Basin. *Science of The Total Environment* **631–632**: 887–894 DOI:

10.1016/j.scitotenv.2018.03.117

Krause P, Boyle DP, Bäse F. 2005. Comparison of different efficiency criteria for hydrological model assessment. *Advances in Geosciences* **5**: 89–97 DOI: 10.5194/adgeo-5-89-2005

Kroeze C, Bouwman L, Seitzinger S. 2012. Modeling global nutrient export from watersheds. *Current Opinion in Environmental Sustainability* **4** (2): 195–202 DOI: 10.1016/j.cosust.2012.01.009

Kummu M, Varis O. 2007. Sediment-related impacts due to upstream reservoir trapping, the Lower Mekong River. *Geomorphology* **85** (3–4): 275–293 DOI: 10.1016/j.geomorph.2006.03.024

Kummu M, Lu XX, Wang JJ, Varis O. 2010. Basin-wide sediment trapping efficiency of emerging reservoirs along the Mekong. *Geomorphology* **119** (3–4): 181–197 DOI: 10.1016/j.geomorph.2010.03.018

Kundzewicz ZW, Nohara D, Tong J, Oki T, Buda S, Takeuchi K. 2009. Discharge of large Asian rivers – Observations and projections. *Quaternary International* **208** (1–2): 4–10 DOI: 10.1016/j.quaint.2009.01.011

Kunz MJ, Wüest A, Wehrli B, Landert J, Senn DB. 2011. Impact of a large tropical reservoir on riverine transport of sediment, carbon, and nutrients to downstream wetlands. *Water Resources Research* **47** (12) DOI: 10.1029/2011WR010996

Lal R. 2003. Soil erosion and the global carbon budget. *Environment International* **29** (4): 437–450 DOI: 10.1016/S0160-4120(02)00192-7

Lal R, Kimble J, Levine E, Stewart BA. 1995. *Soils and global change*. CRC Press: Boca Raton, USA. Available at: https://books.google.fr/books?hl=zh-CN&lr=&id=cQxGGN3vBCAC&oi=fnd&pg=PA131&dq=carbon+transport+to+ocean+by+sediment&ots=i_sclKpAjW&sig=zd6gwiB05VU1M6ksWJEv3aB9krQ#v=onepage&q=carbon transport to ocean by sediment&f=false [Accessed 7 January 2019]

Lauri H, Räsänen TA, Kummu M. 2014. Using Reanalysis and Remotely Sensed Temperature and Precipitation Data for Hydrological Modeling in Monsoon Climate: Mekong River Case Study. *Journal of Hydrometeorology* **15** (4): 1532–1545 DOI: 10.1175/JHM-D-13-084.1

Le T, Sharif H. 2015. Modeling the Projected Changes of River Flow in Central Vietnam under Different Climate Change Scenarios. *Water* **7** (12): 3579–3598 DOI: 10.3390/w7073579

Le TPQ. 2005. Biogeochemical Functioning of the Red River (North Vietnam): Budgets and Modelling.Université Paris VI- Pierre et Marie Curie.

Le TPQ, Billen G, Garnier J, Théry S, Fézard C, Chau M Van. 2005. Nutrient (N, P) budgets for the Red River basin (Vietnam and China). *Global Biogeochemical Cycles* **19** (2): 1–16 DOI: 10.1029/2004GB002405

Le TPQ, Dao VN, Rochelle-Newall E, Garnier J, Lu X, Billen G, Duong TT, Ho CT, Etcheber H, Nguyen TMH, et al. 2017a. Total organic carbon fluxes of the Red River system (Vietnam). *Earth Surface Processes and Landforms* **42** (9): 1329–1341 DOI: 10.1002/esp.4107

Le TPQ, Garnier J, Billen G, Nguyen TMH, Rochelle-Newall E, Lu X, Duong TT, Ho

CT, Le N Da, Tran TBN, et al. 2017b. Riverine carbon flux from the Red River system (Viet Nam and China): a modelling approach. *APN Science Bulletin* **7** (1): 35–41 DOI: 10.30852/sb.2017.53

Le TPQ, Garnier J, Gilles B, Sylvain T, Van Minh C. 2007. The changing flow regime and sediment load of the Red River, Viet Nam. *Journal of Hydrology* **334** (1–2): 199–214 DOI: 10.1016/j.jhydrol.2006.10.020

Le TPQ, Gilles B, Garnier J, Sylvain T, Denis R, Anh NX, Minh C Van. 2010. Nutrient (N, P, Si) transfers in the subtropical Red River system (China and Vietnam): Modelling and budget of nutrient sources and sinks. *Journal of Asian Earth Sciences* **37** (3): 259–274 DOI: 10.1016/j.jseaes.2009.08.010

Le TPQ, Le N Da, Dao VN, Rochelle-Newall E, Nguyen TMH, Marchand C, Duong TT, Phung TXB. 2018. Change in carbon flux (1960–2015) of the Red River (Vietnam). *Environmental Earth Sciences* **77** (18): 658 DOI: 10.1007/s12665-018-7851-2

Le TPQ, Seidler C, Kändler M, Tran TBN. 2012. Proposed methods for potential evapotranspiration calculation of the Red River basin (North Vietnam). *Hydrological Processes* **26** (18): 2782–2790 DOI: 10.1002/hyp.8315

Lehner B, Liermann CR, Revenga C, Vörösmarty C, Fekete B, Crouzet P, Döll P, Endejan M, Frenken K. 2011a. Global Reservoir and Dam (GRanD) database DOI: 10.1128/JCM.01792-10

Lehner B, Liermann CR, Revenga C, Vörösmarty C, Fekete B, Crouzet P, Döll P, Endejan M, Frenken K, Magome J, et al. 2011b. High-resolution mapping of the world's reservoirs and dams for sustainable river-flow management. *Frontiers in Ecology and the Environment* **9** (9): 494–502 DOI: 10.1890/100125

Lever J, Krzywinski M, Altman N. 2017. Principal component analysis. *Nature Methods* **14** (7): 641–642 DOI: 10.1038/nmeth.4346

Li D, Christakos G, Ding X, Wu J. 2018. Adequacy of TRMM satellite rainfall data in driving the SWAT modeling of Tiaoxi catchment (Taihu lake basin, China). *Journal of Hydrology* **556**: 1139–1152 DOI: 10.1016/j.jhydrol.2017.01.006

Li G, Wang XT, Yang Z, Mao C, West AJ, Ji J. 2015. Dam-triggered organic carbon sequestration makes the Changjiang (Yangtze) river basin (China) a significant carbon sink. *Journal of Geophysical Research: Biogeosciences* **120** (1): 39–53 DOI: 10.1002/2014JG002646

Li J, Dong S, Liu S, Yang Z, Peng M, Zhao C. 2013a. Effects of cascading hydropower dams on the composition, biomass and biological integrity of phytoplankton assemblages in the middle Lancang-Mekong River. *Ecological Engineering* **60**: 316–324 DOI: 10.1016/j.ecoleng.2013.07.029

Li M, Peng C, Wang M, Xue W, Zhang K, Wang K, Shi G, Zhu Q. 2017. The carbon flux of global rivers: A re-evaluation of amount and spatial patterns. *Ecological Indicators* **80** (February): 40–51 DOI: 10.1016/j.ecolind.2017.04.049

Li M, Peng C, Zhou X, Yang Y, Guo Y, Shi G, Zhu Q. 2019. Modeling Global Riverine DOC Flux Dynamics From 1951 to 2015. *Journal of Advances in Modeling Earth Systems* **11** (2): 514–530 DOI: 10.1029/2018MS001363

Li S, Bush RT. 2015. Changing fluxes of carbon and other solutes from the Mekong River. *Scientific Reports* **5** (1): 16005 DOI: 10.1038/srep16005

Li S, Lu XX, Bush RT. 2013b. CO2 partial pressure and CO2 emission in the Lower Mekong River. *Journal of Hydrology* **504**: 40–56 DOI: 10.1016/j.jhydrol.2013.09.024

Li X. 2017. Response of runoff to climate change and adaptation strategies in the Yuanjiang River Basin (in Chinese).Yunnan University.

Li X, Li Y, He J, Luo X. 2016a. Analysis of variation in runoff and impacts factors in the Yuanjiang-Red River Basin from 1956 to 2013. *Resources Science (in Chinese)* **38** (6): 1149–1159 DOI: 10.18402/resci.2016.06.14

Li Y, He J, Li X. 2016b. Hydrological and meteorological droughts in the Red River Basin of Yunnan Province based on SPEI and SDI Indices (In Chinese). *Progress In Geography* **35** (6): 758–767 Available at: http://www.progressingeography.com/article/2016/1007-6301/1007-6301-35-6-758.shtml

Li Y, He D, Ye C. 2008. Spatial and temporal variation of runoff of red river basin in Yunnan. *Journal of Geographical Sciences* **18** (3): 308–318 DOI: 10.1007/s11442-008-0308-x

Liu D, Bai Y, He X, Tao B, Pan D, Chen C-TTA, Zhang L, Xu Y, Gong C, Li T, et al. 2019a. Satellite-derived particulate organic carbon flux in the Changjiang River through different stages of the Three Gorges Dam. *Remote Sensing of Environment* **223** (January): 154–165 DOI: 10.1016/j.rse.2019.01.012

Liu D, Pan D, Bai Y, He X, Wang D, Zhang L. 2015. Variation of dissolved organic carbon transported by two Chinese rivers: The Changjiang River and Yellow River. *Marine Pollution Bulletin* **100** (1): 60–69 DOI: 10.1016/j.marpolbul.2015.09.029

Liu X, Yang M, Meng X, Wen F, Sun G. 2019b. Assessing the Impact of Reservoir Parameters on Runoff in the Yalong River Basin using the SWAT Model. *Water* **11** (4): 643 DOI: 10.3390/w11040643

Lloret E, Dessert C, Buss HL, Chaduteau C, Huon S, Alberic P, Benedetti MF. 2016. Sources of dissolved organic carbon in small volcanic mountainous tropical rivers, examples from Guadeloupe (French West Indies). *Geoderma* **282**: 129–138 DOI: 10.1016/j.geoderma.2016.07.014

Lu XX, Siew RY. 2006. Water discharge and sediment flux changes over the past decades in the Lower Mekong River: Possible impacts of the Chinese dams. *Hydrology and Earth System Sciences* **10** (2): 181–195 DOI: 10.5194/hess-10-181-2006

Lu XX, Li S, Kummu M, Padawangi R, Wang JJ. 2014. Observed changes in the water flow at Chiang Saen in the lower Mekong: Impacts of Chinese dams? *Quaternary International* **336**: 145–157 DOI: 10.1016/j.quaint.2014.02.006

Lu XX, Oeurng C, Le TPQ, Thuy DT. 2015. Sediment budget as affected by construction of a sequence of dams in the lower Red River, Viet Nam. *Geomorphology* **248**: 125–133 DOI: 10.1016/j.geomorph.2015.06.044

Ludwig W. 1997. Continental erosion and river transport of organic carbon to the world's oceans.l'Université Louis Pasteur, Strasbourg, France. Available at: https://www.persee.fr/docAsPDF/sgeol_0302-2684_1997_mon_98_1_2368.pdf%0Ahttps://www.persee.fr/doc/sgeol_0302-2684_1997_mon_98_1

Ludwig W, Probst J-L. 1996a. Predicing the oceanic input of organic carbon by continental erosion. *Global Biogeochemical Cycles* **10** (1): 23–41

Ludwig W, Probst JL. 1996b. Predicting the oceanic input of organic carbon by continental erosion. *Global Biogeochemical Cycles* **10** (1): 23–41 DOI: 10.1029/95GB02925

Ludwig W, Probst JL. 1998. River sediment discharge to the oceans: Present-day controls and global budgets. *American Journal of Science* **298** (4): 265–295 DOI: 10.2475/ajs.298.4.265

Lupker M, France-Lanord C, Lavé J, Bouchez J, Galy V, Métivier F, Gaillardet J, Lartiges B, Mugnier JL. 2011. A Rouse-based method to integrate the chemical composition of river sediments: Application to the Ganga basin. *Journal of Geophysical Research: Earth Surface* **116** (4): F04012 DOI: 10.1029/2010JF001947

Luu TNM, Garnier J, Billen G, Le TPQ, Nemery J, Orange D, Le LA. 2012. N, P, Si budgets for the Red River Delta (northern Vietnam): How the delta affects river nutrient delivery to the sea. *Biogeochemistry* **107** (1–3): 241–259 DOI: 10.1007/s10533-010-9549-8

Luu TNM, Garnier J, Billen G, Orange D, Némery J, Le TPQ, Tran HT, Le LA. 2010. Hydrological regime and water budget of the Red River Delta (Northern Vietnam). *Journal of Asian Earth Sciences* **37** (3): 219–228 DOI: 10.1016/j.jseaes.2009.08.004

Lweendo MK, Lu B, Wang M, Zhang H, Xu W. 2017. Characterization of droughts in humid subtropical region, upper kafue river basin (Southern Africa). *Water (Switzerland)* **9** (4): 242 DOI: 10.3390/w9040242

Ma C, Sun L, Liu S, Shao M, Luo Y. 2015. Impact of climate change on the streamflow in the glacierized Chu River Basin, Central Asia. *Journal of Arid Land* **7** (4): 501–513 DOI: 10.1007/s40333-015-0041-0

Mai VT, van Keulen H, Hessel R, Ritsema C, Roetter R, Phien T. 2013. Influence of paddy rice terraces on soil erosion of a small watershed in a hilly area of Northern Vietnam. *Paddy and Water Environment* **11** (1–4): 285–298 DOI: 10.1007/s10333-012-0318-2

Manh N Van, Dung NV, Hung NN, Kummu M, Merz B, Apel H. 2015. Future sediment dynamics in the Mekong Delta floodplains: Impacts of hydropower development, climate change and sea level rise. *Global and Planetary Change* **127**: 22–33 DOI: 10.1016/j.gloplacha.2015.01.001

Mann HB. 1945. Nonparametric tests against trend. *Econometrica* **13** (3): 245–259 Available at: https://www.jstor.org/stable/1907187

Manninen N, Soinne H, Lemola R, Hoikkala L, Turtola E. 2018. Effects of agricultural land use on dissolved organic carbon and nitrogen in surface runoff and subsurface drainage. *Science of the Total Environment* **618**: 1519–1528 DOI: 10.1016/j.scitotenv.2017.09.319

Manton MJ, Della-Marta PM, Haylock MR, Hennessy KJ, Nicholls N, Chambers LE, Collins DA, Daw G, Finet A, Gunawan D, et al. 2001. Trends in extreme daily rainfall and temperature in Southeast Asia and the South Pacific: 1961-1998. *International Journal of Climatology* **21** (3): 269–284 DOI: 10.1002/joc.610

Marhaento H, Booij MJ, Hoekstra AY. 2018. Hydrological response to future land-use change and climate change in a tropical catchment. *Hydrological Sciences Journal* **63** (9): 1368–1385 DOI: 10.1080/02626667.2018.1511054

Marques da Silva R, Dantas JC, Beltrão J de A, Santos CAG. 2018. Hydrological simulation in a tropical humid basin in the Cerrado biome using the SWAT model. *Hydrology Research* **49** (3): 908–923 DOI: 10.2166/nh.2018.222

Martin J, Meybeck M. 1979. Elemental mass-balance of material carried by major world rivers. *Marine Chemistry* **7** (3): 173–206 DOI: 10.1016/0304-4203(79)90039-2

McClelland JW, Stieglitz M, Pan F, Holmes RM, Peterson BJ. 2007. Recent changes in nitrate and dissolved organic carbon export from the upper Kuparuk River, North Slope, Alaska. *Journal of Geophysical Research: Biogeosciences* **112** (G4): n/a-n/a DOI: 10.1029/2006JG000371

Mekonnen MM, Hoekstra AY. 2016. Four billion people facing severe water scarcity. *Science Advances* **2** (2): e1500323 DOI: 10.1126/sciadv.1500323

Miao C, Ni J, Borthwick AGL, Yang L. 2011. A preliminary estimate of human and natural contributions to the changes in water discharge and sediment load in the Yellow River. *Global and Planetary Change* **76** (3–4): 196–205 DOI: 10.1016/j.gloplacha.2011.01.008

Milliman JD, Meade RH. 1983. World-wide delivery of river sediment to the oceans. *journal of geology* **91** (1) DOI: 10.1086/628741

Milliman JD, Syvitski JPM. 1992. Geomorphic/Tectonic Control of Sediment Discharge to the Ocean: The Importance of Small Mountainous Rivers. *The Journal of Geology* **100** (5): 525–544 DOI: 10.1086/629606

Min SK, Zhang X, Zwiers FW, Hegerl GC. 2011. Human contribution to more-intense precipitation extremes. *Nature* **470** (7334): 378–381 DOI: 10.1038/nature09763

Montanher OC, Novo EML de M, Souza Filho EE de. 2018. Temporal trend of the suspended sediment transport of the Amazon River (1984–2016). *Hydrological Sciences Journal* **63** (13–14): 1901–1912 DOI: 10.1080/02626667.2018.1546387

Moreira-Turcq P, Seyler P, Guyot JL, Etcheber H. 2003. Exportation of organic carbon from the Amazon River and its main tributaries. *Hydrological Processes* **17** (7): 1329–1344 DOI: 10.1002/hyp.1287

Moriasi DN, Arnold JG, Van Liew MW, Bingner RL, Harmel RD, Veith TL. 2007. Model Evaluation Guidelines for Systematic Quantification of Accuracy in Watershed Simulations. *Transactions of the ASABE* **50** (3): 885–900 DOI: 10.13031/2013.23153

Nachtergaele F, Petri M, Biancalani R, Van Lynden G, Van Velthuizen H, Bloise M. 2010. Global land degradation information system (GLADIS). Beta version. An information database for land degradation assessment at global level. Available at: http://www.fao.org/soils-portal/soil-degradation-restoration/global-soil-health-indicators-and-assessment/soil-heath-physical/en/

Nash JE, Sutcliffe J V. 1970. River Flow Forecasting Through Conceptual Models Part I-a Discussion of Principles*. *Journal of Hydrology* **10**: 282–290 DOI: 10.1016/0022-1694(70)90255-6

Neitsch S., Arnold J., Kiniry J., Williams J. 2009. Soil and Water Assessment Tool

Theoretical Documentation Version 2009. *Texas Water Resources Institute*: 1–647 DOI: 10.1016/j.scitotenv.2015.11.063

Ngo TS, Nguyen DB, Rajendra PS. 2015. Effect of land use change on runoff and sediment yield in Da River Basin of Hoa Binh province, Northwest Vietnam. *Journal of Mountain Science* **12** (4): 1051–1064 DOI: 10.1007/s11629-013-2925-9

Nguyen-Tien V, Elliott RJR, Strobl EA. 2018. Hydropower generation, flood control and dam cascades: A national assessment for Vietnam. *Journal of Hydrology* **560**: 109–126 DOI: 10.1016/j.jhydrol.2018.02.063

Nguyen HTM, Billen G, Garnier J, Le TPQ, Pham QL, Huon S, Rochelle-Newall E. 2018. Organic carbon transfers in the subtropical Red River system (Viet Nam): insights on CO2 sources and sinks. *Biogeochemistry* **138** (3): 277–295 DOI: 10.1007/s10533-018-0446-x

Nguyen VT, Orange D, Laffly D, Pham VC. 2011. Consequences of large hydropower dams on erosion budget within hilly agricultural catchments in Northern Vietnam by RUSLE modeling. In *International Conference Sediment Transport Modeling in Hydrological Watersheds and Rivers*Istanbul. Available at: http://horizon.documentation.ird.fr/exl-doc/pleins_textes/divers13-06/010058374.pdf

Ni H, Lu F, Luo X, Tian H, Zeng EY. 2008a. Riverine inputs of total organic carbon and suspended particulate matter from the Pearl River Delta to the coastal ocean off South China. *Marine Pollution Bulletin* **56** (6): 1150–1157 DOI: 10.1016/j.marpolbul.2008.02.030

Ni J-R, Li X-X, Borthwick AGL. 2008b. Soil erosion assessment based on minimum polygons in the Yellow River basin, China. *Geomorphology* **93** (3–4): 233–252 DOI: 10.1016/j.geomorph.2007.02.015

Nijssen B. 2004. Effect of precipitation sampling error on simulated hydrological fluxes and states: Anticipating the Global Precipitation Measurement satellites. *Journal of Geophysical Research* **109** (D2): D02103 DOI: 10.1029/2003JD003497

Nijssen B, O'donnell GM, Hamlet AF, Lettenmaier DP. 2001. Hydrologic sensitivity of global rivers to climate change. *Climatic Change* **50** (1–2): 143–175 DOI: 10.1023/A:1010616428763

Nohara D, Kitoh A, Hosaka M, Oki T. 2006. Impact of Climate Change on River Discharge Projected by Multimodel Ensemble. *Journal of Hydrometeorology* **7** (5): 1076–1089 DOI: 10.1175/JHM531.1

Ouillon S. 2018. Why and how do we study sediment transport? Focus on coastal zones and ongoing methods. *Water (Switzerland)* **10** (4) DOI: 10.3390/w10040390

Ouyang W, Cai G, Huang W, Hao F. 2016. Temporal–spatial loss of diffuse pesticide and potential risks for water quality in China. *Science of The Total Environment* **541**: 551–558 DOI: 10.1016/j.scitotenv.2015.09.120

Ouyang W, Hao F, Skidmore AK, Toxopeus AG. 2010. Soil erosion and sediment yield and their relationships with vegetation cover in upper stream of the Yellow River. *Science of The Total Environment* **409** (2): 396–403 DOI: 10.1016/j.scitotenv.2010.10.020

Park J-H, Nayna OK, Begum MS, Chea E, Hartmann J, Keil RG, Kumar S, Lu X, Ran L, Richey JE, et al. 2018. Reviews and syntheses: Anthropogenic perturbations to carbon fluxes in Asian river systems – concepts, emerging trends, and research challenges. *Biogeosciences* **15** (9): 3049–3069 DOI: 10.5194/bg-15-3049-2018

Park JH, Duan L, Kim B, Mitchell MJ, Shibata H. 2010. Potential effects of climate change and variability on watershed biogeochemical processes and water quality in Northeast Asia. *Environment International* **36** (2): 212–225 DOI: 10.1016/j.envint.2009.10.008

Peng J, Chen S, Dong P. 2010. Temporal variation of sediment load in the Yellow River basin, China, and its impacts on the lower reaches and the river delta. *CATENA* **83** (2–3): 135–147 DOI: 10.1016/j.catena.2010.08.006

Phan DB, Wu CC, Hsieh SC. 2010. Land Use Change Effects on Discharge and Sediment Yield of Song Cau Catchment in Northern Vietnam. *Journal of Environmental Science & Engineering* **5**: 92–101 Available at: http://search.proquest.com/docview/876309039?accountid=28676 http://sfxeu11.hosted.exlibrisgroup.com/sfxslub?url_ver=Z39.88-2004&rft_val_fmt=info:ofi/fmt:kev:mtx:journal&genre=article&sid=ProQ:ProQ:pqdienvsci&atitle=Land+Use+Change+Effects+on+Discharge+an

Phan Ha HA, Huon S, Henry des Tureaux T, Orange D, Jouquet P, Valentin C, De Rouw A, Tran Duc T. 2012. Impact of fodder cover on runoff and soil erosion at plot scale in a cultivated catchment of North Vietnam. *Geoderma* **177**–**178**: 8–17 DOI: 10.1016/j.geoderma.2012.01.031

Piman T, Shrestha M. 2017. Case study on sediment in the Mekong River Basin: Current state and future trends: 49

Piman T, Cochrane TA, Arias ME. 2016. Effect of Proposed Large Dams on Water Flows and Hydropower Production in the Sekong, Sesan and Srepok Rivers of the Mekong Basin. *River Research and Applications* **32** (10): 2095–2108 DOI: 10.1002/rra.3045

Piman T, Cochrane TA, Arias ME, Green A, Dat ND. 2013. Assessment of Flow Changes from Hydropower Development and Operations in Sekong, Sesan, and Srepok Rivers of the Mekong Basin. *Journal of Water Resources Planning and Management* **139** (6): 723–732 DOI: 10.1061/(ASCE)WR.1943-5452.0000286

Podwojewski P, Orange D, Jouquet P, Valentin C, Nguyen VT, Janeau JL, Tran DT. 2008. Land-use impacts on surface runoff and soil detachment within agricultural sloping lands in Northern Vietnam. *Catena* **74** (2): 109–118 DOI: 10.1016/j.catena.2008.03.013

Qu HJ, Kroeze C. 2012. Nutrient export by rivers to the coastal waters of China: management strategies and future trends. *Regional Environmental Change* **12** (1): 153–167 DOI: 10.1007/s10113-011-0248-3

Rahman M, Dustegir M, Karim R, Haque A, Nicholls RJ, Darby SE, Nakagawa H, Hossain M, Dunn FE, Akter M. 2018. Recent sediment flux to the Ganges-Brahmaputra-Meghna delta system. *Science of The Total Environment* **643**: 1054–1064 DOI: 10.1016/j.scitotenv.2018.06.147

Ran L, Lu XX, Sun H, Han J, Li R, Zhang J. 2013. Spatial and seasonal variability of organic carbon transport in the Yellow River, China. *Journal of Hydrology* **498**: 76–88 DOI: 10.1016/j.jhydrol.2013.06.018

Ran L, Lu XX, Xin Z. 2014. Erosion-induced massive organic carbon burial and carbon emission in the Yellow River basin, China. *Biogeosciences* **11** (4): 945–959 DOI: 10.5194/bg-11-945-2014

Ranasinghe R, Wu CS, Conallin J, Duong TM, Anthony EJ. 2019. Disentangling the relative impacts of climate change and human activities on fluvial sediment supply to the coast by the world's large rivers: Pearl River Basin, China. *Scientific Reports* **9** (1): 9236 DOI: 10.1038/s41598-019-45442-2

Ranzi R, Le TH, Rulli MC. 2012. A RUSLE approach to model suspended sediment load in the Lo river (Vietnam): Effects of reservoirs and land use changes. *Journal of Hydrology* **422**–**423**: 17–29 DOI: 10.1016/j.jhydrol.2011.12.009

Ren J, He D, Fu K, Li Y. 2007. Sediment variation in the Yuanjiang (the Red River Basin) driven by climate change and human activities (in Chinese). *Chinese Science Bulletin* **52** (Z2): 142–147 DOI: https://doi.org/10.1360/csb2007-52-zkII-142

Rice SK. 2007. Suspended Sediment Transport in the Ganges-Brahmaputra River System, Bangladesh.Texas A&M University, USA. Available at: https://oaktrust.library.tamu.edu/handle/1969.1/ETD-TAMU-1588

Ringnér M. 2008. *What is principal component analysis?* Nature Publishing Group. DOI: · 10.1038/nbt0308-303

Ritson JP, Croft JK, Clark JM, Brazier RE, Templeton MR, Smith D, Graham NJD. 2019. Sources of dissolved organic carbon (DOC) in a mixed land use catchment (Exe, UK). *Science of The Total Environment* **666**: 165–175 DOI: 10.1016/j.scitotenv.2019.02.228

Rizinjirabake F, Abdi AM, Tenenbaum DE, Pilesjö P. 2018. Riverine dissolved organic carbon in Rukarara River Watershed, Rwanda. *Science of The Total Environment* **643**: 793–806 DOI: 10.1016/j.scitotenv.2018.06.194

Rodrigues V de P, Tavares M, Singh VP, Pereira E, Campos C, Morat R, Silveira R, Salviano FA, Rodrigues AC. 2018. Simulation of stream flow and hydrological response to land-cover changes in a tropical river basin. *Catena* **162** (November 2017): 166–176 DOI: 10.1016/j.catena.2017.11.024

Rousseau J-F. 2014. Green Energies the Socialist Way: Hydropower, Energy Crops and Handai Livelihoods along the Red River, Yunnan Province, China.McGill University, Canada. Available at: http://digitool.library.mcgill.ca/webclient/StreamGate?folder_id=0&dvs=1557823421120~210

Runkel RL, Crawford CG, Conh TA. 2004. Load Estimator (LOADEST): A FORTRAN Program for Estimating Constituent Loads in Streams and Rivers. In *Techniques and Methods Book 4, Chapter A5*U.S. Geological Survey: Reston, Virginia; 69.

Schlesinger WH, Melack JM. 1981. Transport of organic carbon in the world's rivers. *Tellus* **33** (2): 172–187 DOI: 10.3402/tellusa.v33i2.10706

Schlünz B, Schneider RR. 2000. Transport of terrestrial organic carbon to the oceans by rivers: Re-estimating flux- and burial rates. *International Journal of Earth Sciences* **88** (4): 599–606 DOI: 10.1007/s005310050290

Schmutz S, Moog O. 2018. Dams: Ecological Impacts and Management. In *Riverine*

*Ecosystem Management*Springer International Publishing: Cham; 111–127. DOI: 10.1007/978-3-319-73250-3_6

Seitzinger SP, Mayorga E, Bouwman AF, Kroeze C, Beusen AHW, Billen G, Van Drecht G, Dumont E, Fekete BM, Garnier J, et al. 2010. Global river nutrient export: A scenario analysis of past and future trends. *Global Biogeochemical Cycles* **24** (2) DOI: 10.1029/2009GB003587

Shaxson TF, Barber RG, Food and Agriculture Organization of the United Nations. 2003. *Optimizing soil moisture for plant production : the significance of soil porosity*.

Shi G, Peng C, Wang M, Shi S, Yang Y, Chu J, Zhang J, Lin G, Shen Y, Zhu Q. 2016. The Spatial and Temporal Distribution of Dissolved Organic Carbon Exported from Three Chinese Rivers to the China Sea (J Mao, ed.). *PLOS ONE* **11** (10): e0165039 DOI: 10.1371/journal.pone.0165039

Shrestha B, Cochrane TA, Caruso BS, Arias ME. 2018. Land use change uncertainty impacts on streamflow and sediment projections in areas undergoing rapid development: A case study in the Mekong Basin. *Land Degradation & Development* **29** (3): 835–848 DOI: 10.1002/ldr.2831

Sickman JO, Zanoli MJ, Mann HL. 2007. Effects of Urbanization on Organic Carbon Loads in the Sacramento River, California. *Water Resources Research* **43** (11) DOI: 10.1029/2007WR005954

Simons G, Bastiaanssen W, Ngô L, Hain C, Anderson M, Senay G. 2016. Integrating Global Satellite-Derived Data Products as a Pre-Analysis for Hydrological Modelling Studies: A Case Study for the Red River Basin. *Remote Sensing* **8** (4): 279 DOI: 10.3390/rs8040279

Sirisena TAJG, Maskey S, Ranasinghe R, Babel MS. 2018. Effects of different precipitation inputs on streamflow simulation in the Irrawaddy River Basin, Myanmar. *Journal of Hydrology: Regional Studies* **19**: 265–278 DOI: 10.1016/j.ejrh.2018.10.005

Spencer RGM, Hernes PJ, Dinga B, Wabakanghanzi JN, Drake TW, Six J. 2016. Origins, seasonality, and fluxes of organic matter in the Congo River. *Global Biogeochemical Cycles* **30** (7): 1105–1121 DOI: 10.1002/2016GB005427

Stenback GA, Crumpton WG, Schilling KE, Helmers MJ. 2011. Rating curve estimation of nutrient loads in Iowa rivers. *Journal of Hydrology* **396** (1–2): 158–169 DOI: 10.1016/j.jhydrol.2010.11.006

Stibig H-J, Achard F, Carboni S, Raši R, Miettinen J. 2014. Change in tropical forest cover of Southeast Asia from 1990 to 2010. *Biogeosciences* **11** (2): 247–258 DOI: 10.5194/bg-11-247-2014

Suif Z, Fleifle A, Yoshimura C, Saavedra O. 2016. Spatio-temporal patterns of soil erosion and suspended sediment dynamics in the Mekong River Basin. *Science of The Total Environment* **568**: 933–945 DOI: 10.1016/j.scitotenv.2015.12.134

Syvitski JP, Morehead MD, Bahr DB, Mulder T. 2000. Estimating fluvial sediment transport: The rating parameters. *Water Resources Research* **36** (9): 2747–2760 DOI: 10.1029/2000WR900133

Syvitski JPM, Kettner A. 2011. Sediment flux and the Anthropocene. *Philosophical*

Transactions of the Royal Society A: Mathematical, Physical and Engineering Sciences **369** (1938): 957–975 DOI: 10.1098/rsta.2010.0329

Syvitski JPM, Peckham SD, Hilberman R, Mulder T. 2003. Predicting the terrestrial flux of sediment to the global ocean: A planetary perspective. *Sedimentary Geology* **162** (1–2): 5–24 DOI: 10.1016/S0037-0738(03)00232-X

Syvitski JPM, Vorosmarty CJ, Kettner AJ, Green P. 2005. Impact of Humans on the Flux of Terrestrial Sediment to the Global Coastal Ocean. *Science* **308** (5720): 376–380 DOI: 10.1126/science.1109454

Tamm T, Nõges T, Järvet A, Bouraoui F. 2008. Contributions of DOC from surface and groundflow into Lake Võrtsjärv (Estonia). *Hydrobiologia* **599** (1): 213–220 DOI: 10.1007/s10750-007-9189-8

Tan ML, Gassman PW, Srinivasan R, Arnold JG, Yang X. 2019. A Review of SWAT Studies in Southeast Asia: Applications, Challenges and Future Directions. *Water* **11** (5): 914 DOI: 10.3390/w11050914

Tan NQ, Hung LQ. 2015. Viet Nam Case Study Prepared for FAO as part of the State of the World ' s Forests 2016 (SOFO). Hanoi.

the World Commission on Dams. 2000. Dams and Development: A New Framework for Decision-Making Available at: http://www.dams.org

Thiet N Van, Didier O, Dominique L, Cu P Van. 2012. Consequences of large hydropower dams on erosion budget within hilly agricultural catchments in Northern Vietnam by RUSLE modeling. In *International Conference Sediment Transport Modeling in Hydrological Watersheds and Rivers*Istanbul, Turkey; 14–16. Available at: http://www.documentation.ird.fr/hor/fdi:010058374

Tian YQ, Yu Q, Feig AD, Ye C, Blunden A. 2013. Effects of climate and land-surface processes on terrestrial dissolved organic carbon export to major U.S. coastal rivers. *Ecological Engineering* **54**: 192–201 DOI: 10.1016/j.ecoleng.2013.01.028

Tong Y, Zhao Y, Zhen G, Chi J, Liu X, Lu Y, Wang X, Yao R, Chen J, Zhang W. 2015. Nutrient Loads Flowing into Coastal Waters from the Main Rivers of China (2006–2012). *Scientific Reports* **5** (1): 16678 DOI: 10.1038/srep16678

Tuan VD, Hilger T, MacDonald L, Clemens G, Shiraishi E, Vien TD, Stahr K, Cadisch G. 2014. Mitigation potential of soil conservation in maize cropping on steep slopes. *Field Crops Research* **156**: 91–102 DOI: 10.1016/j.fcr.2013.11.002

USDA Soil Conservation Service. 1972. *National Engineering Handbook-Part 630 Hydrology, Chapter 4-10*.

Valcu AM. 2013. Agricultural Nonpoint Source Pollution and Water Quality Trading: Empirical Analysis under Imperfect Cost Information and Measurement Error.Iowa State University, USA. Available at: https://lib.dr.iastate.edu/etd/13444

Valentin C, Agus F, Alamban R, Boosaner A, Bricquet JP, Chaplot V, de Guzman T, de Rouw A, Janeau JL, Orange D, et al. 2008. Runoff and sediment losses from 27 upland catchments in Southeast Asia: Impact of rapid land use changes and conservation practices. *Agriculture, Ecosystems and Environment* **128** (4): 225–238 DOI: 10.1016/j.agee.2008.06.004

Vezina K, Bonn F, Van CP. 2006. Agricultural land-use patterns and soil erosion vulnerability of watershed units in Vietnam's northern highlands. *Landscape*

Ecology **21** (8): 1311–1325 DOI: 10.1007/s10980-006-0023-x

Vigiak O, Malagó A, Bouraoui F, Vanmaercke M, Poesen J. 2015. Adapting SWAT hillslope erosion model to predict sediment concentrations and yields in large Basins. *Science of the Total Environment* **538**: 855–875 DOI: 10.1016/j.scitotenv.2015.08.095

Vinh VD, Ouillon S, Thanh TD, Chu L V. 2014. Impact of the Hoa Binh dam (Vietnam) on water and sediment budgets in the Red River basin and delta. *Hydrology and Earth System Sciences* **18** (10): 3987–4005 DOI: 10.5194/hess-18-3987-2014

Vörösmarty CJ, Meybeck M, Fekete B, Sharma K. 1997. The potential impact of neo-Castorization on sediment transport by the global network of rivers. *Human Impact on Erosion and Sedimentation* **245**: 261–273

Vörösmarty CJ, Meybeck M, Fekete B, Sharma K, Green P, Syvitski JPM. 2003. Anthropogenic sediment retention: Major global impact from registered river impoundments. *Global and Planetary Change* **39** (1–2): 169–190 DOI: 10.1016/S0921-8181(03)00023-7

Vu MT, Raghavan S V., Liong SY. 2012. SWAT use of gridded observations for simulating runoff - A Vietnam river basin study. *Hydrology and Earth System Sciences* **16** (8): 2801–2811 DOI: 10.5194/hess-16-2801-2012

Walling DE. 2005. Tracing suspended sediment sources in catchments and river systems. *Science of The Total Environment* **344** (1–3): 159–184 DOI: 10.1016/j.scitotenv.2005.02.011

Walling DE, Fang D. 2003. Recent trends in the suspended sediment loads of the world's rivers. *Global and Planetary Change* **39** (1–2): 111–126 DOI: 10.1016/S0921-8181(03)00020-1

Wang H, Saito Y, Zhang Y, Bi N, Sun X, Yang Z. 2011. Recent changes of sediment flux to the western Pacific Ocean from major rivers in East and Southeast Asia. *Earth-Science Reviews* **102** (1–2): 80–100 DOI: https://doi.org/10.1016/j.earscirev.2011.06.003

Wang H, Yang Z, Saito Y, Liu JP, Sun X. 2006. Interannual and seasonal variation of the Huanghe (Yellow River) water discharge over the past 50 years: Connections to impacts from ENSO events and dams. *Global and Planetary Change* **50** (3–4): 212–225 DOI: 10.1016/j.gloplacha.2006.01.005

Wang W, Lu H, Yang D, Sothea K, Jiao Y, Gao B, Peng X, Pang Z. 2016. Modelling Hydrologic Processes in the Mekong River Basin Using a Distributed Model Driven by Satellite Precipitation and Rain Gauge Observations (GJ-P Schumann, ed.). *PLOS ONE* **11** (3): e0152229 DOI: 10.1371/journal.pone.0152229

Wang X, Ma H, Li R, Song Z, Wu J. 2012. Seasonal fluxes and source variation of organic carbon transported by two major Chinese Rivers: The Yellow River and Changjiang (Yangtze) River. *Global Biogeochemical Cycles* **26** (2) DOI: 10.1029/2011GB004130

Wang X, Quine TA, Zhang H, Tian G, Yuan W. 2019. Redistribution of Soil Organic Carbon Induced by Soil Erosion in the Nine River Basins of China. *Journal of Geophysical Research: Biogeosciences* **124** (4): 1018–1031 DOI: 10.1029/2018JG004781

Wei X, Sauvage S, Le TPQ, Ouillon S, Orange D, Vinh VD, Sanchez-Perez JM. 2019a. A Modeling Approach to Diagnose the Impacts of Global Changes on Discharge and Suspended Sediment Concentration within the Red River Basin. *Water* **11** (5): 958 DOI: 10.3390/w11050958

Wei X, Sauvage S, Ouillon S, Le TPQ, Orange D, Hermann M, Sanchez-Perez JM. 2019b. A drastic decrease of suspended sediment fluxes in the Red River related to climate variability and dam constructions. *Hydrological Processes* **submitted**

Wilkinson BH, McElroy BJ. 2007. The impact of humans on continental erosion and sedimentation. *Geological Society of America Bulletin* **119** (1–2): 140–156 DOI: 10.1130/B25899.1

Wilkinson SN, Prosser IP, Rustomji P, Read AM. 2009. Modelling and testing spatially distributed sediment budgets to relate erosion processes to sediment yields. *Environmental Modelling & Software* **24** (4): 489–501 DOI: 10.1016/j.envsoft.2008.09.006

Williams JR. 1975. Sediment Routing for Agricultural Watersheds. *JAWRA Journal of the American Water Resources Association* **11** (5): 965–974 DOI: 10.1111/j.1752-1688.1975.tb01817.x

Wold S, Esbensen K, Geladi P. 1987. Principal component analysis. *Chemometrics and Intelligent Laboratory Systems* **2** (1–3): 37–52 DOI: 10.1016/0169-7439(87)80084-9

World Economic Forum. 2015. Global Risks 2015, 10th Edition. Geneva. Available at: http://www3.weforum.org/docs/WEF_Global_Risks_2015_Report15.pdf

Wu CS, Yang SL, Lei Y. 2012. Quantifying the anthropogenic and climatic impacts on water discharge and sediment load in the Pearl River (Zhujiang), China (1954–2009). *Journal of Hydrology* **452**–**453**: 190–204 DOI: 10.1016/j.jhydrol.2012.05.064

Wu L, Liu X, Ma X. 2016. Spatio-temporal evolutions of precipitation in the Yellow River basin of China from 1981 to 2013. *Water Science and Technology: Water Supply* **16** (5): 1441–1450 DOI: 10.2166/ws.2016.072

Wu Y, Bao H, Yu H, Zhang J, Kattner G. 2015. Temporal variability of particulate organic carbon in the lower Changjiang (Yangtze River) in the post-Three Gorges Dam period: Links to anthropogenic and climate impacts. *Journal of Geophysical Research: Biogeosciences* **120** (11): 2194–2211 DOI: 10.1002/2015JG002927

Xia X, Dong J, Wang M, Xie H, Xia N, Li H, Zhang X, Mou X, Wen J, Bao Y. 2016. Effect of water-sediment regulation of the Xiaolangdi reservoir on the concentrations, characteristics, and fluxes of suspended sediment and organic carbon in the Yellow River. *Science of The Total Environment* **571**: 487–497 DOI: 10.1016/j.scitotenv.2016.07.015

Xie S. 2002. The Hydrological Characteristics of the Red River Basin. *Hydrology (in Chinese)* **22** (4): 57–63 DOI: 10.3969/j.issn.1000-0852.2002.04.017

Xu ZX, Pang JP, Liu CM, Li JY. 2009. Assessment of runoff and sediment yield in the Miyun Reservoir catchment by using SWAT model. *Hydrological Processes* **23** (25): 3619–3630 DOI: 10.1002/hyp.7475

Yaduvanshi A, Sharma RK, Kar SC, Sinha AK. 2018. Rainfall–runoff simulations of

extreme monsoon rainfall events in a tropical river basin of India. *Natural Hazards* **90** (2): 843–861 DOI: 10.1007/s11069-017-3075-0

Yan R, Zhang X, Yan S, Chen H. 2018. Estimating soil erosion response to land use/cover change in a catchment of the Loess Plateau, China. *International Soil and Water Conservation Research* **6** (1): 13–22 DOI: 10.1016/j.iswcr.2017.12.002

Yang D, Kanae S, Oki T, Koike T, Musiake K. 2003. Global potential soil erosion with reference to land use and climate changes. *Hydrological Processes* **17** (14): 2913–2928 DOI: 10.1002/hyp.1441

Yang J, Reichert P, Abbaspour KC, Xia J, Yang H. 2008. Comparing uncertainty analysis techniques for a SWAT application to the Chaohe Basin in China. *Journal of Hydrology* **358** (1–2): 1–23 DOI: 10.1016/j.jhydrol.2008.05.012

Yang SL, Xu KH, Milliman JD, Yang HF, Wu CS. 2015. Decline of Yangtze River water and sediment discharge: Impact from natural and anthropogenic changes. *Scientific Reports* **5** (1): 12581 DOI: 10.1038/srep12581

Yu Y, Wang H, Shi X, Ran X, Cui T, Qiao S, Liu Y. 2013. New discharge regime of the Huanghe (Yellow River): Causes and implications. *Continental Shelf Research* **69**: 62–72 DOI: 10.1016/j.csr.2013.09.013

Zarfl C, Lumsdon AE, Berlekamp J, Tydecks L, Tockner K. 2015. A global boom in hydropower dam construction. *Aquatic Sciences* **77** (1): 161–170 DOI: 10.1007/s00027-014-0377-0

Zhang LJ, Wang L, Cai W-J, Liu DM, Yu ZG. 2013. Impact of human activities on organic carbon transport in the Yellow River. *Biogeosciences* **10** (4): 2513–2524 DOI: 10.5194/bg-10-2513-2013

Zhang Q, Tao Z, Ma Z, Gao Q, Deng H, Xu P, Ding J, Wang Z, Lin Y. 2019. Hydro-ecological controls on riverine organic carbon dynamics in the tropical monsoon region. *Scientific Reports* **9** (1): 11871 DOI: 10.1038/s41598-019-48208-y

Zhang Q, Xiao M, Singh VP, Li J. 2012. Regionalization and spatial changing properties of droughts across the Pearl River basin, China. *Journal of Hydrology* **472**–**473**: 355–366 DOI: 10.1016/j.jhydrol.2012.09.054

Zhang S, Chen D, Li F, He L, Yan M, Yan Y. 2018. Evaluating spatial variation of suspended sediment ratingcurves in the middle Yellow River basin, China. *Hydrological Processes* **32** (11): 1616–1624 DOI: https://doi.org/10.1002/hyp.11514

Zhang S, Lu XX, Higgitt DL, Chen CTA, Han J, Sun H. 2008. Recent changes of water discharge and sediment load in the Zhujiang (Pearl River) Basin, China. *Global and Planetary Change* **60** (3–4): 365–380 DOI: 10.1016/j.gloplacha.2007.04.003

Zhang S, Lu XX, Sun H, Han J, Higgitt DL. 2009. Geochemical characteristics and fluxes of organic carbon in a human-disturbed mountainous river (the Luodingjiang River) of the Zhujiang (Pearl River), China. *Science of The Total Environment* **407** (2): 815–825 DOI: 10.1016/j.scitotenv.2008.09.022

Zhang W, Zhao Z, Tan S, Li Y, Wang A. 2017. Study on the soil erosion in the Yuanjiang - Honghe boundary river areas (in Chinese). *Geological Survey of China* **4** (3): 64–69 DOI: 10.19388 /j.zgdzdc.2017. 03.10

Zhao M, Running SW. 2010. Drought-Induced Reduction in Global Terrestrial Net Primary Production from 2000 Through 2009. *Science* **329** (5994): 940–943 DOI: 10.1126/science.1192666

Zhao S, Peng C, Jiang H, Tian D, Lei X, Zhou X. 2006. Land use change in Asia and the ecological consequences. *Ecological Research* **21** (6): 890–896 DOI: 10.1007/s11284-006-0048-2

Zhu Y, Chen C, Jiang H. 2012. Preliminary study on water resources protection in the Yuanjiang dry-hot valley of the Honghe river basin (In Chinese). *Pearl River* **1**: 15–17 DOI: 10.3969/j.issn.1001-9235.2012.01.005

Zimmerman JB, Mihelcic JR, Smith J. 2008. Global stressors on water quality and quantity DOI: 10.1021/es0871457

Abstract:

The Asian river basins are great contributors to sediments and organic carbon to the seas. However, these river basins are subject to the influence of climate variability and human activities, which alters the transport and fate of water and associated matter in rivers, and then modifies the coastal biochemical processes. The Red River is a representative Asian river basin and plays an important role in the economy and agriculture in China and Vietnam. However, lack of data sharing between countries and difficulty in in-situ observations and samplings, make the study through the whole basin difficult both spatially and temporally. In order to overcome these issues and better understand the water resources and matters transfer dynamics, interactive use of in-situ measurements, remote sensing observations and numerical modellings are necessary.

This work proposed a modelling approach to simulate the transfer dynamics of water, suspended sediment (SS) and organic carbon at a daily scale in the Red River, and to understand and quantify their responses to the impacts of climate variability and dam constructions. The physical-based SWAT model, combining the remote sensing data, was used in this study to simulate the water regime and suspended sediment. Six dams (two were operated before the study period and the other four started operation since 2008) were implemented in this model. The model was calibrated based on observed discharge (Q) and suspended sediment concentration (SSC) data from 2000 to 2013 at five gauge stations (the outlets of the main tributaries and of the continent basin) at a daily time step. After Q and SSC calibrated under actual conditions, a scenario of natural conditions (without any dams inside the basin) was modelled to disentangle and quantify the impacts of climate variability and dams on Q and sediment fluxes (SF). Dissolved and particulate organic carbon (DOC, POC) were calibrated based on observed Q, SSC and in-situ organic carbon sampling data. According to these relationships, the organic carbon concentrations and fluxes under actual and natural conditions are calculated, in order to further quantify the impacts of climate variability and dams on DOC and POC transfer.

This study highlighted the strong impacts of dams on sediment fluxes (-80%) and organic carbon (POC, -85%; DOC, -13%), and the impacts of climate variability on Q (-9%). Without dams, the Red River basin would have a high specific sediment yield (779 t km^{-2} yr^{-1}) compared to other Asian river basins, though its sediment export was low compared to them. The high soil erosion due to precipitation, slope and agricultural practice in the middle part of the basin is the main factor contributing to the specific sediment yield. The specific yields of DOC (1.62 t km^2 yr^{-1}) and POC (2.96 t km^2 yr^{-1}) of the Red River basin were more than twice those of other Asian basins. Soil organic carbon content and high soil erosion and leaching were the main influencing factors. The percentage of POC in total organic carbon (TOC) decreased from 86% to 74% until 2007 then to 47% with new dams. Dam constructions altered the TOC yield and POC/TOC ratio. Furthermore, simple rating curves between monthly mean Q and SF were established in this study for estimating SF at the outlet of the tributaries and the Red River, which enables stakeholders to estimate the monthly SF without using the SWAT model. Future studies on other nutrients and contaminants transfer and global changes can be carried on based on this modelling.

Résumé:

Les bassins fluviaux asiatiques sont un important contributeur de matières en suspension et de carbone organique vers les océans. Cependant, ces bassins sont soumis à la variabilité climatique et aux activités humaines, modifiant le transport et le devenir de l'eau et des matières associées dans les fleuves, ainsi que les processus biochimiques côtiers. Le Fleuve Rouge est un bassin fluvial représentatif des fleuves asiatiques et joue un rôle important dans l'économie et l'agriculture en Chine et au Vietnam. Cependant, le manque de partage de données entre les pays et la difficulté des observations et des échantillonnages in situ rendent l'étude difficile pour l'ensemble du bassin, à la fois spatialement et temporellement. Afin de surmonter ces problèmes et de mieux comprendre la dynamique de transfert des ressources en eau et des matières et proposer des outils aux gestionnaires de l'eau, une utilisation interactive des mesures in situ, des observations de télédétection et des modélisations numériques est nécessaire.

Ce travail propose de simuler la dynamique de transfert de l'eau, des sédiments en suspension (SS) et du carbone organique à l'échelle journalière dans le Fleuve Rouge, pour comprendre et quantifier leurs réponses aux impacts de la variabilité climatique et de la construction de barrages. Le modèle hydro-agro-environnemental à base physique SWAT, combinant les données de télédétection pour les variables climatiques, a été appliqué dans cette étude pour simuler les débits et les sédiments en suspension. Six barrages (dont quatre mis en service depuis 2008) ont été implémentés. Le modèle a été calibré sur la base des données de débit observées (Q) et de concentration de matières en suspension (CSC) de 2000 à 2013 au niveau de cinq stations de mesure à un pas de temps journalier. Un scénario simulant les impacts de la variabilité climatique et des barrages sur Q et SS a été simulé. Les concentrations et les flux de carbone organique pour ces mêmes conditions, ont été calibrés puis simulés via le même scénario afin de quantifier séparément les impacts de la variabilité climatique et des barrages sur le transfert de COD et de COP.

Cette étude a mis en évidence les impacts importants des barrages sur les flux de sédiments (-80%) et sur le carbone organique (COP, -85%; COD, -13%) ainsi que les impacts de la variabilité climatique sur Q (-9%). Sans barrages, le bassin du Fleuve Rouge aurait un flux spécifique élevé en matières en suspension (779 t km^{-2} an^{-1}) par rapport aux autres bassins asiatiques, bien que son exportation en flux soit faible en comparaison. L'érosion du sol due aux précipitations, à la pente et aux pratiques agricoles dans la zone centrale du bassin est le principal facteur contribuant au flux spécifique. Les flux spécifiques en COD (1.62 t km^2 an-1) et en COP (2.96 t km^2 an^{-1}) du bassin du Fleuve Rouge sont plus de deux fois supérieurs à ceux des autres bassins asiatiques. Le contenu en carbone organique des sols, l'érosion et le lessivage sont les facteurs les plus influents. Le pourcentage de POC dans le Carbonne Organique Total (COT) a diminué de 86% à 74% jusqu'en 2007 puis à 47% après les nouveaux barrages. La construction de barrages a aussi modifié le rapport COP / COT. De simples relations entre la moyenne mensuelle Q et SF ont été établies dans cette étude pour estimer la SF à la sortie des affluents et du Fleuve Rouge, ce qui permet aux parties prenantes d'estimer la SF mensuelle sans utiliser le modèle SWAT. Les futures études sur le transfert d'autres éléments nutritifs et contaminants ainsi que l'impact des changements globaux peuvent être poursuivies sur la base de ce projet de modélisation.